

**CUSHMAN FOUNDATION FOR FORAMINIFERAL RESEARCH**

---

**SPECIAL PUBLICATION NO. 13**

**DISSOLUTION OF DEEP-SEA CARBONATES**

*Edited by*

**WILLIAM V. SLITER**

U.S. Geological Survey  
345 Middlefield Road  
Menlo Park, California 94025

**ALLAN W. H. BÉ**

Lamont-Doherty Geological Observatory of Columbia University  
Palisades, New York 10964

and

**WOLFGANG H. BERGER**

Scripps Institution of Oceanography  
University of California  
La Jolla, California 92037

JANUARY 31, 1975

Price \$12.00 Individuals  
\$20.00 Libraries

## PREFACE

This volume of eleven publications is partially an outgrowth of a conference dealing with "CaCO<sub>3</sub> Dissolution in the Deep Sea," held on January 19–21, 1974 in Santa Barbara, California, under the sponsorship of the National Science Foundation. Sixty-three scientists with diverse backgrounds in geochemistry, sedimentology, micropaleontology, and biostratigraphy convened for three days to discuss the long-standing problem of understanding the rules governing the dissolution of CaCO<sub>3</sub> in sea water and the sea bed.

CaCO<sub>3</sub> skeletons secreted by planktonic foraminifera and Coccolithophoridae form important constituents of deep-sea sediments. Our knowledge of paleoclimates and paleoecology rests primarily on studies of these fossils. It is this same CaCO<sub>3</sub> which will eventually neutralize the CO<sub>2</sub> being generated by the combustion of fossil chemicals fuels. Thus our ultimate understanding of both past and future climates requires that we comprehend fully the processes leading to dissolution of CaCO<sub>3</sub> in the deep sea. This seemingly elementary chemical problem has proven to be a real brain twister. The more we learn about it, the less certain we become about what is really taking place in the deep sea. The problem has been approached in myriad ways. The contributions of sedimentologists, paleontologists, geo-

chemists, physical oceanographers, and physical chemists have all proven important. The scanning electron microscope, the Weyl saturoimeter, the moored buoy, stable and radioisotope measurements, global sediment coring (including the Deep Sea Drilling Project), high pressure inorganic chemistry, and factor analysis have all been brought to bear on the problem.

The idea of holding a CaCO<sub>3</sub> Dissolution Conference to bring together specialists from diverse fields was conceived and brought to fruition by Professor Wallace S. Broecker of Columbia University. The Santa Barbara meeting provided a unique opportunity for scientists from a variety of disciplines to communicate on this subject. Twenty-nine papers were presented. The eleven papers in this volume represent a cross-section of those presented at the conference and show a variety of research ideas and applications, although the full spectrum of the conference papers could not be presented here due to limitations of space and cost.

This volume is dedicated to Professor Wallace S. Broecker, who managed to assemble the motley group of scientists under one roof with financial support from the National Science Foundation (Grant GA-41323).

The Editors.

## CONTENTS

Dissolution of deep-sea carbonates: an introduction	Wolfgang H. Berger	7
Carbonate chemistry of sea water and the calcite compensation depth in the oceans	Taro Takahashi	11
Progressive dissolution and ultrastructural breakdown in planktonic foraminifera	Allan W. H. Bé, John W. Morse, and Stanley M. Harrison	27
Experimental studies on the dissolution of planktonic foraminifera	Alan D. Hecht, Eric V. Eslinger, and Lucille B. Garmon	56
On the dissolution of planktonic foraminifera and associated microfossils during settling and on the sea floor	Charles G. Adelseck, Jr., and Wolfgang H. Berger	70
Deep-sea carbonates: dissolution profiles from foraminiferal preservation	Wolfgang H. Berger	82
Distribution and dissolution of coccoliths in the south and central Pacific	Peter H. Roth and Wolfgang H. Berger	87
Dissolution of suspended coccoliths in the deep-sea water column and sedimentation of coccolith ooze	Susumu Honjo	114
Late Pleistocene carbonate dissolution cycles in the eastern equatorial Atlantic	James V. Gardner	129
CaCO <sub>3</sub> solution in the tropical east Pacific during the past 130,000 years	Boaz Luz and Nicholas J. Shackleton	142
Differentiating dissolution and transport effects in foraminiferal sediments from the Panama Basin	Chiye Yamashiro	151

# DISSOLUTION OF DEEP-SEA CARBONATES: AN INTRODUCTION

WOLFGANG H. BERGER

Scripps Institution of Oceanography  
University of California, San Diego  
La Jolla, California 92037

---

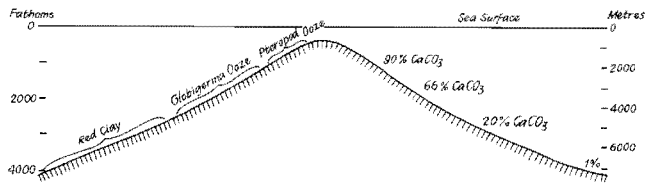
Of all the distinct types of veneers covering the Earth's crust—be it soil, sediment, or snow and ice—none are more widespread than red clay and calcareous ooze. Not surprisingly, the rate of accumulation of the ooze, its composition, and the fact that it is essentially restricted to the shallower half of the deep sea floor leaving the abyss to red clay, contain messages about first-order geochemical processes on the skin of our planet. The rate of accumulation of calcareous ooze, say, one centimeter per thousand years on the average, reflects the rate at which continents are being denuded to deliver the necessary calcium carbonate. The variations of this rate between different areas where dissolution does not interfere span roughly a factor of ten and indicate the range of large-scale, long-term productivity differences between oceanic regions. The distribution of maxima and minima—regions of mixing and upwelling versus central gyres—makes it obvious that mixing processes across the thermocline are the factor controlling this productivity. The composition of calcareous ooze—*foraminifera* in sand and silt fractions, *coccoliths* and skeletal crystallites in silt and clay—provides the reason why carbonate supply exactly follows fertility patterns: all the carbonate is precipitated by organisms. Thus, the rate of precipitation of the carbonate is limited by the nutrient supply from deep waters to the nutrient-poor euphotic zone where *forams* and *coccolithophores* grow.

This elementary chain of reasoning also provides the clue to the problem why a large part of the carbonate, once deposited, goes back into solution. Precipitation being controlled by nutrient supply, it can easily exceed the input of carbonate from land. This "excess precipitation" leads to an "excess supply" of carbonate to the sea floor, essentially robbing the ocean waters of what they consider their fair share of dissolved carbon-

ate and thus driving them toward undersaturation to the extent that the ensuing dissolution rate balances the excess precipitation. While this general model is applicable to all substances involved in biogenic deposition and redissolution, there is a special twist to the carbonate cycle. Carbonate dissolution increases with depth due to increasing pressure and decreasing temperature. Any dissolution therefore will preferably involve the abyss, with the effect that the input from land is balanced by output of carbonate on the more elevated regions of the sea floor. This phenomenon, of course, was known to John Murray of the Challenger Expedition, who in fact proposed a bathymetric zonation based on carbonate percentages and on the degree of preservation of the calcareous fossils contained in the ooze (Murray and Renard, 1891; see text fig. 1).

Murray's comparison of carbonate percentages with depth of deposition has spawned a plethora of carbonate depth plots since. An important result of this activity was the suggestion by Bramlette (1961) that the depth zone separating carbonate-rich from carbonate-poor sediments is rather narrow and well defined in several oceanic regions. This observation gave rise to the concept of "calcium carbonate compensation depth" (see text fig. 2). This concept has since been variously attacked as being fictitious and defended as being real. It has been explained chemically as a level of switch-over from saturation to undersaturation, or from inhibited to uninhibited dissolution, and explained arithmetically as the zone where clay contents get high enough to become noticeably different from their initial low percentages. Recently, the level has been mapped (see text fig. 3).

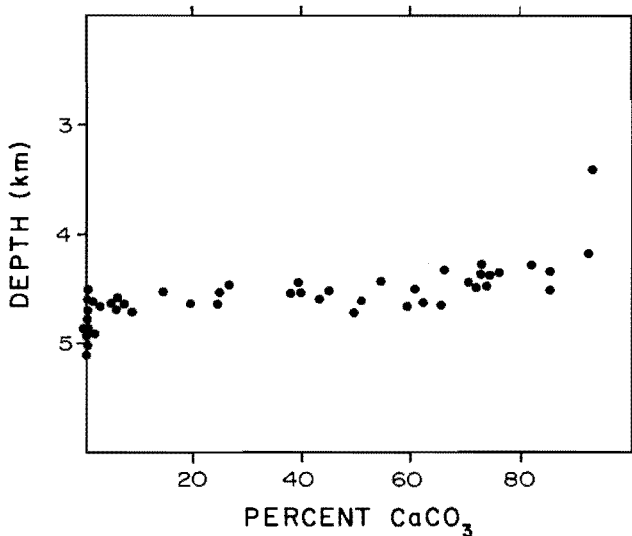
The first-order features of the surface describing the compensation depth are: (1) the mean elevation at 4.5 km depth, just halfway between ridge crest elevations and the deepest parts of the sea floor other than



TEXT FIGURE 1

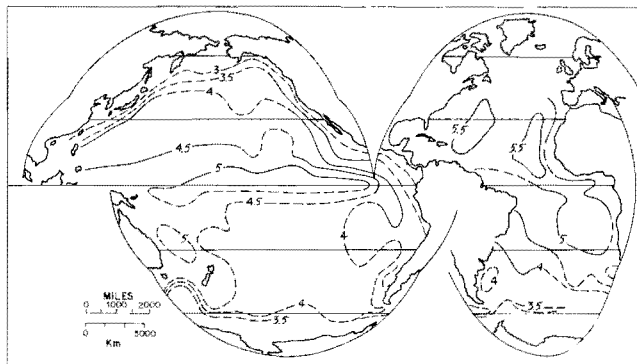
Murray's concept of dissolution of deep-sea carbonate: "Diagram showing gradual disappearance of calcium carbonate with increasing depth" (Murray and Hjort, p. 173, fig. 142).

trenches; (2) the great difference between Atlantic and Pacific which is due to the accumulation of old, CO<sub>2</sub>-rich deep waters in the Pacific; (3) the great depression under the Pacific equatorial system, which is due to increased productivity resulting from equatorial upwelling; and (4) the rise of the compensation depth toward the continents which also is related to increased fertility, but of a kind that supplies the means of dissolution—carbon dioxide—to a greater extent than the means of carbonate accumulation. Obviously, this contrasting role of fertility in changing the calcite compensation depth poses a major challenge for future investigation.



TEXT FIGURE 2

Bramlette's concept of the calcium carbonate compensation depth: "... factors related to a rather narrow depth difference are more important than has previously been indicated. . ." (Bramlette, 1961, p. 355, fig. 5). Points plotted are samples from the central equatorial Pacific, 15°N to 5°S and 120°W to 135°W.

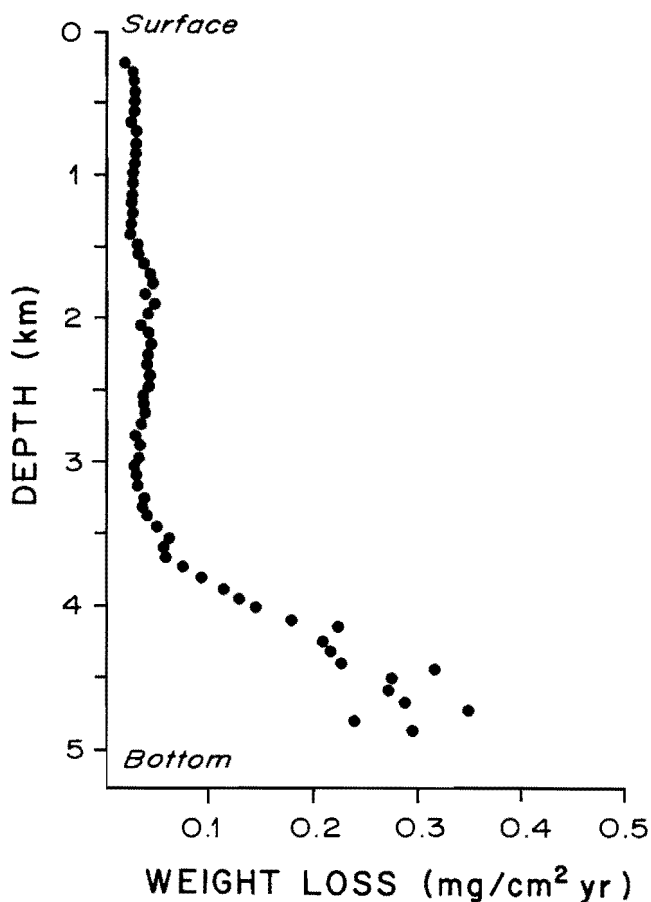


TEXT FIGURE 3

Bathymetric contours of the calcite compensation depth in Pacific and Atlantic, after Berger and Winterer (1974).

Murray's other main suggestion regarding carbonate dissolution, that is the differential dissolution of calcareous fossils, was taken less seriously on the whole, being of a more qualitative nature. Arrhenius' (1952) introduction of foram fragmentation as a quantitative index of preservation state also went essentially unnoticed until quite recently. The impetus to search systematically for partial dissolution of calcareous sediments above the compensation depth came from the results of the buoy experiment by Peterson (1966). This experiment established two important facts: (1) dissolution occurred over a wide range of depths above the compensation depth, and (2) a sharp increase in dissolution rate occurred at a level not far from the compensation depth but distinctly shallower than this depth (see text fig. 4). The sedimentologic implications of these findings were obvious: virtually all of the carbonate deposits have to be checked for evidence of partial dissolution, and such evidence would be most striking in the zone immediately above the compensation depth. A zone of partial dissolution is indeed evident: Schott (1935) had already noted something like it. The upper limit of this zone of poorly preserved calcareous assemblages was dubbed "lysocline"; in the central Atlantic it was found to follow the boundary between Antarctic Bottom Water and North Atlantic Deep Water (see text fig. 5).

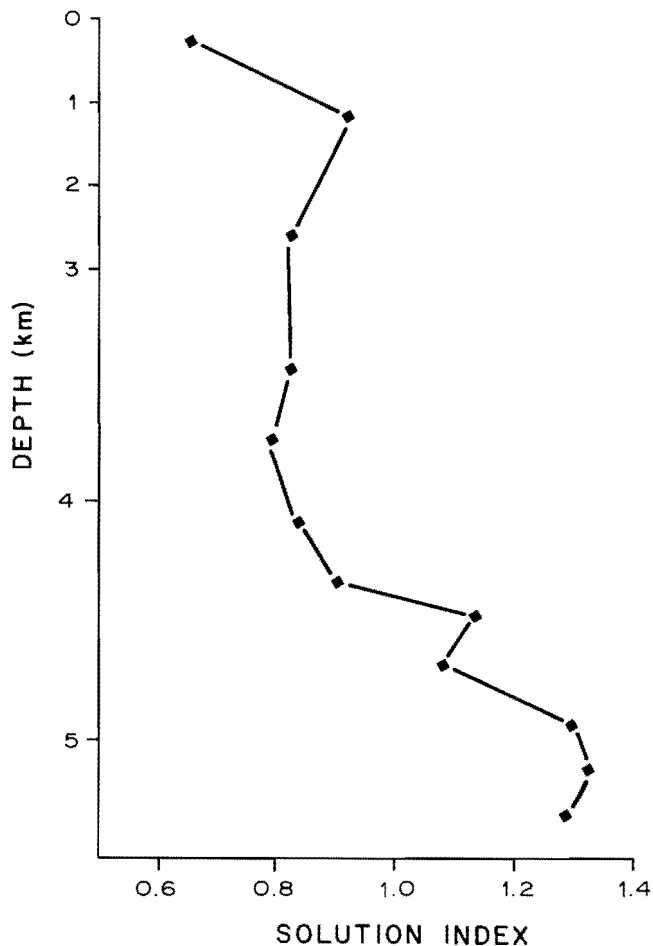
Initially, the mapping of the (foraminiferal) lysocline on the sea floor was meant to obviate the need for further Peterson-type experiments in other parts of the ocean. However, the study and the mapping of preservation facies has developed a life quite its own, as demonstrated by many of the articles in this volume.



TEXT FIGURE 4

Profile of dissolution rate of optical calcite on a moored buoy in the central Pacific demonstrating the existence of a level of rapid increase of dissolution near 3,700 m. From Peterson (1966).

Whether Peterson's level of rapid dissolution increase, the "hydrographic lysocline," invariably has a sedimentary counterpart remains to be seen and proved. Such proof has to come from study of sedimentation rate profiles (Heath and Culberson, 1970; Broecker and Broecker, 1974). Information from the Deep Sea Drilling Project on sedimentation rates in the eastern tropical Pacific is consistent with a general linear increase of dissolution rates below 3 km depth (text fig. 6). The average rate increase amounts to about 1 cm/1,000 yrs additional carbonate dissolved for each km depth increase. While a level of accelerated dissolution is not apparent in these data, its existence is not precluded, because (1) the rate increase is av-

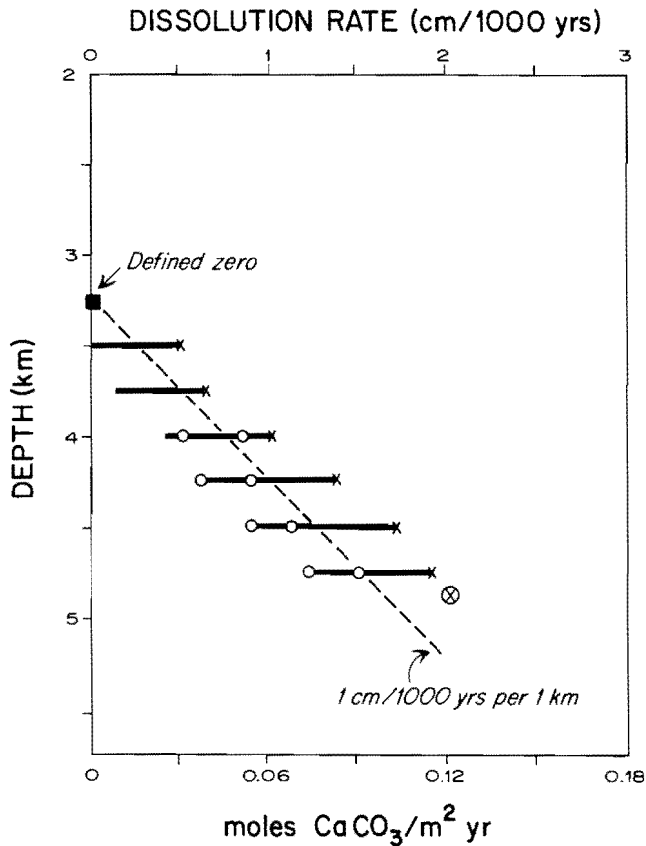


TEXT FIGURE 5

Profile of the preservation aspect ("solution index") of foraminifera in the central Atlantic, demonstrating an abrupt transition from well-preserved to poorly preserved foram assemblages (foram "lysocline"). Points plotted are averages (mean N = 7). From Berger (1968).

craged over the post-Eocene Tertiary and reflects, in part, the range of fluctuation in the depth of pronounced dissolution, (2) if the rate increase is a reasonable estimate for other regions also, it can only apply at depths approaching the CCD, since 1 to 2 cm/1,000 yrs represents the maximum sedimentation rate for many areas, and (3) paleontologic evidence suggests that dissolution of calcite above, say, 3 km depth in the deep sea is of minor importance although the subject warrants further study.

Clearly, the relationship between facies distribution, dissolution rate profiles and degree-of-saturation profiles such as given by Takahashi in the following article



TEXT FIGURE 6

Depth distribution of sedimentation rate differences in the eastern tropical Pacific, west of the Rise, within 10° of the equator. The differences are interpreted as dissolution rates. Circles: points at the local CCD. Crosses: points at paleo-equator. Data from generalized sedimentation rate distributions for post-Eocene sediments recovered by the Deep Sea Drilling Project (as given in Berger, 1973, fig. 11).

are still completely unresolved, with new information mostly adding complexities at this stage. Such complications, of course, are good news for chemists, sedimentologists and paleontologists alike, because it gives

us something to look for, to think about, and to talk and argue about—although not always necessarily in this sequence.

## REFERENCES

- ARRHENIUS, G., 1952, Sediment cores from the East Pacific: Swedish Deep-Sea Exped. (1947-1948) Repts. v. 5, nos. 1-4, p. 1-228.
- BERGER, W. H., 1968, Planktonic foraminifera: selective solution and paleoclimatic interpretation: *Deep-Sea Research*, v. 15, p. 31-43.
- , 1973, Cenozoic sedimentation in the Eastern Tropical Pacific: *Geol. Soc. America Bull.*, v. 84, p. 1941-1954.
- BERGER, W. H., and WINTERER, E. L., 1974, Plate stratigraphy and the fluctuating carbonate line, in Hsü, K. J., and Jenkyns, H. C., eds., *Pelagic sediments on land and under the sea*: Internat. Assoc. Sedimentologist Spec. Pub., v. 1, p. 59-96.
- BRAMLETTE, M. N., 1961, Pelagic sediments, in Sears, M., ed., *Oceanography*: Am. Assoc. Adv. Sci. Pub., v. 67, p. 345-366.
- BROECKER, W. S., and BROECKER, S., 1974, Carbonate dissolution on the flank of the East Pacific Rise: *Soc. Econ. Paleontologists Mineralogists Spec. Pub.*, v. 20, p. 44-57.
- HEATH, G. R., and CULBERSON, C., 1970, Calcite: degree of saturation, rate of dissolution, and the compensation depth in the deep oceans: *Geol. Soc. America Bull.*, v. 81, p. 3157-3160.
- MURRAY, J., and HJORT, J., 1912, *The depths of the ocean*: London, Macmillan. 821 p.
- MURRAY, J., and RENARD, A. F., 1891, Report on deep-sea deposits based on the specimens collected during the voyage of H. M. S. Challenger in the years 1872 to 1876: London, Longmans, Rept. Voyage Challenger, 525 p. (reprinted by Johnson Reprint Corp., New York, 1965).
- PETERSON, M. N. A., 1966, Calcite: rates of dissolution in a vertical profile in the Central Pacific: *Science*, v. 154, p. 1542-1544.
- SCHOTT, W., 1935, Die Foraminiferen in dem äquatorialen Teil des Atlantischen Ozeans: *Wiss. Ergebn. der deutsch. Atl. Exped. "Meteor" 1925-1927, Bd. III (3), Sec. B*, p. 43-134.

# CARBONATE CHEMISTRY OF SEA WATER AND THE CALCITE COMPENSATION DEPTH IN THE OCEANS

TARO TAKAHASHI

Queens College, City University of New York,  
Flushing, N.Y., 11367

---

## ABSTRACT

The physicochemical parameters needed for the calculation of the degree of saturation of calcium carbonate in deep sea from the chemical data measured at ambient barometric pressures are reviewed. When the alkalinity and total carbon dioxide concentrations are used to calculate total  $\text{CO}_3^{2-}$  species, the result is not sensitively affected by the choice of the available sets of the apparent dissociation constants for carbonic and boric acids in sea water determined by Lyman (1957), Hansson (1973a), and Mehrbach and others (1974). The apparent solubility products of calcite in seawater determined by Ingle and others (1973) at 1 bar total pressure are preferred over those determined by McIntyre (1965), because of the possible disequilibrium conditions existing in McIntyre's experiments. An inconsistency of an order of  $10 \text{ cm}^3/\text{mole}$  for the partial molal volumes of  $\text{Ca}^{++}$  and/or  $\text{CO}_3^{2-}$  are present among the available data. This would cause an uncertainty of about 15 percent in the degree of saturation calculated for a pressure of 500 bars (or a 5,000 meter depth). The degree of saturation of calcite in the Atlantic and Pacific Oceans has been calculated from about 4,000 sets

of the alkalinity and total  $\text{CO}_2$  measurements obtained during GEOSECS. It has been found that the calcite compensation depths obtained by Berger and Winterer (1974) coincide with the level of 75 and 65 percent undersaturation respectively in the Atlantic and the Pacific Oceans with an exception of the southern extreme of those oceans. In the southern extreme ( $\sim 60^\circ \text{ S}$ ), the calcite compensation depths become shallower coinciding with a level of 90 percent undersaturation. On the basis of the rates of dissolution of calcite in seawater determined by Morse and Berner (1972) and the calculated pH values at in situ pressure and temperature conditions, the dissolution rates for calcite at the calcite compensation depths have been estimated. General agreement between the dissolution rates thus obtained and the carbonate productivity in the surface water suggests that the calcite compensation depth in the oceans is controlled by the biological productivity of carbonates in the surface water and the degree of undersaturation of calcite in seawater which, in turn, regulates the rate of dissolution. Specific areas of studies needed to be investigated are summarized.

---

## INTRODUCTION

The observed correlation between water depth and calcium carbonate concentration in deep-sea sediments has been an enigma to oceanographers, and has been investigated with different approaches by a number of researchers in the field. The most direct approach

was taken by Peterson (1966) who measured the rate of weight loss over a period of several months from polished spheres of calcite suspended at various depths of water at deep-sea moorings in the central North Pacific. He observed that the rate of solution increases abruptly at a water depth of about 3,700 meters, and it remains high below this depth. Berger (1967) conducted similar experiments using calcitic shells of fora-

minifera, and observed a weight loss of several percent below 1,000 meters, and a greater rate of weight loss below 3,000 meters. The results of these experiments clearly indicate that the deep water of the North Pacific Ocean below about 3,000 meters dissolves calcite at a measurable rate, hence, accounting qualitatively for the observed lack of calcium carbonate in deep-sea sediments below water depths of 4,500 meters in the area of the moorings.

Since mooring experiments are neither suited for a rapid survey of the world oceans, nor measurements of the degree of saturation, Ben-Yaakov and Kaplan (1971) adapted the carbonate saturometer of Weyl (1961) for the study of the degree of saturation of calcite and/or aragonite in the deep oceans. The degree of saturation of calcium carbonate in sea water at in situ temperature and pressure conditions was obtained from the difference between the EMF for a calomel-glass electrode pair immersed in sea water in situ and one immersed in a sea water saturated column of powdered carbonate crystals. They observed that in the eastern North Pacific Ocean off Southern California the sea water between 400 and 1,650 meters deep and that below about 2,250 meters is undersaturated with respect to calcite.

In contrast to the first two methods described above, a third type of study offers a less direct approach, but has been most commonly used by a number of investigators. The degree of saturation of carbonate in sea water can be calculated if two of the following four carbonate chemistry parameters, i.e., alkalinity, total dissolved  $\text{CO}_2$  concentration, pH, and  $\text{pCO}_2$ , are measured in discrete water samples collected at various depths. The effects of temperature and pressure on the apparent dissociation constants for carbonic and boric acids and on the apparent solubility products for calcite and aragonite must be known for the calculation. However, due to insufficient knowledge of the compatibility of the different methods used for the measurements of the carbonate chemistry parameters, and also due to the diversity of the data on the effects of temperature and pressure on the necessary chemical parameters, it has not been possible to compare the results obtained at various geographical locations by different investigators using different techniques. Hence, the systematic variation of the degree of carbonate saturation within an ocean has not been well documented. During the recent Geochemical Ocean Section Studies (GEOSECS) expeditions in the Atlantic and Pacific Oceans, several thousand measurements of alkalinity and total  $\text{CO}_2$  concentration were made,

and thus, it has become possible to study the systematic variation of the carbonate saturation in sea water on the basis of sets of data which were obtained by a single method at various water depths and over wide geographical locations.

The objectives of this paper are (1) to review the available basic physicochemical data needed to compute the degree of saturation of calcium carbonate in sea water, and (2) to discuss the implications of the calcite saturation values calculated from the GEOSECS alkalinity and total carbon dioxide values to the origin of the calcite compensation depths in the oceans.

### COMPUTATION OF THE DEGREE OF SATURATION OF CALCIUM CARBONATE IN SEA WATER

The degree of saturation of calcium carbonate in sea water is defined in terms of the ratio of the product of the calcium and carbonate ion concentrations in sea water,  $(\text{Ca}^{++}) \cdot (\text{CO}_3^{=})$ , to the equilibrium solubility product of calcite or aragonite,  $K'_{sp}$ . Namely, if  $(\text{Ca}^{++}) \cdot (\text{CO}_3^{=}) / K'_{sp} > 1$ , sea water is supersaturated with respect to calcium carbonate; if  $(\text{Ca}^{++}) \cdot (\text{CO}_3^{=}) / K'_{sp} = 1$ , it is in equilibrium with calcium carbonate; and if  $(\text{Ca}^{++}) \cdot (\text{CO}_3^{=}) / K'_{sp} < 1$ , it is undersaturated with respect to calcium carbonate and dissolution of carbonate crystals should occur. Therefore, in order to study the degree of saturation of calcium carbonate crystals in sea water, it is necessary to know the concentrations of  $\text{Ca}^{++}$  and  $\text{CO}_3^{=}$  ions in sea water and the equilibrium solubility products for calcite or aragonite in sea water as a function of temperature, pressure and chlorinity (or salinity). Since the concentration or activity of carbonate ions cannot be measured directly, it is calculated using the dissociation constants of the carbonic acid and measurable parameters such as the total  $\text{CO}_2$  species dissolved in sea water, alkalinity, pH and partial pressure of  $\text{CO}_2$  exerted by sea water.

The total carbon dioxide species dissolved in sea water,  $\Sigma\text{CO}_2$ , is expressed by:

$$\Sigma\text{CO}_2 = \alpha_s \cdot \text{pCO}_2 + (\text{HCO}_3^-) + (\text{CO}_3^{=}) \quad (1)$$

where  $\alpha_s$  is the solubility of carbon dioxide gas in a sea-water sample with a salinity  $S$ ;  $\text{pCO}_2$ , the partial pressure of carbon dioxide exerted by the sea-water sample; and  $(\text{HCO}_3^-)$  and  $(\text{CO}_3^{=})$  are respectively the concentrations of bicarbonate and carbonate ions. Since both bicarbonate and carbonate ions form various ion complexes by reacting with such cations as  $\text{Na}^+$ ,  $\text{Mg}^{++}$

and  $\text{Ca}^{++}$  present in sea water, the concentrations of  $(\text{HCO}_3^-)$  and  $(\text{CO}_3^{=})$  represent the sum of the concentrations of simple ions and complex ion associations such as  $\text{NaHCO}_3^0$ ,  $\text{MgHCO}_3^+$  and  $\text{CaCO}_3^0$  (e.g., see Garrels and Christ, 1965). The three terms in equation (1) are related to each other by equations (2) and (3):

$$K'_1 = a_{\text{H}} \cdot (\text{HCO}_3^-) / \alpha_s \cdot p\text{CO}_2 \quad (2)$$

$$K'_2 = a_{\text{H}} \cdot (\text{CO}_3^{=}) / (\text{HCO}_3^-), \quad (3)$$

where  $a_{\text{H}}$  is the activity of hydrogen ions.  $K'_1$  and  $K'_2$  are called apparent dissociation constants as opposed to the thermodynamic constants which are defined in terms of the activities for uncomplexed ionic species.

The total alkalinity,  $\Sigma A$ , of sea water is defined commonly as:

$$\begin{aligned} \Sigma A &= (\text{HCO}_3^-) + 2(\text{CO}_3^{=}) + (\text{H}_2\text{BO}_3^-) \\ &\quad + (\text{OH}^-) - (\text{H}^+) \\ &= (\text{K}^+) + (\text{Na}^+) + 2(\text{Ca}^{++}) \\ &\quad + 2(\text{Mg}^{++}) - (\text{Cl}^-) - 2(\text{SO}_4^{=}) \end{aligned} \quad (4)$$

where the parentheses denote the concentrations of both simple ionic and complexed species as well. Since the concentrations of  $\text{OH}^-$  and  $\text{H}^+$  ions in sea water are negligible compared to others, equation (4) can be rewritten as:

$$\Sigma A = (\text{HCO}_3^-) + 2(\text{CO}_3^{=}) + \Sigma B \cdot K'_B / (K'_B + a_{\text{H}}) \quad (5)$$

where

$$K'_B = a_{\text{H}} \cdot (\text{H}_2\text{BO}_3^-) / (\text{H}_3\text{BO}_3), \quad \text{and} \quad (6)$$

$$\Sigma B = (\text{H}_2\text{BO}_3^-) + (\text{H}_3\text{BO}_3). \quad (7)$$

$K'_B$  is the apparent dissociation constant for boric acid in sea water,  $\Sigma B$  is the total boron concentration in sea water, and the parentheses denotes the concentrations.

In equations (1), (2), (3) and (5),  $\alpha_s$ ,  $K'_1$ ,  $K'_2$ ,  $K'_B$  and  $\Sigma B$  are knowns, and  $\Sigma A$ ,  $\Sigma \text{CO}_2$ ,  $a_{\text{H}}$ ,  $p\text{CO}_2$ ,  $(\text{HCO}_3^-)$  and  $(\text{CO}_3^{=})$  are unknowns. Hence, if any two of the first four unknowns, i.e.,  $\Sigma A$ ,  $\Sigma \text{CO}_2$ ,  $a_{\text{H}}$  and  $p\text{CO}_2$ , are measured, this set of four equations can be solved, and the concentration of  $(\text{CO}_3^{=})$  can be calculated.

Recent improved titrimetric technique for alkalinity determination developed by Edmond (1970) made it possible to determine the alkalinity values with a precision of  $\pm 0.2$  percent and the total  $\text{CO}_2$  concentrations with an accuracy of  $\pm 0.7$  percent. Since the technique allows determination of both the total alka-

linity and the total  $\text{CO}_2$  from a single sample, errors such as those resulting from two separate measurements of sample volumes will be minimized. In addition, both  $\Sigma A$  and  $\Sigma \text{CO}_2$  are oceanographically significant parameters since their variations may be used to estimate addition of carbon dioxide due to oxidation of organic matter and dissolution of  $\text{CaCO}_3$  in a water column. Thus, these parameters appear to be a highly desirable pair of carbonate parameters if they are measured with a satisfactory accuracy.

The activity of hydrogen ions in sea water (or pH) can be measured aboard ship with a desired accuracy (e.g.,  $\pm 0.003$  pH) as done by Culberson (Takahashi and others, 1970; Culberson, 1972). The accuracy of the pH measurements obtained on board has been, in general, less than satisfactory due to systematic errors introduced by the loss of  $\text{CO}_2$  from water samples, and by the difference between the concentrations of various ionic species present in sea water and in the pH standard solutions used for calibrating the electrodes (i.e., liquid junction potential).

As an alternative to  $a_{\text{H}}$ , the partial pressure of  $\text{CO}_2$  exerted by a sample water is measured with satisfactory accuracy using a gas-water equilibrator and an infrared  $\text{CO}_2$  analyzer as done by Li and others (1969) and Takahashi and others (1970). The  $\text{CO}_2$  gas analyzer is standardized using  $\text{CO}_2$ - $\text{N}_2$  gas mixtures which have been calibrated volumetrically, and hence the  $p\text{CO}_2$  values are directly related to the fundamental thermodynamic reference state of  $\text{CO}_2$  gas without ambiguity. Therefore, the  $p\text{CO}_2$  measurement is more desirable than the pH measurement which is affected by the difference between the liquid junction potentials for electrodes in sea water and standard solutions and the temperature coefficient for the electrode EMF. However, the measurements of  $p\text{CO}_2$  require a relatively large volume (5 liters or more) of water sample, and a large laboratory space for storage of bulky standard gas containers. Furthermore,  $p\text{CO}_2$  is a physically meaningful parameter only near the ocean surface (characterizing the direction of the  $\text{CO}_2$  gas exchange between the ocean water and the atmosphere), and has little physical significance in deep waters, as opposed to the total  $\text{CO}_2$  and alkalinity values, which are independent of temperature and water pressure when expressed in a per kilogram unit and may be used to study the mass balance of the dissolved species in water masses. Thus, the  $p\text{CO}_2$  measurement in deep sea-water samples has not been commonly undertaken as a routine shipboard program.

In the following section, various sets of constants

TABLE 1

Comparison of the  $a_{\text{H}}$  and  $(\text{CO}_3^{2-})$  values calculated with  $K'_1$ ,  $K'_2$  and  $K'_B$  of Lyman (1957), Hansson (1973a) and Mehrbach and others (1974) at 20°C, 10°C and 0°C for a sea water having  $S = 35.00 \text{ ‰}$ ,  $\Sigma A = 2.320 \text{ meq/kg}$ ,  $\Sigma \text{CO}_2 = 2.150 \text{ mM/kg}$  and  $\Sigma B = 0.411 \text{ mM/kg}$ .

$K'_1$ and $K'_2$	Lyman (1957)	Hansson (1973a)	Mehrbach and others (1974)
$K'_B$	Lyman (1957)	Hansson (1973a)	Lyman (1957)
T (°C)	20.00	20.00	20.00
$K'_1$ ( $10^{-7}$ )	9.59	12.44	9.44
$K'_2$ ( $10^{-10}$ )	7.05	9.41	6.54
$K'_B$ ( $10^{-9}$ )	1.78	2.16	1.78
$a_{\text{H}}$ ( $10^{-8}$ )	1.067	1.386	1.017
pH	7.972	7.858	7.993
$(\text{CO}_3^{2-})$ ( $10^{-4} \text{ M/kg}$ )	1.32	1.35	1.29
T (°C)	10.00	10.00	10.00
$K'_1$ ( $10^{-7}$ )	8.43	9.86	8.00
$K'_2$ ( $10^{-10}$ )	5.35	6.43	4.74
$K'_B$ ( $10^{-9}$ )	1.41	1.62	1.41
$a_{\text{H}}$ ( $10^{-8}$ )	0.833	0.986	0.770
pH	8.079	8.006	8.114
$(\text{CO}_3^{2-})$ ( $10^{-4} \text{ M/kg}$ )	1.28	1.30	1.24
T (°C)	0.00	0.00	0.00
$K'_1$ ( $10^{-7}$ )	7.14	7.69	6.35
$K'_2$ ( $10^{-10}$ )	4.06	4.27	3.51
$K'_B$ ( $10^{-9}$ )	1.12	1.19	1.12
$a_{\text{H}}$ ( $10^{-8}$ )	0.647	0.685	0.586
pH	8.189	8.164	8.232
$(\text{CO}_3^{2-})$ ( $10^{-4} \text{ M/kg}$ )	1.26	1.25	1.21

used for the computation of the degree of saturation of calcite in seawater will be briefly discussed in order to depict the degree of certainty for the computed results.

#### APPARENT DISSOCIATION CONSTANTS FOR CARBONIC AND BORIC ACIDS IN SEA WATER

The apparent dissociation constants for carbonic and boric acids in sea water have been determined at 1 bar total pressure as a function of temperature and salinity by Buch and others (1932), Lyman (1957), Hansson (1973a), and Mehrbach and others (1974). The values obtained by Buch and others (1932), Lyman (1957), and other workers such as Disteché and Disteché (1967) were critically reviewed by Edmond and Gieskes (1970).

Since the concentration of  $\text{CO}_3^{2-}$  is the quantity needed for the study of the degree of saturation of carbonates in sea water, it was calculated for a given sea-water sample using various sets of the dissociation

constants in order to see the effect of those constants on the calculated value for  $\text{CO}_3^{2-}$ . Table 1 shows the results of calculation for a sea-water sample with a typical salinity, alkalinity and total carbon dioxide concentration value for the North Atlantic Deep Water, using the dissociation constants of Lyman (1957), Hansson (1973a) and Mehrbach and others (1974) respectively. Since Mehrbach and others (1974) did not determine  $K'_B$  for boric acid, Lyman's  $K'_B$  values were used for the computation. The results of calculation reveal the following facts.

1. Although the value for those three sets of  $K'_1$ ,  $K'_2$  and  $K'_B$  differ as much as 30 percent, the calculated  $\text{CO}_3^{2-}$  values differ by no more than 4 percent. However, as shown by Hansson (1973a), the concentrations of  $(\text{CO}_3^{2-})$  calculated using the dissociation constants of Buch and others (1932) are about 10 percent greater than those calculated using the constants of Hansson and of Lyman. Therefore, the constants of Buch and others (1932) will not be further considered in the present discussion.

2. The calculated values for the hydrogen ion activity, however, vary widely, as much as 30 percent. Such a variation in hydrogen ion activities may be due to the difference in the ways in which the pH of solutions was measured by those workers. Lyman (1957) standardized his electrodes in the NBS pH 4.0 buffer solution; and Mehrbach and others (1974) standardized their electrodes in the NBS pH 7.4 buffer solution and assumed the effect of temperature on the electrodes to be theoretical. On the other hand, Hansson (1973a, 1973b) used a pH scale based on a synthetic sea water:  $\text{pH (NBS)} - \text{pH (sea-water scale, } S = 35 \text{ ‰}) = 0.159$ .

3. Hence, when the alkalinity and total carbon dioxide concentration are measured and used to calculate the  $\text{CO}_3^{2-}$  concentration, the resulting  $\text{CO}_3^{2-}$  concentration (and, hence, the degree of saturation of calcium carbonate in sea water) is insensitive to the choice of those three sets of the dissociation constants. Since an uncertainty of  $\pm \frac{1}{4}$  percent in alkalinity measurements and an uncertainty of  $\pm \frac{1}{2}$  percent in total carbon dioxide concentration measurements would cause an uncertainty of  $\pm 3$  percent and  $\pm 5$  percent in the calculated  $\text{CO}_3^{2-}$  concentrations respectively, the effect of the use of different sets of dissociation constants, which cause a maximum of 4 percent variation in the calculated  $\text{CO}_3^{2-}$  concentrations, would become unimportant.

4. If the concentration of  $\text{CO}_3^{2-}$  is calculated using a measured value of  $a_{\text{H}}$  (or pH) or  $\text{pCO}_2$ , the results

would be highly sensitive to a choice of those sets of the dissociation constants.

5. Simpson and Broecker (1973) measured  $p\text{CO}_2$  exerted by sea-water samples (an Atlantic surface water sample near Bermuda Island and a Pacific deep-water sample) as a function of added KOH and boric acid, and observed that, at temperatures of 17.5°C and 25.2°C, the concentration of  $\text{CO}_3^{2-}$  calculated using their experimental data agree with those calculated from Lyman's apparent dissociation constants within approximately 3 percent. Kanwisher (1960) has experimentally determined the effect of temperature on the partial pressure of  $\text{CO}_2$  for surface ocean water to be 4.4 percent/°C, a value which agrees with that of 4.3 percent/°C calculated for the similar salinity and temperature range using Lyman's constants. The results of about 120 measurements of  $p\text{CO}_2$  for the Atlantic water samples collected at various depths agree with those calculated from the alkalinity and total  $\text{CO}_2$  data of GEOSECS using Lyman's constants (Kaiteiris, 1974). In addition to the reasons stated above, Lyman's constants are based on the NBS scale and also include  $K'_B$  [whereas Mehrbach and others (1974) did not determine  $K'_B$ ]. Hence, the apparent dissociation constants of Lyman (1957) will be used for the following discussion.

#### THE EFFECT OF PRESSURE ON THE APPARENT DISSOCIATION CONSTANTS OF CARBONIC AND BORIC ACIDS IN SEA WATER

The effect of pressure on an equilibrium constant,  $K'$ , can be expressed in terms of the difference between the partial molal volume of reactants and products,  $\Delta\bar{V}$ , using a basic thermodynamic equation:

$$K'(P)/K'(1) = \exp [-\Delta\bar{V}^*(P-1)/RT] \quad (8)$$

where  $R$  is the gas constant (e.g., 83.143 bar  $\text{cm}^3/\text{mole deg}$ );  $T$ , temperature in °K; and  $K'(P)$  and  $K'(1)$  respectively the equilibrium constant at pressures  $P$  and 1 bar.  $\Delta\bar{V}^*$  is assumed to be independent of pressure.

On the basis of the experimental data of Culberson and others (1967), Culberson and Pytkowicz (1968) and Edmond and Gieskes (1970) expressed the  $\Delta\bar{V}^*$  values for the apparent dissociation constants,  $K'_1$ ,  $K'_2$  and  $K'_B$ , as a function of temperature and judged them as the best set of the data available:

$$\begin{aligned} \Delta\bar{V}^{*1} &= -(24.2 - 0.085 t) \text{ cm}^3 \text{ for } K'_1 \\ \Delta\bar{V}^{*2} &= -(16.4 - 0.040 t) \text{ cm}^3 \text{ for } K'_2 \\ \Delta\bar{V}^{*B} &= -(27.5 - 0.095 t) \text{ cm}^3 \text{ for } K'_B \end{aligned}$$

where  $t$  = temperature in °C.

TABLE 2

The effect of the  $\Delta\bar{V}^*$  values of the  $\text{CO}_3^{2-}$  concentrations and solubility product of calcium carbonates calculated for a sea water ( $S = 35.00 \text{ ‰}$ ,  $\Sigma\text{Ca} = 1.026 \times 10^{-2} \text{ M/kg}$ ,  $\Sigma\text{A} = 2.320 \times 10^{-3} \text{ eq/kg}$ ,  $\Sigma\text{CO}_2 = 2.150 \times 10^{-3} \text{ M/kg}$ ,  $\Sigma\text{B} = 4.106 \times 10^{-4} \text{ M/kg}$ ) at 0° C and 500 bars using Lyman's apparent dissociation constants in sea water.

	P = 1 bar	P = 500 bars	
$\Delta\bar{V}^{*1}$ ( $\text{cm}^3$ )	—	-24.2 <sup>1</sup>	-19.0 <sup>2</sup>
$\Delta\bar{V}^{*2}$ ( $\text{cm}^3$ )	—	-16.4 <sup>1</sup>	-10.7 <sup>2</sup>
$\Delta\bar{V}^{*B}$ ( $\text{cm}^3$ )	—	-27.5 <sup>1</sup>	-23.1 <sup>2</sup>
$K'_1$ (P) ( $10^{-9}$ )	0.714	1.215	1.084
$K'_2$ (P) ( $10^{-10}$ )	4.057	5.816	5.132
$K'_B$ (P) ( $10^{-6}$ )	1.122	2.052	1.863
$a_B$ ( $10^{-9}$ )	6.474	10.146	9.043
pH	8.189	7.994	8.044
$(\text{CO}_3^{2-})$ ( $10^{-4} \text{ M/kg}$ )	1.257	1.157	1.146
$(\text{Ca}^{++})(\text{CO}_3^{2-})$ ( $10^{-6} \text{ M}^2/\text{kg}^2$ )	1.295	1.191	1.180

<sup>1</sup>  $\Delta\bar{V}^*$  values are from the equations listed above, and are based on Culberson and Pytkowicz (1968).

<sup>2</sup> The values are the 22° C values of Disteché and Disteché (1967).

Millero and Berner (1972) compared the values of  $\Delta\bar{V}^*$ 's obtained by Culberson and Pytkowicz (1968) and those by Disteché and Disteché (1967) ( $\Delta\bar{V}^{*1} = -19.0 \text{ cm}^3$ ,<sup>†</sup>  $\Delta\bar{V}^{*2} = -10.7 \text{ cm}^3$  and  $\Delta\bar{V}^{*B} = -23.1 \text{ cm}^3$  at 22°C for  $\text{Cl} = 20 \text{ ‰}$ ), and supported the values of Culberson and Pytkowicz (1968) on the basis of the recent direct measurements of molal volumes of  $\text{K}_2\text{CO}_3$  and  $\text{Na}_2\text{CO}_3$  by Duedall (1972).

Table 2 lists the concentrations of  $\text{CO}_3^{2-}$  and the ion concentration products calculated using the  $\Delta\bar{V}^*$  values of Culberson and Pytkowicz (1968) and Disteché and Disteché (1967). Since the latter investigators reported the  $\Delta\bar{V}^*$  values only at 22°C, their values were taken for the calculation at 0°C. The results of calculation show that, when the alkalinity and total  $\text{CO}_2$  values are known, the concentration of  $\text{CO}_3^{2-}$  and the solubility product are insensitive to the choice of the  $\Delta\bar{V}^*$  values. However, since the values of Culberson and Pytkowicz (1968) are internally consistent with the apparent dissociation constants of carbonic and boric acids of Lyman (1957), the expressions listed above for  $\Delta\bar{V}^*$ 's are used for computation of  $(\text{CO}_3^{2-})$  using the GEOSECS data.

<sup>†</sup> The superscript \* denotes the quantity in sea water, and, hence, it indicates the partial molal volume difference including simple ions and complex ion associations.

TABLE 3

Apparent solubility products,  $K'_{sp}$ , for calcite as a function of temperature. The  $\pm$  values indicate one standard deviation from the least-squares fit to the experimental data.

Experimenters	S(‰)	$K'_1$ and $K'_2$ Used	$K'_{sp}$ ( $M^2/kg^2$ ) = A + B t ( $^{\circ}C$ )	
			A ( $10^{-7} M^2/kg^2$ )	B ( $10^{-9} M^2/Kg^2/^{\circ}C$ )
Ingle and others (1973)	35.00	Mehrbach and others (1974)	$4.87 \pm 0.04$	$-1.1 \pm 0.2$
McIntyre (1965)	34.33	Mehrbach and others (1974)	$5.72 \pm 0.13$	$-3.4 \pm 0.6$
Ingle and others (1973)	35.00	Lyman (1957)	$5.61 \pm 0.04$	$-3.2 \pm 0.2$
McIntyre (1965)	34.33	Lyman (1957)	$6.62 \pm 0.13$	$-5.9 \pm 0.6$

#### SOLUBILITY OF CALCITE AND ARAGONITE IN SEA WATER AT 1 BAR PRESSURE

The solubility of calcium carbonate crystals in sea water is one of the most critical parameters needed for the calculation of the degree of saturation of calcium carbonate in sea water. Accordingly, it was studied by a number of investigators but yielded widely varying results. The results of solubility determinations at 1 bar total pressure for calcite and aragonite (Wattenberg, 1933, 1936); Wattenberg and Timmerman (1936); Smith (1941); Hindman (1942); Kramer (1958); McIntyre (1965)) were reviewed by Li and others (1969) and by Edmond and Gieskes (1970). Since the study of McIntyre (1965) is the only one which covers the temperature range of the oceanographic significance,  $0^{\circ}$  to  $40^{\circ}C$ , his results for calcite and aragonite are widely used for the interpretation of field data. More recently, Ingle and others (1973) determined the apparent solubility product of calcite for a temperature range of  $0^{\circ}$  to  $25^{\circ}C$  in a synthetic sea water of 35 ‰ S prepared according to the recipe of Kester and others (1967) with the exception that boric acid was omitted. In contrast to McIntyre's experiments, in which a small quantity of calcite crystals were equilibrated with a 1.5 liter synthetic sea-water sample, they chose to measure the pH of the interstitial water in a calcite-sea water slurry as in the saturometer of Weyl (1961). Since their  $K'_{sp}$  values are calculated using the  $K'_1$  and  $K'_2$  values determined by Mehrbach and others (1974), a new set of  $K'_{sp}$  values have been computed using Lyman's constants, so that their values can be compared with McIntyre's  $K'_{sp}$  values. The results of the computation are summarized in table 3.

Table 3 shows that, at  $0^{\circ}C$ , the  $K'_{sp}$  value of Ingle and others (1973) is about 17 percent smaller than that of McIntyre (1965), and the effect of temperature on  $K'_{sp}$  by Ingle and others (1973) is about 50 per-

cent of that by McIntyre (1965). It also shows that the scatter of the experimental data by Ingle and others (1973) is nearly one-third of that of McIntyre (1965). Thus, at  $0^{\circ}C$ , the degree of saturation of calcite in sea water,  $(CA^{++}) \cdot (CO_3^{=}) / K'_{sp}$ , calculated using the  $K'_{sp}$  values of McIntyre (1965) is about 17 percent smaller (or less saturated with respect to calcite) than that calculated using the  $K'_{sp}$  values of Ingle and others (1973). The difference is decreased at higher temperatures due to the difference in their temperature coefficients (the term B in table 3), and it becomes negligible at temperatures above  $30^{\circ}C$ . However, since the temperature of deep sea-water ranges  $0^{\circ}$  to  $2^{\circ}C$ , the difference between the solubility values of Ingle and others (1973) and McIntyre (1965) is quite significant with respect to the degree of saturation of calcite in deep oceans.

McIntyre (1965) filled the air space above the sea-water sample in the equilibration vessel with gases having  $pCO_2$  values of  $3 \times 10^{-4}$ , 0.5 or 1.0 atm. However, the equilibrium  $pCO_2$  values calculated from his pH and alkalinity data for the 24 calcite-runs charged or flushed through with 1 atm  $pCO_2$  ranged between 0.37 and 0.76 atm with the exception of two runs ( $pCO_2 = 0.95$  and  $0.86$  atm). Among the 10 calcite-runs charged with gas mixtures having  $3 \times 10^{-4}$  or 0.5 atm  $pCO_2$ , 7 runs showed a satisfactory agreement between the calculated  $pCO_2$  values and those used for the experiments. Thus, in 25 calcite solubility experiments out of 34, the gaseous phase was not in equilibrium with the aqueous phase. This suggests that at least 75 percent of his experimental data appear to be subject of systematic errors arising from disequilibrium. The degree of the disequilibrium corresponds to an average pH of 0.3, whereas the discrepancy between the  $K'_{sp}$  values of McIntyre and Ingle and others corresponds to an error in the pH values of 0.08 at  $0^{\circ}C$ . The discrepancy between the

two sets of  $K'_{sp}$  values for calcite appears to be well within the uncertainty of McIntyre's pH values resulting from the disequilibrium in his experiments. Hence, the  $K'_{sp}$  values of Ingle and others (1973) are preferred and used for the following discussion.

Edmond and Gieskes (1970) have demonstrated that the apparent solubility product of calcite is proportional to salinity (or chlorinity). Accordingly the  $K'_{sp}$  values of Ingle and others (1973) are corrected for salinity for the calculation of the degree of saturation of calcite in the oceans.

#### EFFECT OF PRESSURE ON THE APPARENT SOLUBILITY PRODUCT OF CALCIUM CARBONATE IN SEA WATER

Edmond and Gieskes (1970) and Culberson (1972) expressed the experimental data of Pytkowicz and his associates (Pytkowicz and Connors, 1964; Pytkowicz and Fowler, 1967; Pytkowicz and others 1967; Hawley and Pytkowicz, 1969) in terms of the apparent partial molal volume for the reaction in sea water,  $-\Delta\bar{V}^{\circ}$  ( $K'_{sp}$ ) in  $\text{cm}^3$ :

	Edmond and Gieskes (1970)	Culberson (1972)
Calcite	35.4 - 0.23 t ( $^{\circ}\text{C}$ )	36.0 - 0.20 t ( $^{\circ}\text{C}$ )
Aragonite	32.8 - 0.23 t ( $^{\circ}\text{C}$ )	33.3 - 0.22 t ( $^{\circ}\text{C}$ )

The apparent partial molal volume for the dissolution of calcium carbonate is defined as:

$$\Delta\bar{V}^{\circ} (K'_{sp}) = \bar{V}^{\circ} (\text{Ca}^{++}) + \bar{V}^{\circ} (\text{CO}_3^{--}) - V (\text{CaCO}_3) \quad (9)$$

where  $\bar{V}^{\circ} ( )$  denotes the apparent partial molal volume in sea water for an ionic species specified (the ion associations inclusive) within the parentheses, and  $V (\text{CaCO}_3)$  denotes the molal volume of crystalline calcium carbonate.

At  $25^{\circ}\text{C}$ , Culberson's formula yields a  $\Delta\bar{V}^{\circ} (K'_{sp})$  value for calcite of  $-30.9 \text{ cm}^3$ . If the  $\bar{V}^{\circ} (\text{CO}_3^{--})$  value of  $19.2 \text{ cm}^3/\text{mole}$  based on Duedall (1972) is accepted and a value of  $36.9 \text{ cm}^3/\text{mole}$  for  $V (\text{CaCO}_3)$  is used for calcite, then a value of  $-13.2 \text{ cm}^3/\text{mole}$  is obtained for  $\bar{V}^{\circ} (\text{Ca}^{++})$  according to equation (9). This value is about a half of  $-24.6 \text{ cm}^3/\text{mole}$  estimated by Millero and Berner (1972) for sea water, and is about two thirds of  $-20.3 \text{ cm}^3/\text{mole}$  obtained by Owen and Brinkley (1941) for a 0.725 m NaCl solution at  $25^{\circ}\text{C}$ . The latter value is based upon their original value of  $-16.6 \text{ cm}^3/\text{mole}$  for  $\bar{V} (\text{Ca}^{++}) - \bar{V} (\text{H}^+)$  in the NaCl solution and  $-3.7 \text{ cm}^3/\text{mole}$  for  $\bar{V}^{\circ} (\text{H}^+)$  of Millero

(1969) in sea water. This inconsistency indicates that either one of the values for  $\Delta\bar{V}^{\circ} (K'_{sp})$ ,  $\bar{V}^{\circ} (\text{Ca}^{++})$  and  $\bar{V}^{\circ} (\text{CO}_3^{--})$  is in error, and that the present knowledge on the effect of pressure on the apparent solubility product for calcium carbonate is far from satisfactory.

To illustrate the effect of the uncertainty in the  $\Delta\bar{V}^{\circ} (K'_{sp})$  value on the degree of saturation of calcite in sea water, it was calculated using two  $\Delta\bar{V}^{\circ}$  values for a typical Atlantic deep water. The values used are  $-36.0 \text{ cm}^3$  at  $0^{\circ}\text{C}$  from Culberson's formula and  $-42.3 \text{ cm}^3$  which was obtained for  $\bar{V}^{\circ} (\text{Ca}^{++}) = -24.6 \text{ cm}^3/\text{mole}$  of Millero and Berner (1972),  $\bar{V}^{\circ} (\text{CO}_3^{--}) = 19.2 \text{ cm}^3/\text{mole}$  of Duedall (1972). The degree of saturation of calcite in sea water is reduced by 7.1 percent at 250 bars and 14.8 percent at 500 bars when the  $\Delta\bar{V}^{\circ} (K'_{sp})$  value is changed from  $-36.0 \text{ cm}^3$  to  $-42.3 \text{ cm}^3$ . Therefore, the uncertainty in the effect of pressure would cause 15 percent uncertainty in the degree of saturation of calcite in deep oceans, whereas the uncertainty in the relative values is expected to be an order of 5 to 10 percent, which is mainly due to the uncertainties in the values for  $K'_1$ ,  $K'_2$  and  $K'_B$ , and to the experimental errors in the measurements of the alkalinity and total dissolved  $\text{CO}_2$  concentration.

#### DEGREE OF SATURATION OF CALCITE IN THE ATLANTIC AND PACIFIC OCEANS

During the GEOSECS expeditions in the Atlantic (July, 1972–April, 1973) and the Pacific (August, 1973–June, 1974) Oceans, nearly 4,000 sets of the alkalinity and total carbon dioxide concentration data were obtained by means of a computer controlled titrimetric method, which was developed by A. E. Bainbridge and M. Morrione, Scripps Institution of Oceanography. The titrimetric method is similar to that reported by Edmond (1970). The precision of most of the Atlantic GEOSECS data was estimated to be  $\pm 1/8$  percent for alkalinity and  $\pm 1/4$  percent for total dissolved carbon dioxide concentration. The accuracy of the measurements was estimated to be similar to the estimated precision. This was substantiated by the agreement of the measured  $\text{pCO}_2$  values with those calculated from the alkalinity and total  $\text{CO}_2$  values within an expected root-mean-squares deviation of  $\pm 4$  percent for about 120 test samples. On the other hand, although the precision of the alkalinity and total  $\text{CO}_2$  data for the Pacific GEOSECS is similar to that for the Atlantic data, the measured  $\text{pCO}_2$  values for the Pacific are systematically about 15 percent smaller than those calculated from the alkalinity and total  $\text{CO}_2$  data ob-

tained by the titration method. Hence, it appears that the internal consistency of the carbonate data for the Pacific Ocean is inferior to that for the Atlantic Ocean. Thus, the uncertainty for the values of the degree of saturation of calcite reported here for the Pacific Ocean is about 0.1, whereas that for the Atlantic Ocean is about 0.03. Salinity and temperature for the samples were determined with an accuracy of  $\pm 0.001$  ‰ S and  $\pm 0.001^\circ\text{C}$  respectively. These data are tabulated in the GEOSECS Preliminary Report Series prepared by the GEOSECS Operations Group, Scripps Institution of Oceanography.

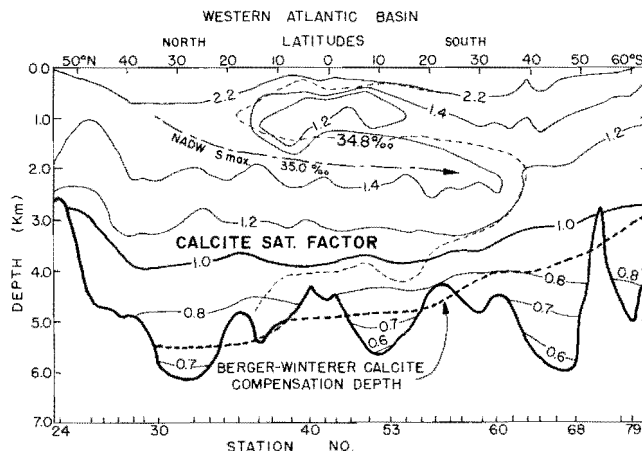
The sources of various constants used for the calculations of the degree of saturation of calcite in sea water are summarized below:

$K'_1, K'_2$ and $K'_B$	Lyman (1957; see table 1)
Effect of pressure on $K'_1, K'_2$ and $K'_B$	Culberson and Pytkowicz (1968; see p. 15)
$K'_{sp}$ for calcite at 1 bar	Ingle and others (1973; see table 3)
Effect of pressure on $K'_{sp}$ for calcite	Culberson (1972); see p. 17
	Pytkowicz and Connors; (1964)
	Pytkowicz and Fowler, (1967) Pytkowicz and others (1967), Hawley and Pytkowicz (1969)
$\Sigma\text{Ca}$	$1.026 \times 10^{-2}$ (S/35) M/kg, Carpenter (1957)
$\Sigma\text{B}$	$2.19 \times 10^{-5}$ Cl (‰) M/kg

The degree of saturation of calcite in sea water is expressed in terms of  $(\text{Ca}^{++})(\text{CO}_3^{=})/K'_{sp}$  corrected to the in situ temperature and pressure. In this paper, this ratio is called Calcite Saturation Factor or CSF, which is equivalent to  $\Omega$  used by Edmond and Gieskes (1970), Gieskes (1974), and  $\text{IP}/K'_{sp}$  used by Ben-Yaakov and Kaplan (1971) and Ben-Yaakov and others (1974a, b). The calcite saturation factors presented here are all based upon the solubility data of Ingle and others (1973) and they should be decreased by approximately 17 percent at 5,000 meters deep if the solubility data of McIntyre (1965) are used.

#### ATLANTIC OCEAN

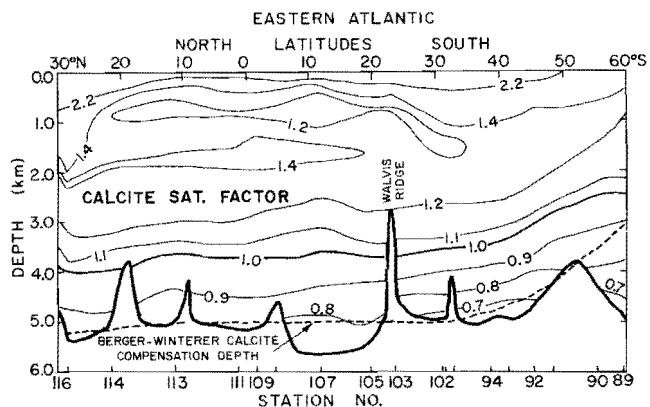
Text figures 1 and 2 show the distribution of calcite saturation factor along the North-South profiles in the western and eastern basins of the Atlantic Ocean respectively, and text figures 3 and 4 show the east-



TEXT FIGURE 1

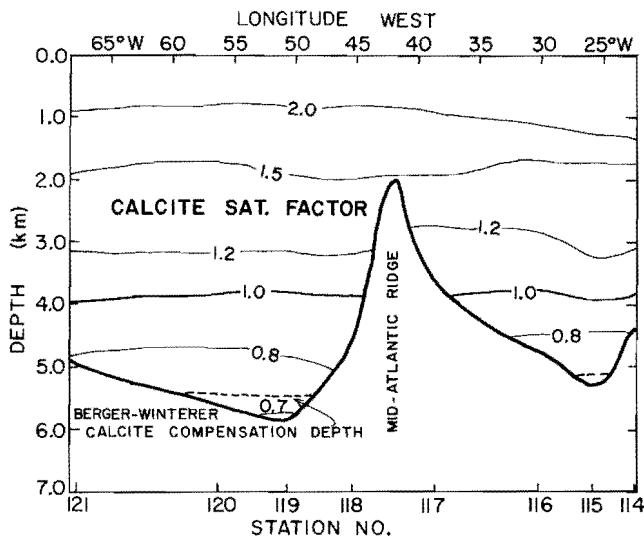
The distribution of the calcite saturation factor (CSF) in the western Atlantic Ocean along the GEOSECS tracks illustrated in text figure 5. The waters undersaturated with respect to calcite are indicated by the CSF values smaller than unity. The calcite compensation depths compiled by Berger and Winterer (1974) are also shown. A curve indicating the salinity maxima ( $S = 35.0$  ‰) is shown to show the core of the North Atlantic Deep Water.

west profiles along approximately lat  $35^\circ$  N. and long  $60^\circ$  S. respectively. The calcite compensation depths which were obtained by Berger and Winterer (1974) on the basis of the calcium carbonate contents in deep-sea sediments, are also shown in these figures. The locations of the stations in the Atlantic are shown in text figure 5.



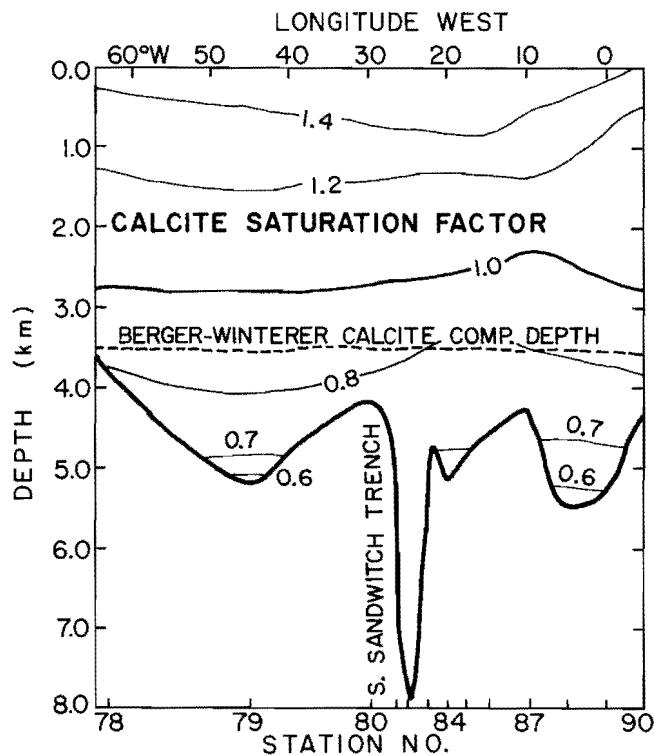
TEXT FIGURE 2

The distribution of the calcite saturation factor in the eastern Atlantic Ocean along the GEOSECS tracks illustrated in text figure 5.



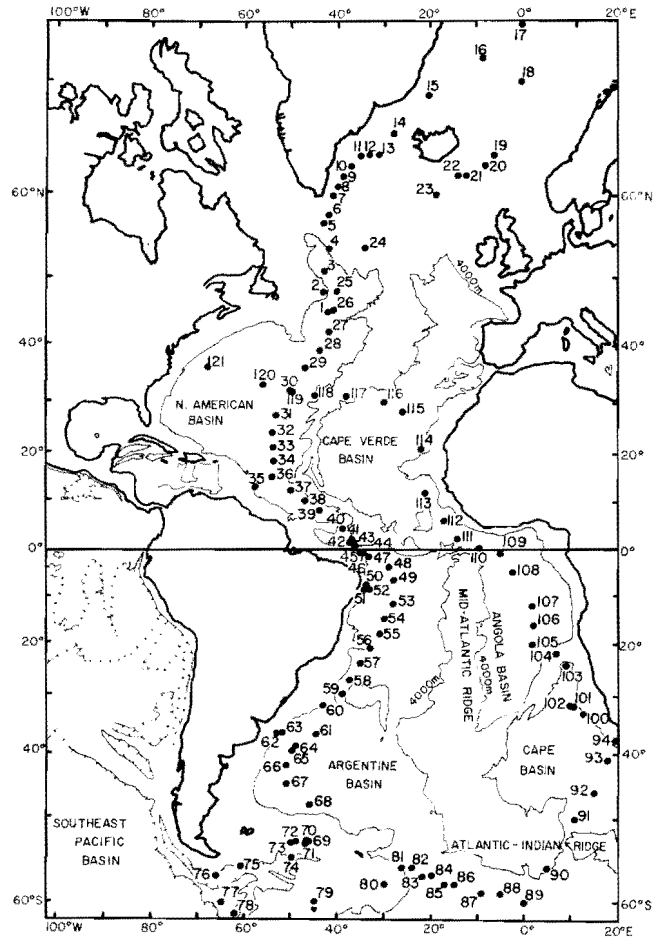
TEXT FIGURE 3

An E-W profile of the North Atlantic Ocean (stations 114 through 121) along  $\sim 35^\circ$  N latitude indicating the distribution of the calcite saturation factor in the eastern and western Atlantic basins.



TEXT FIGURE 4

An E-W profile of the southern extreme of the South Atlantic Ocean along  $\sim 60^\circ$  S latitude indicating the distribution of the calcite saturation factor and the calcite compensation depth.

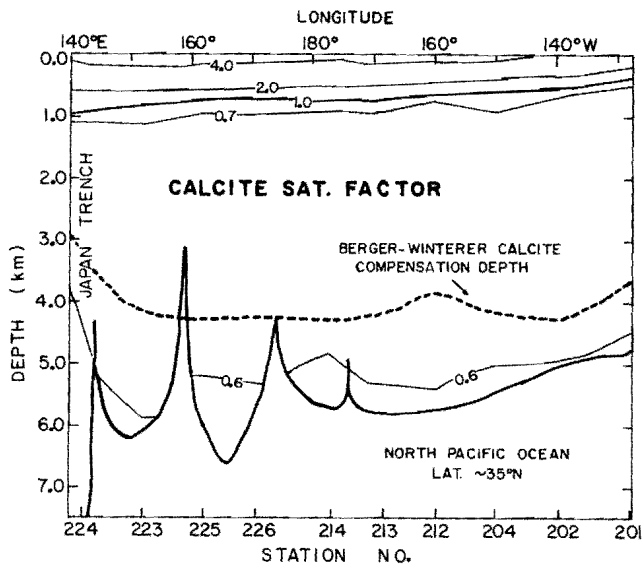


TEXT FIGURE 5

Positions of the GEOSECS Atlantic stations.

In the western Atlantic basin (text fig. 1), the waters below approximately 3,800 meters deep are undersaturated with respect to calcite ( $CSF < 1$ ) between lat  $50^\circ$  N. and  $35^\circ$  S. The saturation level ( $CSF = 1$ ) rises from about 3,500 meters deep at lat  $35^\circ$  S. to about 2,800 meters at lat  $60^\circ$  S. Such a rise in the saturation level is most likely caused by the Antarctic Circumpolar Water. The Berger-Winterer compensation level coincides with the CSF value of 0.75 (or 75 percent of saturation) between lat  $40^\circ$  N. and  $30^\circ$  S., and with the CSF value of 0.8 to 0.9 in the southern extreme of the Atlantic Ocean as shown in text figure 4.

In the eastern Atlantic basin (text fig. 2), the saturation level ( $CSF = 1$ ) is found at a depth of 3,500 to 4,000 meters between lat  $30^\circ$  N. and  $35^\circ$  S., and it rises gradually to 2,500 meters at lat  $60^\circ$  S. as in the case of



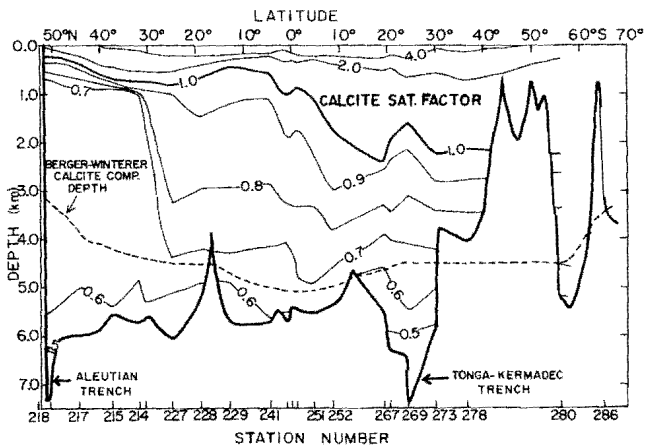
TEXT FIGURE 6

An E-W profile of the North Pacific Ocean along  $\sim 35^\circ$  N (San Diego, Calif. to Tokyo) showing the distribution of the calcite saturation factor and the calcite compensation depth.

the western Atlantic basin. The effect of the Walvis Ridge, which dams the northward flow of the Antarctic Deep Water, on the CSF is clearly seen. In the north of the Walvis Ridge, the CSF values are greater than 0.75, whereas in the south of it, the CSF values as small as 0.65 are observed. The east-west profile along  $35^\circ$  N. latitude (text fig. 3) shows virtually no significant difference in the CSF between the eastern and western basins. However, because of the greater depths of water present in the western basin along the track, the CSF values as small as 0.70 are found in the western basin, whereas the CSF values in the eastern basin remain greater than 0.7. In this profile, the calcite compensation depths coincide with the CSF level of about 0.73.

#### PACIFIC OCEAN

Text figures 7 and 6 show respectively a north-south profile of the CSF in the Pacific along longitude  $180^\circ$  between lat  $53^\circ$  N. and  $56^\circ$  S., and an east-west profile along lat  $35^\circ$  N. (San Diego to Tokyo). Text figure 7 shows that, in contrast to the Atlantic Ocean, the saturation level (CSF = 1) deepens from 200 meters at the northern extreme to about 2,200 meters at lat  $56^\circ$  S. This clearly depicts the basic difference between



TEXT FIGURE 7

A N-S profile of the North Pacific Ocean along  $\sim 180^\circ$  longitude between  $53^\circ$  N and  $56^\circ$  S showing the distribution of the calcite saturation factor and the calcite compensation depth.

the chemistry of the Atlantic and Pacific Oceans. In the Pacific, both the alkalinity and total carbon dioxide concentration are several percent greater than those in the Atlantic, and the  $\Sigma A/\Sigma CO_2$  ratios in the Pacific are smaller than those in the Atlantic. Accordingly, the Pacific water is, in general, more acidic than the Atlantic water. Other features to be noted in text figure 6 are that the CSF values decrease very slowly with depth between 1,000 and 5,500 meters north of lat  $30^\circ$  N. and that the depth for a CSF value of 0.7 increases abruptly from 1,000 meters at lat  $33^\circ$  N. to 4,500 meters at lat  $25^\circ$  N. These features are associated with the Subarctic Water mass in the northern North Pacific, which is characterized by high total  $CO_2$  values ( $\sim 2.35$  mM/kg).

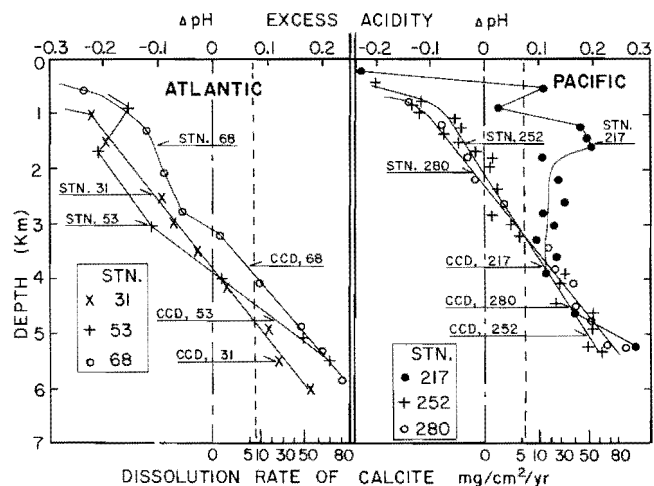
The east-west profile in the North Pacific (text fig. 6) shows that the saturation level (CSF = 1) deepens from the west at 300 meters to the east at 1,000 meters, whereas no significant trend in the distribution of CSF in the deep waters of the Pacific is observable. With the exception of the southern extreme of the Pacific, the calcite compensation depths of Berger and Winterer (1974) coincide with the CSF level of about 0.65. Although the CSF values for the calcite compensation depths in the Pacific appear to be smaller than those in the Atlantic (CSF  $\approx 0.75$ ), this difference may not be significant in view of the relatively large uncertainties in the CSF values arising from the internal inconsistencies in the Pacific data as discussed above.

RELATIONSHIP BETWEEN THE CALCITE  
COMPENSATION DEPTH AND THE DEGREE OF  
SATURATION OF CALCITE IN SEA WATER

Whether the calcite compensation depth represents the thermodynamic equilibrium boundary between super- and undersaturation of calcite in sea water or the reaction kinetic boundary has been extensively debated in the literature. In the North Pacific Ocean, the depths for calcite saturation ( $CSF = 1$ ) in sea water calculated from the GEOSECS and other sets (e.g., Wyatt and others, 1970) of data are no deeper than 1,000 meters, even when the maximum uncertainties in the calculations are assumed, whereas the calcite compensation depth lies at about 4,000 meters. Therefore, the calcite saturation level lies several thousand meters above the compensation depth, and it does not coincide with the compensation depth.

On the other hand, the results of the direct dissolution experiments for calcite by Peterson (1966) and for calcitic foraminifera shells by Berger (1967) at deep-sea moorings in the central North Pacific Ocean have demonstrated that rapid dissolution occurs at depths greater than 3,500–4,500 meters, although small amounts of dissolution were observed at depths between 200 and 3,500 meters. The calcite compensation depth in the area lies at about 4,500 meters, virtually the depth at which an abrupt increase in the dissolution rate of calcite was observed. Thus, it appears that the calcite compensation depth represents a kinetically controlled phenomenon.

Morse and Berner (1972) and Berner and Morse (1974) have demonstrated in their laboratory experiments that the rate of dissolution of calcite (both a chemical grade calcite and a calcareous deep-sea sediment sample at 25°C and one bar total pressure) increases linearly from 0 to 4 mg/cm<sup>2</sup>/yr when the sea water sample becomes more acid than the presumed equilibrium condition by 0.15 pH unit. They also observed that the rate increases abruptly by more than one order of magnitude from 4 to 55 mg/cm<sup>2</sup>/yr as the excess acidity ( $\Delta pH$ ) was increased from 0.15 to 0.24 pH unit. However, their  $\Delta pH$  values were calculated using a  $K'_{sp}$  value of  $9.5 \times 10^{-7}$  (M/kg H<sub>2</sub>O)<sup>2</sup>, which is nearly twice as large as the value of Ingle and others ( $4.74 \times 10^{-7}$  (M/kg)<sup>2</sup> at 25°C and 34.5‰ salinity), and a  $K'_2$  value of  $1.0 \times 10^{-9}$ , which is about 20 percent greater than the value of Lyman ( $0.8 \times 10^{-9}$  at 25°C and 34.5‰ salinity). Therefore, in order to make their  $\Delta pH$  values internally consistent with the degree of saturation calculations presented in this paper,



TEXT FIGURE 8

Excess acidity as a function of depth in the Atlantic and Pacific Oceans. The excess acidity,  $\Delta pH$ , is defined as the difference between the pH of the seawater at in situ temperature and pressure and that at the equilibrium of seawater with calcite. A positive value of  $\Delta pH$  indicates undersaturation, and a negative value indicates supersaturation of calcite in seawater. Three stations in each of the oceans represent the northern, equatorial and southern portions of the oceans: Stations 31 and 217 are located in the northern latitudes, Stations 53 and 252 are located in the equatorial latitudes, and Stations 68 and 280 are located in the southern latitudes. The calcite compensation depths (CCD) are those of Berger and Winterer (1974), and the dissolution rate of calcite is based on Morse and Berner (1972). For each  $\Delta pH$  profile, the rate of dissolution of calcite at a calcite compensation depth can be read from  $\Delta pH$ -depth-dissolution curve at a given calcite compensation depth.

their experimental data for a sea water sample ( $PO_4^{3-} = 1.6$  micromoles/l), which are listed in Table B (p. 133) of Berner and Morse (1974), have been used to compute new  $\Delta pH$  values using the  $K'_1$  and  $K'_2$  values of Lyman (1957) and the  $K'_{sp}$  value of Ingle and others (1973). The new  $\Delta pH$  values thus calculated are smaller than the  $\Delta pH$  values of Berner and Morse (1974) by 0.07. Accordingly, the abrupt increase in the rate of dissolution of calcite occurs at a  $\Delta pH$  of 0.08 instead of 0.15 as originally reported by Morse and Berner (1972).

Text figure 8 shows a variation of the excess acidity,  $\Delta pH$ , as a function of the depths at three stations located in the northern, equatorial, and southern portions of the Atlantic and Pacific Oceans. The  $\Delta pH$  value is the difference between the pH value for the calcite-sea water equilibrium and that of sea water calculated from the alkalinity and total  $CO_2$  data at in

situ pressure and temperature conditions. The former is based on the calcite solubility product of Ingle and others (1973). A negative value of  $\Delta\text{pH}$  represents that the sea water is supersaturated with respect to calcite, and a positive value represents undersaturation. Also shown in the figure are the calcite compensation depths (CCD) reported by Berger and Winterer (1974), and the dissolution rates of calcite, which are based on the data of Berner and Morse (1974), and the revised  $\Delta\text{pH}$  scale. The dissolution rates for the Atlantic and Pacific profiles correspond respectively to the  $\text{PO}_4^-$  concentrations of 1.6 and 2.2 micromoles/l. The dashed vertical straight line at 0.08  $\Delta\text{pH}$  indicates the  $\Delta\text{pH}$  value, at which the rate of dissolution increases abruptly with increasing  $\Delta\text{pH}$ .

In the Atlantic, the calcite compensation depths at the three stations (Station 31 at lat  $27^\circ$  N.; Station 53 at lat  $12^\circ$  S.; and Station 68 at lat  $49^\circ$  S. in the western basin) occur at  $\Delta\text{pH}$  values of 0.07 at Station 68, 0.11 at Station 53 and 0.14 at Station 31. The precision for those  $\Delta\text{pH}$  values has been estimated to be  $\pm 0.01$ , which is due mainly to the experimental errors in the measurements of the alkalinity and total  $\text{CO}_2$ . However, the accuracy of the  $\Delta\text{pH}$  values should be  $\pm 0.03$  due to the uncertainty in the effect of pressure on the solubility product of calcite. In text figure 8, it is observed that the calcite compensation depths at three stations occur nearly at a same  $\Delta\text{pH}$  value of 0.08. The observed displacements of three profiles, particularly below 4 km deep, are due most likely to the differences in the chemistry of the North Atlantic and Antarctic Deep Water masses, Station 31 profile representing the former and Station 68 profile representing the latter. The rates of dissolution corresponding to those  $\Delta\text{pH}$  values at the respective calcite compensation depths range between  $5 \pm 3$  and  $20 \pm 10$   $\text{mg}/\text{cm}^2$  sea floor/yr, assuming that one  $\text{cm}^2$  of calcite surface is available for dissolution over one  $\text{cm}^2$  of sea floor (see appendix 1).

In the study of the material balance, Li and others (1969) estimated that the average biological production of calcium carbonate in the surface water of the Atlantic and Pacific Oceans is approximately  $2 \text{ mg}/\text{cm}^2/\text{yr}$ . On the basis of their deep-sea sediment study, Biscaye and others (1972) determined that the calcite sedimentation rate in high productivity areas in the Atlantic during the past 17,000 years is approximately  $4 \text{ mg}/\text{cm}^2/\text{yr}$ . Although the uncertainties in the rates of dissolution estimated from the chemical data are too great to permit a quantitative statement, it appears that, at a calcite compensation depth, the rate of sedimentation of calcite

is equal to or is exceeded by the rate of dissolution of calcite estimated on the basis of the laboratory experiments of Berner and Morse (1974). Thus, the thermodynamic and kinetic data for the calcite-sea water system appear to be consistent with the definition of the calcite compensation depth—a depth at which the rate of calcite dissolution exceeds the rate of sedimentation of calcite.

In the Pacific Ocean, the excess acidity increases almost linearly below a depth of 1 km at Stations 252 (lat  $8^\circ$  S.) and 280 (lat  $56^\circ$  S.), whereas it is nearly constant at a  $\Delta\text{pH}$  of 0.12 between the depths of 2 and 4 km at Station 217 (lat  $45^\circ$  N.) in the northern North Pacific. The large  $\Delta\text{pH}$  values observed in the intermediate depths of 1 to 4 km are due to high total  $\text{CO}_2$  concentrations, and can be correlated with the Subarctic Water mass. Unlike the Atlantic Ocean, the  $\Delta\text{pH}$ -depth profiles for those three stations are similar at depths greater than 4 km. This may be a reflection of the more homogeneous nature of the deep water of the Pacific, in which the deep water is mainly generated in its southern extreme alone rather than in the northern and southern extremes as in the case of the Atlantic. The dissolution rate for calcite estimated at the calcite compensation depths in the Pacific range between 15 and  $50 \text{ mg}/\text{cm}^2/\text{yr}$ , and are unrealistically large compared to the sedimentation rate of calcite on deep sea floors. This may be attributed to a systematic error in the measurements of the alkalinity and/or the total  $\text{CO}_2$  concentration. As mentioned earlier, the alkalinity and total  $\text{CO}_2$  data obtained in the Pacific yield  $\text{pCO}_2$  values which are consistently 15 percent greater than those measured. If the alkalinity/total  $\text{CO}_2$  ratio is adjusted to yield a  $\text{pCO}_2$  value consistent with the measured one, a  $\Delta\text{pH}$  value of 0.06 smaller than those plotted in text figure 8 is obtained. Therefore, the  $\Delta\text{pH}$  values computed for the Pacific may be too large by as much as 0.06. Accordingly, if a correction of 0.06  $\Delta\text{pH}$  is applied to the Pacific profiles in text figure 8, the dissolution rates of calcite at the calcite compensation depth are estimated to range between  $3 \pm 2 \text{ mg}/\text{cm}^2/\text{yr}$  at Station 217 (lat  $44^\circ$  N.) and  $20 \pm 10 \text{ mg}/\text{cm}^2/\text{yr}$  at Station 252 (lat  $8^\circ$  S.). The highest rate of dissolution is estimated at the equatorial station, even after such a systematic correction has been applied. Considering those uncertainties, it appears that the rate of dissolution estimated at the calcite compensation depths are consistent with the biological calcite productivity of the oceans and the calcite sedimentation rates. However, it must be noted that the rates of calcite dissolution estimated above are based upon the laboratory

experiments, in which the stirring environments and the surface conditions of the calcite particles are different from the oceanographic environment near the sediment-water interface. When the water is strongly turbulent causing the surface of calcite particles to be free of non-calcareous substances, or when the rate of calcite deposition is far greater than that of noncalcareous particles, the rates of calcite dissolution on the ocean floor should be nearly the same as those determined in the laboratory at a given  $\Delta\text{pH}$ . On the other hand, when the rate of calcite deposition is much slower than the rate of deposition of noncalcareous sediments or when the surfaces of calcite particles are coated with organic matter, the rate of dissolution of calcite on the ocean floor is expected to be slower than that for the laboratory experiments at a given  $\Delta\text{pH}$ . Admittedly, the effects of various sedimentary conditions on the dissolution rate of calcite are difficult to characterize quantitatively. However, the information presented above appears to point out that the degree of undersaturation of calcite in sea water, the rate of dissolution of calcite in sea water, and the sedimentation rate of calcite are three major factors that control the calcite compensation depth in the oceans. Since the dissolution rate of calcite increases drastically when the excess acidity ( $\Delta\text{pH}$ ) exceeds 0.08, a sharp boundary between the calcareous and noncalcareous sediments is expected in the area where the calcite sedimentation rate is high and hence the  $\Delta\text{pH}$  value at calcite compensation depths is large. This question is currently being studied in order to further test the adequacy of the interpretation presented above.

#### COMPARISON BETWEEN THE RESULTS OF GEOSECS AND OTHER STUDIES

Edmond and Gieskes (1970) reported the alkalinity and total dissolved carbon dioxide values obtained in the Brazil Basin in the equatorial Atlantic Ocean Circe 9 Cruise, Station 245, lat  $7^{\circ} 9' \text{ S}$ , long  $21^{\circ} 21' \text{ W}$ .) and calculated the degree of saturation of calcite in sea water using constants similar to those used in this paper with an exception of using McIntyre's solubility data for calcite. When their data are recalculated using the solubility data of Ingle and others (1973) for calcite, their data yield a saturation depth (where  $\text{CSF} = \Omega = 1.0$ ) of 3,800 meters and a CSF value of 0.57 at 5,385 meters. These values are in excellent agreement with the values reported in this paper.

Culberson (1972) calculated the degree of saturation of calcite in the North Pacific (lat  $38^{\circ} 00' \text{ N}$ ., long  $124^{\circ} 45' \text{ W}$ .) using the alkalinity and pH data re-

ported by Wyatt and others (1970) and the calcite solubility data of McIntyre (1965). When their data are used to calculate the CSF values using the calcite solubility data of Ingle and others (1973), the data of Wyatt and others yield a CSF value of 1.0 and 0.68 respectively at 300 meters and 3,928 meters (the deepest sample obtained at this station). These recalculated values are in agreement with the results of the present paper and within the uncertainty of the data used.

Li and others (1969) calculated the degree of saturation of calcite in the Atlantic and Pacific Oceans based upon their measurements of  $\text{pCO}_2$  and total  $\text{CO}_2$  and the solubility data of McIntyre (1965) for calcite. In addition, the pressure dependence for the dissociation constants used for their study is substantially different from those used in this paper. Therefore, their CSF values cannot be directly compared with those in this paper. A subsequent investigation conducted by R. F. Weiss (Takahashi and others, 1970) has shown that the total  $\text{CO}_2$  values reported in Li and others (1969) are 2 to 3 percent too high, perhaps due to the biological contamination during sample storage. When this correction is applied the total  $\text{CO}_2$  data of Li and others (1969) are in agreement with the GEOSECS data. The  $\text{pCO}_2$  data of Li and others (1969) are consistent with those obtained during GEOSECS in the Atlantic and Pacific Oceans.

Ben-Yaakov and others (1974a, 1974b) reported the results of their deep-sea saturometer measurements obtained at 13 stations (lat  $32^{\circ} 31' - 33^{\circ} 56' \text{ N}$ . and long  $118^{\circ} 42' - 121^{\circ} 47' \text{ W}$ .) located 180 miles west of San Diego, California, and at 2 stations located 500 miles northeast and 300 miles east of Oahu Island, Hawaii. At the two Hawaiian stations they observed that the degree of saturation of calcite in sea water is nearly constant at 0.95 between 1,200 and 4,000 meters and it decreases linearly with depth from 0.93 at 4,000 meters to 0.77 at 5,300 meters. Their values are based upon the calcite solubility data of McIntyre (1965), and if the solubility data of Ingle and others (1973) are used, their calcite saturation values of 0.93 and 0.77 correspond to the CSF values of 1.1 and 0.92 respectively. At GEOSECS Station 204 (lat  $31^{\circ} \text{ N}$ ., long  $150^{\circ} \text{ W}$ .) which is located at about 250 miles northeast of their Station 11, the CSF values are 0.71 and 0.55 respectively at 3,890 and 5,225 meters. Hence, the saturometer values of Ben-Yaakov and others (1974b) are 0.4 greater than the values of the present study. Similar discrepancy between the results of saturometer measurements at stations off San Diego

and those of GEOSECS Station 201 (lat 34° N., long 128° W.) and YALOC-69 (Culberson, 1972) are found. The causes for those discrepancies are currently being investigated.

#### SUMMARY AND CONCLUSIONS

1. When the alkalinity and total dissolved carbon dioxide concentration in sea water are determined and used to calculate the concentration of the total  $\text{CO}_3^{=}$  species, the result is insensitive to the choice of the apparent dissociation constants, and the effect of pressure on those constants.
2. The apparent solubility product of calcite in sea water at 1 bar total pressure determined by McIntyre (1965) is about 17 percent greater than that by Ingle and others (1973) at the oceanographically significant temperature range of 0 to 5°C. Because of possible disequilibrium conditions in McIntyre's experiments, the solubility data of Ingle and others (1973) for calcite are preferred, and were used for the present study.
3. As previously pointed out by Millero and Berner (1972), an inconsistency of an order of 10  $\text{cm}^3/\text{mole}$  in the partial molal volumes for  $\text{CO}_3^{=}$  and/or  $\text{Ca}^{++}$  exists. Thus, the uncertainties in the effect of pressure on the solubility product of calcite in sea water would cause an uncertainty of 15 percent (at 5,000 meters) in the calculated degree of saturation.
4. The calcite saturation factor in the Atlantic and Pacific Oceans was computed using about 4,000 sets of the alkalinity and total carbon dioxide data of GEOSECS, using Lyman's apparent dissociation constants for carbonic and boric acids, and other selected values for the effect of pressure and temperature on those constants. The calcite compensation depth of Berger and Winterer (1974) appears to coincide with the CSF level of 0.75 in the Atlantic and 0.65 in the Pacific. The rate of calcite dissolution at the calcite compensation depth was estimated from the excess acidity in the oceans and the calcite dissolution rate determined by Morse and Berner (1972) in the laboratory. The dissolution rates for calcite thus estimated at the calcite compensation depths in the Atlantic and Pacific Oceans appear to be consistent with the rates of sedimentation of calcitic shells on the deep sea floor. Therefore, the calcite compensation depth in the oceans appear to be controlled by the rate of calcite sedimentation and the degree of undersatura-

tion of calcite in ocean water, which is, in turn, a major factor for regulating the rate of dissolution of calcite.

5. Additional studies on (a) the apparent solubility of calcite in sea water, (b) the effect of pressure and temperature on the solubility of calcite, (c) the effect of pressure and temperature on the dissolution kinetics of calcite in sea water, and (d) simultaneous measurements of the chemical parameters (such as alkalinity and the total carbon dioxide concentrations) and the degree of saturation by a deep-sea saturometer would be fruitful for answering the century old enigma of the relationship between the water chemistry and the calcite compensation depth.

#### ACKNOWLEDGMENTS

The author is deeply grateful to W. S. Broecker for stimulating and constructive discussions on land and at sea. He is grateful to A. E. Bainbridge for his most ingenious design and construction of the shipboard titrimetric system, without which the acquisition of a large number of high precision alkalinity and total  $\text{CO}_2$  data would have been impossible. Mike Morrione, Ed Slater, David Boss, Don Lingle, and Ann Gilbert of the GEOSECS Operation Group at the Scripps Institution of Oceanography worked long hours on board ship to make the titration measurements. Assistance of Jack Spiegelberg, Arnold Mantyla, Robert Williams, J. Scott Weaver, Linda Prince, Peter Kaiteris, and Mark Nodell in various stages of this study is gratefully acknowledged. The author has benefited from discussions with Allan Bé regarding the condition of foraminiferal shells in deep sea sediments.

The present work has been supported by the grants from the International Decade of Ocean Exploration Program of the National Science Foundation, NSF GX-33293 and NSF GX-33293A#1 to Queens College, City University of New York and GX-28162 to GEOSECS Operations Group, Scripps Institution of Oceanography.

#### REFERENCES

- Bé, A. W. H., HARRISON, S. M., and LOTT, L., 1973, *Orbulina universa d'Orbigny* in the Indian Ocean: Micropaleontology, v. 19, 150-192.
- Bé, A. W. H., MORSE, J. W., and HARRISON, S. M., 1975, Progressive dissolution and ultrastructural breakdown of planktonic foraminifera in Sliter, W. V., Bé, A. W. H., and Berger, W. H., eds., Dissolution of deep-sea carbonates:

- Cushman Found. Foram. Research Spec. Pub. No. 13, p. 27-55.
- BEN-YAAKOV, S., and KAPLAN, I. R., 1971, Deep sea *in situ* calcium carbonate saturometry: *Jour. Geophys. Research*, v. 76, p. 722-731.
- BEN-YAAKOV, S., RUTH, E., and KAPLAN, I. R., 1974a, Calcium carbonate saturation in northeastern Pacific: *in situ* determination and geochemical implications: *Deep-Sea Research*, v. 21.
- , 1974b, Carbonate compensation depth: relation to carbonate solubility in ocean waters: *Science*, v. 184, p. 982-984.
- BERNER, R. A., and MORSE, J. W., 1974, Dissolution kinetics of calcium carbonate in sea water IV. Theory of calcite dissolution: *Am. Jour. Sci.*, v. 274, p. 108-134.
- BERGER, W. H., 1967, Foraminiferal Ooze: Solution at Depths: *Science*, v. 156, p. 383-385.
- BERGER, W. H., and WINTERER, E. L., 1974, Plate stratigraphy and the fluctuating carbonate line, *in* Hsu, K. J., and Jenkins, H., eds., *Pelagic sediments on land and in the oceans*: *Internat. Assoc. Sedimentologists Spec. Pub. 1*.
- BISCAYE, P., BÉ, A., ELLIS, D., GARDNER, J., KELLOG, T., MCINTYRE, A., PRELL, W., ROCHE, M., and VENKATARATHNAM, K., 1972, Holocene vs. glacial (17,000 yrs. B. P.) patterns of sedimentation in the Atlantic Ocean: *Geol. Soc. America 1973 Ann. Mtg. Abstracts*, v. 5, no. 7, p. 551.
- BUCH, K., HARVEY, H. W., WATTENBERG, H., and GRIPENBERG, S., 1932, Über der Kohlensäuresystem in Meerwasser: *Rapp. Proc. Verb. C.P.I.E.M.*, v. 79, p. 1-70.
- CARPENTER, J. H., 1957, The determination of calcium in natural waters: *Limnology and Oceanography*, v. 2, p. 271-280.
- CULBERSON, C., KESTER, D. R., and PYTKOWICZ, R. M., 1967, High pressure dissociation of carbonic and boric acids in seawater: *Science*, v. 157, p. 59-61.
- CULBERSON, C. H., and PYTKOWICZ, R. M., 1968, Effect of pressure on carbonic acid, boric acid and the pH in sea water: *Limnology and Oceanography*, v. 13, p. 403-417.
- CULBERSON, C. H., 1972, Processes affecting the oceanic distribution of carbon dioxide: Ph.D. dissertation, Oregon State Univ., 178 p.
- DISTECHE, A., and DISTECHE, S., 1967, The effect of pressure on the dissociation of carbonic acid from measurements with buffered glass electrode cells: *Journal Electrochem. Soc.*, v. 114, p. 330-340.
- DUEDALL, I. W., 1972, The partial molal volume of calcium carbonate in seawater: *Geochim. et Cosmochim. Acta*, v. 36, p. 729-734.
- EDMOND, J. M., 1970, High precision determination of titration alkalinity and total carbon dioxide content of sea water by potentiometric titration: *Deep-Sea Research*, v. 17, p. 737-750.
- EDMOND, J. M., and GIESKES, J. M., 1970, On the calculation of the degree of saturation of sea water with respect to calcium carbonate under *in situ* conditions: *Geochim. et Cosmochim. Acta*, v. 34, p. 1261-1291.
- GARRELS, R. M., and CHRIST, C. L., *Solutions, minerals and equilibria*: New York, Harper and Row, 450 p.
- GIESKES, J. M., 1974, The alkalinity-total carbon dioxide system, *in* Goldberg, E. D., ed., *The Sea*: New York, John Wiley and Sons, v. 5, p. 123-151.
- HANSSON, I., 1973a, A new set of acidity constants for carbonic acid and boric acid in sea water: *Deep-Sea Research*, v. 20, p. 461-478.
- , 1973b, A new set of pH-scales and standard buffers for seawater: *Deep-Sea Research*, v. 20, p. 479-491.
- HAWLEY, J., and PYTKOWICZ, R. M., 1969, Solubility of calcium carbonate in sea water at high pressures and 2°C: *Geochim. et Cosmochim. Acta*, v. 33, p. 1557-1561.
- HINDMAN, J. C., 1942, Properties of the system CaCO<sub>3</sub>-CO<sub>2</sub>-H<sub>2</sub>O in sea water and NaCl solutions: Ph.D. dissertation, Univ. California at Los Angeles.
- INGLE, S. E., CULBERSON, C. H., HAWLEY, J. E., and PYTKOWICZ, R. M., 1973, The solubility of calcite in sea water at atmospheric pressure and 35 ‰ salinity: *Marine Chem.*, v. 1, p. 295-307.
- KAITERIS, P., 1974, Internal consistency of the GEOSECS Atlantic carbonate data and the evaluation of dissociation constants of carbonic acid in sea water: M.S. Thesis, Queens College, City College of New York, 55 p.
- KANWISHER, J., 1960, pCO<sub>2</sub> in seawater and its effect on the movement of CO<sub>2</sub> in nature: *Tellus*, v. 12, p. 209-215.
- KESTER, D. R., DUEDALL, I. W., CONNORS, D. N., and PYTKOWICZ, R. M., 1967, Preparation of artificial seawater: *Limnology and Oceanography*, v. 12, p. 176-179.
- KRAMER, J. R., 1958, Study on calcite and dolomite in sea water (abs.): *Geol. Soc. America, Bull.*, v. 69, p. 160.
- LI, Y-H, TAKAHASHI, T., and BROECKER, W. S., 1969, Degree of saturation of CaCO<sub>3</sub> in the oceans: *Jour. Geophys. Research*, v. 74, p. 5507-5525.
- LYMAN, J., 1957, Buffer mechanism of sea water: Ph.D. dissertation, Univ. California at Los Angeles, 196 p.
- MCINTYRE, W. G., 1965, The temperature variation of the solubility product of calcium carbonate in sea water: *Fisheries Res. Board Canada Manuscript Rept. Series*, v. 200, 153 p.
- MEHRBACH, C., CULBERSON, C. H., HAWLEY, J. E., and PYTKOWICZ, R. M., 1974, Measurement of the apparent dissociation constants of carbonic acid in seawater at atmospheric pressure: *Limnology and Oceanography*, v. 19.
- MILLERO, F. J., 1969, The partial molal volumes of ions in seawater: *Limnology and Oceanography*, v. 14, p. 376-385.
- MILLERO, F. J., and BERNER, R. A., 1972, Effect of pressure on carbonate equilibria in seawater: *Geochim. et Cosmochim. Acta*, v. 36, p. 92-98.
- MORSE, J. W., and BERNER, R. A., 1972, Dissolution kinetics of calcium carbonate in sea water: II. A kinetic origin for the lysocline: *Am. Jour. Sci.*, v. 272, p. 840-851.
- OWEN, B. B. and BRINKLEY, S. R., JR., 1941, Calculation of the effect of pressure upon ionic equilibria in pure water and in salt solutions: *Chem. Rev.*, v. 29, p. 461-474.
- PETERSON, M. N. A., 1966, Calcite: Rates of dissolution in a vertical profile in the central Pacific: *Science*, v. 154, p. 1542-1544.
- PYTKOWICZ, R. M., and CONNORS, V. N., 1964, High pressure solubility of CaCO<sub>3</sub> in sea water: *Science*, v. 144, p. 840-841.

- PYTKOWICZ, R. M., DISTECHE, A., and DISTECHE, S., 1967, Calcium carbonate solubility in seawater at *in situ* pressures: Earth & Planetary Sci. Letters, v. 2, p. 430-432.
- PYTKOWICZ, R. M. and FOWLER, G. A., 1967, Solubility of foraminifera in sea water at high pressures: Geochem. Jour., v. 1, p. 169-182.
- SIMPSON, H. J. and BROECKER, W. S., 1973, A new method for determining the total carbonate ion concentration in saline waters: Limnology and Oceanography, v. 18, p. 426-440.
- SMITH, C. L., 1941, The solubility of calcium carbonate in tropical sea water: Marine Biol. Assoc. United Kingdom Jour., v. 25, p. 235-242.
- TAKAHASHI, T., WEISS, R. F., CULBERSON, C. H., EDMOND, J. M., HAMMOND, D. E., WONG, C. S., LI, Y-H. and BAINBRIDGE, A. E., 1970, A carbonate chemistry profile at the 1969 GEOSECS intercalibration station in the eastern Pacific Ocean: Jour. Geophys. Research, v. 75, p. 7648-7666.
- WATTENBERG, H., 1933, Über die Titrationsalkalinität und den Kalziunikarbonatgehalt des Meerwassers, Deutsche Atlantische Exped., Meteor 1925-1927, Wiss. Ergeb., v. 8 (2), p. 122-231.
- , 1936, Kohlensäure und Kalzium karbonat im Meer: Fortschr. Mineralogie, v. 20, p. 168-195.
- WATTENBERG, H., and TIMMERMAN, E., 1936, Über die Sättigung des Seewassers an  $\text{CaCO}_3$ , und die anorganogene Bildung von Kalksedimenten: Ann. Hydrograph. Mar. Meteorol., p. 23-31.
- WEYL, P. K., 1961, The carbonate saturometer: Jour. Geology, v. 69, p. 32-43.
- WYATT, B., GILBERT, W., GORDON, L., and BASTROW, D., 1970, Hydrographic data from Oregon waters, 1969: Oregon State Univ., Dept. Oceanography, Data Rept., 155 p.

## APPENDIX 1

### RELATIONSHIP BETWEEN THE CALCITE DISSOLUTION RATES MEASURED IN THE LABORATORY AND IN THE OCEANS

The rate of dissolution of calcite determined by Morse and Berner (1972) in their laboratory experiments is expressed in a unit of  $\text{mg CaCO}_3/\text{cm}^2/\text{yr}$ , in which "cm<sup>2</sup>" refers to the surface area of calcite grains. The rate of dissolution of calcite on the ocean floor is similarly expressed in a unit of  $\text{mg CaCO}_3/\text{cm}^2/\text{yr}$ . However, in contrast to the former case, "cm<sup>2</sup>" refers to the area of the ocean floor. Therefore, in order to apply the laboratory dissolution data of Morse and Berner

(1972) to a study of dissolution rates at ocean floor, a conversion factor is needed.

Although foraminiferal tests grow in a variety of sizes, shapes, and structures, and with or without the spines (e.g., Bé and others, 1973), the shells deposited on the deep ocean floor may be approximated by an array of hemispheres of equal dimension, each having a surface area of  $4\pi r^2/2$ , where  $r$  is the radius of a hemisphere. It is assumed that the lower half of a sphere is buried in sediments and only the upper half of a sphere (hemisphere) is exposed to the overlying sea water for dissolution. If these hemispheres are arranged in a hexagonal-close-packed configuration on a  $1 \text{ cm}^2$  area of ocean floor, the total number of the hemispherical shells of a radius  $r \text{ cm}$  is  $(\frac{1}{4}r^2 \sin 60^\circ =) \frac{1}{2}\sqrt{3} r^2$ . Hence, the total surface area of the hemispherical shells exposed to the overlying sea water over  $1 \text{ cm}^2$  ocean floor area is independent of the size of the hemispheres and is  $1.8 \text{ cm}^2$ . If those shells are broken to smooth platy pieces and cover the ocean floor completely exposing only the upper surface to the overlying sea water, then the surface area of calcite crystals available for reaction with sea water would be close to  $1 \text{ cm}^2$  per  $\text{cm}^2$  of ocean floor area. On the other hand, the sediments which occur near the calcite compensation depth contain less than 10 percent calcite, and, therefore, the surface area of calcite crystals directly in contact with the sea water may be much smaller than  $1 \text{ cm}^2$  per  $\text{cm}^2$  of ocean floor due to the deposition of noncalcareous matter onto the surface of calcitic shells to hinder the dissolution reaction. However, as shown by Bé and others (1974), foraminiferal shells break down to highly porous fragments in advanced stages of dissolution, and, therefore, the surface area of calcite crystals available for dissolution would be increased to counteract against the decrease of calcite contents in sediments and the masking effect of noncalcareous sediments.

The discussion presented above demonstrates the difficulties in pinpointing a single value for the conversion factor applicable to the entire oceanic areas. Since the conditions of the sediment-water interface change with time and space due to varying degree of the turbulence of deep ocean water, it is not possible to estimate a conversion factor applicable to specific areas, unless the *in situ* conditions of the interface and the states of calcitic shells are well characterized, and documented with time. Meanwhile, in the absence of such data, a time-space average of the conversion factor has been assumed to be  $1 \text{ cm}^2$  calcite surface area per  $\text{cm}^2$  of ocean floor area, and used for the present paper. The interpretation of the data presented in this paper is accordingly subject of the verification of the conversion factor used.

# PROGRESSIVE DISSOLUTION AND ULTRASTRUCTURAL BREAKDOWN OF PLANKTONIC FORAMINIFERA

ALLAN W. H. BÉ\*, JOHN W. MORSE\*\* AND STANLEY M. HARRISON\*

---

## ABSTRACT

Progressive structural breakdown of planktonic foraminiferal shells was obtained by three types of laboratory dissolution experiments. First, individual specimens of *Globorotalia truncatulinoides* and *Orbulina universa* were dissolved in sea water baths at a pH of 6.5. Percent dissolution, determined by weight loss, ranged from a few percent to 83 percent. Second, a single specimen of *G. truncatulinoides* and a suite of specimens of *Pulleniatina obliquiloculata* were subjected to repeated exposures in an acetic acid bath at a pH of 6. Third, four aliquots of a death assemblage of planktonic foraminifera were dissolved to varying degrees in the pH-stat of Morse (1974) at a pH of 7.53 at 5°C. Changes in the species composition were noted with increasing dissolution. The sequential breakdown of shell ultrastructures in each experiment was observed in a scanning electron microscope. For *G. truncatulinoides*, this breakdown was similar in each experimental method and closely resembles those occurring in nature.

Tests were carried out to determine specimen orientation during laboratory dissolution. It was observed that

*G. truncatulinoides* assumed a preferred spiral-side resting position after being stirred in a cylindrical container. In some of our experiments this preferred orientation determined the final shell morphology by selectively exposing certain parts of the shell to dissolution.

Natural species assemblages from four surface sediment samples of various depths in the west-central North Atlantic reflected changes in species composition caused by natural dissolution. However, the trends of relative resistance to dissolution of individual species in these natural assemblages showed only minor agreement with the trends of species dissolved in the laboratory.

The effects of natural dissolution was studied for *Pulleniatina obliquiloculata*, because this species is highly dissolution-resistant and possesses a relatively homogeneous surface texture (cortex) in the adult stage. This species is potentially useful as an indicator of the degree of dissolution of planktonic foraminiferal assemblages on the sea floor.

---

## INTRODUCTION

The dissolution of biogenous CaCO<sub>3</sub> on the deep-sea bed is an important geochemical process that is being investigated at an increasing tempo in recent years. Most organically derived CaCO<sub>3</sub> is secreted by cocco-

lithophorids and planktonic foraminifera, Pteropoda and Heteropoda in euphotic waters. This vast calcareous debris from the plankton is lost to the ocean floor unless it is recycled to the ocean reservoir. Such recycling does indeed occur as varying amounts find their way back into the ocean through the dissolution of the calcareous skeletons.

Since planktonic foraminifera and other calcareous plankton play a vital role in interpreting paleoclimatic and paleoecological conditions, we need to understand

---

\* Lamont-Doherty Geological Observatory, Palisades, New York 10964.

\*\* Department of Oceanography, Florida State University, Tallahassee, Florida 32306.

the rules governing their dissolution and the extent they are removed from the fossil record. We already know that this dissolution process affects different groups and different species at varying rates. For example, the aragonitic shells of pteropods and heteropods are much less resistant to dissolution than skeletons made of calcite. Moreover, the general consensus is that the calcitic shells of planktonic foraminifera are more readily dissolved than the calcitic placoliths of coccolithophorids (Hay, 1970, p. 669–672). Even among the planktonic foraminifera, there is ample evidence that different species resist corrosion to different extents (Ruddiman and Heezen, 1967; Berger, 1968).

Presently there are two approaches to the measurement of calcium carbonate dissolution in deep-sea sediments. The first method is based on the determination of weight percent calcium carbonate in the sediment. The second method is based on the relative species abundance of planktonic foraminifera and their relative resistance to dissolution (Berger, 1970). These two methods have several common aspects. Both require a region of sufficient topographic relief so that samples can be obtained from a wide depth range. Samples from relatively shallow depths are assumed to have undergone little or no dissolution and are used as a base for comparison of samples from greater depths. There also must be evidence that other factors such as the non-calcium carbonate sedimentation rate, surface productivity and species composition are constant over the region being investigated. As a result of these restrictions, neither of these methods can be applied to large areas of the deep sea or to single cores.

One of the primary aims of this paper is to test the feasibility of developing a third approach to the calcium carbonate dissolution problem. The basis of this approach is the idea that it may be possible to quantify the amount of dissolution an individual shell has undergone from an examination of its surface morphology. If this can be done, the following step would be the dissolution, to various extents, of a group of shells from the same species. Next, the statistical distribution of the degree of dissolution of individual shells would be determined of species from the “poorly,” “moderately,” and “highly” solution-resistant classes of foraminifera. They could then be used as “key” species for the quantitative study of the dissolution of assemblages. This could ultimately result in a method whereby the examination of several shells from perhaps three different species of foraminifera could yield a quantitative answer as to how much dissolution had occurred and what species would have a high probability of being com-

pletely lost to dissolution. A major advantage of this method would be that it could be applied to single cores without the restrictions found in the other two methods.

Perhaps the most important question to be resolved for the development of this method is whether laboratory experiments can meaningfully duplicate selective dissolution found on the ocean floor? Our approach is to examine with the scanning electron microscope the ultrastructural features of shells that have undergone dissolution in laboratory experiments and to compare these results with naturally dissolved specimens and species assemblages from varying depths within a confined region of the central North Atlantic.

#### EXPERIMENTAL METHODS

Three different methods were used in the laboratory dissolution experiments. These experimental methods were used as a test of the effectiveness of different procedures in duplicating shell surface textures produced by dissolution under natural conditions. A general consideration was the work of Berner and Morse (1974) which indicated that markedly different surface textures on reagent grade calcite are produced by dissolution conducted at undersaturations where either diffusion or surface reactions are rate-limiting. Although all experiments were carried out at undersaturations significantly greater than generally found in the deep ocean, diffusion was not rate-limiting in any of the experiments.

The foraminiferal specimens obtained from experimental and natural dissolution conditions were photographed in a Cambridge Mark IIA Scanning Electron Microscope (SEM).

*Method 1. Dissolution of Individual Shells in Sea Water Baths:* In Experiments 1, 2, and 5 individual shells of *Globorotalia truncatulinoides* and *Orbulina universa* were etched in separate flasks containing sea water in which the pH had been adjusted to 6.5. The volume of artificial sea water (35 ‰) used was sufficiently large so that the pH remained essentially constant ( $\pm 0.05$ ). Percent dissolution (= “Dissolution Loss”) was determined by weight loss of shells. Weighing was done on a Mettler M5S/A microbalance, with a precision of  $\pm 1$  microgram. Reproducibility, including handling error was  $\pm 3$  micrograms or approximately 2 percent possible error in the calculated degree of dissolution. A possible source of error in experiments where a large amount of dissolution took place was fragmentation and loss of internal clay and coccoliths. This could lead to calculation of degrees of dis-

solution which are higher than actually took place. Another source of possible error in samples which underwent small amounts of dissolution is the salt derived from entrained sea water during drying. In an attempt to avoid this problem, samples were repeatedly washed in pH adjusted distilled water, prior to initial and final weighing.

*Method 2. Dissolution of Individual Shells in Acetic Acid Bath:* In Experiments 3 and 4 individual shells were placed in a beaker containing 15 ml of acetic acid solution with a pH of 6.0 at room temperature. The bath was prepared by adding 28 percent acetic acid 1 drop at a time to 0.1 molar solution of sodium acetate until a pH of 6.0 was obtained. The sodium acetate acts as a buffer to help maintain a constant pH as CaCO<sub>3</sub> of the dissolving specimens goes into solution.

For Experiment 4, 8 specimens of *Pulleniatina obliquiloculata* were placed in the acetic acid bath. During a period of 8 hours, one specimen was removed each hour for SEM observations.

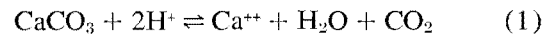
For Experiment 3 a single specimen of *G. truncatulinoides* was dissolved at six successively greater dissolution stages in the acetic acid bath. Each stage involved the following steps:

1. Specimen was mounted on a SEM stub with silver glue.
2. Specimen was carbon coated.
3. Specimen was photographed in the scanning electron microscope.
4. Specimen was removed from the SEM stub and washed with acetone, then with distilled water.
5. Carbon coating on specimen was removed in Tracerlab Low Temperature Asher (Model LTA-600) at 100 radio frequency watts for 15 minutes at 100°–150°C.
6. Specimen was placed in the acetic acid bath for 30 minutes.
7. Specimen was again glued to the stub and the cycle was repeated.

A "control" specimen was carbon-coated, photographed and ashed (but not dissolved) at each of the 6 stages to determine if the ashing process altered the foraminiferal shell with each successive step. The result showed no morphological alteration of the shell.

*Method 3. pH-Stat Dissolution:* In Experiment 6 natural assemblages of planktonic foraminifera were dissolved in the pH-stat described by Morse (1974).

Use of the pH-stat allows an accurate maintenance of the degree of undersaturation. The basis for the maintenance of a constant state of disequilibrium comes from the consideration of the dissolution or growth of calcium carbonate via reaction 1. Equation 2 shows that there are only three concentration variables in the dissolution or growth of calcium carbonate, assuming the activity of water is close to constant, when reaction 1 is followed ( $m_{Ca^{++}}$ ,  $a_{H^+}$ , and  $P_{CO_2}$ ).



$$\Omega = \frac{a_{Ca^{++}} a_{CO_3^{--}}}{K_c} = K' \left( \frac{m_{Ca^{++}} P_{CO_2}}{a_{H^+}^2} \right) \quad (2)$$

Where:  $\Omega$  = the degree of saturation

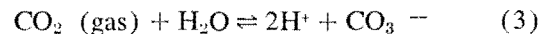
$a$  = activity

$m$  = total molality (free ions plus ion pairs)

$$K' = \frac{K_{012} \gamma T_{Ca^{++}}}{K_c}$$

$K_c$  = equilibrium ion activity product of calcite under experimental conditions

$K_{012}$  = the activity equilibrium constant for the reaction:



$\gamma T_{Ca^{++}}$  = total activity coefficient of calcium ion

$P_{CO_2}$  = partial pressure of carbon dioxide

Thus, at constant  $a_{H^+}$ ,  $m_{Ca^{++}}$ , and  $P_{CO_2}$ , the degree of saturation is constant.

It is possible to hold  $P_{CO_2}$  constant by bubbling a CO<sub>2</sub>-air mixture of constant composition through the solution during reaction. The concentration of calcium ( $m_{Ca^{++}}$ ) is essentially constant because a negligibly small amount of CaCO<sub>3</sub> can be dissolved or precipitated relative to the amount of calcium originally present in the solution. For example, the dissolution of 1 mg of calcite in 1 liter of sea water, in equilibrium with the atmosphere would result in a change in the calcium concentration by only a factor of 1.005. Although the change in the calcium concentration in this example would be negligibly small, the change in hydrogen ion concentration would be by a factor of approximately 1,000. It is, therefore, necessary to add either acid (HCl) or base (NaOH) to the solution in order to maintain a nearly constant pH and, consequently, a close to constant degree of saturation. The hydrogen ion activity can be monitored on a pH meter, and the rate and amount of either acid or base added to maintain a constant pH can then be used as a precise method of determining the reaction rate and

amount of calcium carbonate dissolved via the stoichiometry of reaction 1 (Morse, 1974).

Experiments on the breakage of shells due to stirring (with a suspended magnetic stirrer) with time, drift characteristics of the pH-stat system, and knowledge of the dissolution kinetics of calcite (Berner and Morse, 1974) indicated that the optimum conditions for our present experiments are a pH = 7.53 at a  $P_{CO_2}$  of  $10^{-3.50}$  atm for phosphate free artificial sea water (35 ‰) at 5°C. This resulted in a dissolution rate of approximately 1 percent per hour. A minimum of 10 mg of calcium carbonate was found necessary for accurate results.

#### SAMPLE LOCALITIES FOR FORAMINIFERAL SPECIMENS

Most of the specimens for Experiments 1 through 6 were obtained from a single surface sediment sample in the north-central Sargasso Sea (V17-106 SBT, lat 35°06'N., long 45°56'W., 3400 m depth).

The natural assemblages of planktonic foraminifera discussed in the section on natural observations were collected from the following localities:

Sample	Location	Depth
V20-248 TW Top	33°30'N., 62°24'W.	1575 m
V7-65 TW Top	32°07'N., 64°47'W.	2743 m
V26-172 TW Top	32°02'N., 66°20'W.	4803 m
V26-9 TW Top	31°43'N., 56°12'W.	5546 m

The specimens of *Pulleniatina obliquiloculata* showing natural dissolution features (pl. 10) are from V20-248, V17-106, V26-172, V26-9, and V16-25 (lat 5°04'N., long 36°48'W., 4254 m water depth; 245 and 285 cm core depth levels).

The single specimen of *Globorotalia truncatulinoides* in Experiment 3 (pl. 5) was obtained from sample V20-248.

#### SPECIMEN ORIENTATION DURING DISSOLUTION EXPERIMENTS

The orientation of the planktonic foraminiferal shells in the dissolution containers during Experiments 1 to 5 has an important bearing on the relative exposure of the shell surface area to the surrounding liquid. If a non-random orientation occurred after the shells settle to the bottom of the bath, certain parts of the shells would rest in a protected position against the container floor for a large percentage of the time. This could result in selective dissolution of some shell parts and thus influence the final gross morphology of the shells.

In order to check this possibility we examined the resting positions of eight representative species: *Pulleniatina obliquiloculata*, *Globigerinoides sacculifer*, *Globoquadrina dutertrei*, *Globorotalia menardii*, *G. crassaformis*, *G. inflata*, *G. hirsuta* and *G. truncatulinoides* [illustrations of these species are shown in Bé (in press)]. The resting positions of ten specimens of each species were recorded after (a) settling through a column of water in a 400 ml beaker, (b) gentle and vigorous swirling in the same beaker; and (c) inducing unidirectional flow in a partitioned tray. Each test was repeated five times, so that for each method 50 observations were recorded per species, as shown in table 1.

As intuitively expected, species whose gross shell forms are globular or spherical (e.g., *Globigerinoides sacculifer*, *Pulleniatina obliquiloculata* or *Orbulina universa*) are randomly oriented when they settle in a container, even after being stirred or subjected to unidirectional flow. At first, *P. obliquiloculata* was found to rest invariably on its apertural side in all three sets of observations. However, this preferred orientation is caused by air trapped inside the shells. By repeating these observations with *P. obliquiloculata* specimens from plankton tows whose shells were filled with protoplasm, we obtained random resting positions for the three sets of observations. Thus when empty shells are tested, it is necessary that any trapped air be evacuated.

*Globorotalia menardii* (with relatively flat to slightly convex sides) and *Globorotalia crassaformis* (with relatively flat spiral side and convex apertural side) had slight preferences of resting on their spiral sides in the three sets of observations.

*Globoquadrina dutertrei* (with a convex spiral side and concave to flat apertural side) had a slight preference of landing on its spiral side after settling, but it was randomly oriented after swirling and had a moderate preference for an apertural resting position after unidirectional flow.

*Globorotalia inflata* (with flat to slightly convex spiral side and strongly convex apertural side) had a random orientation after settling, but a moderate preference of a spiral-side resting position after swirling and unidirectional flow.

*Globorotalia hirsuta* (with a convex to flat spiral side and concave apertural side) and *Globorotalia truncatulinoides* (with a flat spiral side and conical apertural side) showed striking reversals in their strongly preferred orientations. After settling *G. hirsuta* and *G. truncatulinoides* both had strong preferences of

TABLE 1

Specimen orientation of eight species of planktonic foraminifera after settling, swirling and unidirectional flow. The ratios of spiral-side resting positions to apertural-side resting positions are recorded for five tests of ten specimens per species.

	<i>Pulleniatina obliquiloculata</i>	<i>Globigerinoides sacculifer</i>	<i>Globorotalia menardii</i>	<i>Globoquadrina dutertrei</i>	<i>Globorotalia crassaformis</i>	<i>Globorotalia inflata</i>	<i>Globorotalia hirsuta</i>	<i>Globorotalia truncatulinoides</i>
Settling	Random	4:6	7:3	7:3	8:2	7:3	4:6	4:6
		6:4	6:4	7:3	3:7	4:6	7:3	1:9
		7:3	7:3	4:6	6:4	5:5	7:3	0:10
		4:6	2:8	5:5	6:4	4:6	8:2	1:9
		5:5	6:4	6:4	5:5	6:4	6:4	2:8
		26:24	28:22	29:21	28:22	26:24	32:18	8:42
Swirling	Random	4:6	7:3	6:4	7:3	8:2	3:7	5:5
		6:4	6:4	3:7	7:3	6:4	2:8	8:2
		4:6	7:3	6:4	5:5	7:3	2:8	9:1
		7:3	2:8	7:3	6:4	7:3	1:9	9:1
		5:5	5:5	2:8	5:5	5:5	3:7	9:1
		26:24	27:23	24:26	30:20	33:17	11:39	40:10
Unidirectional flow	Random	5:5	8:2	4:6	8:2	9:1	2:8	9:1
		4:6	8:2	3:7	6:4	4:6	3:7	8:2
		5:5	4:6	8:2	3:7	7:3	1:9	9:1
		6:4	3:7	1:9	6:4	4:6	1:9	10:0
		4:6	3:7	4:6	3:7	8:2	4:6	9:1
		24:26	26:24	20:30	26:24	32:18	11:39	45:5

resting on their spiral and apertural sides, respectively. However, after swirling and unidirectional flow *G. hirsuta* had a strongly preferred apertural-side resting position and *G. truncatulinoides* a strongly preferred spiral-side resting position. The ratio of spiral-side vs. apertural-side resting positions of *G. truncatulinoides* obtained after swirling was 40:10. The same ratio after unidirectional flow was 45:5. These results indicate that the spiral-side of *G. truncatulinoides* is hydrodynamically a stable resting position in contrast to the unstable resting position of the apertural side.

Since in our dissolution experiments 1 and 2 the specimens of *G. truncatulinoides* were swirled and assumed a preferred spiral-side resting position, it helps to explain why the walls of the apertural side are corroded first while the spiral side is still well preserved (pls. 3 and 4).

The preferred resting positions may also be significant in explaining why in laboratory and field observations the chambers of the last whorl are sometimes preserved and the inner chambers are dissolved, as in the specimens of *Globorotalia inflata* and *G. truncatulinoides* in plate 9, figures 3 and 4. By contrast, the reverse condition when the last whorl is corroded and the inner chambers remain intact also occurs—as in

our laboratory experiments 1 and 2 (pls. 3 and 4) and in nature (see Thiede, 1971, pl. 10, figs. 2 and 3). In addition to any preferred resting positions, the flow rate of liquid around and within the shells is probably also a decisive factor in the resulting two types of shell preservation.

#### SHELL STRUCTURE OF PLANKTONIC FORAMINIFERA AND PROGRESSIVE DISSOLUTION

An understanding of the shell structure of planktonic foraminifera is necessary before we can discuss problems of their dissolution in laboratory experiments or under natural conditions on the sea bed. Bé (in press) has recently reviewed our status of knowledge of how planktonic foraminifera grow their shells, and, therefore, we shall here confine our discussion to their shell structure only. The following description is based on *Globorotalia truncatulinoides*, whose shell ultrastructure is similar and representative of most *Globorotalia* species.

When the shell of an adult *G. truncatulinoides* is fractured, several layers are apparent in a cross-section of a fully developed wall (pl. 1). For con-

venience, we shall distinguish three types of layers based on the size of their crystallite units; actually, these three layers grade into each other. The inner or proximal layer is the initial one secreted by the organism and consists of anhedral microgranules (about  $0.2\mu$  in diameter). The small size and close packing of the microgranules produces a homogeneous, smooth texture when seen from top view (pl. 2, fig. 1). Under the light microscope with dark-filled illumination this "Microgranular Layer" distinctly contrasts with the radial structure of the "Euhedral Layer" or calcite crust (Pessagno and Miyano, 1968).

An intermediate layer between the Microgranular and Euhedral Layers is composed of subrhombic calcite crystallites (pl. 2, fig. 5). This so-called "Subrhombic Layer" is secreted on top of the Microgranular Layer and is the early stage in the development of the calcite crust. It can thus be considered as an incipient part of the Euhedral Layer. The surface texture of the Subrhombic Layer is coarser than that of the Microgranular Layer, due to the appearance of well-defined subhedral crystallite units (about  $0.6-1.0\mu$  long). Each crystallite appears to have a triangular outline and collectively they form a mosaic of neatly fitted triangles (pl. 2, fig. 5).

Further wall thickening results in the formation of a thick "calcite crust" or "Euhedral Layer" which consists of large euhedral calcite crystallites (about  $10-15\mu$  long) (pl. 1; pl. 2, fig. 9). These euhedral crystallites are the product of the gradual enlargement of the subrhombic crystallites and thus no distinct boundary separates these two layers.

We have depicted an idealized sequence of the progressive ultrastructural breakdown of each of the three layers in plate 2. The scanning electron micrographs were chosen from different specimens and placed in a sequence which we believe best illustrates the progressive ultrastructural breakdown during the dissolution process. It is important to keep in mind in subsequent discussions and interpretations of the laboratory dissolution experiments, that the morphological end-products are largely influenced by the shell size and wall thickness of each specimen and species. Depending upon the ontogenetic stage of an individual for-

minifer, its outer shell surface may be covered by varying proportions of the three ultrastructural types—Microgranular, Subrhombic or Euhedral. The thinner (younger) the shell wall the greater the likelihood that its surface is Microgranular. The thicker (older) the shell wall the more likely its surface is of the Euhedral type. Thus, since it is possible for an individual to have all three types occurring concurrently on its shell surface, it is difficult to make comparisons of dissolution features between different shells. Ideally, stages in progressive dissolution should be followed for a single specimen, as we have done in Experiment 3. Less ideally, morphological comparisons should be made for homologous ultrastructures, if different specimens are to be examined.

Plate 2 illustrates our view of the sequence of progressive ultrastructural breakdown for each of the three layers. The Microgranular Layer is first etched (pl. 2, fig. 2), before it reveals a "jig-saw puzzle" suture pattern which probably reflects first-order structural units (pl. 2, fig. 3). Very advanced dissolution widens the sutures and exposes the individual microgranules (pl. 2, fig. 4).

The irregular, interlocking units bounded by sinuous sutures that make up the "jig-saw puzzle" mosaic (pl. 2, fig. 2) may be homologous to those occurring commonly in benthic foraminifera (e.g., Towe and Cifelli, 1967, pl. 91; Murray and Wright, 1970, pl. 37; Stapleton, 1973, pl. 2, pl. 7).

Solution etching of the Subrhombic Layer results in a characteristically triangular suture pattern (pl. 2, fig. 6). Further etching causes rounding of the "triangular" crystallites (pl. 2, fig. 7) and ultimately produces needle-like prisms (pl. 2, fig. 8).

Solution etching of the Euhedral Layer becomes evident with the appearance of dissolution steps (Berner and Morse, 1974) on the previously smooth faces of the euhedral crystallites (pl. 2, fig. 10) and the widening of sutures between the crystallites themselves (pl. 2, fig. 11). The ultimate end-product of dissolution of the Euhedral Layer has not been completely investigated by us.

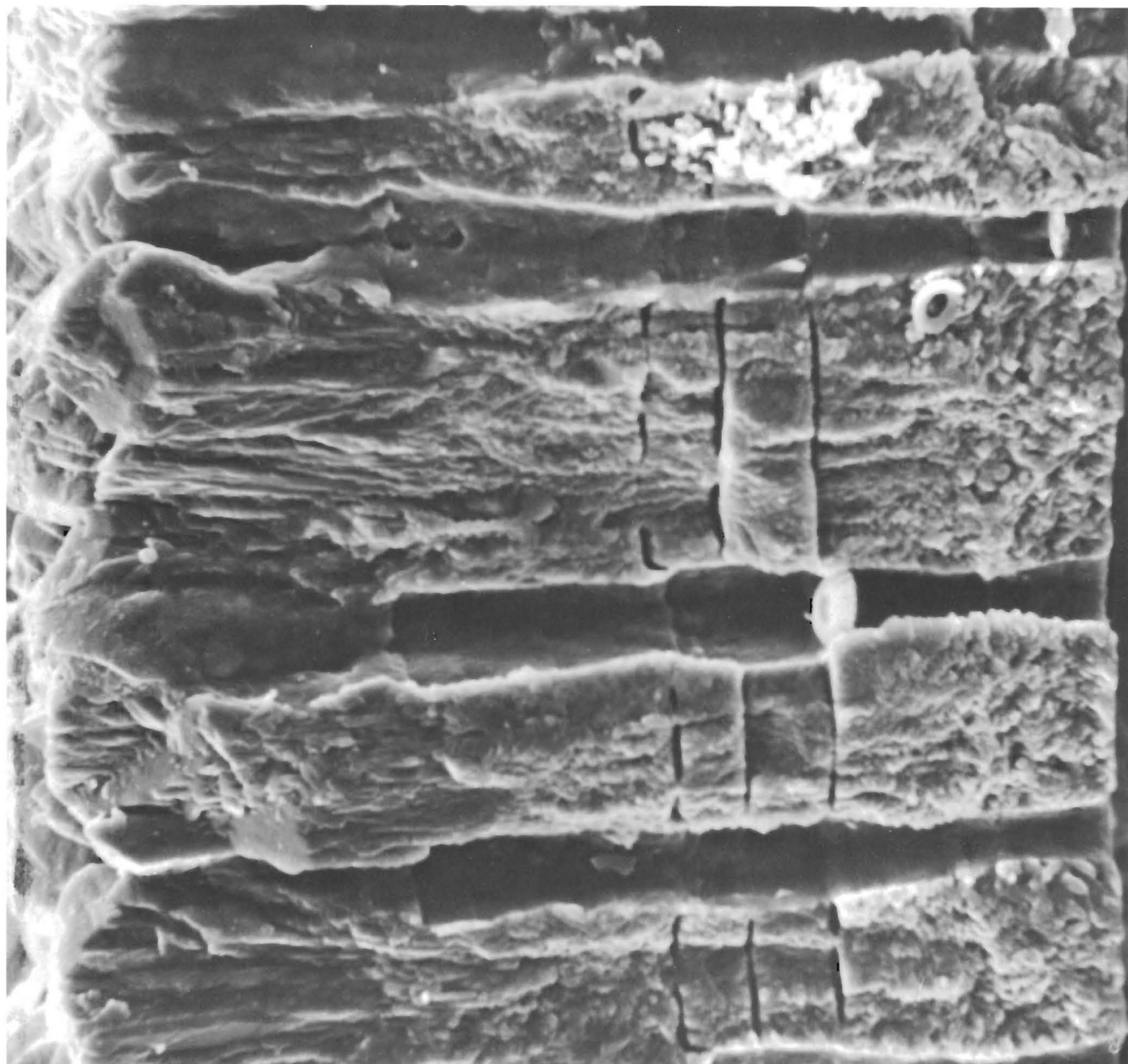
With the morphological sequences in plate 2 in mind, we can now proceed with the laboratory experiments

---

## PLATE 1

Oblique cross-sectional view of a fully developed wall of *Globorotalia truncatulinoides* from sample V17-106 magnified  $\times 3,600$ . The euhedral crystallites appear on the outer surface.

The boundary between the Subrhombic and Euhedral Layers is gradational and not distinct. Compare the three ultrastructural layers with those in plate 2.



EUHEDRAL  
LAYER

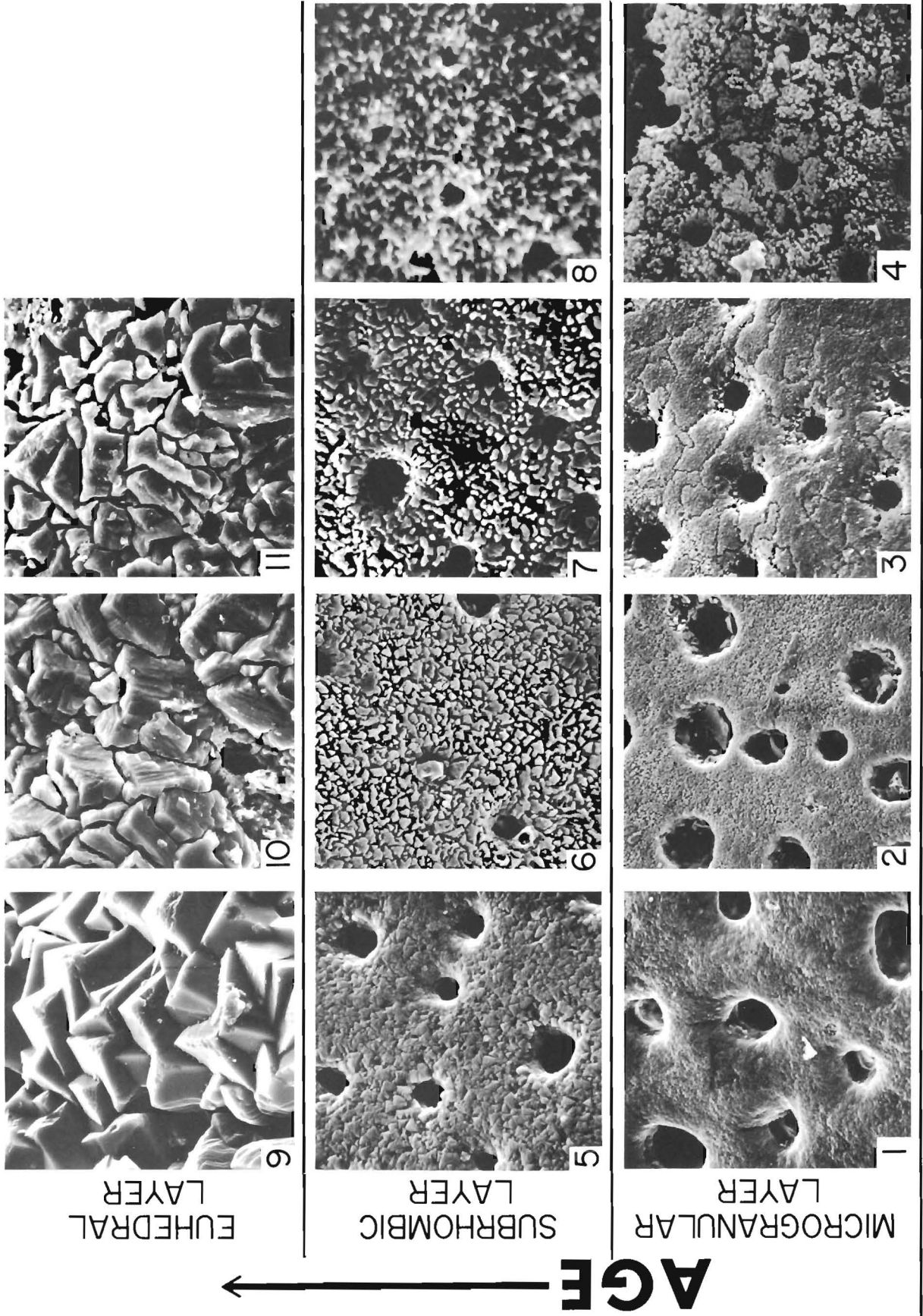


SUBRHOMBIC  
LAYER



MICROGRANULAR  
LAYER

**PROGRESSIVE DISSOLUTION** —————→



and observations of natural assemblages. These we shall discuss under the following two categories:

#### EXPERIMENTAL OBSERVATIONS

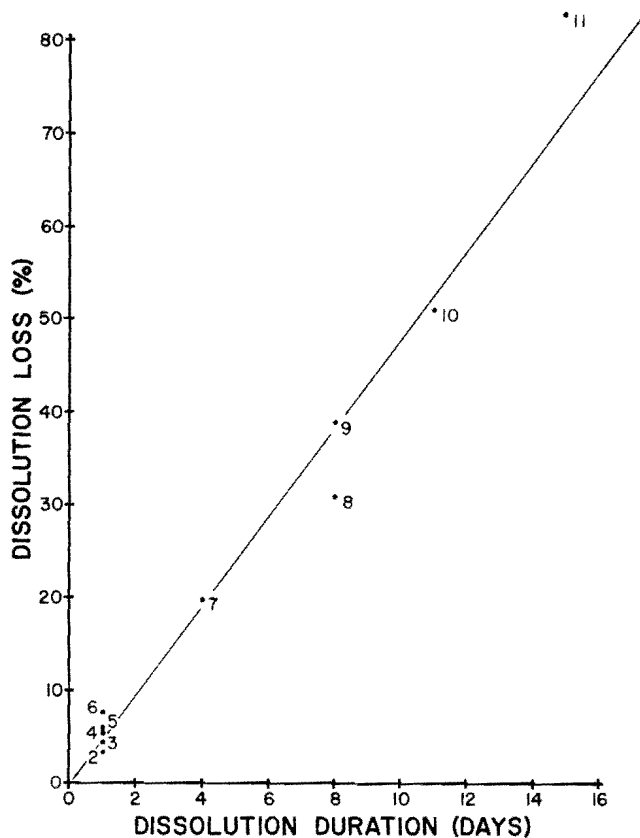
1. Experiment 1—Laboratory dissolution of 10 individual specimens of *Globorotalia truncatulinoides* in sea water bath.
2. Experiment 2—Laboratory dissolution of 14 specimens of *G. truncatulinoides* in sea water bath.
3. Experiment 3—Laboratory dissolution of a single specimen of *G. truncatulinoides* in acetic acid bath.
4. Experiment 4—Laboratory dissolution of 8 individual specimens of *Pulleniatina obliquiloculata* in acetic acid bath.
5. Experiment 5—Laboratory dissolution of 9 individual specimens of *Orbulina universa* in sea water bath.
6. Experiment 6—Laboratory dissolution by pH-stat method of a natural assemblage of planktonic foraminifera.

#### NATURAL OBSERVATIONS

1. Natural dissolution of four assemblages of planktonic foraminifera from different oceanic localities.
2. Natural dissolution of *P. obliquiloculata* from different oceanic localities.

### RESULTS OF EXPERIMENTAL OBSERVATIONS EXPERIMENT 1

Ten specimens of *Globorotalia truncatulinoides* from surface sediment sample V17-106 were subjected to dissolution in separate flasks of undersaturated sea water. The shells were removed successively after various durations of dissolution, ranging from 1 to 15 days. Weight losses of the shells were calculated as percentages of



TEXT FIGURE 1

A roughly linear relationship exists between dissolution loss and dissolution duration (in days) for the ten specimens used in Experiment 1. The specimens, numbered 2 through 11, are shown in plate 3.

their original weight. The "weight loss" or "dissolution loss" for the 10 specimens ranged from 3 to 83 percent (pl. 3). A plot of "dissolution loss" against "dissolution duration" indicates a roughly linear relationship

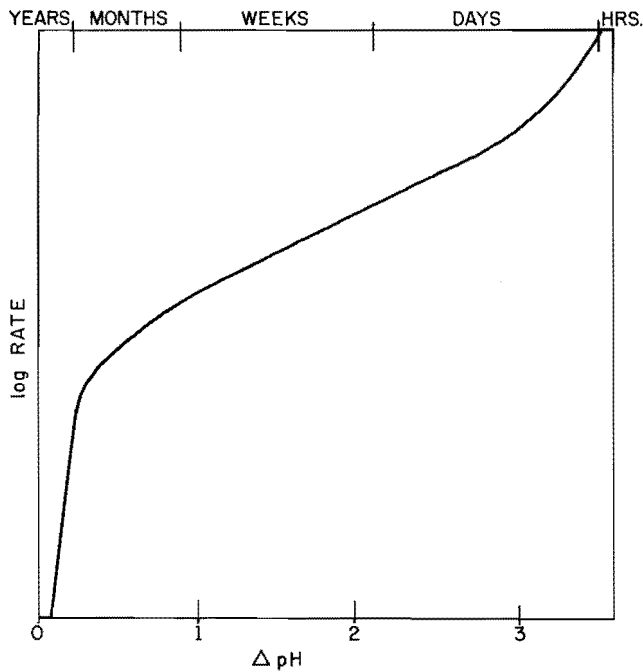
#### PLATE 2

Idealized series of progressive ultrastructural breakdown of *Globorotalia truncatulinoides* shell wall, which is made up of three types of ultrastructural layers. The Microgranular Layer is secreted first, followed by the Subrhombic and Euhedral

Layers. Sample localities are listed under "Methods." All specimens were dissolved to varying degrees in the laboratory, except those in figures 1, 5 and 9 which came directly from sediment samples.

	Sample
1. × 2,262	V5-8
2. × 2,262	V17-106
3. × 2,262	V17-106
4. × 2,262	V17-106
5. × 2,262	V5-8
6. × 2,262	V17-106

	Sample
7. × 2,262	V17-106
8. × 2,262	V17-106
9. × 905	V26-9
10. × 905	V20-248
11. × 905	V20-248



TEXT FIGURE 2

Log Rate ( $\text{mg cm}^{-2}\text{yr}^{-1}$ ) versus pH based on the results of Berner and Morse (1974). At the top of the figure is the approximate time necessary to dissolve a single specimen of *Globorotalia truncatulinoides*. No scale is given on the log Rate axis because variable rates have been found for different calcite samples even when normalized by surface area.

(text fig. 1). This is probably indicative that, although the total amount of  $\text{CaCO}_3$  is changing, the surface area exposed for dissolution is approximately constant.

In text figure 2 the approximate time necessary for complete dissolution of an individual shell of *G. truncatulinoides* as a function of  $\Delta\text{pH}$  (distance from equilibrium  $\text{pH} = -\frac{1}{2} \log \Omega$ , Berner and Wilde, 1972) is shown. The plot of rate vs.  $\Delta\text{pH}$  is based on the work of Berner and Morse (1974).

Progressive changes in the surface texture of the final chamber were visible from a comparison of the scanning electron micrographs taken at various magnifications (pl. 3). However, these changes are often obscured by the great biological variability among individual shells, because the surface texture of each final chamber may reflect different growth stages or wall thickness. The results of Experiment 1 (pl. 3) indicate the following:

1. The preferred spiral-side resting position of *G. truncatulinoides* during this as well as the two subsequent experiments resulted in greater exposure of

the apertural side to the surrounding liquid, while the spiral side is less vulnerable to dissolution. The significance of this orientation is discussed further in the specimen orientation section (p. 30).

2. Solution etching of the outer shell surface is already apparent at very low (3–4%) dissolution loss.
3. The  $\times 1,700$  magnification series shows:
  - a. At 3 and 5 percent dissolution loss, etching accentuates the “triangular” crystallites of the Subrhombic Layer.
  - b. At 4 percent, deep etching produces a jig-saw puzzle pattern of the Microgranular Layer.
  - c. At 6 percent, the Subrhombic Layer is partly removed to expose the Microgranular Layer, which is deeply etched to show the jig-saw puzzle pattern.
  - d. At 8 percent, the jig-saw puzzle units are composed of second-order microgranules.
  - e. At 20 percent, a deeper layer (i.e., Microgranular Layer) is exposed which appears to be smooth and relatively undissolved.
  - f. At 31 percent, continued dissolution of the Microgranular Layer reveals that the “jig-saw puzzle” units consist of second-order microgranules.
  - g. At 39, 51 and 83 percent advanced dissolution has reduced the texture to a spongy mass. Note elongated calcite units at 39 percent.
4. Dissolution attacks the shell by layers. Sometimes the outer one is weaker and is peeled off first (see  $\times 68$  at 4% dissolution loss). At other times, a stronger outer veneer protects a weaker inner layer (see  $\times 340$ ,  $\times 1,700$  at 6% dissolution loss).
5. The final chamber was breached by a large hole and a smaller one at 20 percent dissolution loss. The final and penultimate chambers were destroyed at 31 percent. At 83 percent all the chambers of the last whorl were corroded.

## EXPERIMENT 2

After Experiment 1 had shown that breaching of the final chamber in *Globorotalia truncatulinoides* occurred at approximately the 20 percent dissolution loss level, it was decided that a second series of specimens be placed in separate flasks of undersaturated sea water to examine the gross effects on shell breakdown at high dissolution levels, i.e.,  $> 20$  percent weight (dissolution) loss. Thus, fourteen specimens of *G. truncatulinoides* from surface sediment sample V17-106 were subjected to dissolution for periods ranging from

4 to 14 days until their dissolution losses ranged from 22 to 81 percent.

The following results were interpreted from plate 4:

1. Final chamber was destroyed at all stages.
2. Penultimate chambers were destroyed at 28 percent and higher stages. In many of these specimens, the final chamber has been completely removed.
3. Peeling off of layers is apparent at all stages. This is especially noticeable at 42 percent.
4. Earliest whorl (innermost chambers) were preserved longer and dissolved later than the thicker outer whorl. The significance of this observation is discussed in the specimen orientation section (p. 30).

The two bottom figures in plate 4 are from a *G. truncatulinoides* with 49 percent dissolution loss. The high-magnification detail shows a gradational sequence of ultrastructures that is remarkably similar to those shown in plate 1. Relatively well-preserved subrhombic crystallites are found on the left side and grade to progressively more corroded, needle-like structures to the right.

### EXPERIMENT 3

In our third experiment, we dissolved a single specimen of *G. truncatulinoides* from surface sediment sample V20-248 in order to observe progressive ultrastructural changes of an individual shell. This required an elaborate procedure of dissolving the shell in six stages with dissolution periods ranging from 0.5 to 2.5 hours. Each stage involved SEM photography, removal from the SEM stub, removal of the carbon-coating by low temperature ashing, dissolution in acetic acid buffered with 0.1 sodium acetate at pH 6.0. This procedure allowed us to observe the same spot on the shell at successively greater dissolution stages and at various magnifications from  $\times 50$  to  $\times 1,350$  (pl. 5). In conjunction with this experiment, we also carried out parallel tests of evaluating whether the low temperature asher and repeated carbon coatings create any artifacts or cause structural changes in the foraminiferal shell. As far as we were able to determine, no such

artificial changes were introduced. One disadvantage of using carbon-coating only instead of the normal carbon and gold-palladium coating in scanning electron microscopy, is the inferior quality of the SEM photos obtained by the former method. Experiments 3 and 4 were carried out at a higher acid concentration and consequently at an accelerated dissolution rate in comparison to Experiments 1 and 2.

The following results of Experiment 3 are shown in plate 5:

1. Solution etching of the final (F) chamber is evident at the earliest stage (0.5 hour). This is followed by peeling off of the upper Subrhombic Layer after 1 hour. After 1.5 hours, the Subrhombic Layer breaks up into needle-like prisms and reveals an underlying "jig-saw puzzle" Microgranular Layer. After 2.5 hours the Microgranular Layer also disintegrates into needle-like prisms.
2. On the penultimate (F-1) chamber, the Subrhombic Layer is considerably etched after 1 hour and almost totally disintegrated after 1.5 hours. After 2 hours, the Microgranular Layer is exposed.
3. On the F-3 chamber (i.e., third chamber previous to the final chamber), the euhedral crystallites of the calcite crust retained their smooth faces up to one hour of dissolution. After 1.5 hours there was considerable rounding of the formerly sharp edges of the crystallites. According to Berner and Morse (1974) this rounding could indicate diffusion-controlled dissolution. However, considering the undersaturation at which the experiment was conducted it is more probable that the rounding was due to inherent microstructural characteristics. This hypothesis is substantiated by the observation that after 2 hours, plate-like growth steps developed on the crystallite faces. And after 2.5 hours wide sutures were formed between the crystallites indicative of surface reaction control of the dissolution rate.
4. Except for the accelerated dissolution process, the morphological sequence of structural features were similar to those observed in Experiments 1 and 2 conducted in the sea water baths.

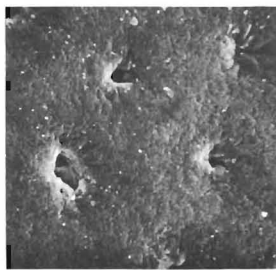
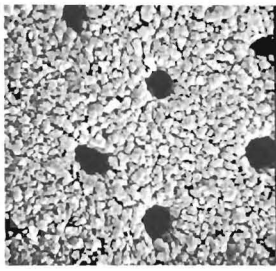
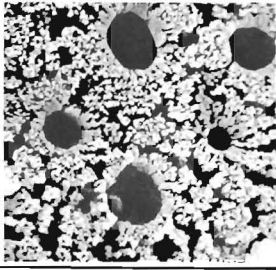
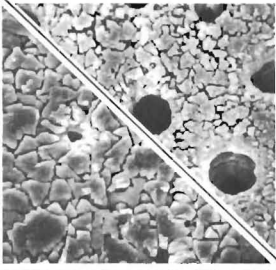
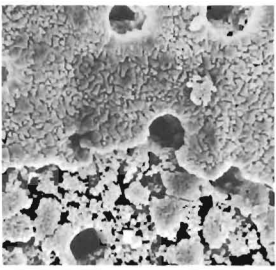
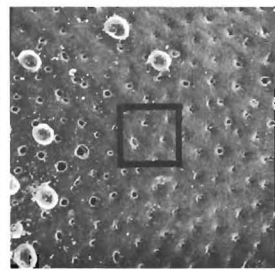
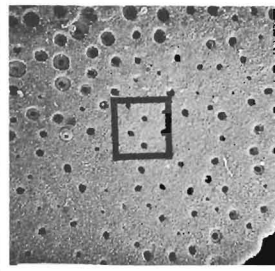
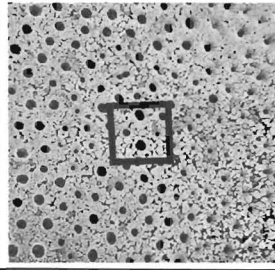
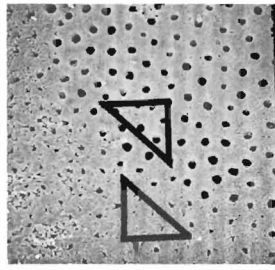
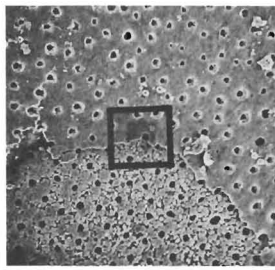
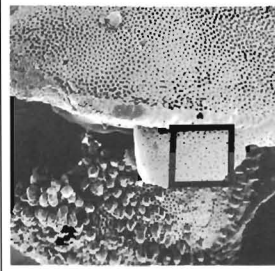
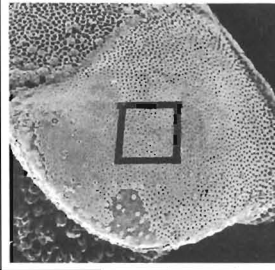
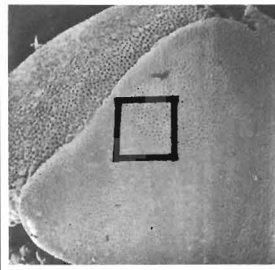
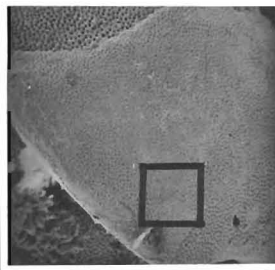
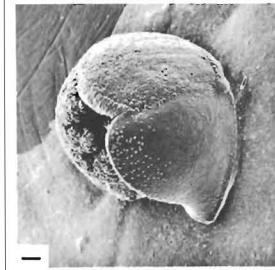
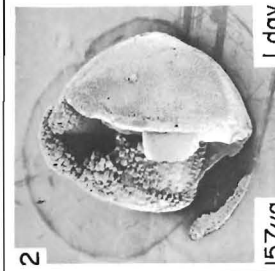
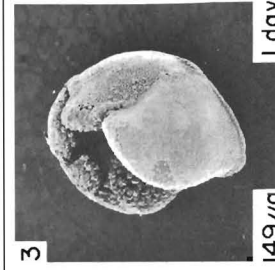
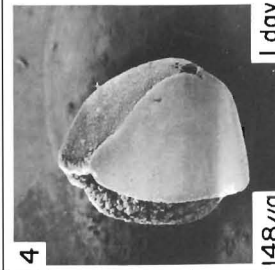
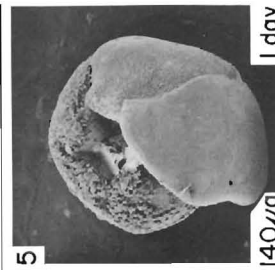
---

### PLATE 3

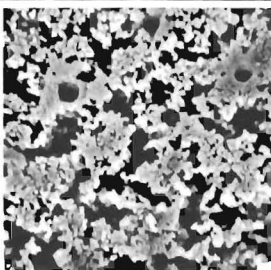
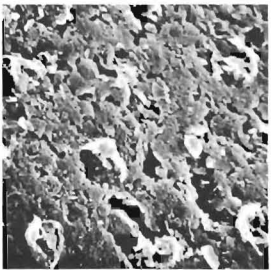
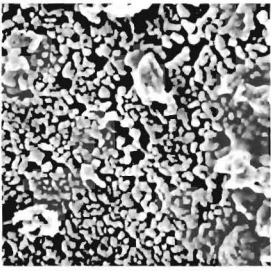
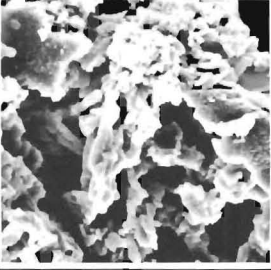
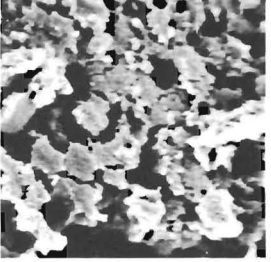
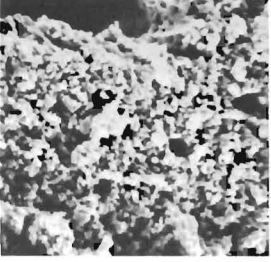
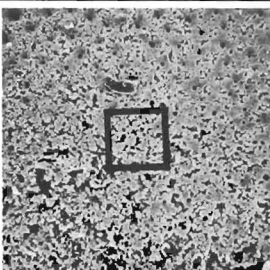
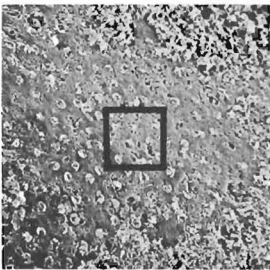
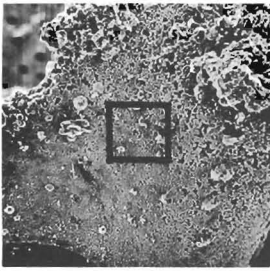
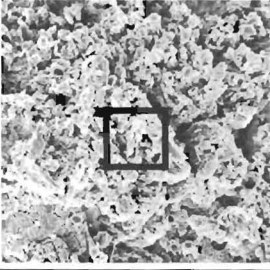
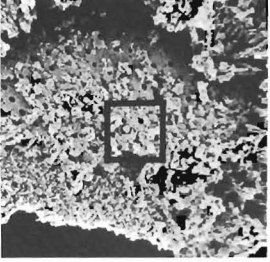
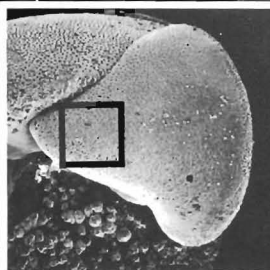
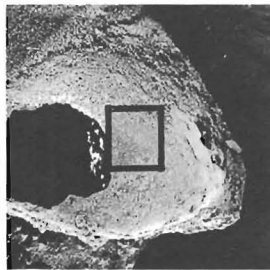
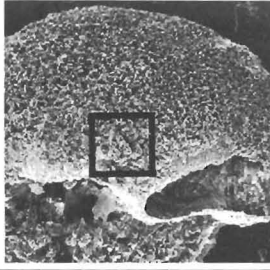
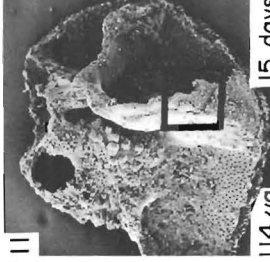
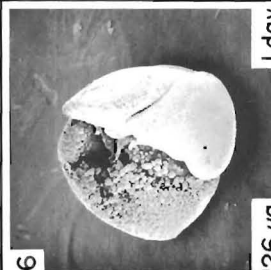
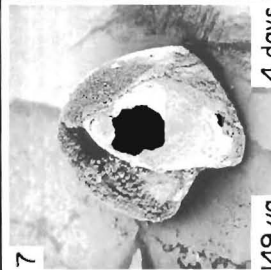
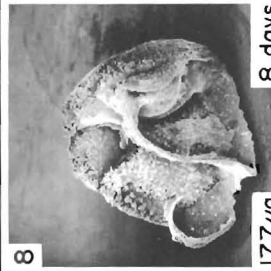
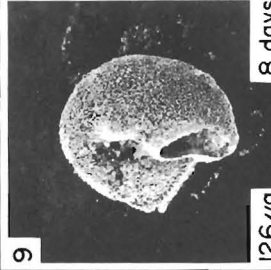
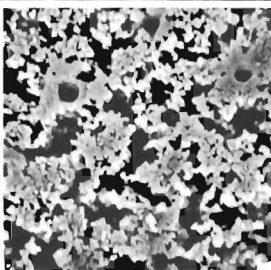
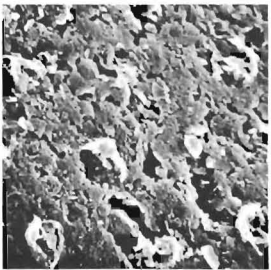
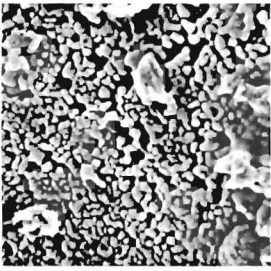
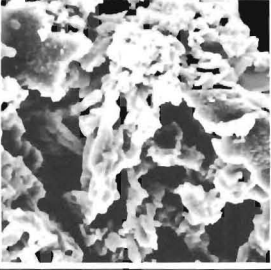
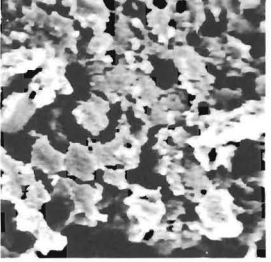
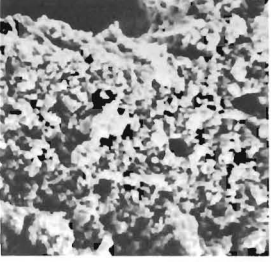
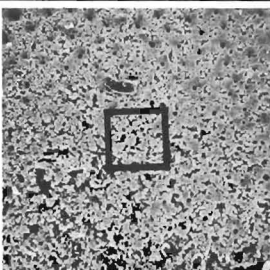
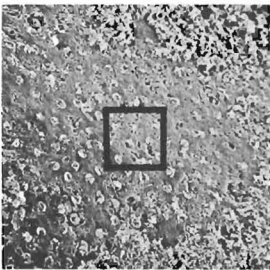
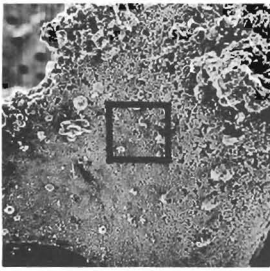
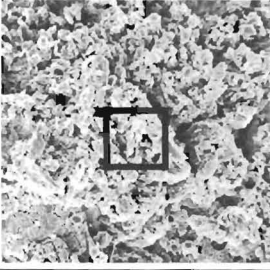
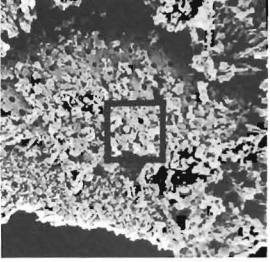
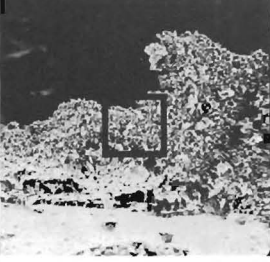
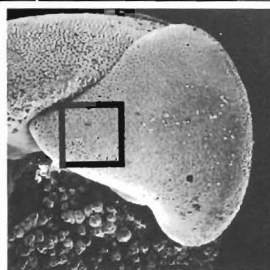
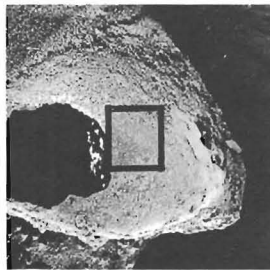
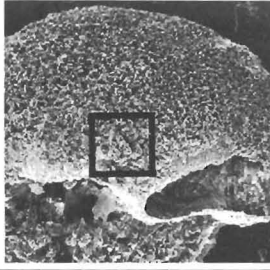
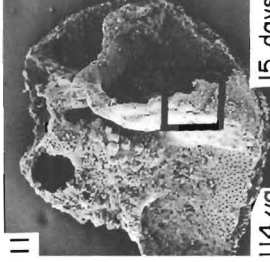
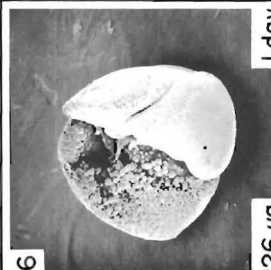
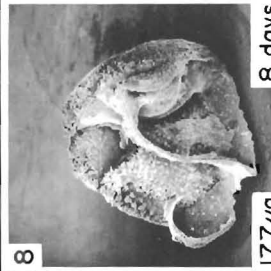
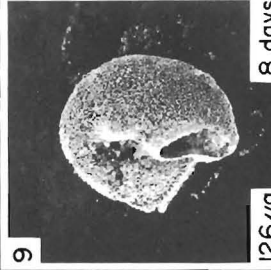
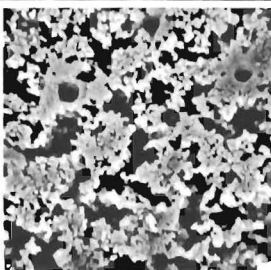
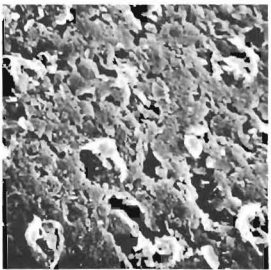
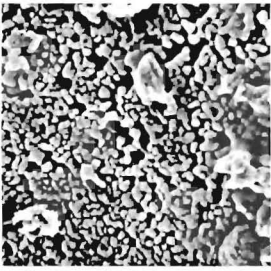
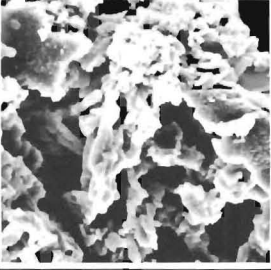
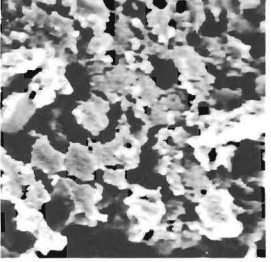
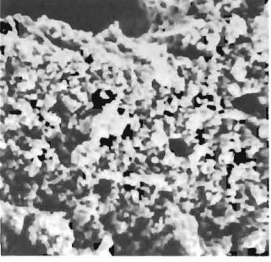
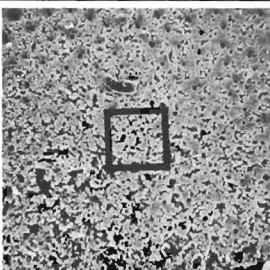
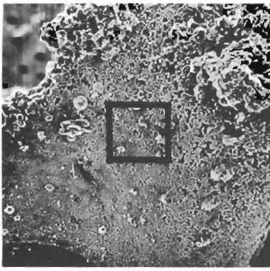
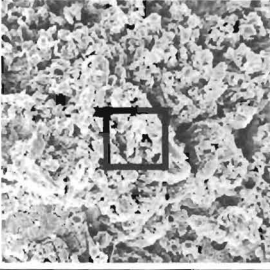
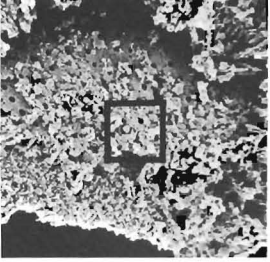
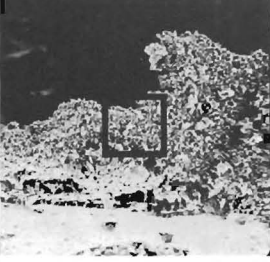
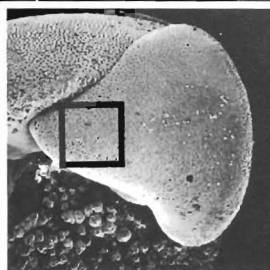
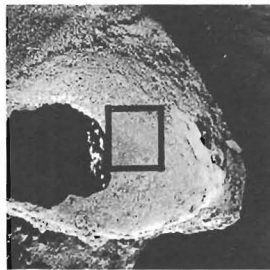
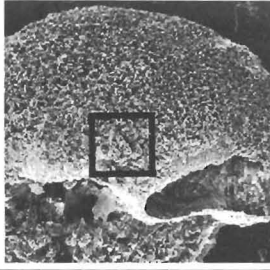
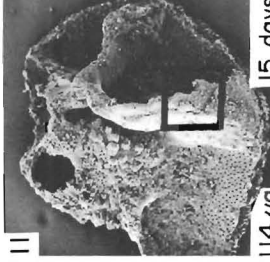
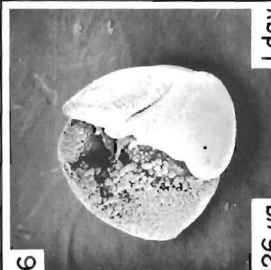
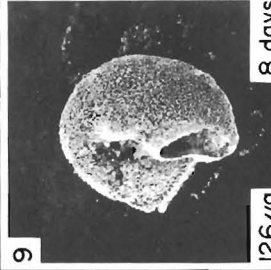
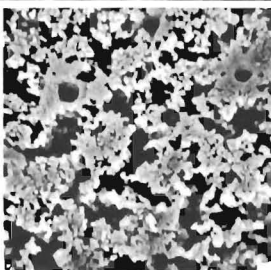
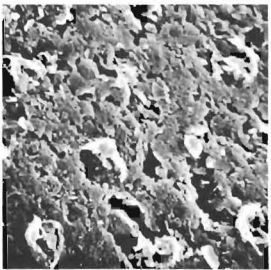
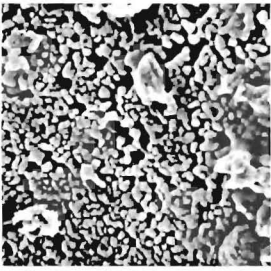
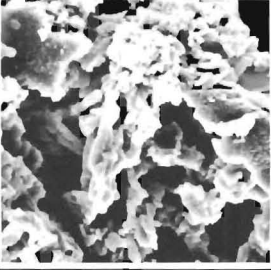
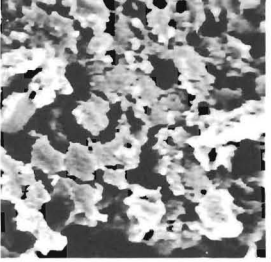
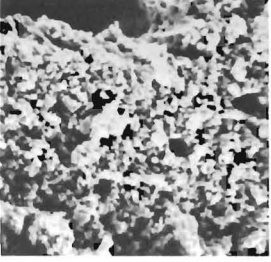
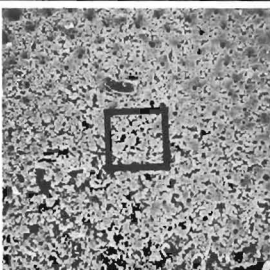
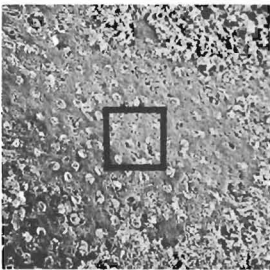
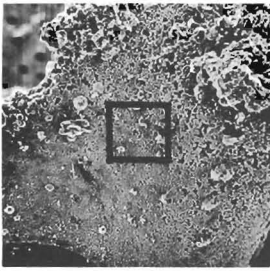
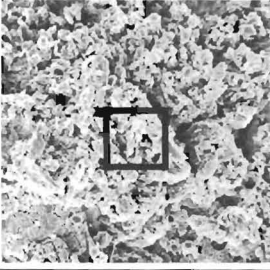
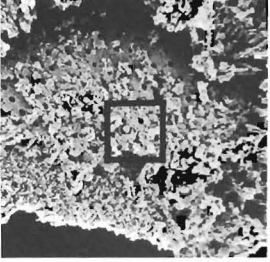
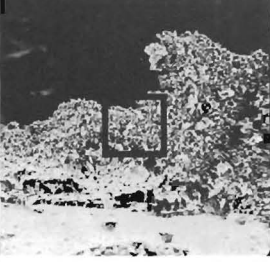
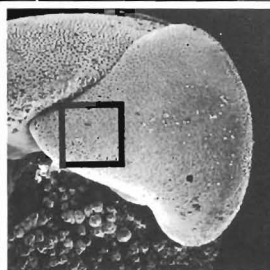
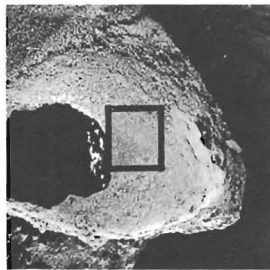
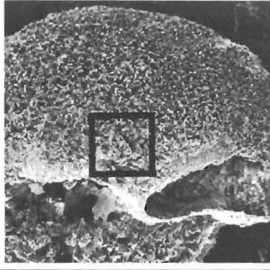
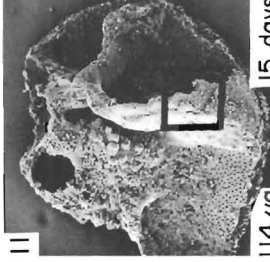
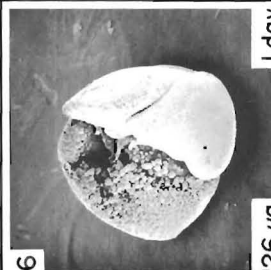
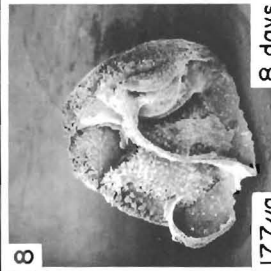
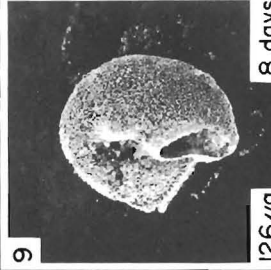
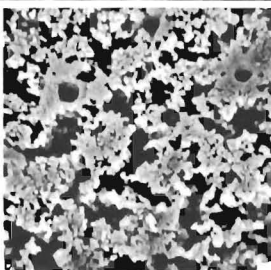
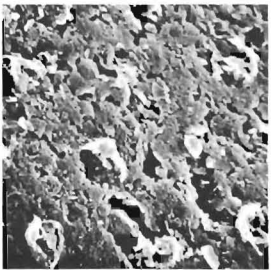
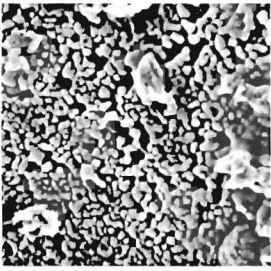
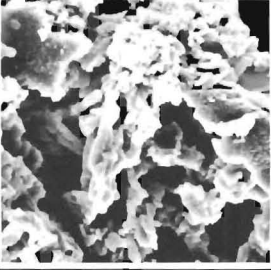
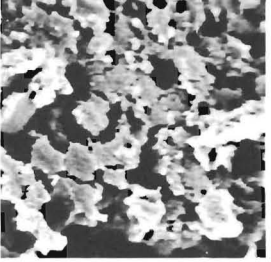
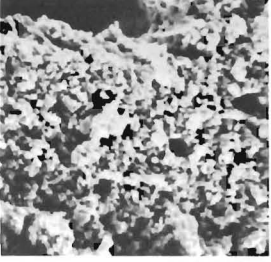
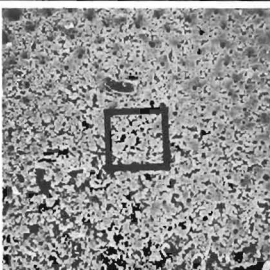
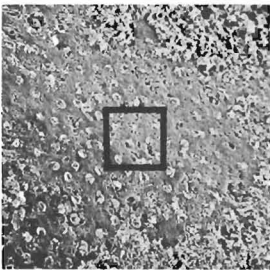
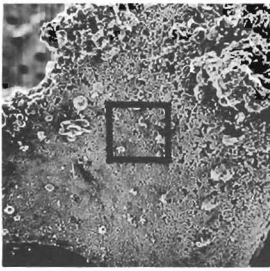
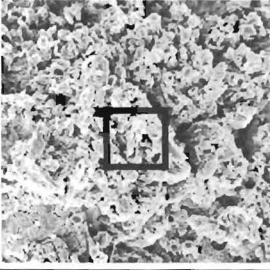
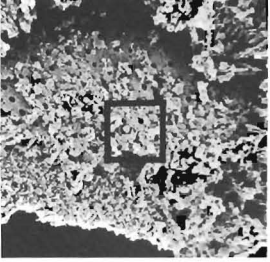
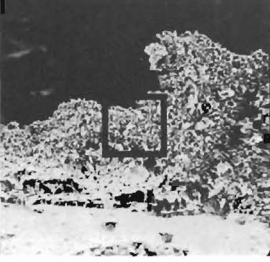
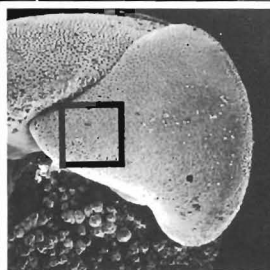
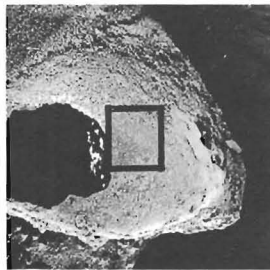
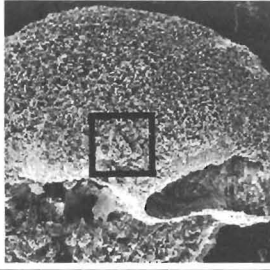
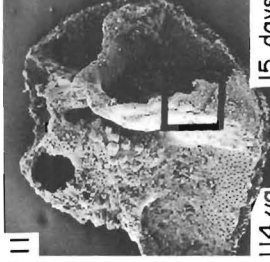
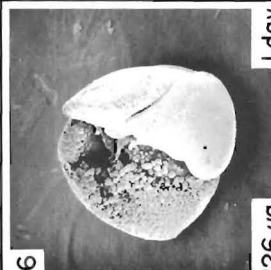
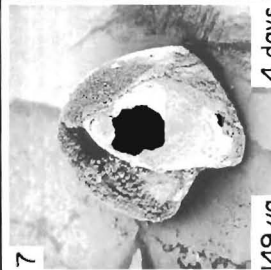
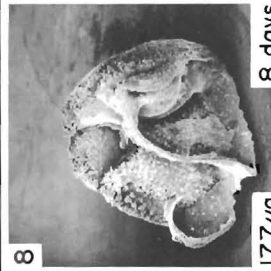
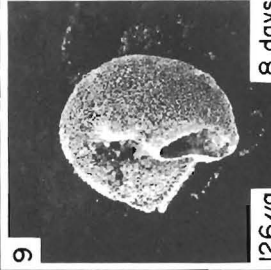
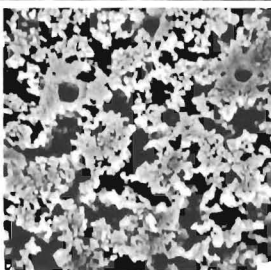
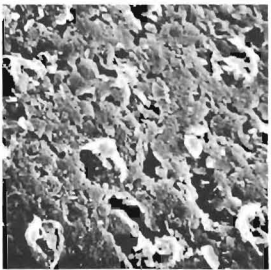
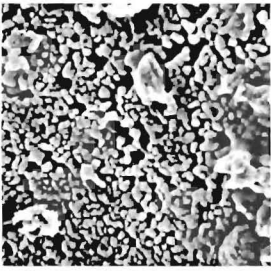
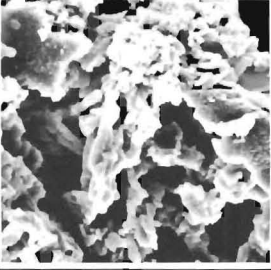
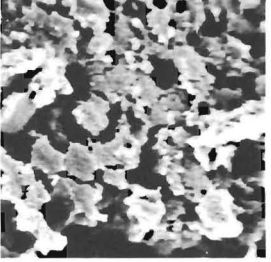
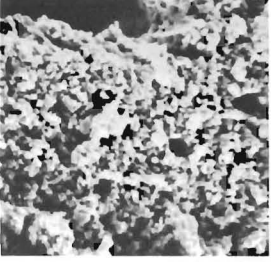
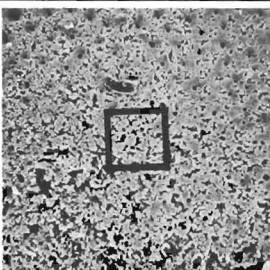
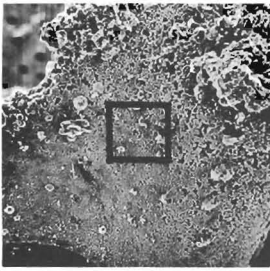
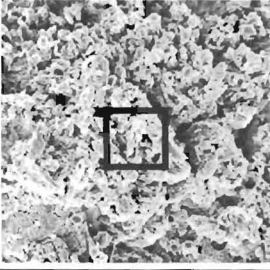
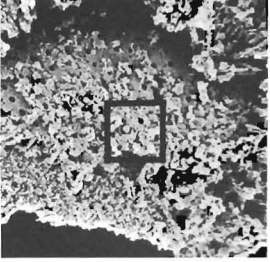
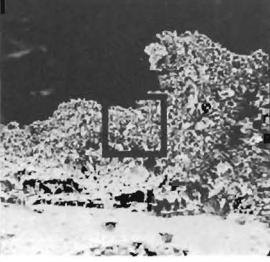
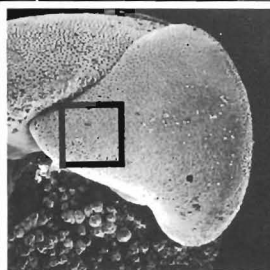
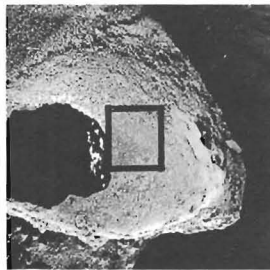
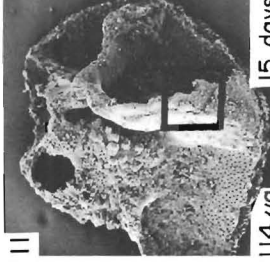
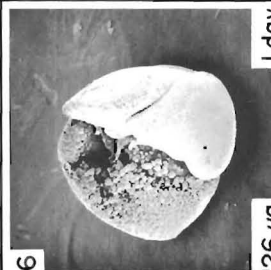
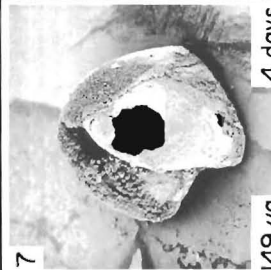
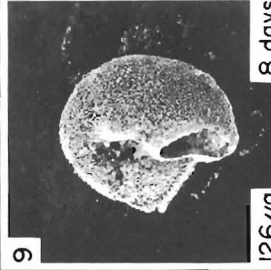
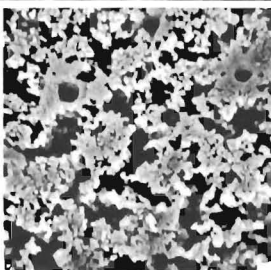
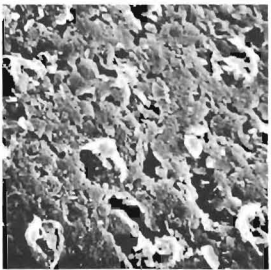
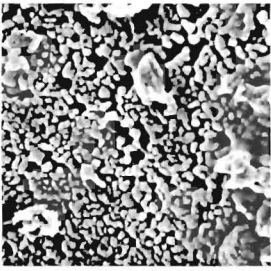
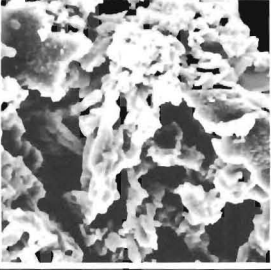
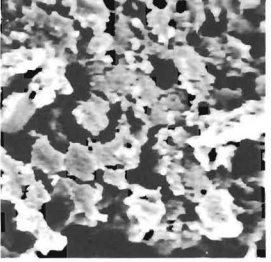
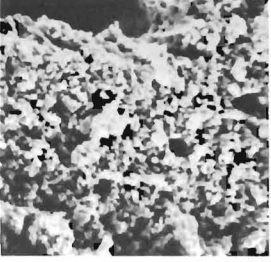
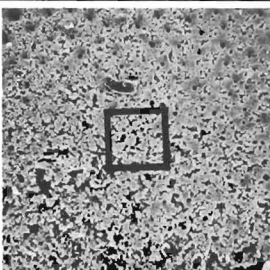
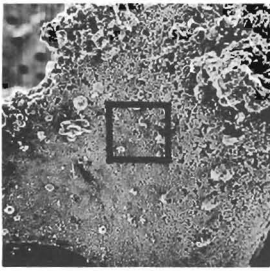
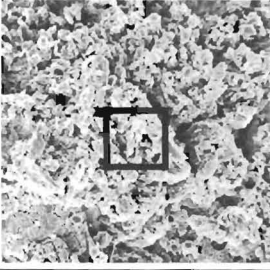
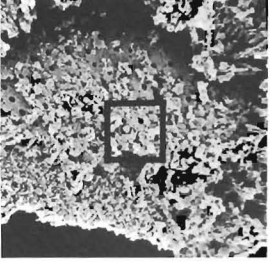
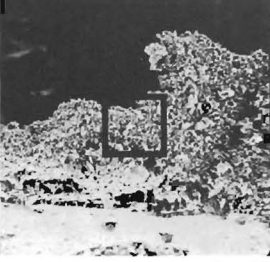
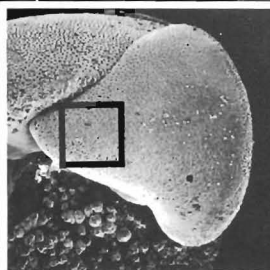
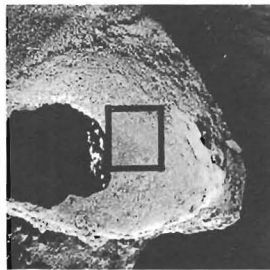
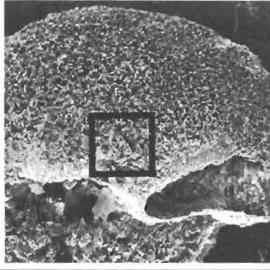
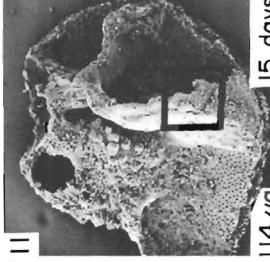
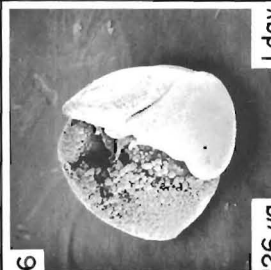
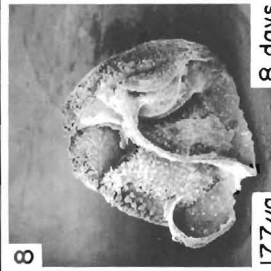
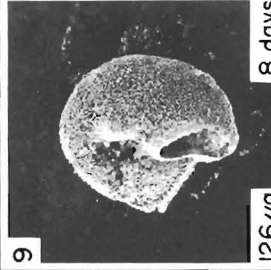
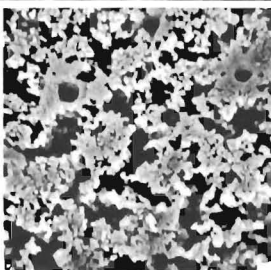
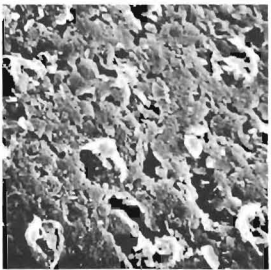
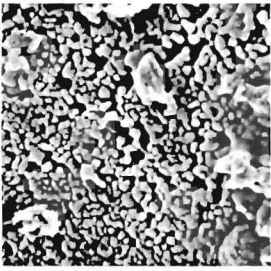
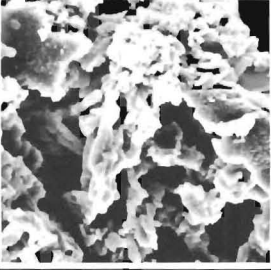
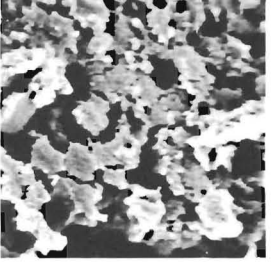
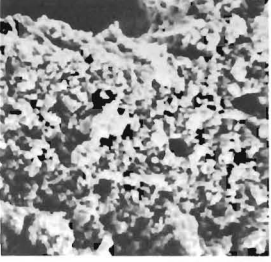
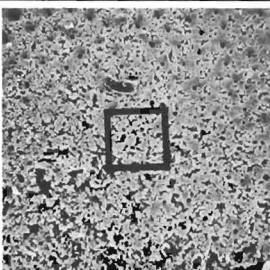
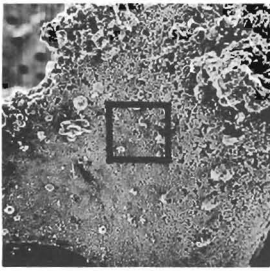
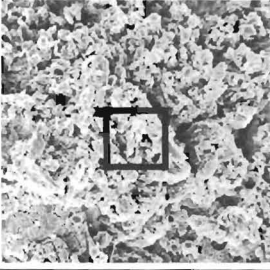
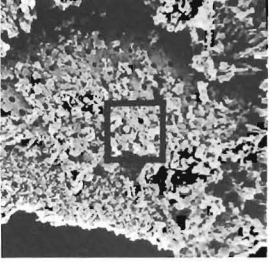
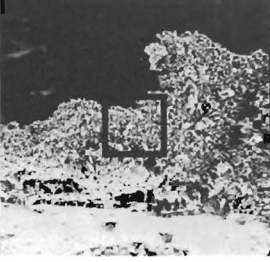
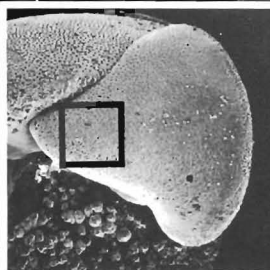
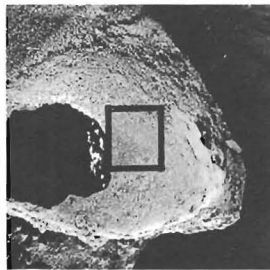
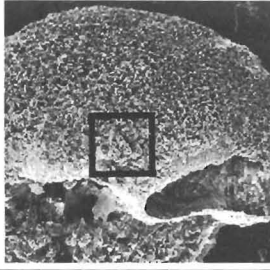
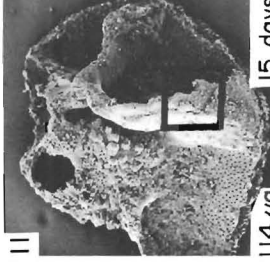
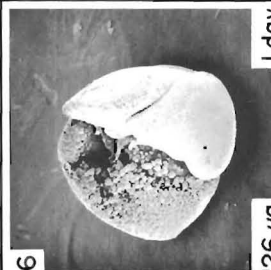
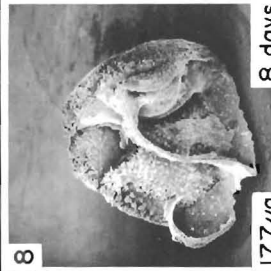
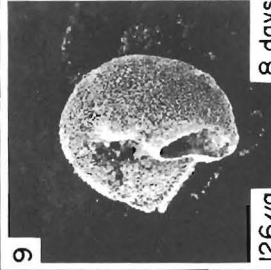
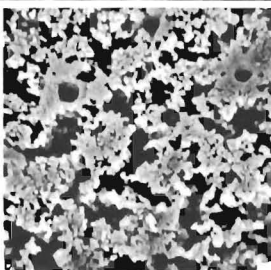
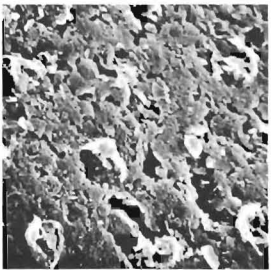
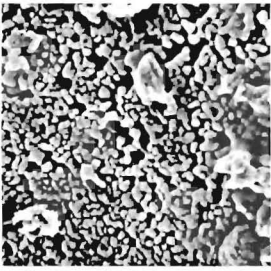
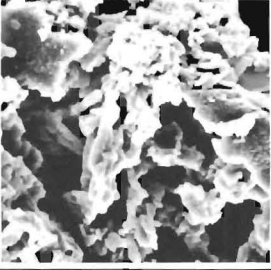
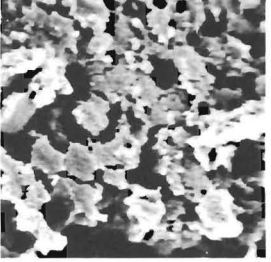
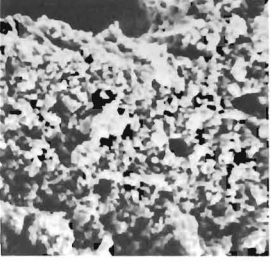
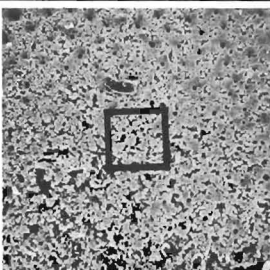
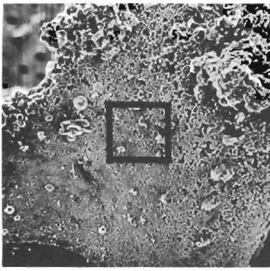
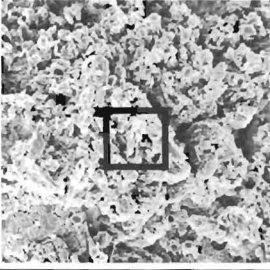
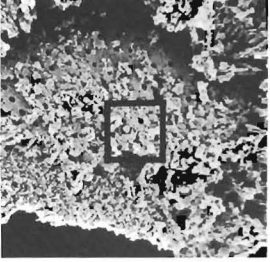
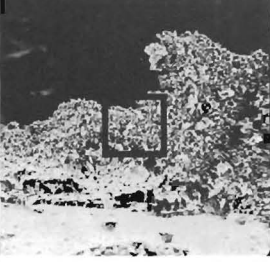
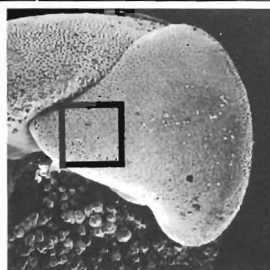
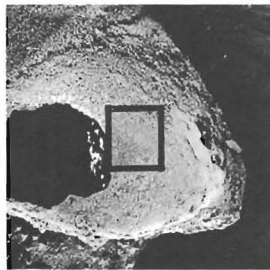
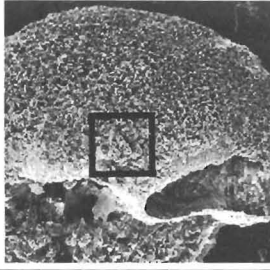
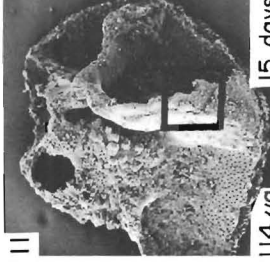
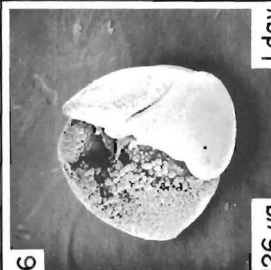
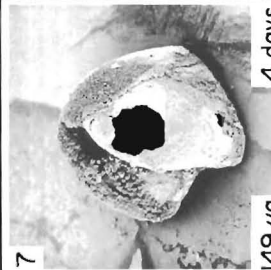
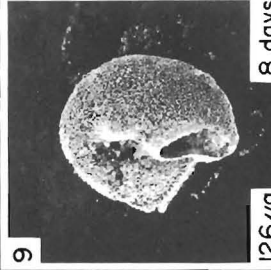
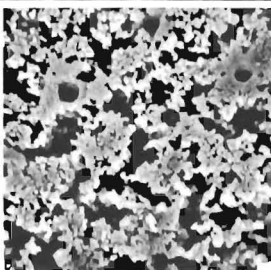
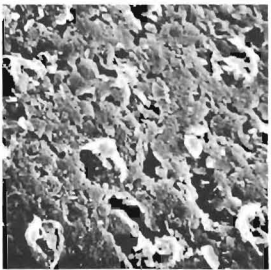
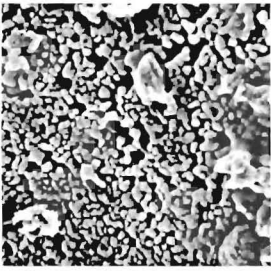
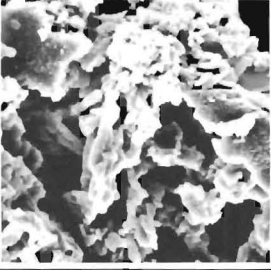
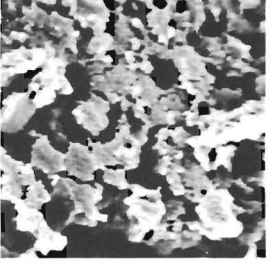
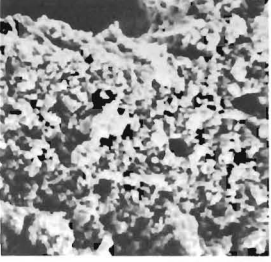
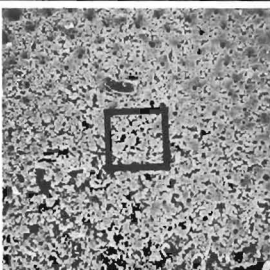
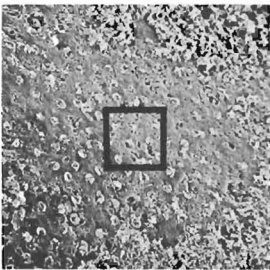
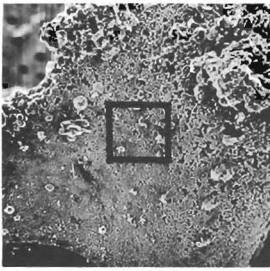
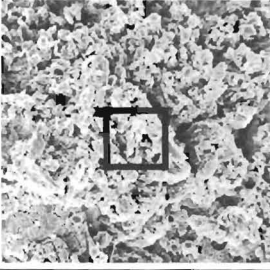
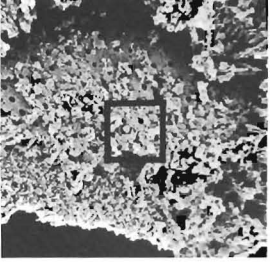
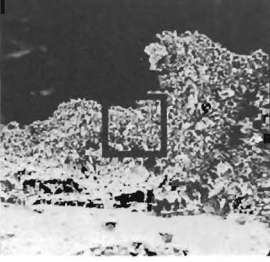
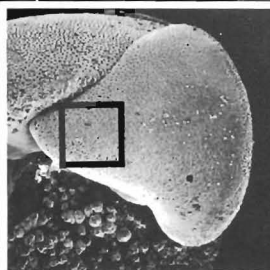
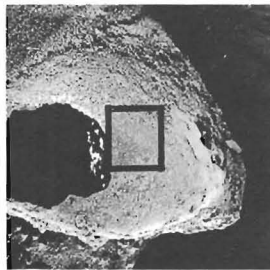
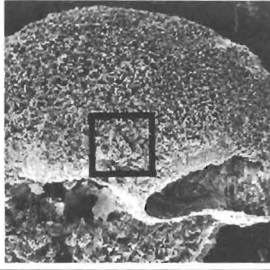
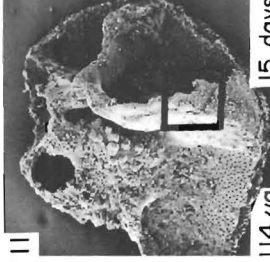
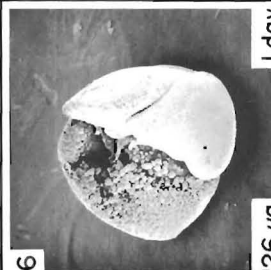
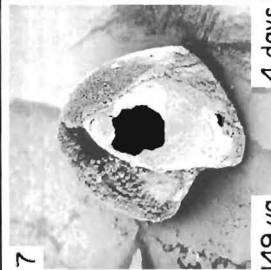
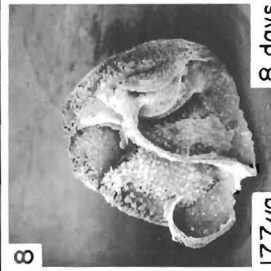
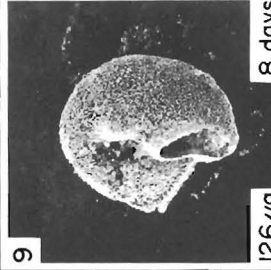
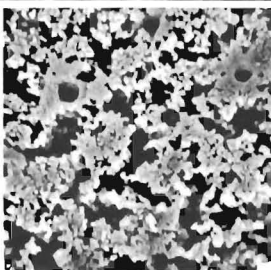
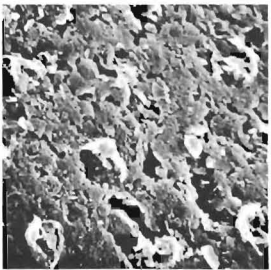
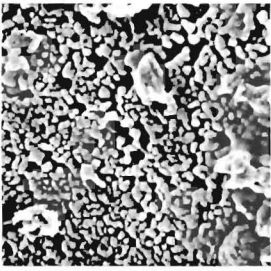
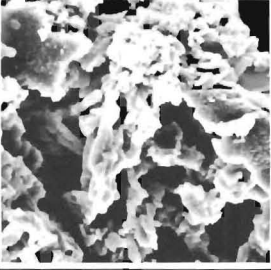
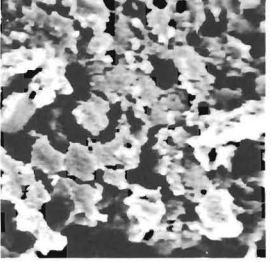
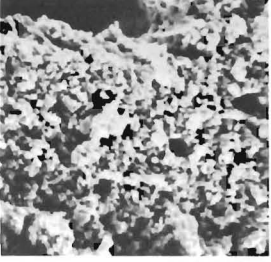
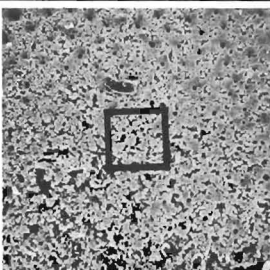
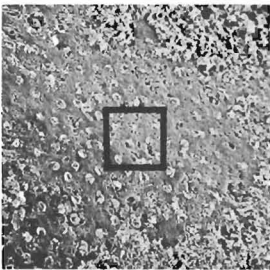
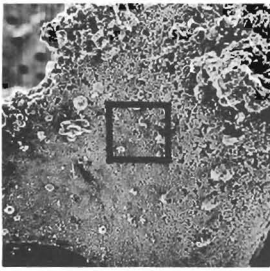
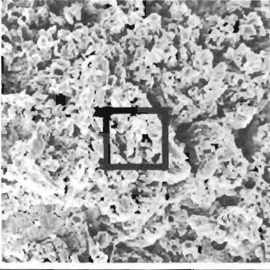
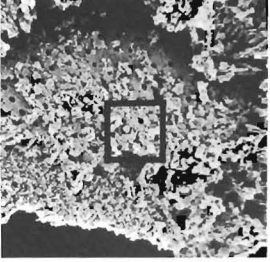
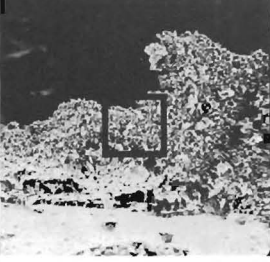
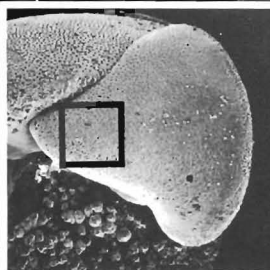
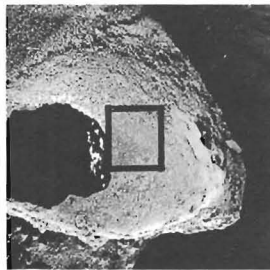
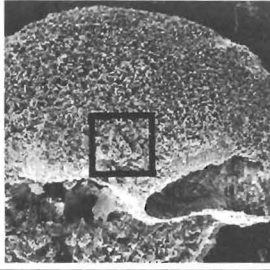
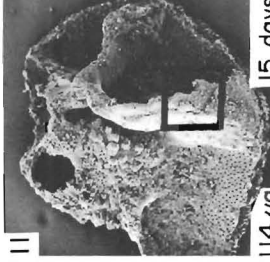
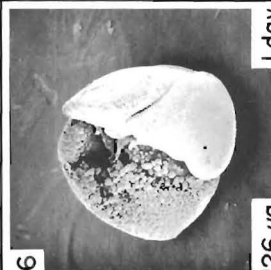
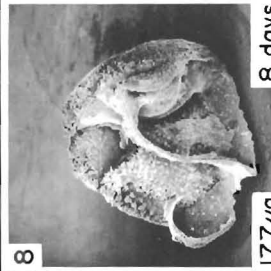
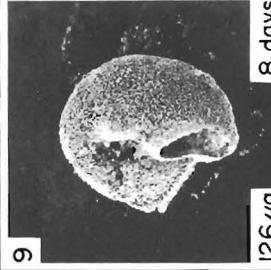
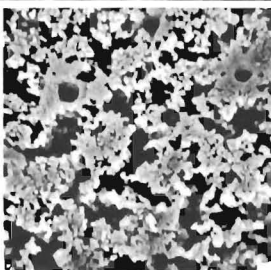
Experiment 1. Progressive ultrastructural breakdown in *Globorotalia truncatulinoides*, based on the dissolution of ten specimens in undersaturated sea water baths. The weights of individual specimens and the dissolution duration (in days)

are noted on the bottom figures; compare with text figure 1. (Note: the final chamber at 3% dissolution loss was intact after removal from the bath, but was accidentally broken during mounting on the SEM stub.)

# DISSOLUTION LOSS

	0%	3%	4%	5%	6%
<b>X 1700</b>					
<b>X 340</b>					
<b>X 68</b>					
<b>X 34</b>					
		1 157μg 1 day	2 149μg 1 day	3 148μg 1 day	4 140μg 1 day

# DISSOLUTION LOSS

	8%	20%	31%	39%	51%	83%
<b>X 1700</b>						
<b>X 340</b>						
<b>X 68</b>						
<b>X 34</b>						
						
						
						
						
						
						
						
						
						
						
						
						
						
						
						
						
						
						
						
						
						
						
						
						
						
						
						
						
						
						
						
						
						
						
						
						
						
						
						
						
						

#### EXPERIMENT 4

Because *Globorotalia truncatulinoides* exhibits great variability in surface texture that hinders comparisons between different specimens, we decided to study a species that has minimum surface texture variability. The species selected was *Pulleniatina obliquiloculata*, which in its adult stage secretes an extremely smooth outer layer or cortex that is homogeneous in texture. *Pulleniatina obliquiloculata* is one of the most resistant species to solution among the planktonic foraminifera according to Berger (1970).

The eight specimens of *P. obliquiloculata* from surface sediment sample V17-106 that were dissolved in an acetic acid bath and removed after successive 1-hour intervals show the following results (pl. 6):

1. Before the dissolution experiment (0 hr), *P. obliquiloculata*'s cortex surface texture is extremely smooth, but does reveal some slight etching and a few solution pits.
2. After 1 hour, pronounced etching is evident. The closed pores exhibit a "spider" suture pattern. The region between pores is composed of small rounded units.
3. After 2 hours, a small portion of the cortex (uppermost layer) begins to peel. An oblique view of the cortex shows that it is made up of small prismatic units. Etching of the interpore region has accentuated these small units and has obscured the pores.
4. After 3 hours, the "spider" suture pattern of the pores is still apparent. A "jig-saw puzzle" pattern occurs on the cortex veneer. Extensive corrosion has partly exposed an underlying layer.
5. After 4 hours, etching has further widened the spaces between the small units and a large number of pores are visibly enlarged.
6. After 5 hours, the final chamber is breached. Etching at this and subsequent stages have advanced to the point that the interpore units become needle-like prisms and big gashes have replaced the pores.
7. After 8 hours, large holes in the final and penultimate chambers have reduced the apparent surface area of the adult shell by about 40 percent.

8. In summary, dissolution of the initially very smooth cortex shows a progressive breakdown of the sub-rhombic units, proceeding from a homogeneously granular texture to a "jig-saw puzzle" pattern (3 hours) and deeply etched surface (4 hours) before the widened sutures further reduce the subrhombic units to needle-like prisms (5–8 hours).

It is interesting to note that *P. obliquiloculata* (as well as some other planktonic foraminiferal species) close off their pores completely in their gerontic growth stage. The physiological significance of this phenomenon is as yet unexplained.

#### EXPERIMENT 5

Nine specimens of *Orbulina universa* from sediment sample V17-106 were dissolved in separate flasks of undersaturated sea water for successively longer periods, ranging from 6 to 10 days, until their dissolution (weight) losses ranged from 15 to 47 percent.

The following results are evident from plate 7:

1. *Orbulina universa* is a less solution resistant species than *G. truncatulinoides* (pls. 3 and 4) or *P. obliquiloculata* (pl. 6), because *O. universa* shows more severe dissolution effects at all stages between 15 and 47 percent dissolution losses.
2. *Orbulina universa* undergoes the same sequence of ultrastructural changes as *G. truncatulinoides* and *P. obliquiloculata*. From an initially smooth surface texture (0%) etching produces deep sutures and a "jig-saw puzzle" pattern (24%) until finally needle-like prisms remain (27%). This process is repeated layer by layer, as seen at 36 percent dissolution loss when small remnants of an overlying layer appear as islands upon a "jig-saw puzzle" layer.
3. At 27 percent and higher dissolution losses, it is difficult to determine with certainty which layer is being examined. The peeling off of layers is particularly noticeable at the 28 and 44 percent stages.
4. At 28 percent and higher stages, the shells are cracked and fragmented.

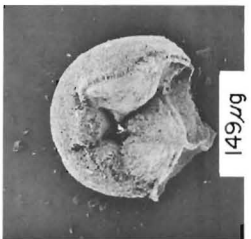
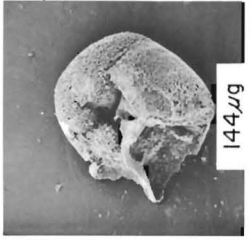
---

#### PLATE 4

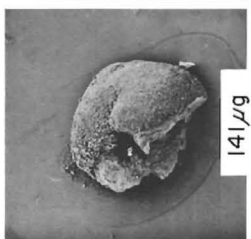
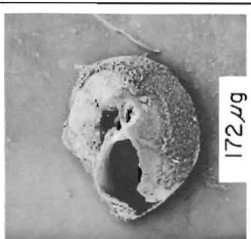
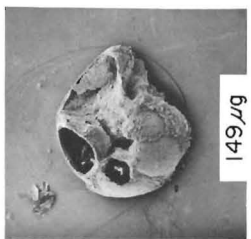
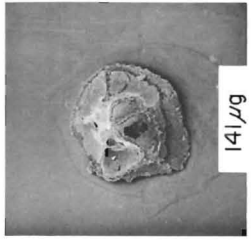
Experiment 2. Progressive dissolution of fourteen specimens of *Globorotalia truncatulinoides* in undersaturated seawater baths. The two bottom figures are of a *G. truncatulinoides*

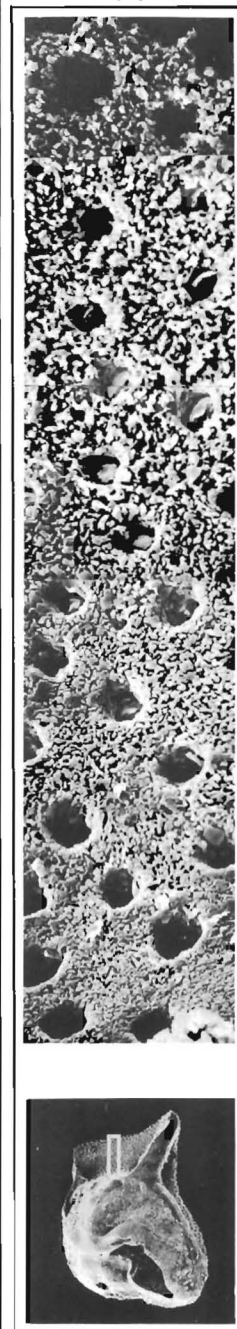
with 49 percent weight loss. The detail shows a gradation of progressively greater dissolution structures from left to right.

# DISSOLUTION LOSS

<b>22%</b>		<b>167 μg</b>
<b>28%</b>		<b>133 μg</b>
<b>29%</b>		<b>149 μg</b>
<b>38%</b>		<b>144 μg</b>
<b>42%</b>		<b>124 μg</b>
<b>46%</b>		<b>180 μg</b>

**X 30**

<b>57%</b>		<b>141 μg</b>
<b>61%</b>		<b>172 μg</b>
<b>71%</b>		<b>149 μg</b>
<b>76%</b>		<b>141 μg</b>
<b>81%</b>		<b>124 μg</b>



**X 60**

**X 1520**

# DISSOLUTION TIME

	0 hr.	.5 hr.	1 hr.	1.5 hrs.	2 hrs.	2.5 hrs.
<p><b>CHAMBER</b> F-3 X 540</p>						
<p><b>CHAMBER</b> F-1 X 1350</p>						
<p><b>CHAMBER</b> F X 1350</p>						
<p><b>FINAL (F)</b> <b>CHAMBER</b> X 270</p>						
<p><b>X 54</b></p>						

EXPERIMENT 6

In Experiment 6, four aliquots of a single natural assemblage of planktonic foraminifera were dissolved in the pH-stat for varying duration spanning from 4 to 40 hours until their dissolution losses ranged from 4.2 to 39 percent (table 2). It should be understood that the "undissolved" assemblage (0% dissolution loss) represents the initial assemblage, which may have undergone some natural dissolution on the sea floor prior to its collection.

The initial species assemblage as well as the four assemblages with progressively greater degrees of dissolution are listed in table 2. Arrows pointing to the left indicate species whose relative abundance decrease with increasing dissolution levels; they are therefore solution-prone species. Arrows pointing to the right are solution-resistant species whose relative abundance increases with increasing dissolution levels.

The following results can be interpreted from table 2 and plate 8:

1. Solution-prone species are: *Globigerina bulloides*, *G. falconensis*, *Globigerinita glutinata*, and *Globigerinoides ruber*.
2. Solution-resistant species are: *Globorotalia inflata*, *G. hirsuta*, *G. truncatulinoides*, *Globigerinoides conglobatus* and *Globigerinita humilis*. The relative sensitivity to dissolution of these two species groups is in general agreement with Berger's (1970) findings.
3. The percentage of shell fragments relative to the total fragmented and unfragmented shells in the 74-149 $\mu$  fraction increases with increasing dissolution level, i.e., from 20.5 to 88.5 percent.
4. The 39 percent dissolution loss sample has undergone dissolution to such an extent that only 17 specimens belonging to 11 species remained, while 15 species and varieties have disappeared. This has resulted in a disproportionate percentage increase for the remaining species and produced some

TABLE 2

Experiment 6. Changes in species composition of planktonic foraminifera (> 149 $\mu$  fraction) in four dissolution stages obtained by the pH-stat method. The initial, natural assemblage (0%) as well as the other four assemblages are from a single sediment sample. Arrows to left indicate solution-prone species; arrows to right are solution-resistant species. The 39 percent sample is too fragmented for a valid species composition. Compare with plate 8.

Species	Dissolution loss				
	0%	4.2%	9.5%	16%	39%
<i>Globoquadrina pachyderma</i> (left)	—	0.3	—	—	5.9
<i>Globoquadrina pachyderma</i> (right)	5.9	4.9	6.7	1.4	—
<i>Globigerinita humilis</i>	0.2	0.8	0.4	0.5	5.9
<i>Globigerina bulloides</i>	14.3	12.8	7.3	1.4	17.6
<i>Globigerina falconensis</i>	9.7	6.6	3.5	1.0	5.9
<i>Globorotalia inflata</i>	12.4	17.1	19.0	32.3	—
<i>Globigerina quinqueloba</i>	0.5	0.3	0.4	0.5	5.9
<i>Globorotalia hirsuta</i>	7.8	10.3	15.3	22.7	17.6
<i>Globorotalia truncatulinoides</i> (left)	6.7	12.0	14.9	19.8	11.8
<i>Globorotalia truncatulinoides</i> (right)	2.5	3.7	3.5	2.9	—
<i>Globorotalia sciutula</i>	1.7	2.6	1.5	—	5.9
<i>Globoquadrina dutertrei</i>	0.2	0.6	0.2	1.0	—
<i>Globigerinita glutinata</i>	9.2	1.1	0.9	—	11.7
<i>Pulleniatina obliquiloculata</i>	0.2	0.3	0.2	0.5	—
<i>Orbulina universa</i>	1.0	—	0.2	0.5	—
<i>Globigerina rubescens</i>	1.6	2.0	3.4	2.4	5.9
<i>Globigerinoides tenellus</i>	1.3	0.6	0.4	—	—
<i>Globigerinoides ruber</i> (pink)	0.6	0.6	—	—	—
<i>Globigerinoides ruber</i> (white)	15.9	20.0	18.5	9.2	—
<i>Globigerina digitata</i>	0.2	—	—	—	—
<i>Globigerinella aequilateralis</i>	2.4	—	—	—	—
<i>Globigerinella calida</i>	3.7	0.8	—	—	5.9
<i>Globorotalia menardii</i>	0.6	0.6	1.5	0.5	—
<i>Globorotalia umida</i>	—	—	0.2	—	—
<i>Globigerinoides sacculifer</i>	1.4	1.7	0.9	1.0	—
<i>Globigerinoides conglobatus</i>	—	0.3	1.1	2.4	—
Total	100.0	100.0	100.0	100.0	100.0
No. specimens counted	628	350	464	207	17
% of shell fragments in 74-149 $\mu$ fraction	20.5	47.2	49.5	57.3	88.5

←

PLATE 5

Experiment 3. Progressive dissolution of a single specimen of *Globorotalia truncatulinoides* in acetic acid bath. The same areas of the final chamber (see squares) as well on the ante-

penultimate (F-1) and F-3 chambers (see arrows) are viewed at various magnifications at each successive dissolution stage.

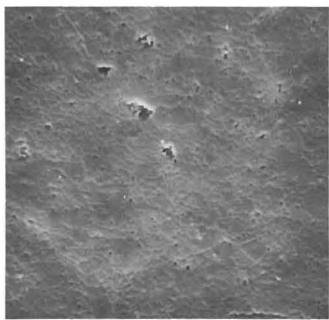
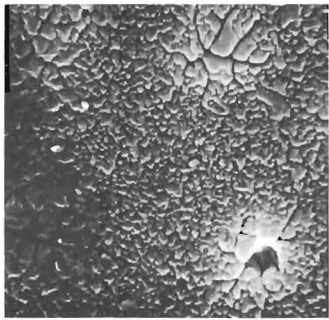
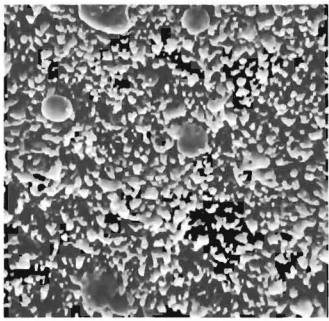
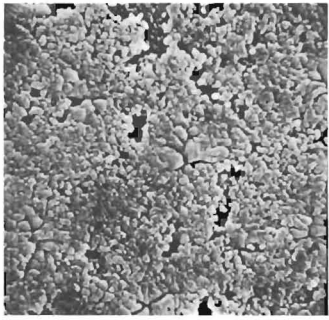
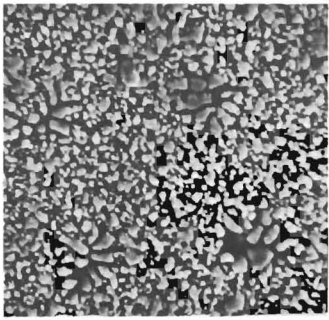
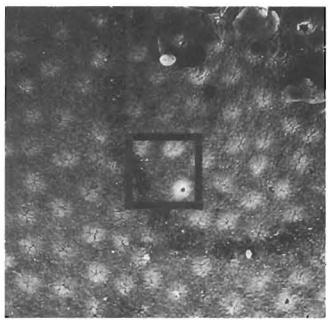
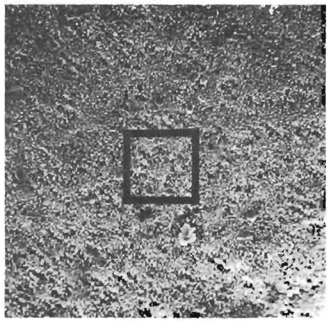
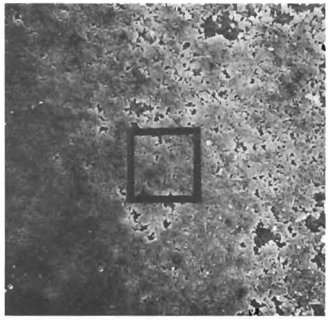
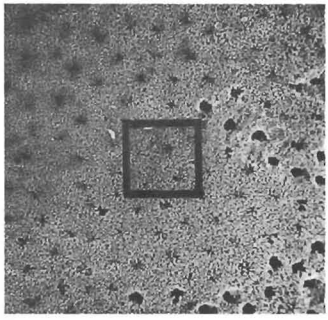
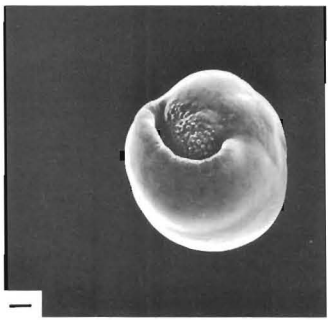
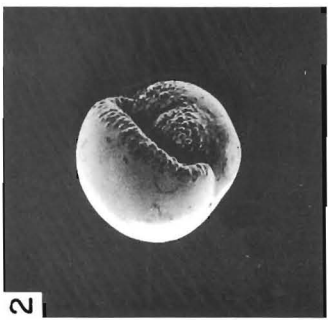
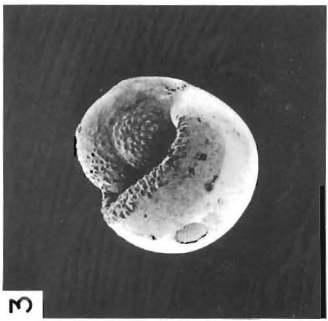
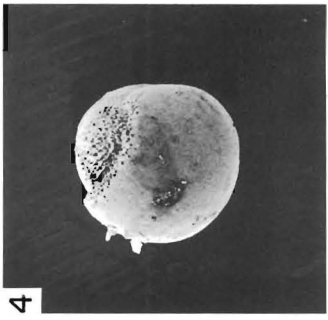
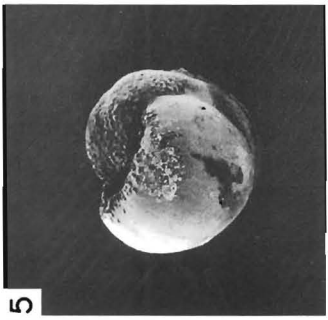
→

PLATE 6

Experiment 4. Progressive dissolution of eight specimens of *Pulleniatina obliquiloculata* in an acetic acid bath. Ultrastructural details of the final chamber of each specimen are viewed

at  $\times 400$  and  $\times 2,000$  magnification. Specimen no. 1 was not reacted and serves as a control.

# DISSOLUTION TIME

	0 hr.	1 hr.	2 hrs.	3 hrs.	4 hrs.
X 2000					
X 400					
X 40					

# DISSOLUTION TIME

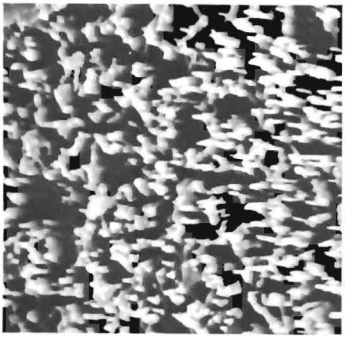
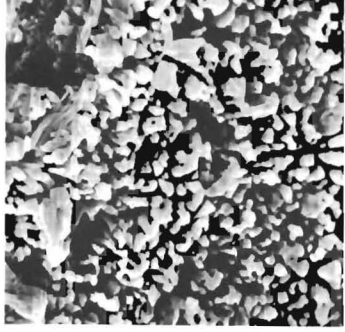
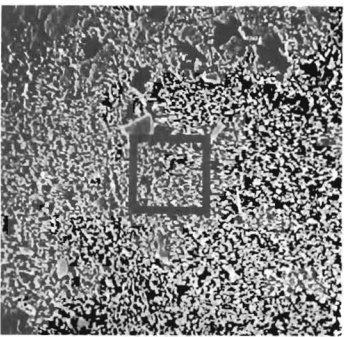
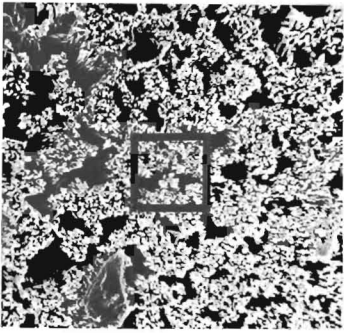
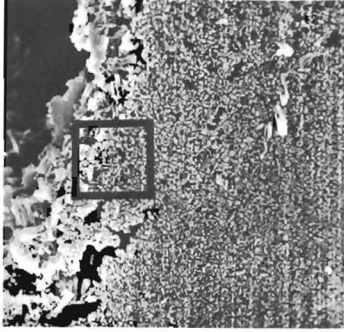
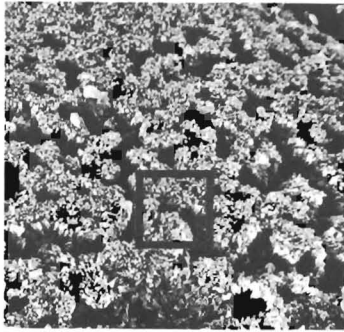
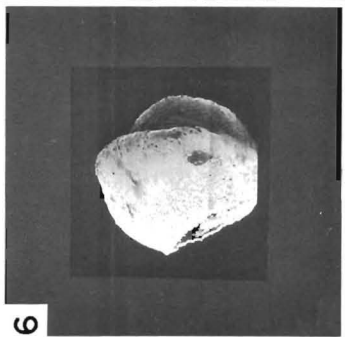
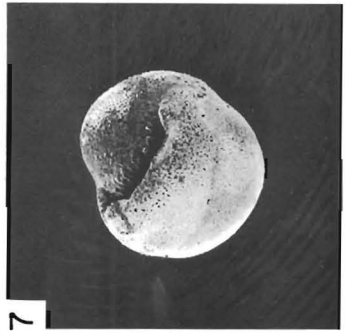
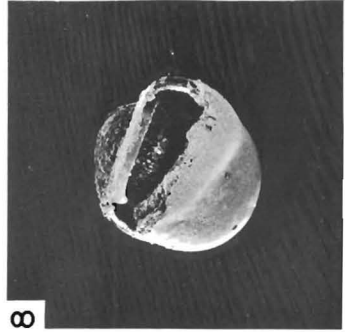
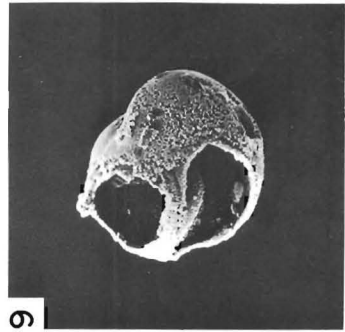
	5 hrs.	6 hrs.	7 hrs.	8 hrs.
<b>X 2000</b>				
<b>X 400</b>				
<b>X 40</b>				

TABLE 3

Species composition of planktonic foraminifera (< 149 $\mu$  fraction) in four natural assemblages of various depths in the west-central North Atlantic. The faunal variations are interpreted to be largely due to natural dissolution. Arrows to left indicate solution-prone species; arrows to right are solution-resistant species.

Species	1575m V20-248	2743m V7-65	4803m V26-172	5546m V26-9
<i>Globoquadrina pachyderma</i> (left)	—	—	—	1.0
<i>Globoquadrina pachyderma</i> (right)	6.9	0.6	2.6	2.5
<i>Globigerinita humilis</i>	[ —	0.3	0.7	1.3] $\blacktriangleright$
<i>Globigerina bulloides</i>	16.0	17.9	18.6	11.3
<i>Globigerina falconensis</i>	$\blacktriangleleft$ [ 8.8	3.3	3.3	— ]
<i>Globorotalia inflata</i>	[ 10.1	4.2	10.9	39.5] $\blacktriangleright$
<i>Globigerina quinqueloba</i> (left)	—	—	0.1	—
(right)	—	—	0.6	—
<i>Globorotalia hirsuta</i>	4.3	6.8	4.0	8.8
<i>Globorotalia</i> <i>truncatulinoides</i> (left)	6.8	12.7	6.4	0.6
(right)	1.1	0.6	1.0	—
<i>Globorotalia scitula</i>	$\blacktriangleleft$ [ 0.2	0.3	—	— ]
<i>Globoquadrina dutertrei</i>	0.9	1.0	0.9	—
<i>Globigerinita glutinata</i>	6.5	8.1	8.1	1.0
<i>Pulleniatina</i> <i>obliquiloculata</i>	0.9	—	0.1	0.6
<i>Orbulina universa</i>	0.4	2.3	1.7	0.3
<i>Globigerina rubescens</i>	1.4	3.2	0.7	—
<i>Globigerinoides tenellus</i>	0.7	1.6	2.0	—
<i>Globigerinoides ruber</i> (pink)	1.1	1.0	1.2	—
(white)	[ 21.8	21.8	28.5	29.8] $\blacktriangleright$
<i>Globigerina digitata</i>	0.2	0.3	0.1	0.3
<i>Globigerinella</i> <i>aequilateralis</i>	$\blacktriangleleft$ [ 4.3	5.9	2.0	0.6 ]
<i>Globigerinella calida</i>	$\blacktriangleleft$ [ 4.1	4.6	2.0	0.6 ]
<i>Hastigerina pelagica</i>	$\blacktriangleleft$ [ 0.2	0.3	—	— ]
<i>Globorotalia menardii</i>	0.2	1.0	0.3	0.3
<i>Globorotalia tumida</i>	0.2	—	—	—
<i>Globigerinoides sacculifer</i> w/out sac	2.7	0.6	2.4	0.6
with sac	—	0.3	1.3	—
<i>Globigerinoides</i> <i>conglobatus</i>	—	1.3	0.4	0.9
<i>Globigerinita iota</i>	0.2	—	0.1	—
Total .....	100.0	100.0	100.0	100.0
No. of specimens counted	445	308	701	319

confusing trends. For example, the curious presence of some weakly resistant species, such as *G. bulloides*, *G. falconensis*, *G. glutinata*, *G. rubescens*, and *G. calida*, in the 39 percent sample has increased their percentages to an artificially high de-

gree. Thus, only the first four assemblages are useful for indicating trends of relative resistance to dissolution for the individual species.

## NATURAL OBSERVATIONS

### NATURAL ASSEMBLAGES

In order to observe the effect of natural dissolution on planktonic foraminiferal assemblages on the sea floor, we compared four surface sediment samples from successively greater water depths and close proximity to each other. The assemblages selected are from core-top samples of 1,575 m, 2,743 m, 4,803 m and 5,546 m depths and are located within a relatively stable oceanic region of the west-central North Atlantic. The shallowest sample (V20-248) comes from the slope of Muir Seamount. V7-65 (2,743 m) and V26-172 (4,803 m) are from the slope and base of the Bermuda Pedestal. V26-9 (5,546 m) is the nearest and deepest surface sediment sample available to us and is located in the Sohm Abyssal Plain about 820 km east of Bermuda. The latter sample is very near the calcite compensation depth, which in this region is at about 5,500 m according to Berger and Winterer (1974). Assuming that the surface sediment samples represent recent-most, undisturbed death assemblages and that the faunal composition at these four locations was originally similar, we would expect to see a trend of increasing dissolution with greater depth that would selectively preserve the robust shells and destroy the fragile ones (Berger, 1968; Ruddiman and Heezen, 1967). The results do not indicate such clear-cut trends, as we interpret the following findings from table 3:

1. Only 8 out of 25 species show well-defined trends towards selective dissolution. Of these, *Globorotalia inflata* and *Globigerinita humilis* are highly solution-resistant species, whereas *Globigerina falconensis*, *Globorotalia scitula*, *Globigerinella aequilateralis*, *G. calida* and *Hastigerina pelagica* are solution-prone species. In general, they agree with Berger's species ranking (1970).
2. *Globigerinoides ruber's* percentage increase with increasing depth makes it a solution-resistant species, thus contradicting Berger's ranking as well as our Experiment 6 results. Our scanning electron micrographs of *G. ruber* from 5,546 m depth show that it is of small size (<200 $\mu$ ) with restricted apertures and encrusted with euhedral crystallites (pl. 9, figs. 1, 2). The calcite crust has most likely protected it from dissolution. These specimens are unlike

the normal *G. ruber*, which generally has thin walls and large apertures. If the calcite crust of *G. ruber* is secreted at relatively deep levels, as it is believed to be the case for other planktonic foraminiferal species (Bé and Lott, 1964), we must then revise our present consideration of this species as exclusively a surface dweller.

3. It is noteworthy that we observed in the natural assemblages *Globorotalia inflata* and *Globorotalia truncatulinoides* with calcite crusts, whose inner chamber were dissolved (pl. 9, figs. 3 and 4). This contrasts with the observations in Experiments 1 and 2 in which the chambers of the final whorl of *G. truncatulinoides* were dissolved first and the inner chambers were still intact. The significance of these two types of shell preservation is discussed in more detail in the section on specimen orientation (p. 30).
4. The lack of clear-cut trends either towards or against solution resistance may partly be due to the high species diversity in this region and also due to the small number of samples examined.

#### COMPARISON OF RESULTS BETWEEN EXPERIMENTAL AND NATURAL DISSOLUTION ASSEMBLAGES

We have compared the relative abundances of the species listed in tables 2 and 3 in order to determine to what extent the laboratory results conform with field observations. In the following list we have assigned each species into three categories: + for solution-resistant species, showing increase in relative abundance

in more dissolved samples and greater water depths; – for solution-prone species, showing decrease in relative abundance in more dissolved samples and greater water depths; and 0 for species showing inconclusive trends in either direction:

Species	Laboratory Experiments	Natural Assemblages
1. <i>Globigerina falconensis</i>	–	–
2. <i>Globigerinella aequilateralis</i>	–	–
3. <i>Globigerinella calida</i>	–	–
4. <i>Hastigerina pelagica</i>	–	–
5. <i>Globorotalia scitula</i>	0	–
6. <i>Globigerinita glutinata</i>	–	0
7. <i>Globigerinoides tenellus</i>	–	0
8. <i>Globigerinoides ruber</i> (pink)	–	0
9. <i>Globigerina bulloides</i>	–	0
10. <i>Globoquadrina pachyderma</i>	0	0
11. <i>Globoquadrina dutertrei</i>	0	0
12. <i>Globigerina quinqueloba</i>	0	0
13. <i>Pulleniatina obliquiloculata</i>	0	0
14. <i>Orbulina universa</i>	0	0
15. <i>Globigerina rubescens</i>	0	0
16. <i>Globigerina digitata</i>	0	0
17. <i>Globorotalia menardii</i>	0	0
18. <i>Globorotalia tumida</i>	0	0
19. <i>Globigerinoides sacculifer</i>	0	0
20. <i>Globigerinita iota</i>	–	0
21. <i>Globigerinita humilis</i>	0	+
22. <i>Globorotalia hirsuta</i>	+	0
23. <i>Globorotalia truncatulinoides</i>	+	0
24. <i>Globigerinoides conglobatus</i>	+	0
25. <i>Globorotalia inflata</i>	+	+
26. <i>Globigerinoides ruber</i> (white)	–	+

The above-mentioned results indicate that the majority of the species do not show good agreement in relative abundance trends between the two sets of

#### PLATE 7

Experiment 5: Progressive dissolution of nine specimens of *Orbulina universa* in undersaturated sea-water baths. Specimen

no. 1 serves as a control.

#### PLATE 8

Experiment 6. Progressive dissolution by the pH-stat method of four assemblages of planktonic foraminifera from the same sediment sample (V17-106). Dissolution (weight) losses ranged from 4.2 to 39 percent. The 0 percent sample serves as a con-

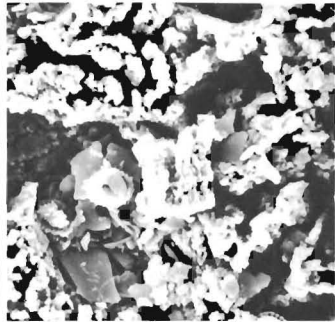
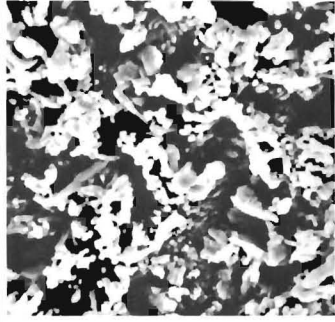
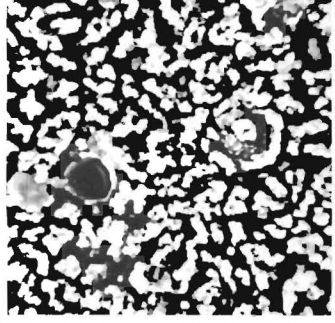
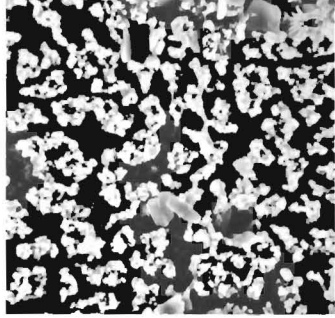
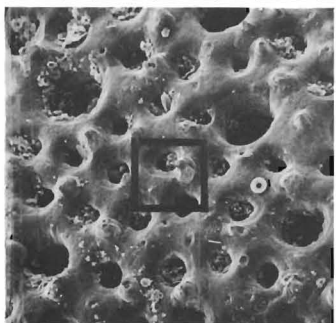
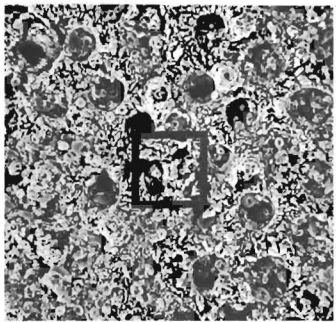
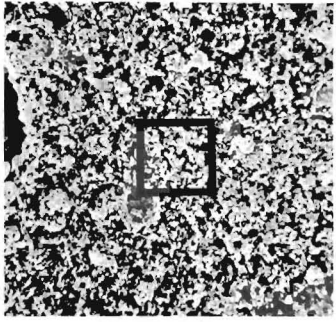
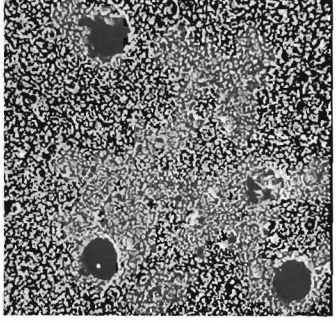
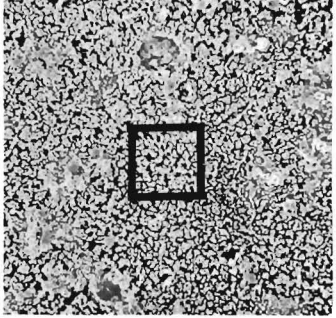
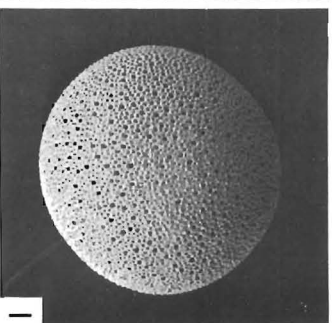
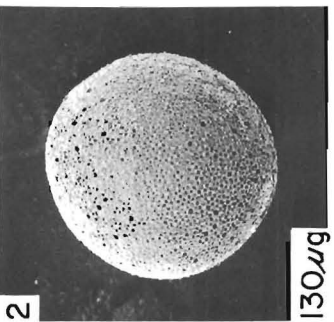
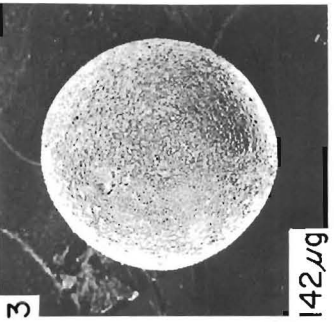
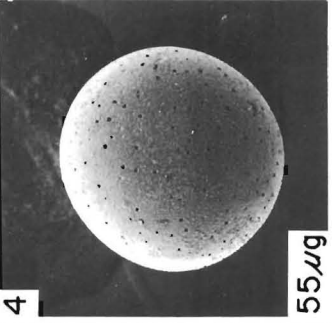
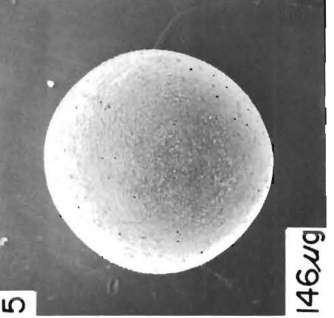
trol. Note the selective preservation of *Globorotalia* species in the 9.5 and 16 percent samples and the increase in fragmentation with greater dissolution. All views are magnified  $\times 19$ .

#### PLATE 9

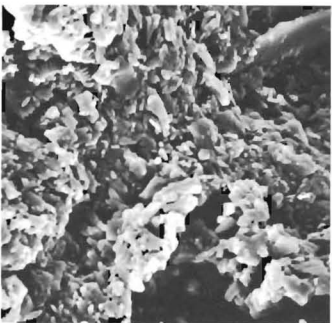
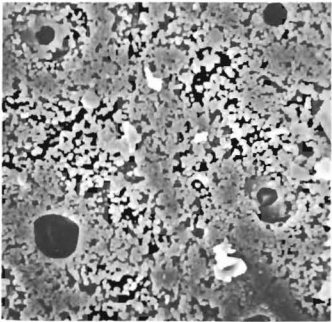
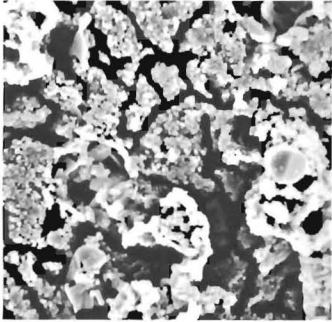
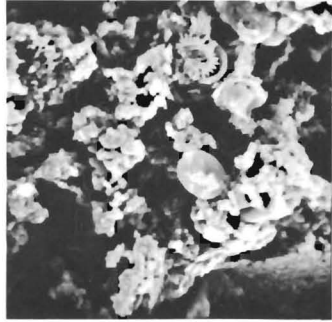
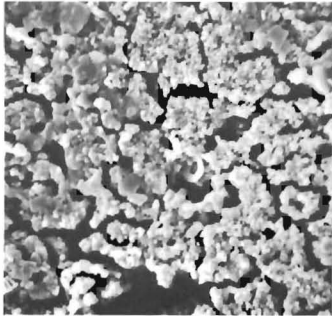
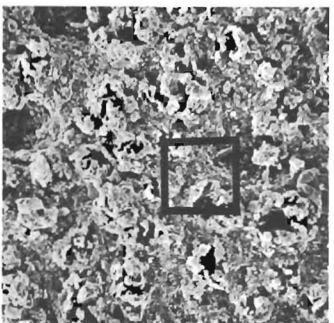
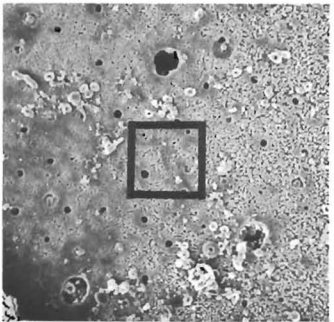
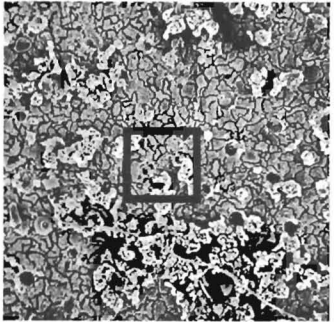
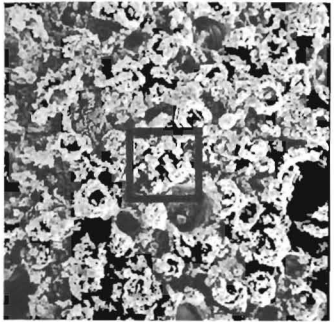
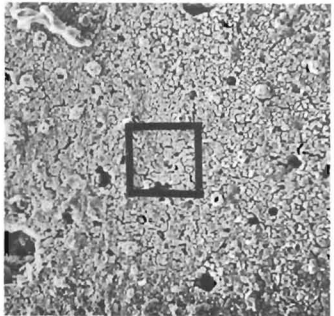
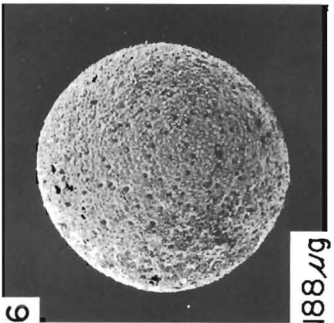
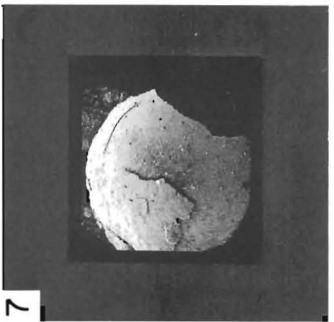
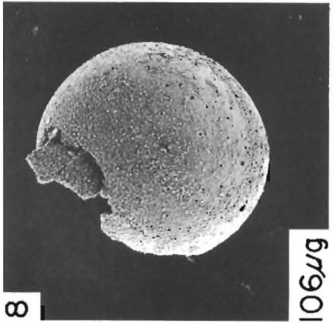
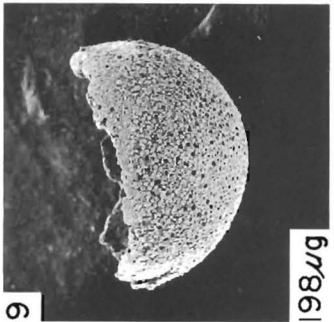
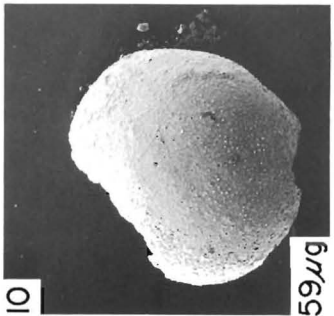
- 1, 2 *Globigerinoides ruber* of small size (188 $\mu$  length) with abnormally thick calcite crust. The abundance of this species at great depth (5,546 m) in sample V26-9 is unusual. 1,  $\times 395$ . 2,  $\times 1,575$ .
- 3, 4 *Globorotalia inflata* (left) and *Globorotalia truncatuli-*

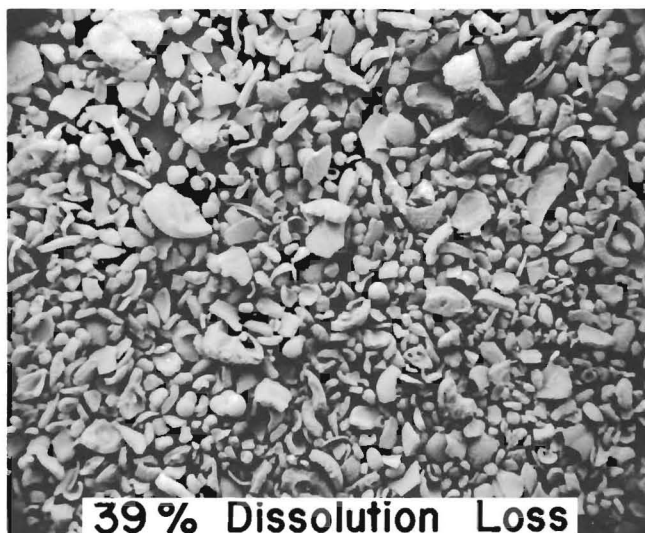
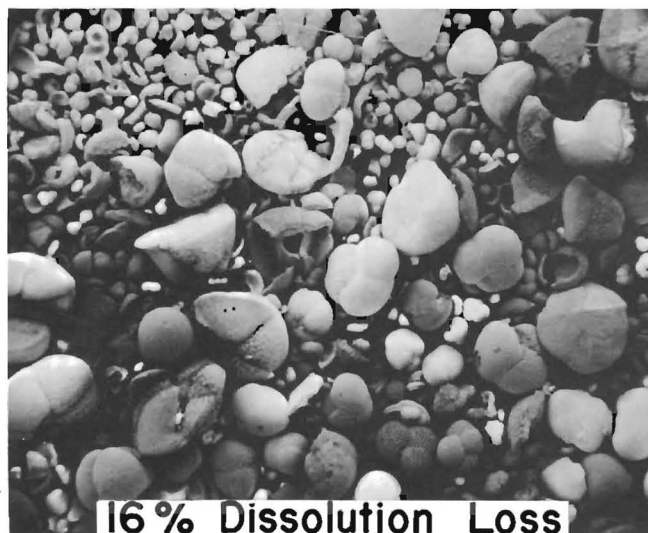
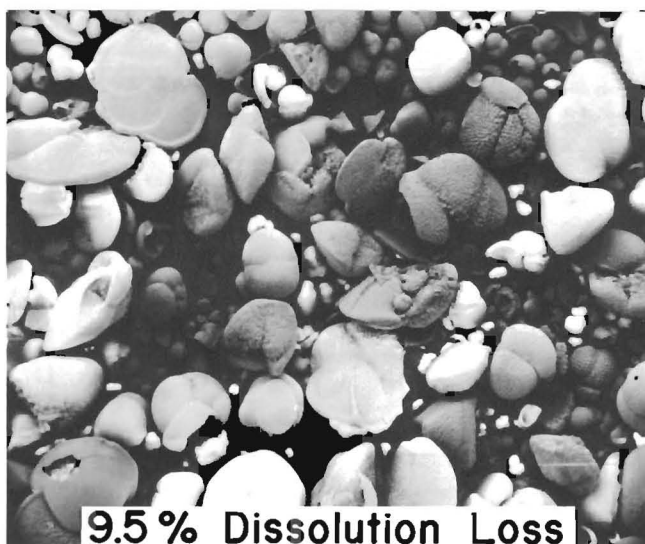
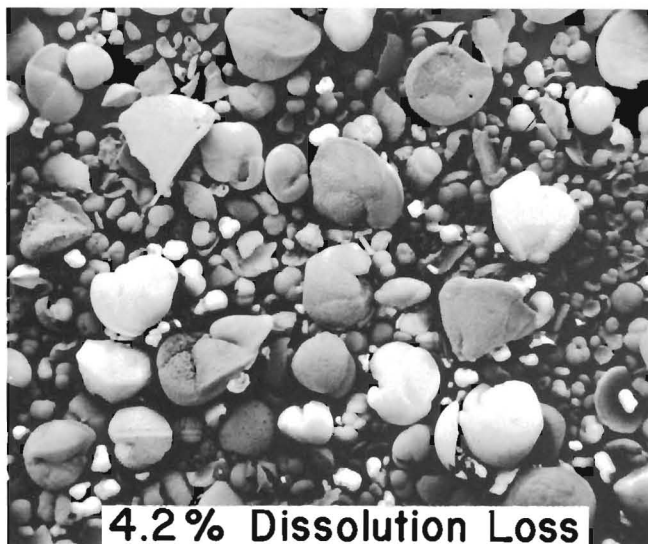
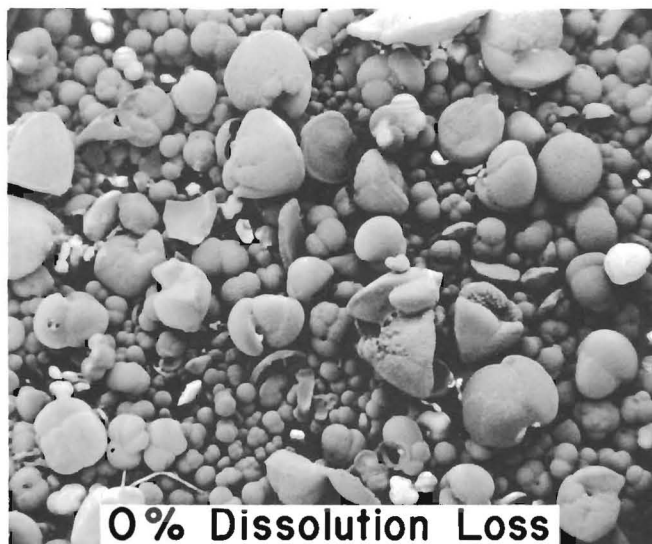
*noides* (right) from RC11-99 TW Top, lat 46°31'S, long 61°02'E, 4,449 m depth, showing dissolution of inner chambers and well-preserved outer calcite crust. Compare with plate 4. 3 and 4 both  $\times 175$ .

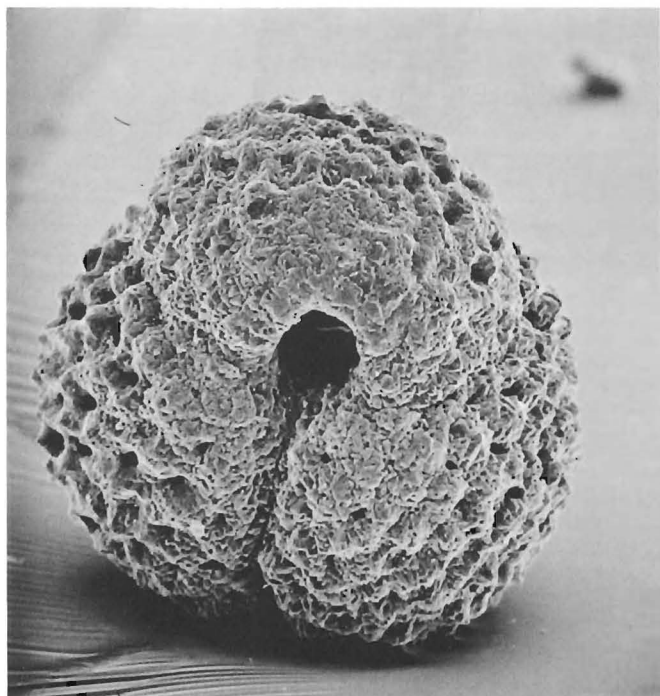
# DISSOLUTION LOSS

	0%	15%	18%	20%	24%
<b>X 2000</b>					
<b>X 400</b>					
<b>X 40</b>					
	1	2	3	4	5
		130 μg	142 μg	55 μg	146 μg

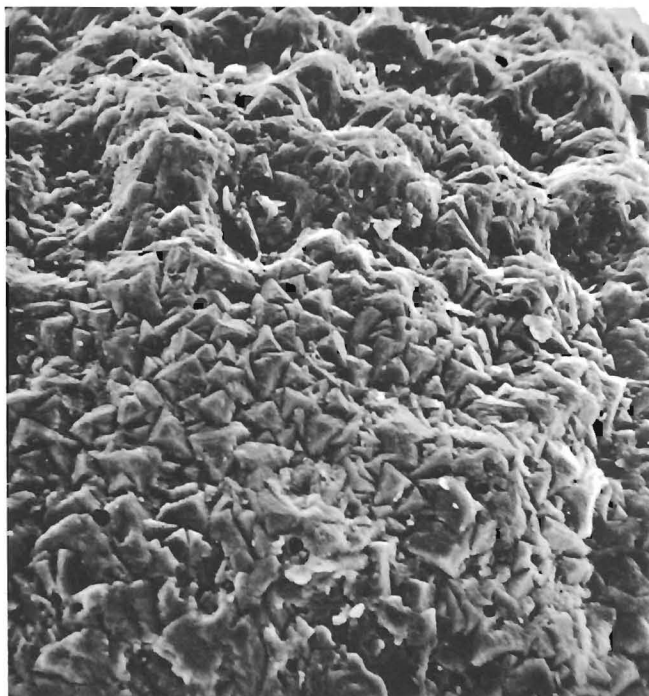
# DISSOLUTION LOSS

	27%	28%	36%	44%	47%
<b>X 2000</b>					
<b>X 400</b>					
<b>X 40</b>	 188µg	 106µg	 98µg	 59µg	 10µg

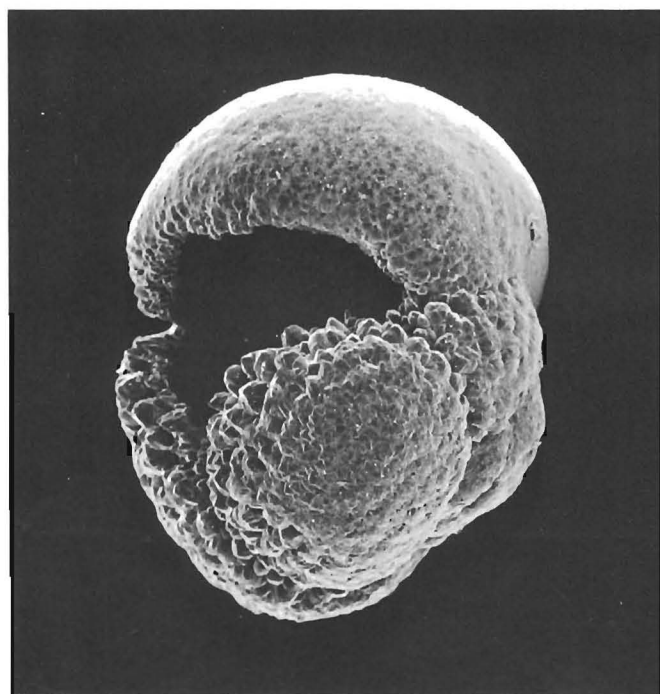




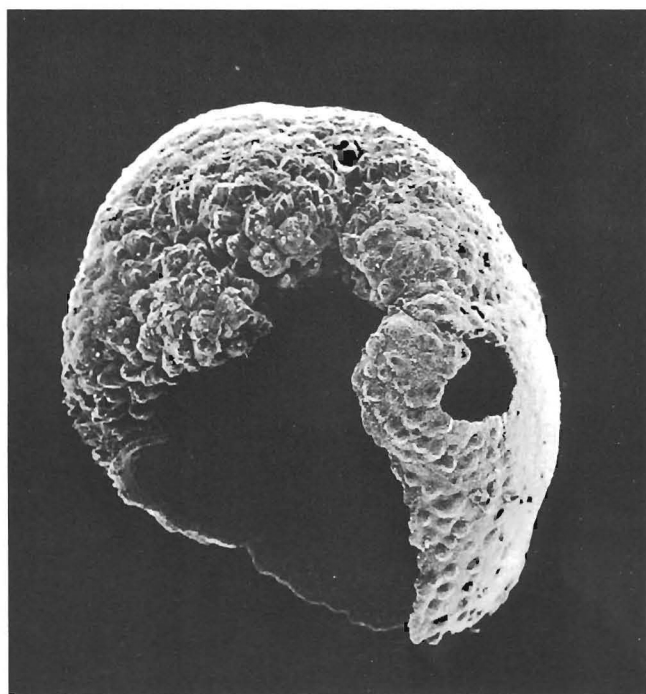
1



2



3



4

observations. Best agreement is apparent for *Globorotalia inflata* as a solution-resistant species, and for *Globigerina falconensis*, *Globigerinita glutinata*, *Globigerinella aequilateralis*, and *G. calida* for solution-prone species.

*Globigerinoides ruber* is an enigmatic species that was weakly solution-resistant in laboratory experiments, but appeared in increasingly greater percentages in the four samples from progressively greater depths. We believe, however, that the great majority of *G. ruber* has a thin shell that should be considered highly susceptible to dissolution and that the thick-walled variety is relatively rare and selectively preserved on occasion.

#### SINGLE SPECIES

As a final project, we examined the relationship between dissolution and ultrastructural changes in the smooth cortex of *Pulleniatina obliquiloculata* from successively deeper depths. We selected specimens from the same samples as in the previous discussion, except for the substitution of V7-65 (2743 m) by V17-106 SBT (3,400 m). Our reason for selecting *P. obliquiloculata*, partly explained in Experiment 4, is to explore the possibility that this species could serve as a "solution indicator" for the degree of dissolution that a foraminiferal assemblage may have undergone on the seafloor. Our results shown in plate 10 indicate that such a possibility may exist.

*Pulleniatina obliquiloculata* from 1,575 m depth had uniformly smooth cortex surfaces which showed no or little solution pitting. *Pulleniatina obliquiloculata* from 3,400 m depth had considerable solution etching, but retained many patches of the cortex (dark gray areas in the  $\times 1,665$  magnification). *Pulleniatina obliquiloculata* from 4,803 m depth was deeply etched and revealed a predominantly triangular pattern of rhombic crystallite units. *Pulleniatina obliquiloculata* from 5,546 m depth showed the beginning of larger lines of weakness, large solution pits and rounding of the rhombic crystallites.

We were unable to find any severely corroded specimens of *P. obliquiloculata* in these four surface sediment samples. However, we did encounter such speci-

mens in core V16-25 at the 245 cm and 285 cm levels representing approximately the Early Wisconsin Glacial Stage (about 70,000 and 78,000 Y. B. P.) in the western equatorial Atlantic (Bé, Damuth, Lott and Free, in press). The cortex in the final chambers of these *P. obliquiloculata* exhibited extremely deep solution etching, widening of the pores and loss of identity of the rhombic crystallites (pl. 10). The highly corroded ultrastructure in the right-most specimen from core V16-25 (245 cm) closely resembles the needle-like prisms that remain of the cortexes in specimens which have undergone experimental dissolution (pl. 6).

Our present results are still fragmentary, but sufficiently promising to warrant further investigations towards the potential application of certain planktonic foraminiferal species as indicators of the degree of dissolution of  $\text{CaCO}_3$  on the sea floor.

#### SUMMARY

The results of this investigation indicate that laboratory experiments on the dissolution of foraminiferal shells can yield meaningful results for the interpretation of dissolution under natural conditions. Three different experimental methods all gave results which were in close agreement with observations on natural material. These experiments indicate that it is possible to quantify the extent of dissolution based on surface morphology. Species with generally homogeneous surface textures (e.g., *Pulleniatina obliquiloculata*) are much better for this purpose than other species with variable surface textures (e.g., *Globorotalia truncatulinoides*). Future work may allow the selection of key species from poorly, moderately and highly solution-resistant classes of foraminifera as dissolution indicators. This should provide a much more precise method for the determination of dissolution than the present species ratio methods.

An interesting supplementary finding, that is undergoing further investigation, is that hydrodynamic factors at the time of deposition influence the orientation of the shells (at least for *G. truncatulinoides*). This in turn is reflected in the dissolution morphology of

---

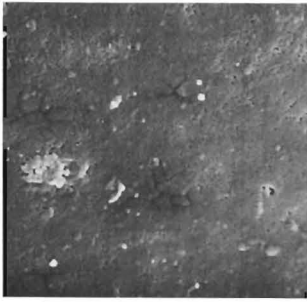
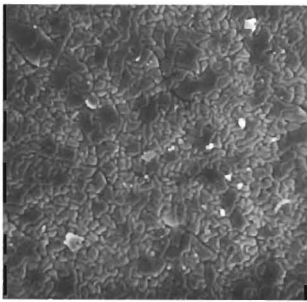
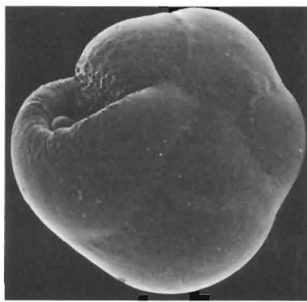
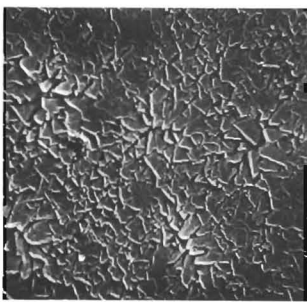
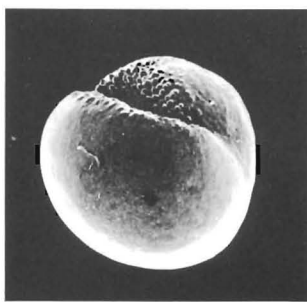
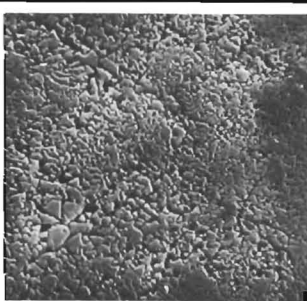
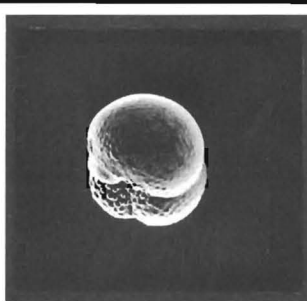
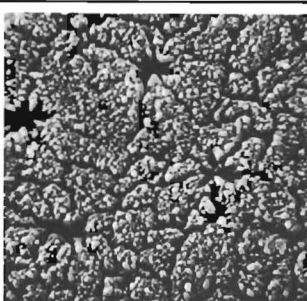
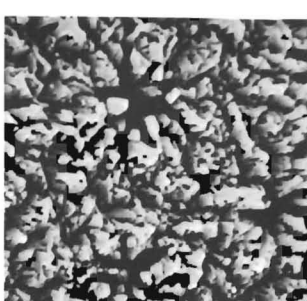
#### PLATE 10

Natural dissolution stages of *Pulleniatina obliquiloculata* from four surface sediment samples of the west-central North Atlantic. The two highly corroded specimens to the right are from 285 cm and 245 cm depth levels in core V16-25 from the

western equatorial Atlantic. The ultrastructure of the right-most specimen closely resembles the needle-like prisms in specimens of *P. obliquiloculata* that have undergone artificial dissolution in Experiment 4 (pl. 6).

# NATURAL DISSOLUTION STAGES

OCEAN DEPTH (M) & CORE LEVEL (CM)

<b>X 1665</b>	<b>1575 M</b> <b>0 CM</b>		
	<b>3400 M</b> <b>0 CM</b>		
<b>X 50</b>	<b>4803 M</b> <b>0 CM</b>		
	<b>5546 M</b> <b>0 CM</b>		
	<b>4254 M</b> <b>285 CM</b>		
	<b>4254 M</b> <b>245 CM</b>		



the shell. Development of this finding may result in a method for the determination of paleocurrents in calcareous deep sea sediments.

#### ACKNOWLEDGMENTS

We would like to thank Leroy Lott for help in preparing the illustrations, Rosemary Free for the faunal analyses in tables 2 and 3, Saijai Tuntivate for assistance in the scanning electron microscope laboratory, Harvey Bliss for assistance in the specimen orientation experiments, Taro Takahashi and Boaz Luz for reviewing the manuscript.

This study received support from a National Science Foundation Grant No. GA 31,388X. It is Lamont-Doherty Geological Observatory Contribution No. 2174.

#### REFERENCES

- BÉ, A. W. H., in press, A taxonomic and zoogeographic review of Recent planktonic foraminifera, *in* Ramsay, A. T., ed., *Oceanic micropaleontology*.
- BÉ, A. W. H., DAMUTH, J. E., LOTT, L., and FREE, R., in press, Late Quaternary climatic record in western equatorial Atlantic sediments: *Geol. Soc. America, Mem.* 145.
- BÉ, A. W. H., and LOTT, L., 1964, Shell growth and structure of planktonic Foraminifera: *Science*, v. 145, no. 3634, p. 823-824.
- BERGER, W. H., 1968, Planktonic foraminifera: Selective solution and paleoclimatic interpretation: *Deep-Sea Research*, v. 15, p. 31-43.
- , 1970, Planktonic Foraminifera: Selective solution and the lysocline: *Marine Geology*, v. 8, p. 111-138.
- BERGER, W. H., and WINTERER, E. L., 1974, Plate stratigraphy and the fluctuating carbonate line, *in* Hsu, K. J., and Jenkins, H. C., eds., *Pelagic sediments on land and under the sea*. *Internat. Assoc. Sedimentologists, Spec. Pub.*, v. 1.
- BERNER, R. A., and MORSE, J. W., 1974, Dissolution kinetics of calcium carbonate in sea water: IV. Theory of calcite dissolution: *Am. Jour. Sci.*, v. 274, p. 108-134.
- BERNER, R. A., and WILDE, P., 1972, Dissolution kinetics of calcium carbonate in sea water: I. Saturation state parameters for kinetic calculations: *Am. Jour. Sci.*, v. 272, p. 826-839.
- HAY, W. W., 1970, Sedimentation Rates; Calcium Carbonate Compensation: *Deep Sea Drilling Proj. Initial Repts.*, v. 4, p. 668-672.
- MORSE, J. W., 1974, Dissolution kinetics of calcite in sea water: A new method for the study of carbonate reaction kinetics: *Am. Jour. Sci.*, v. 274, p. 97-107.
- MURRAY, J. W., and WRIGHT, C. A., 1970, Surface textures of calcareous foraminiferids: *Palaeontology*, v. 13, pt. 2, p. 184-187.
- PESSAGNO, E. A., JR., and MIYANO, K., 1968, Notes on the wall structure of the Globigerinacea: *Micropaleontology*, v. 14, no. 1, p. 38-50.
- RUDDIMAN, W. F., and HEEZEN, B. C., 1967, Differential solution of planktonic Foraminifera: *Deep-Sea Research*, v. 14, p. 801-808.
- STAPLETON, R. P., 1973, Ultrastructure of tests of some Recent benthic hyaline Foraminifera: *Palaeontographica*, v. 142(A), p. 16-49.
- THIEDE, J., 1971, Planktonische Foraminiferen in Sedimenten vom ibero-marokkanischen Kontinentalrand: "Meteor" *Forsch.-Ergebnisse*, pt. C, no. 7, p. 15-102.
- TOWE, K. M., and CIFELLI, R., 1967, Wall ultrastructure in the calcareous Foraminifera: Crystallographic aspects and a model for calcification: *Jour. Paleontology*, v. 41, no. 3, p. 742-762.

# EXPERIMENTAL STUDIES ON THE DISSOLUTION OF PLANKTONIC FORAMINIFERA

ALAN D. HECHT<sup>1</sup>, ERIC V. ESLINGER<sup>1</sup>, AND LUCILLE B. GARMON<sup>2</sup>,  
West Georgia College, Carrollton, Georgia 30117

---

## ABSTRACT

Experimental dissolution of *Globigerinoides ruber*, *Globigerinoides trilobus*, *Globorotalia menardii*, and *Orbulina universa* from core top sediments in the Caribbean Sea are being conducted by reaction with a sodium acetate-acetic buffer solution of pH 6.1 at atmospheric pressure and room temperature. Preliminary results suggest that the foraminifera tests are attacked by the solution primarily from the outside surface such that layers of calcite are successively destroyed. SEM micrographs of successively "stripped" layers indicate that a finely crystalline, smooth layer forms the outer shell and that a more coarsely crystalline layer underlies this

surface layer. Ca/Mg analysis of the buffer solutions after successive intervals of dissolution indicate that the calcite dissolving first is richer in Mg than the calcite which dissolves last.  $\delta O^{18}$  concentrations of undissolved and dissolved tests are not significantly different.

Dissolution of foraminifera in size fractions greater and less than 250 microns indicates that the small-size fraction dissolves significantly faster than the coarser one. These laboratory results are compatible with observations of the selective dissolution of foraminifera in Caribbean core P6304-8.

---

## INTRODUCTION

The remains of recent and ancient planktonic foraminifera are abundant and widely distributed within the sediments of all oceans. These organisms have been extensively studied for the past one hundred years, beginning with the Challenger Expedition (1872-1876), and have been shown to be of great value in paleoenvironmental interpretations because the distribution and abundance of the living species are, in large part, determined by the temperature of the water in which they live. Ocean sediments thus provide a valuable record for reconstructing the environmental changes over the last 100 million years. Unfortunately, deep-sea fossil foraminiferal assemblages are often not an accurate representation of the populations that originally lived

in the upper water column, but are biased because the abundance of fragile and thin-shelled species is reduced by selective dissolution. Thus, selective dissolution can bias environmental interpretations derived from deep-sea sediments (Parker and Berger, 1971).

Selective dissolution of planktonic foraminifera has been most recently studied by Berger (1967, 1968, 1971). On the basis of his early experiments (1967) and subsequent analysis of published species abundance in surface sediments, it was apparent that some species of foraminifera dissolved more easily than others. The order in which species dissolved as determined by Berger is given in table 1. Other workers, for example Ruddiman and Heezen (1967), have confirmed these results by showing that in Atlantic Ocean sediments the relative amounts of the more resistant species given to table 1 increase as the depth of water from which the samples were collected increases, even though the distribution of

---

<sup>1</sup>Department of Geology.

<sup>2</sup>Department of Physics.

Contribution Number 59 of West Georgia College.

TABLE 1

Ranking of planktonic species from least resistant (1) to most resistant (15) to dissolution.

- 
1. *Globigerinoides ruber*
  2. *Orbulina universa*
  3. *Globigerinella acquilateralis* (= siphonifera)
  4. *Globigerinoides sacculifer* (and *G. trilobus*)
  5. *Globigerinoides conglobatus*
  6. *Globigerina bulloides*
  7. *Globorotalia hirsuta*
  8. *Globorotalia truncatulinoides*
  9. *Globorotalia inflata*
  10. *Globorotalia menardii*
  11. *Globoquadrina dutertrei* (= eggeri)
  12. *Pulleniatina obliquiloculata*
  13. *Globorotalia crassaformis*
  14. *Sphaerodinella dehiscens*
  15. *Globorotalia tumida*
- 

living species is not dependent on depth of water. Thus, the amount of selective dissolution is recognized to be in large part dependent on the depth of water in which the shell lies.

It is perhaps reasonable to suspect that not all species of foraminifera would undergo dissolution with equal ease because not all species have shells of equal bulk. It has been observed that species that live high in the water column are often more fragile than species that live at greater depths, and are, therefore, more susceptible to dissolution (see, for example, Berger, 1971). Bé (1965), Bé and Lott (1964), Bé and Hemleben (1970) and Orr (1967, 1969) have shown that adult populations of several foraminiferal species that live at relatively deep depths secrete additional calcite in the form of keels or crusts which increase the stability of the test.

Thus, selective dissolution is known to affect the relative percentages of various planktonic foraminiferal species preserved in deep-sea sediments. However, the changes that may occur due to dissolution within a single species population, other than the altering of absolute number of individuals present, are poorly known. It is with such intra-specific changes that this paper is primarily concerned.

The results reported herein and complemented by the paper by Bé, Morse and Harrison (this volume) suggest that laboratory experiments on the dissolution of planktonic foraminifera can be related to the natural environment and, thus, provide insight into the complex problem of foraminiferal dissolution.

Experiments were designed to determine whether or not: (1) large- and small-size specimens are equally susceptible to dissolution; (2) all parts of a shell are of equal resistance to dissolution; (3) shell morphology changes as a result of dissolution; (4) the elemental chemistry of the remaining shell changes as dissolution occurs; and (5) the oxygen isotopic chemistry of the remaining shell changes as dissolution occurs.

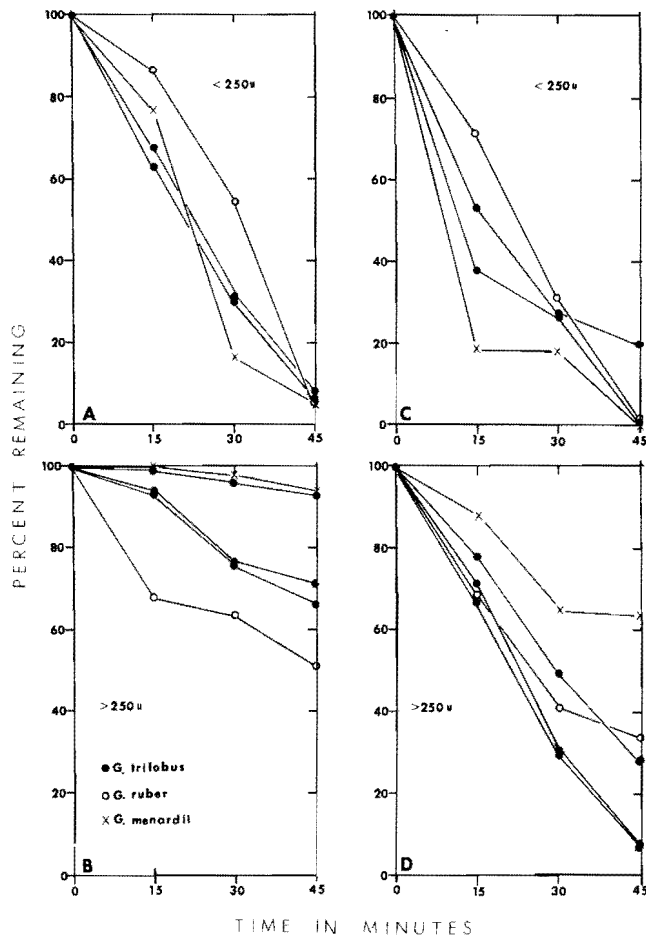
## EXPERIMENTAL TECHNIQUES

The experimental destruction of foraminifera in the laboratory provides a means of directly observing the dissolution of individual specimens or assemblages of specimens. In our studies, we have examined the destruction of foraminiferal tests by both direct observation and by transmission and electron microscopy. Additionally, we have monitored the changes in shell chemistry during the course of the dissolution experiments by atomic absorption spectrophotometry.

In all of our experiments, the dissolving media has been a sodium acetate-acetic acid buffer solution having a pH of 6.1. The experiments were conducted at room temperature and pressure. While these chemical and physical conditions are not the same as those on the ocean floor, we do feel that the geometrical changes that occur during shell destruction in the laboratory approximate those changes that occur on the ocean floor. Samples used in our study are from surface sediments in the Caribbean Sea (core P6304-8). The water depth at this site is 3,927 meters. This depth is well above the present calcite compensation depth in the Caribbean Sea and, as expected, the shells used show few effects of dissolution.

## DISSOLUTION VERSUS SHELL SIZE

In this experiment, we examined three species (*Globigerinoides ruber*, *Globigerinoides trilobus*, and *Globorotalia menardii*) in the size fractions greater and less than 250 microns. For each species, a number of specimens were randomly picked from the two size fractions. The specimens were placed in a petri dish and dissolved for 15 minutes in about five milliliters of the buffer solution. After 15 minutes, the specimens were collected with a brush and mounted on a slide for observation. The number of unbroken and broken specimens of each species were recorded and the general appearance of all the specimens were described. A broken specimen is defined as one that still has most chambers intact, but in which one or more chambers has part of the chamber dissolved completely through to the inside of the



TEXT FIGURE 1

(A and B) Plot of the percentage of the number of original tests remaining (both unbroken and broken) after successive intervals of dissolution in the less-than-250-micron (A) and greater-than-250-micron (B) size fraction.

(C and D) Plot of the percentage of unbroken tests during successive periods of dissolution in the less-than-250-micron (C) and greater-than-250-micron (D) size fractions. The three species *G. ruber*, *G. trilobus*, and *G. menardii* are as indicated.

test. Fragments of individual specimens were not counted. The specimens were then replaced in the petri dish, which had been washed, and fresh buffer was added. After an additional 15 minutes, the samples were removed and again examined. In controlled experiments whereby specimens were transferred from a slide to distilled water and back again, the number of specimens lost due to the transferring operation was always less than 1 percent of the total sample, even for a size fraction that was less than 125 microns.

The results, shown in text figure 1 and table 2, show

the percent of the original sample remaining, and the percent of unbroken shells among those samples remaining after each interval in the solution. Two populations of *Globigerinoides trilobus* in the small-size fraction and three populations of that species in the large-size fraction were dissolved in order to test the reproducibility of this experiment.

In the less-than-250-micron size fraction, no species had more than 10 percent of the shells remaining after 45 minutes in solution, and of these only 20 percent or less were unbroken. However, in the greater-than-250-micron size fraction, 50 percent or more of the shells remained after 45 minutes in solution, and of these as many as 65 percent were unbroken. Thus, in the laboratory, the small-size fraction dissolves significantly quicker than the large-size fraction.

Berger (1967) observed that in his solution experiments where samples of foraminiferal ooze were suspended on buoys in the central Pacific, the larger specimens appeared to dissolve first. Yet, he indicated (1971) that in samples from the South Pacific large-size individuals (> 300 microns) were generally common in samples recovered from great depths, although they constituted only a minor fraction of the living assemblages. Presumably, their abundances were enriched by selective dissolution of small, more fragile specimens.

Additionally, our observation of samples from Caribbean core P6304-8 is that the small-size fraction is significantly more dissolved than the fraction greater than 250 microns. This is true at all depths in the core where dissolution is apparent. Thus, our experimental data are generally compatible with observations of naturally preserved sediments.

The data also indicate that the three species do not dissolve equally fast and that the ranking of the three species as to relative resistance to dissolution is not the same for both size fractions. In the size fraction less than 250 microns, *Globigerinoides ruber* and *G. trilobus* are more resistant to dissolution than *Globorotalia menardii*. Text figure 1 shows that while after 15 minutes in the solution, a greater percentage of tests of *G. menardii* remain than *Globigerinoides trilobus*, a greater percentage of the tests of *Globorotalia menardii* remain than *Globigerinoides trilobus*, a greater percentage of the tests of *Globorotalia menardii* are broken. This is because the test of *G. menardii* is not as homogeneous as the test of *Globigerinoides trilobus*. Populations of *Globorotalia menardii* are characterized by thick ribs that border the chambers which unite to form a keel around the test perimenter. Intra-test partitions and a keel are absent in *Globigerinoides trilobus*

TABLE 2  
Number of unbroken and broken specimens remaining after successive intervals of dissolution.

TOTAL NUMBER OF SPECIMENS RECOVERED									
Less Than 250 Microns					Greater Than 250 Microns				
	Minutes of Dissolution					Minutes of Dissolution			
	0	15	30	45		0	15	30	45
<i>G. trilobus</i>	63	43	19	5	<i>G. trilobus</i>	54	51	42	39
<i>G. trilobus</i>	60	38	19	4	<i>G. trilobus</i>	65	65	63	60
<i>G. ruber</i>	70	61	39	4	<i>G. trilobus</i>	54	51	42	36
<i>G. menardii</i>	35	27	6	2	<i>G. ruber</i>	68	68	64	51
					<i>G. menardii</i>	50	50	49	46

Number of Specimens of Those Recovered That Are Broken									
	Minutes of Dissolution					Minutes of Dissolution			
	0	15	30	45		0	15	30	45
<i>G. trilobus</i>	0	27	14	4	<i>G. trilobus</i>	0	17	29	26
<i>G. trilobus</i>	0	18	14	4	<i>G. trilobus</i>	0	14	32	43
<i>G. ruber</i>	0	18	27	4	<i>G. trilobus</i>	0	15	29	33
<i>G. menardii</i>	0	22	5	2	<i>G. ruber</i>	0	21	38	35
					<i>G. menardii</i>	0	6	17	6

and *G. ruber*. Thus, while the chambers of *Globorotalia menardii* may be dissolved before the chambers of *Globigerinoides trilobus*, the entire test is given additional stability by the presence of the keel margins.

In the large-size fraction, *Globorotalia menardii* is generally more resistant to dissolution than either *Globigerinoides trilobus* or *G. ruber*. However, in our experiments, one of the three *G. trilobus* samples analyzed dissolved nearly as slowly as *Globorotalia menardii*; at present, we have no explanation for this observation.

The simplest model that explains these data is that the larger the test of a particular species, the thicker the test wall such that, assuming the rate of dissolution of large and small tests are equal, the thinner walled small tests are completely dissolved before the thicker walled large ones. Of course, if the walls of a species are not everywhere of equal thickness, as in the case of *G. menardii* which has some of the wall composed of thick ribs, then the model becomes more complex.

It is suggested from these data that it would be desirable for all workers who use species counts of planktonic foraminifera for quantitative paleoclimatic studies to agree upon a standard size fraction to use because species in differing size fractions will have different wall thicknesses. Therefore, in order to compare the relative amounts of selective dissolution that have occurred among different species and different samples, a limited size range should be studied in order to avoid large

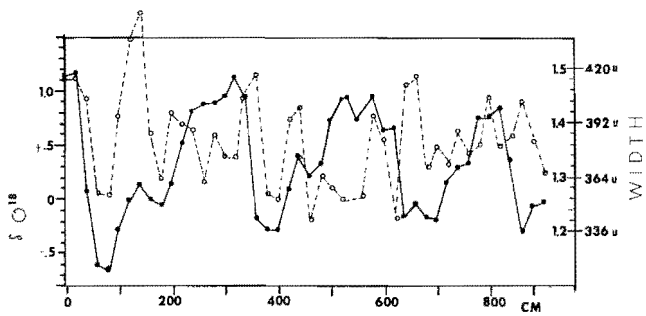
variations in wall thickness. We suggest that the size fraction studied for paleoecologic analysis should have an upper as well as lower size limit.

It is also clear from the observations that the determination of the dissolution ranking of species (as given in table 1) should be reevaluated as a function of size fraction to determine better the degree of bias introduced by individual species.

#### SIZE FREQUENCY CHANGES IN SPECIES POPULATIONS VERSUS DISSOLUTION

The size frequency distribution of foraminiferal species populations might be expected to change due to selective dissolution. The extent to which such changes occur has not been investigated previously. If such changes are significant, they would affect the interpretation of size variations in Pleistocene and Recent foraminiferal populations.

Hecht, for example, has been studying size distributions of individual species in cores from the Caribbean and equatorial Atlantic. Text figure 2 shows the distribution of average width in the greater-than-250-micron split for populations of *Globigerinoides ruber* from Caribbean core P6304-8. Average sizes are based on populations of 30-40 individuals. The size frequency curve, when compared to the oxygen isotope ratios of populations of *G. trilobus* from the same core show major differences, the significance of which will be discussed in another paper. Pertinent to the discussion



DEPTH, P63048  
TEXT FIGURE 2

Plot of the  $\delta O^{18}$  (closed circles) for populations of *G. trilobus* and average width (open circles) for populations of *G. ruber* in Caribbean core P6304-8. Measurements of width were made at 20-cm intervals. The scale on the right vertical axis shows both optical and micron measures. Isotopic data after Emiliani (1966).

herein is to what extent the size frequency data are related to dissolution effects. Observations of the degree of preservation of specimens in this core indicate many levels in which specimens are broken.

To evaluate morphologic changes within the size fraction greater-than-250 microns, three species were again studied. These were *Globigerinoides ruber*, *G. trilobus*, and *Orbulina universa*.<sup>1</sup> For these experiments, individ-

<sup>1</sup>These species were selected because Hecht is presently studying their morphologic variations in surface sediments from the Atlantic Ocean.

uals of each species were randomly picked, mounted on a slide, and their maximum diameters measured with an optical micrometer at 50× (10 units = 280 microns). The specimens were then placed in a petri dish and dissolved in about five milliliters of the bufer solution. After 15 or 30 minutes, all specimens were removed from the solution, remounted on a slide, and measured again. The procedure was repeated until nearly all the specimens were dissolved to the point where they might break when touched with a brush or until no unbroken specimens were preserved.

Intially, three splits of samples were measured before dissolution occurred; from these measurements, an operational error of measurement was determined. For most of the dissolution runs, only one set of measurements were recorded. All samples were measured by one person.

Text figure 3 and table 3 show morphologic data and the size frequency distributions of species measured before and after 30 minutes of dissolution. Only in the case of *Orbulina universa* does dissolution significantly change the size frequency pattern. In this instance, the shift is toward smaller sizes. However, for all species, the mean size change is only slightly outside the limits of observational error. Thus, the large size variations measured on populations of *Globigerinoides ruber*, as shown in text figure 2, may be presumed to be predominately related to environmental rather than dissolution effects. It is our intent to conduct additional experiments of this type to fully study the size frequency changes in foraminiferal populations over a greater size range.

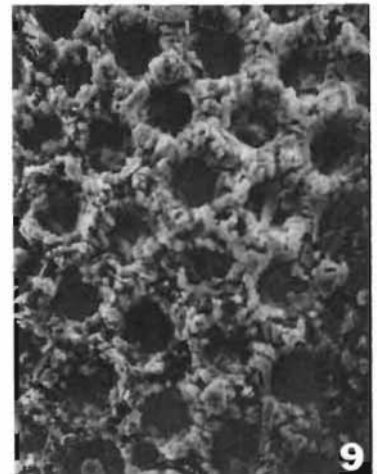
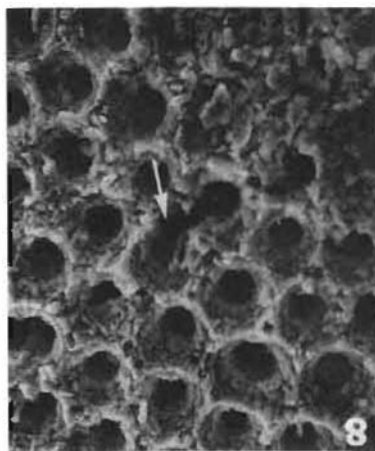
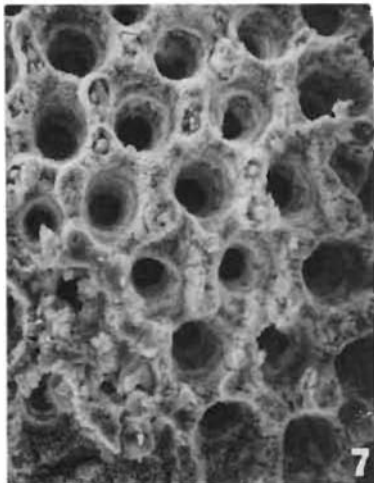
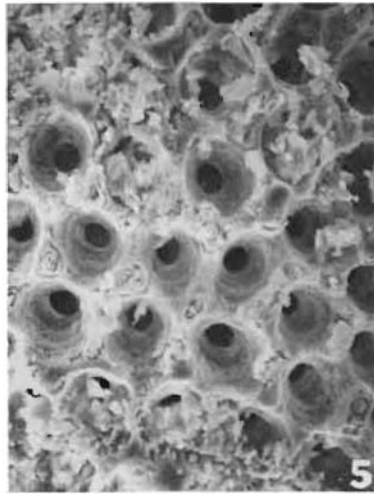
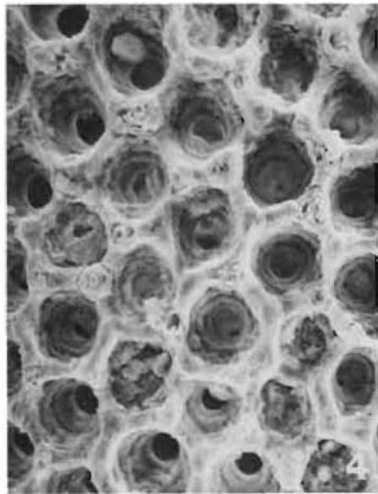
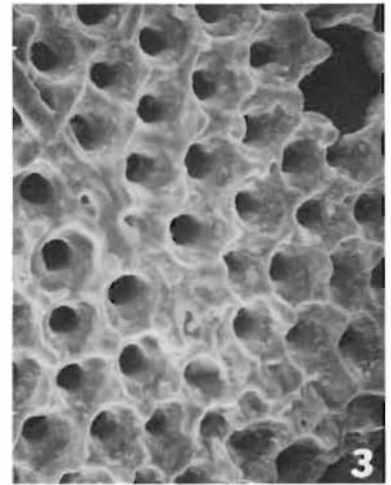
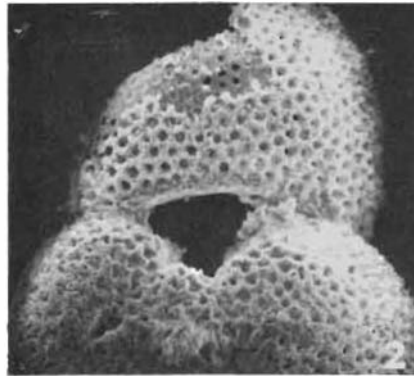
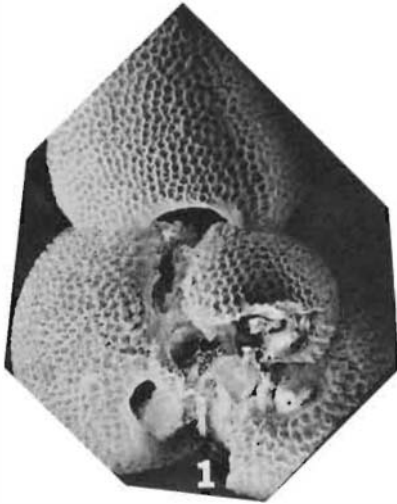
## PLATE 1

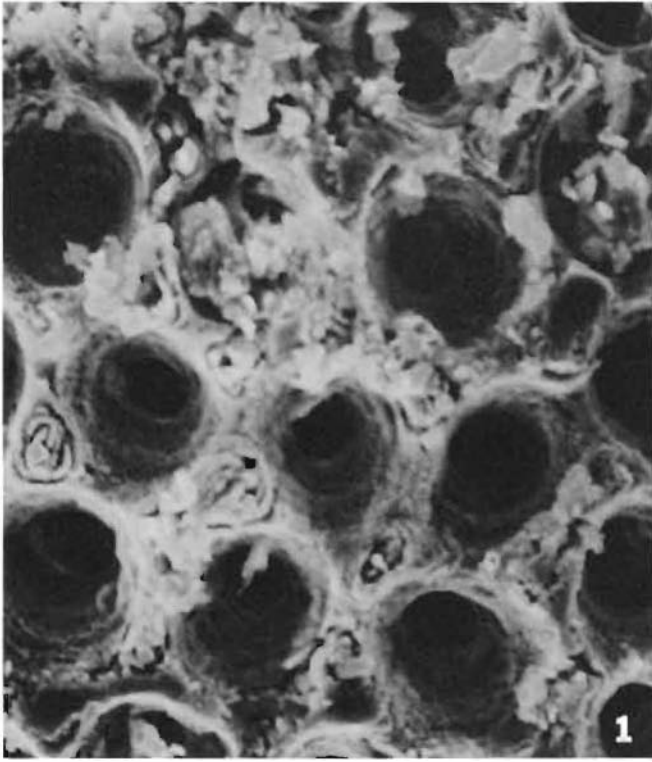
Figures 1-2, *Globigerinoides trilobus* at 200 ×  
Figures 3-9, final chamber of *G. trilobus* at 1,000 ×

- 1 Undissolved specimen of *G. trilobus* from core top sample P6304-8. Specimen mechanically broken during handling. Surface is completely covered with pores. In living organisms, spines radiate from projections surrounding the pore areas.
- 2 *Globigerinoides trilobus* after 75 minutes of dissolution in the laboratory. In all samples studied, the final chamber dissolved first.
- 3 Undissolved *G. trilobus* final chamber. Pores appear to be conical in shape with spine bases surrounding the pore areas. Surface of the test is smooth.
- 4 15 minutes of laboratory dissolution. Signs of erosion in spinal base areas are evident.
- 5 15 minutes of laboratory dissolution. This specimen is

from a different run than the specimen in figure 4. The similarity in surface texture is evident.

- 6 30 minutes of dissolution. External surface is becoming more irregular than the specimens after 15 minutes of dissolution. Spinal base is still evident on some parts of the test.
- 7 Second specimen dissolved for 30 minutes.
- 8 45 minutes of dissolution. Surface texture is highly irregular. Interpore area between spines has been eroded at arrow (see enlargement pl. 2, fig. 2). Base of spines nearly completely eroded away.
- 9 Final chamber of *G. trilobus* after 60 minutes of dissolution. Note the irregular crystal appearance of the test as compared to the undissolved and 15 minutes-dissolved specimens given in figures 3-5.

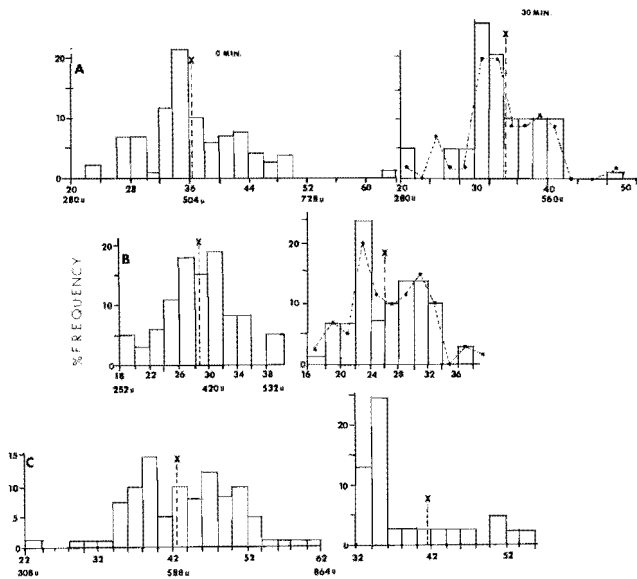




## CHANGES IN SHELL TEXTURE AND CHEMISTRY DURING DISSOLUTION

Changes in shell texture and chemistry were monitored during progressive buffer dissolution of *Globigerinoides trilobus* and *Globorotalia menardii*. Two greater-than-250-micron size fraction samples weighing more than 30 milligrams each of *G. menardii* and one of *Globigerinoides trilobus* were placed in a nalgene test tube with successive aliquots of 10 milliliters of buffer solution and left for intervals of 15 to 60 minutes. The samples were hand agitated every few minutes during the course of the experiment. After each interval, the samples were separated from the buffer by filtration. The buffer was saved for elemental analysis of Ca and Mg. The foraminiferal samples were washed with fresh buffer with the washings being added to the 10 milliliters of buffer that was used during the dissolution interval. The foraminiferal samples were then washed in distilled water and acetone, dried, and weighed. Six to twelve specimens were then removed from each sample and set aside for transmission and electron microscope observation. The samples were then placed in a fresh aliquot of buffer and the procedure repeated. This progressive dissolution was repeated until only about 10 milligrams or less of sample remained. This remaining sample was set aside for oxygen isotopic analysis.

*Changes in Shell Texture:* Plates 1–3 show the results of the dissolution experiments on populations of *Globigerinoides trilobus* and *Globorotalia menardii*. The external shells of *Globigerinoides trilobus* show hexagonal pores which are cone shaped in cross section. Plate 1, figure 1, shows a specimen sampled from the surface sediments in which no experimental dissolution has occurred. The external shell is completely covered with pores. In living specimens, these pores are surrounded by spines projecting from nodes surrounding the pores. In sediment samples, the spines are absent, although in undissolved specimens, the spinal bases or nodes are clearly evident (pl. 1, figs. 3–7). Plate 1, figure 2, shows a typical specimen dissolved for 75



TEXT FIGURE 3

Size frequency distributions for populations of (A) *G. trilobus*, (B) *G. ruber*, and (C) *O. universa* before dissolution (left) and after 30 minutes of dissolution (right). The upper numbers on the horizontal axes correspond to an optical scale (1 unit = 140 microns). The lower numbers are in microns. Actual values are given in table 3. The frequency data for 30 minutes of dissolution shows both unbroken tests (bar histogram) and unbroken plus broken tests (dashed curve). Vertical dashed lines with "X" are mean values of the unbroken tests.

Actually, using the simple model referred to in the previous section, one can predict that there is only one way large shifts in size distribution due to selective dissolution can occur. This would occur in a population with a large size range in which the test sizes of the population were skewed to the smaller sizes. Then, during dissolution, the thin-walled, small tests would be dissolved leaving the larger ones relatively undissolved. Such a phenomena would likely result in an increase in the average shell size of the population.

### PLATE 2

- 1 Enlargement of final chamber in *Globigerinoides trilobus* (2,500 ×) after 15 minutes of dissolution. Surface texture is regular, and spinal base evident. Same area as plate 1, figure 5.
- 2 45 minutes of dissolution shows the beginnings of shell destruction as the interpore areas between spines are

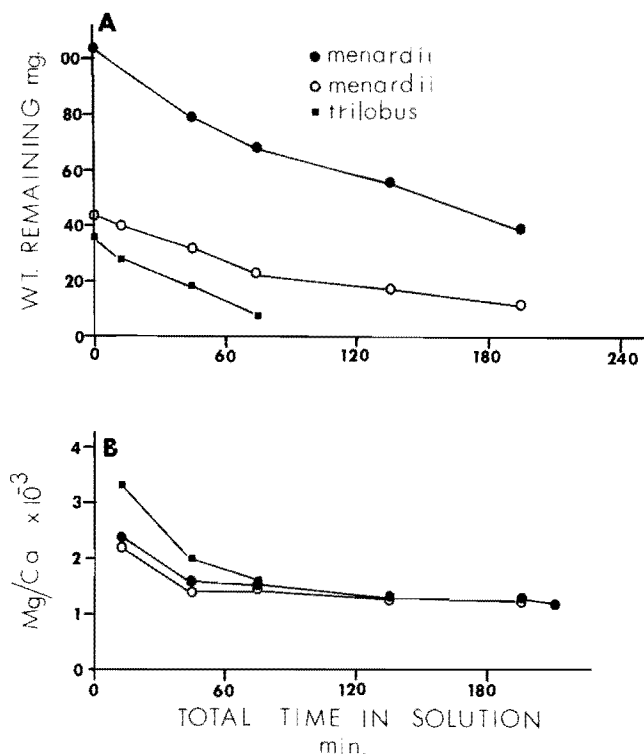
eroded away. Surface texture is highly irregular. Same area shown in plate 1, figure 8, 2,500 ×.

- 3 60 minutes of dissolution. The coarsely crystalline layer of calcite is exposed as dissolution has proceeded to reduce the thickness of the shell. Same area as plate 1, figure 9, 2,500 ×.

TABLE 3

Size measurements of dissolved and undissolved populations of *Globigerinoides trilobus*, *G. ruber*, and *Orbulina universa*.

Species	Mean Width <sup>1</sup> Before Dissolution (microns)	Number of Specimens Before Dissolution	Total <sup>2</sup> Time of Dissolution (min.)	Number of Unbroken Specimens	Number of Broken & Unbroken Specimens	Average Width Unbroken Specimens in Microns	Average Width Broken & Unbroken in Microns
<i>G. trilobus</i>	508.9 ± 12	68	30	19	34	472.8 ± .08	488.3
<i>G. ruber</i>	395.6 ± 12	98	30	32	43	364.0	372.4
<i>O. universa</i>	592.5 ± 11	66	30	18	—	581.8	

<sup>1</sup> Average of 3 sample runs.<sup>2</sup> Consists of two 15-minute dissolution intervals.

TEXT FIGURE 4

Curves showing (A) weight percent of tests remaining and (B) Mg/Ca of test dissolved during progressive dissolution in buffer solution. Horizontal axis is cumulative dissolution time in minutes.

minutes. In all cases studied, the final chamber of the last whorl dissolved first. Details of dissolution of the final chamber during successive intervals of time are shown in plate 1, figures 3–9. Dissolution appears first to reduce the spinal bases (pl. 1, fig. 7–9, and pl. 2, figs. 2–3). In our experiments, erosion of the spinal bases was evident after 30 minutes of dissolution. With increased exposure to the buffer solution, the diameter of the external openings to the pores appears to de-

crease (pl. 1, figs. 3, 4, 8, 9, and pl. 2, figs. 1 and 3). Concurrently, the diameter of the inner pores appears to increase. We feel these observations reflect dissolution of the external test in layers, similar to exfoliation, with additional dissolution occurring along the inside of the pores. This is supported by the appearance of the coarsely crystalline inner layer (pl. 1, fig. 9).

During the process of experimental dissolution, the texture of the final chamber changes from a generally smooth surface (pl. 1, figs. 1–3; pl. 2, fig. 1) to a highly irregular one with individual crystals becoming evident (pl. 1, fig. 9; pl. 2, fig. 3).

The surface structure of *Globorotalia menardii* appears more complex than that of *Globigerinoides trilobus* (pl. 3). This species has been examined in detail by Bé and others (1966), who clearly showed that the external surface is composed of pores of varying size, and that in many parts of the shell, calcite crystals have grown together obscuring the outer pores. Plate 3, figure 1, shows the external characteristics of an undissolved specimen. The surface texture of the final chamber is smooth (pl. 3, fig. 4). The shell is coarse or spinose in earlier chambers of the final whorl and near the keel areas. The surface is also marked by “pustules” (Bé, and others 1966) which surround the aperture (pl. 3, figs. 2 and 10).

Pore sizes vary considerably on specimens and in chambers of individual specimens of *Globorotalia menardii*. Due to this variation, it is difficult to evaluate pore size changes as a function of dissolution unless single specimens are studied (see Bé, Morse and Harrison, this volume). Plate 3, figures 2 and 3, show the dissolution of the test after 75 and 175 minutes. The original smooth surface of the shell is eroded to reveal individual crystals. In earlier chambers of the test (pl. 3, figs. 8–9), the chambers are composed of many calcite crystals grown together to obscure the pores. In some cases, however, the pores are still visible (pl. 3, fig. 8). Comparison of figures 8 and 9 on plate 3 shows

TABLE 4

Run time, weight loss, and Mg/Ca ratios in populations of *Globigerinoides trilobus* and *Globorotalia menardii* during successive periods of dissolution.

Sample	Dissolution Time This Interval (min.)	Total Dissolution Time (min.)	Beginning Weight (Mg) *	Ending Weight (Mg)	Weight Lost This Run (Mg)	Weight Percent Lost of Each Run	Weight Percent of Original Sample Remaining	Mg/Ca of Shell Dissolved ( $\times 10^{-3}$ )
<i>G. menardii</i>								
2-1	15	15	104	—	—	—	—	2.4
2-2	30	45	—	79	—	—	76	1.6
2-3	30	75	78	68	10	13	65	1.6
2-4	60	135	67	56	11	16	54	1.3
2-5	60	195	51	39	12	23	37	1.3
2-6	15	210	30	—	—	—	—	1.2
<i>G. menardii</i>								
3-1	15	15	44	40	4	9	91	2.2
3-2	30	45	39	32	7	18	73	1.4
3-3	30	75	31	23	8	26	52	1.4
3-4	60	135	22	17	5	23	39	1.3
3-5	60	195	16	11	5	31	25	1.3
<i>G. trilobus</i>								
4-1	15	15	36	28	8	22	78	3.3
4-2	30	45	27	19	8	30	53	2.0
4-3	30	75	18	8	10	58	22	1.6

\* Beginning weight for dissolution intervals after the first is less than ending weight for preceding interval due to removal of some specimens for electron microscope work. † Total weight loss during runs 2-1 and 2-2 was 24 milligrams.

very little change in surface texture between specimens dissolved for 15 and 105 minutes. The close packing of crystals, and perhaps greater thickness, gives greater support to the shell and, therefore, dissolution of this portion of the shell is relatively slow. Since *G. menardii*, like other foraminifera, grows by the secretion of calcite in layers, the last formed chamber is often the thinnest and, thus, would be the first to dissolve (pl. 3, figs. 2-3). In undissolved specimens, the keels and chamber separations are highly distinct and are raised above the external shell surface (pl. 3, fig. 1). In the dissolved specimens, however, these keel and chamber partitions are greatly reduced and are less distinctive (pl. 2, fig. 3).

The observations given above suggest that these species dissolve primarily from the external surface inward and partially along the insides of pores. Chambers break up where the shell wall is thinnest, which generally occurs in the last-formed chamber. This observed preferential destruction of the final chamber and the general decrease in wall thickness during dissolution is compatible with the results of the size measurements of the previous section that indicated a small reduction in the width of the tests with increased dissolution.

*Chemical Changes:* Appropriate geochemical data for samples experimentally treated are given in table 4, and are plotted in text figures 4a and 4b. Elemental concentrations of calcium and magnesium were determined using a Perkin-Elmer No. 403 atomic absorption spectrophotometer.

Qualitatively, the results of these experiments appear to be in accord with the results of the previous section on dissolution versus shell size in that in the size fraction greater than 250 microns, *G. menardii* appears to be more resistant to dissolution than *Globigerinoides trilobus* (text fig. 4a). However, because the sample sizes used in the three dissolution experiments were not the same and because agitation of the dissolved material about the dissolving solid tests was not constant, we have not attempted to evaluate weight loss percent data in terms of a diffusion-controlled process (Berner, 1971).

In text figure 4b, the calcium and magnesium concentrations analyzed in the buffer solutions have been corrected for quantities of these elements contained in the original buffer solution, and also for calcium and magnesium leached from and absorbed onto the filter paper.

Text figure 4b indicates that for both species the

TABLE 5

Oxygen isotopic data for undissolved and dissolved populations of *Globigerinoides trilobus* and *Globorotalia menardii*. Isotopic values are given relative to PDB-1 standard.

Sample	Minutes in Buffer	$\delta O^{18}(‰)$
<i>G. menardii</i>	0	$-0.16 \pm 0.1$
<i>G. menardii</i> (2-5)	195	$-0.22 \pm .04$
<i>G. menardii</i> (2-6)	210	$-0.21 \pm .01$
<i>G. menardii</i> (3-5)	195	$-0.27 \pm .05$
<i>G. trilobus</i>	0	$-1.92 \pm .08$
<i>G. trilobus</i> (4-3)	75	$-2.13 \pm .07$

<sup>(c)</sup> Values given are averages of two mass spectrometer runs of the same sample.

Mg/Ca ratio of test material dissolved during the first fifteen-minute interval is significantly greater than the Mg/Ca ratio of test material that dissolved during the next thirty minutes. From the data discussed in previous sections, the parts of the tests that dissolve first are the last-formed chamber and, of course, the outer layers of all chambers. At this time, we do not have enough information to determine why all of the shell material does not have the same Mg concentration. Studies concerning the problem are continuing.

Oxygen isotopic analyses were made on undissolved samples of *Globorotalia menardii* and *Globigerinoides trilobus* and on the portion of the samples that remained after the progressive buffer dissolution. Isotopic values relative to the isotopic standard PDB-1 are given in table 5. There appears to be no significant difference in oxygen isotopic composition between the undissolved

and dissolved samples for either species. Thus, in these laboratory experiments, although there is selective dissolution with respect to the elemental chemistry, there is no selective dissolution with respect to the isotopic chemistry of the test.

## DISCUSSION

In order to determine to what extent the experiments in this study are representative of processes on the ocean floor, we can compare the samples dissolved in this study with samples that have undergone natural dissolution. It is our observation in studying samples from various depths in Caribbean Core P6304-8 that the foraminifera appear to have the same external characteristics as our laboratory-dissolved specimens. It remains for us to fully investigate morphologic changes in foraminiferal populations undergoing natural dissolution as a means of documenting our experimental results.

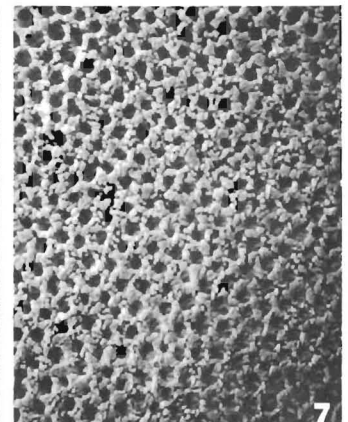
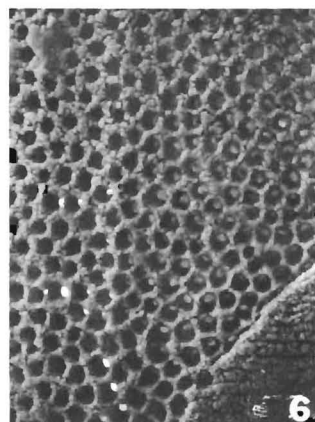
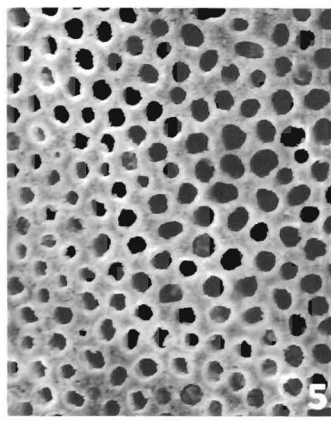
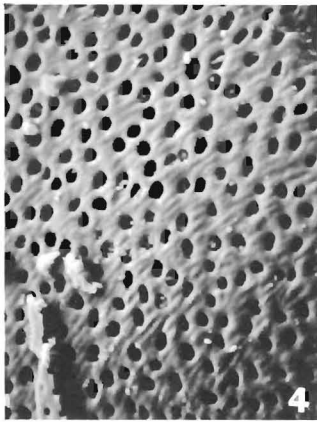
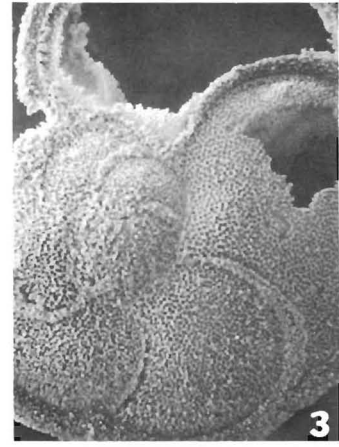
We believe our observations on the greater dissolution of the less-than-250-micron size fraction relative to the greater-than-250 one is supported by the observational data of sediment samples given by Berger (1971). Our geochemical data are also compatible with those suggested by Savin and Douglas (1973) who show that less resistant species of foraminifera have higher concentrations of Mg in their test than those that are more resistant to dissolution.

Although we observed no changes in the isotopic composition of the tests during dissolution, there is still reason to suspect that isotopic analyses of foraminiferal populations may be biased by the selective destruction of smaller size tests. The isotopic temperature of a

## PLATE 3

### *Globorotalia menardii*

- 1 Undissolved specimen (200 ×). Note concentration of pores in the final chamber.
- 2 75 minutes of dissolution. Final chamber is nearly completely dissolved. Keel area and interchamber septa still prominent. "Pustules" evident as indicated by the arrow (see text discussion).
- 3 175 minutes of dissolution. Note the erosion of keel and interchamber septa. Entire surface of test is irregular.
- 4 Final chamber *G. menardii* (1,000 ×) undissolved specimen shows smooth external surface. Same specimen as in plate 3, figure 1.
- 5 Final chamber after 30 minutes of dissolution (1,000 ×). Surface texture becomes irregular. Pore sizes are variable and increase in size.
- 6 Final chamber after 75 minutes of dissolution (1,000 ×). Surface assumes lacework appearance. Individual calcite crystals visible.
- 7 Final chamber after 145 minutes of dissolution just prior to breakup of chamber (1,000 ×).
- 8 Early chamber of the final whorl in *G. menardii* (1,000 ×) after 15 minutes of solution. Note close-packing of crystals has obscured the pores (see arrow).
- 9 Early chamber after 105 minutes of dissolution. Little change is evident in the crystal structure of the early chambers from specimens dissolved for 15 minutes (1,000 ×).
- 10 Enlargement of pustule areas after 75 minutes of dissolution. Large crystals are clearly evident which resist dissolution and lend structural support to the test (1,000 ×). Same specimen as in plate 3, figure 2.





foraminiferal population is an average temperature for the populations which in nature may have occupied a wide range of temperature and depth environments. If those individuals of the population which live in shallow waters are smaller and more susceptible to dissolution (as suggested by Berger, 1968, 1971) than their counterparts living in deeper and cooler waters, then the isotopic composition of the preserved assemblage could be biased toward cooler temperatures. It seems clear that to avoid such biases those populations used for isotopic measurements should, where dissolution is suspected, be restricted by a lower and upper size range.

Finally, our results may be compared to those discussed by Bé, Morse and Harrison (this volume). Bé has experimentally studied the dissolution of single specimens and whole populations. The fact that our results are similar indicates that despite differences in experimental techniques, similar end results are apparent. Our results compare favorably with his observations for specimens preserved in nature which lends credence to the experimental approaches to dissolution problems.

#### ACKNOWLEDGMENTS

The authors gratefully acknowledge the laboratory assistance of Joe Sullivan and Ken Simonton. Scanning electron microscope studies were done with the facilities of the Department of Poultry Science, Auburn University, and the Engineering Experiment Station, Georgia Institute of Technology. Oxygen isotopic analyses were performed by Samuel M. Savin, Case Western Reserve University. Financial support was given by a faculty research grant from West Georgia College. The senior author additionally expresses his appreciation to Drs. Wallace Broecker and Allan Bé, Lamont-Doherty Geological Observatory, for their invitation to participate in a conference on selective dissolution held at Santa Barbara in January 1974. Discussions held during this conference greatly stimulated our research on this problem.

#### BIBLIOGRAPHY

- BÉ, A. W. H., 1965, The influence of depth on shell growth in *Globigerinoides sacculifer* (Brady): *Micropaleontology*, v. 11, p. 81-97.
- BÉ, A. W. H., MORSE, J. W., and HARRISON, S. M., 1975, Progressive dissolution and ultrastructural breakdown of planktonic foraminifera in Sliter, W. V., Bé, A. W. H., and Berger, W. H., eds., *Dissolution of deep-sea carbonates*: Cushman Found. Foram. Research Spec. Pub. 13, p. 27-55.
- BÉ, A. W. H., and HEMLEBEN, C., 1970, Calcification in a living planktonic foraminifera, *Globigerinoides sacculifer*: *Neues Jahrb. Geologie u. Paläontologie Abh.* 134, p. 221-234.
- BÉ, A. W. H., and LOTT, L., 1964, Shell growth and structure of planktonic foraminifera: *Science*, v. 145, p. 823-824.
- BÉ, A. W. H., MCINTYRE, ANDREW, and BERGER, D. L., 1966, Shell microstructure of a planktonic foraminifera, *Globorotalia menardii*: *Eclogae Geol. Helvetiae*, v. 59, p. 885-896.
- BERGER, W. H., 1967, Foraminiferal ooze: solution at depth: *Science*, v. 156, p. 383-385.
- , 1968, Planktonic foraminifera: selective solution and paleoclimatic interpretation: *Deep-Sea Research*, v. 15, p. 31-43.
- , 1971, Sedimentation of planktonic foraminifera: *Marine Geology*, v. 11, p. 325-358.
- BERNER, ROBERT A., 1971, *Principles of chemical sedimentology*: New York, McGraw Hill Book Co., 240 p.
- EMILIANI, C., 1966, Paleotemperature analysis of Caribbean Cores P6304-8 and P6304-9 and a generalized temperature curve for the last 425,000 years: *Jour. Geology*, v. 74, p. 109-126.
- ORR, W., 1967, Secondary calcification in the foraminiferal genus *Globorotalia*: *Science*, v. 157, p. 1554-1555.
- , 1969, Variation and distribution of *Globigerinoides ruber* in the Gulf of Mexico: *Micropaleontology*, v. 15, p. 373-379.
- PARKER, F. L., and BERGER, W. H., 1971, Faunal and solution patterns of planktonic foraminifera in surface sediments of the South Pacific: *Deep-Sea Research*, v. 18, p. 73-107.
- RUDDIMAN, W. F., and HEEZEN, B. C., 1967, Differential solution of planktonic foraminifera: *Deep-Sea Research*, v. 14, p. 301-308.
- SAVIN, SAMUEL M., and DOUGLAS, R. G., 1973, Stable isotope and trace element geochemistry of Recent planktonic foraminifera from the South Pacific: *Geol. Soc. America Bull.*, v. 84, p. 2327-2342.

# ON THE DISSOLUTION OF PLANKTONIC FORAMINIFERA AND ASSOCIATED MICROFOSSILS DURING SETTLING AND ON THE SEA FLOOR

CHARLES G. ADELSECK, JR. AND WOLFGANG H. BERGER

Scripps Institution of Oceanography, University of California, San Diego  
La Jolla, California 92037

---

## ABSTRACT

The problem of whether planktonic forams and associated microfossils dissolve during settling or on the sea floor was investigated in the eastern tropical Pacific Ocean. Net tow samples, from 3,000 meters depth and deeper, showed excellent preservation of most microfossils. Relatively rapid-settling forams ( $> 150 \mu$ ) were well preserved showing only minor etching, whereas effects of dissolution were noticeable in the finer fraction. Whole pteropod tests were common, in part showing considerable etching. Several tows collected abundant large centric diatom frustules, the valves being generally intact and the preservation excellent. Box cores recovered assemblages of foraminifera at the sediment-sea water interface at depths well below the regional

calcite compensation depth. The assemblages contained a wide range of preservation states, that is, delicately spined individuals having experienced no dissolution as well as keel fragments of *Globorotalia* species being the final stages of solution of some of the most resistant species. Such mixed assemblages are expected if dissolution occurs mainly on the sea floor.

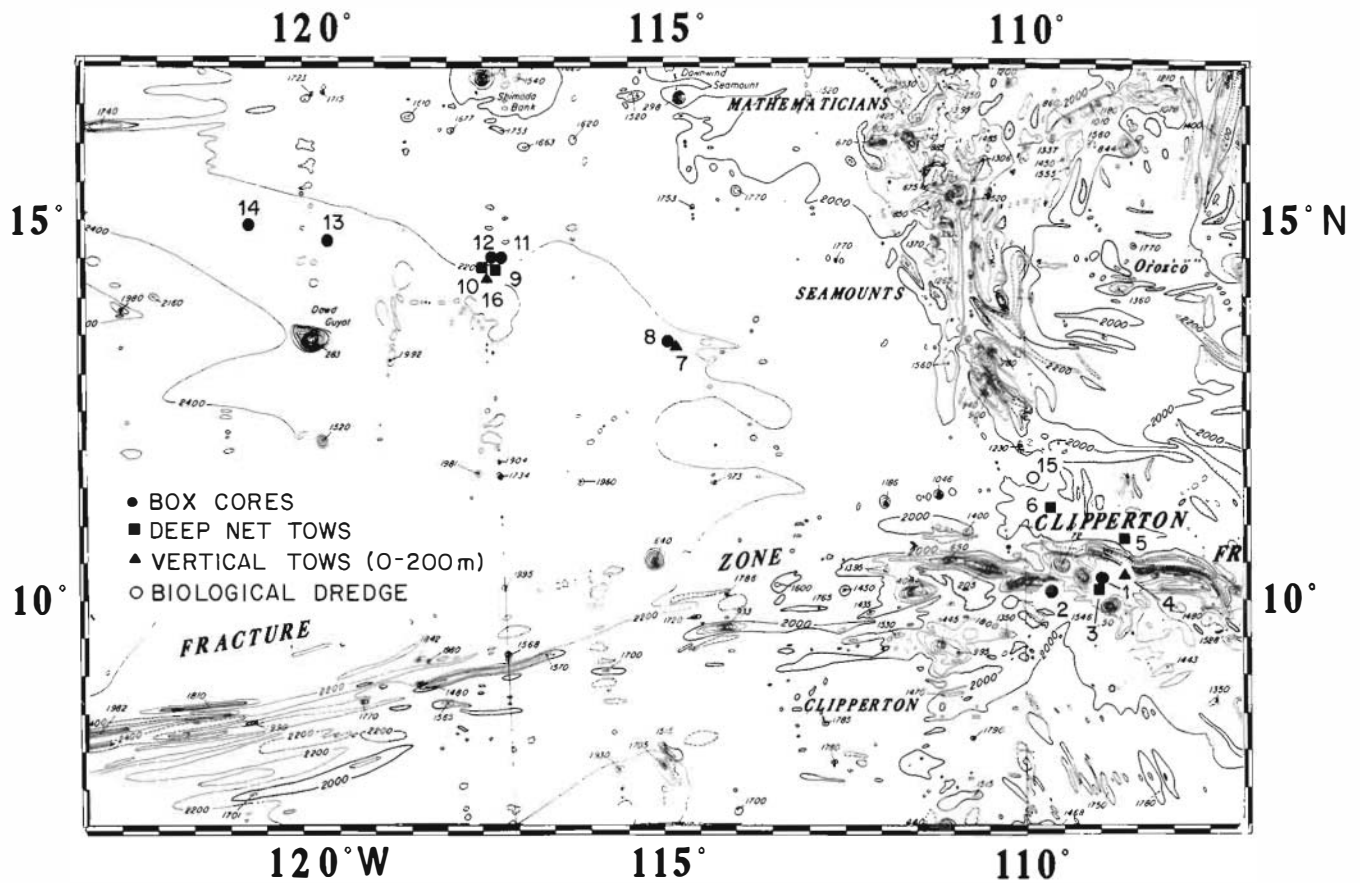
The results from deep net tow and box core samples indicate that larger forams and pteropods experience little solution during settling: solution occurs mainly at the sediment-sea water interface. Estimates of the average residence time of foram tests on the sea floor before disintegration yield a value on the order of one month for the area studied.

---

## INTRODUCTION

The question of whether planktonic foraminifera dissolve during settling or after reaching the sea floor has remained unanswered since the problem was first identified by Murray and Renard (1891). Theoretical considerations (Pond and others, 1969; Lal and Lerman, 1973) are inconclusive, but oceanographic observations suggest that alkalinity (and perhaps dissolved silica) resemble conservative properties in deep waters which would exclude any significant input from dissolution during settling (Bacon and Edmond, 1972; Gieskes, 1974). Kuenen (1950) and Bramlette (1961) believed that because the settling time is short relative to the exposure time at the sediment-sea water interface, most

solution must occur after the foraminifera reached the bottom. Experiments on dissolution rates of optical calcite and of foraminifera in the water column (Peterson, 1966; Berger, 1967) have provided pertinent data which when combined with experimentally determined settling rates indeed suggest that foram tests larger than  $150\mu$  reach the sea floor essentially unharmed (Berger and Piper, 1972). This conclusion is supported by observations by Saidova (1968) who reports foram-rich gut contents in sediment-eating holothurians from the Kermadec Trench at depths well below the regional calcite compensation depth (CCD). Her observations were interpreted as indicating the presence of an interface assemblage enriched in recently arrived forams (Berger, 1974).



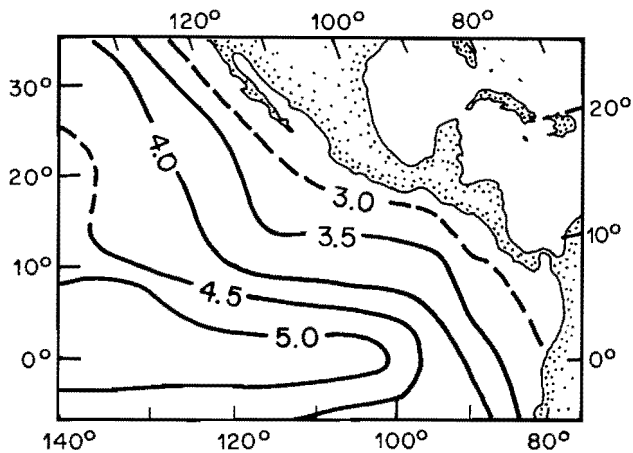
TEXT FIGURE 1

Locations of vertical tows (0–200m), deep net tows, box cores, and the biological dredge (bathymetry by Chase and others, 1971). (1) Box Core 10, 3,400 meters. (2) Box Core 50, 3,655 meters. (3) Bongo Net Tow 1; upper nets 2,000 meters, lower nets 3,000 meters. (4) Vertical Net Tow 3, 0–200 meters. (5) Bongo Net Tow 2; upper nets 2,000 meters, lower nets 3,000 meters. (6) Bongo Net Tow 3; upper nets 340 meters, lower nets 1,340 meters. (7) Vertical Net Tow 6, 0–200 meters. (8) Box Core 56, 4,158 meters. (9) Bongo Net Tow 4; upper nets 2,000 meters, lower nets 3,000 meters. (10) Bongo Net Tow 5; upper nets 3,000 meters, lower nets 4,000 meters. (11) Box Core 63, 4,045 meters. (12) Box Core 74, 3,980 meters. (13) Box Core 82, 4,258 meters. (14) Box Core 83, 4,226 meters. (15) Biological Dredge, 3,750 meters. (16) Vertical Net Tow 7, 0–200 meters.

To test the validity of these hypotheses, we carried out a sampling program involving vertical net tows (0–200 m), opening and closing Bongo net tows ( $\geq 3,000$  m), box coring and biological dredging. Concurrently, satrometer measurements were made in the water column by the geochemistry group at UCLA (see Ben-Yaakov and Kaplan, 1971; Ben-Yaakov and others, 1974). Here we report on the results of the sedimentological program which was part of the “Benthiface Cruise” to the eastern tropical Pacific Ocean aboard the R/V MELVILLE, in May and June of 1973.

The bathymetry of the fieldwork area (text fig. 1) and the regional depth of the CCD (text fig. 2) indicate

the presence of both carbonate-rich and carbonate-poor sediments in this region. Geographic contrasts are substantial. To the south lies the Clipperton Fracture Zone which is characterized by rugged topography. The area around Clipperton Island shows greater than 5,200 meters relief and was studied for patterns of regional sedimentation from above the lysocline to below the CCD as well as for the effects of redeposition. North of the Clipperton Fracture Zone and to the west of the Mathematician Seamounts the area is dominated by low relief abyssal hills topography. Here we report on studies concerning the direct sedimentation of microfossils, relatively free from the effects of redeposition.



TEXT FIGURE 2

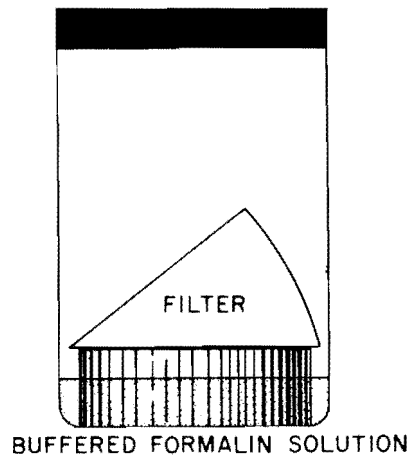
Approximate topography of the calcite compensation depth (CCD) in the area of investigation.

#### SAMPLING AND STORAGE OF SAMPLES

Vertical net tow samples were taken with a one-meter plankton net of  $153\ \mu$  mesh. The net was lowered to 200 meters and retrieved at 20 meters per minute. The ship was maneuvered to maintain wire angles of less than 20 degrees. Samples were stored in a solution of buffered formalin and sea water. Jars were regularly checked and gently stirred to maintain a pH greater than 7. In preparation for counting, aliquots of the original sample were dried and combusted at  $500^\circ\text{C}$  to remove all organic carbon. From previous work (Berger, 1971) we consider that essentially all specimens in the upper 200 meters of the water column were alive at the time of sampling.

Deep net tows were taken using a 0.7-meter opening and closing Bongo frame. Each frame was fitted with two nets ( $53\ \mu$  and  $153\ \mu$  mesh). The contents of the cod ends were washed into a fine filter. The filter was then folded and placed in a jar on top of a plastic cap to avoid contact with a buffered formalin-sea water solution in the bottom of the jar (text fig. 3). The poisonous atmosphere in the jar and freezing of the sample prevented decomposition. For analysis the samples were wet sieved into three fractions ( $43\ \mu$ – $149\ \mu$ ,  $149\ \mu$ – $1,000\ \mu$ , and  $> 1,000\ \mu$ ), and then wet counted before mounting individual specimens for Scanning Electron Microscope (SEM) viewing.

In sampling the sediment-water interface best success was achieved using a box core described by Bouma and Marshall (1964). It was modified with additional gaskets to improve the seal around the box, prevent-



TEXT FIGURE 3

Storage of Bongo Net Tow samples. Samples were stored within a paper filter sitting on top of a plastic cap, forming an island in a buffered seawater formalin solution.

ing washing of the sample during retrieval. The box took a 20- by 30-cm areal sample of the interface with up to 45 cm of penetration. Upon retrieval the water covering the surface of the sediment was carefully siphoned off. Subcores were taken with regular piston core liner and approximately  $40\ \text{cm}^2$  of the interface was scraped off to an average depth of 0.3 cm. This is referred to as the "interface sample" in the following text. Samples were stored at  $4^\circ\text{C}$  until analysis.

Biological dredge samples were placed in buffered formalin-sea water solution and stored until analysis.

#### RESULTS AND DISCUSSION

Our results may be summarized as follows:

1. The deep net tows contain a settling assemblage with a sampling bias towards test with a slow fall rate, and thus different from the actual death assemblage. Despite this selection, which enhances the dissolution aspect of the sampled assemblage, preservation is excellent with the exception of the smaller tests from the deepest tow. Aragonitic shells of petropods also are intact.
2. The interface samples, from the box cores, contain a planktonic foraminifera assemblage at depths well below the CCD, showing a wide range of preservation states. Well-preserved tests represent recent arrivals to the interface whereas fragments, including remnants of very resistant species, con-

stitute the residue of tests that have had a considerably longer time to dissolve. As expected, the assemblage is enriched in the species most resistant to solution.

3. The density of whole foram tests at the interface suggests that for the area studied the average residence time on the bottom before dissolution is approximately a month. Species susceptible to solution will have much shorter residence times and resistant species have somewhat longer ones.
4. Two small brittle stars were recovered from below the CCD by dredging, each containing about 0.06 ml of sediment, mainly brown clay. One of these guts yielded three calcareous foram tests (two planktonic, one benthonic), and one planktonic foram fragment. Cocoliths from a fecal pellet within the brittle star's gut showed much better preservation than the few cocoliths in the other ingested sediment, apparently due to the recent arrival of the cocolith-bearing fecal pellet.
5. We found no evidence to support the possibility that predation and fecal pellet transport are important contributors of sand-sized microfossils to the sediments.

Details of the observations illustrate and amplify these main results, as follows.

#### VERTICAL NET TOWS, 0–200 METERS

The species counts from three vertical tows (table 1) underscore the large variability occurring in the plankton assemblage. Assuming a 70 percent filtering efficiency for the 153  $\mu$  mesh nets, the average foraminiferal population densities in the upper 200 meters of the water column for Vertical Tows 3, 6, and 7 are 8.6, 19.4, and 12.8 individuals/ $m^3$  respectively. These values are somewhat higher than the ones published by Bradshaw (1959) for this area, reflecting the difference in mesh size of the nets. The population densities of pteropods for the same samples are 11.3, 10.7, and 5.3 individuals/ $m^3$ . An unusually high abundance of *Globorotalia cultrata* abnormal forms (3%) were found in Vertical Tows 6 and 7 where this species is dominant.

#### DEEP BONGO NET TOWS

Five casts were taken, each with an upper and a lower double net. The amount of greenish-brown organic matter (mainly algal remains) tends to decrease with depth. Concomitantly, the proportion of

shelled plankton increases, and at depth the bulk of organic matter is provided by empty copepod carapaces rather than by algal matter. Since these carapaces settle very slowly (on the order of 100 m/day), they must resist decomposition for a long time, probably several weeks. The same is true for the abundant diatom frustules recovered, especially in the eastern tows, numbers 1 and 2 (pl. 1, fig. 2). These frustules sink even more slowly than the carapaces (approximately 10 m/day; Smayda, 1970). As is readily observed in the Scanning Electron Microscope (SEM), the diatoms are excellently preserved. The prevalence of a *Coscinodiscus* species is noteworthy. This dominance is interpreted as an effect of selective shell supply from the euphotic zone as well as selective preservation during settling. In *Coscinodiscus* a special protective organic layer may prevent dissolution of the opaline test during settling (Smayda, 1970). Radiolarians, both polycystins and phaeodarians, show excellent preservation. There is considerable diversity although acantharians were not seen. Table 2 summarizes the occurrence and preservation of the microfossils.

Fecal pellet transport of diatoms, radiolarians, and, to a lesser degree, cocoliths, was also observed. Inspection by SEM, both of free fecal material and of gut contents of copepods and other crustaceans, showed the predation to be "destructive" by mechanical breakage. The paleontologically laudable "preserving" predation described by Schrader (1971) was not encountered. In general, the few cocoliths seen were poorly preserved. The fecal matter observed apparently is largely from deep living organisms and may have little bearing on the transfer of particles from the euphotic zone to great depths.

Pteropod shells were observed in all net tow samples, including the deepest ones. The shells, even rather small ones, are well preserved. Many are clear, but signs of etching also are common (pl. 1, figs. 1, 3, and 5). Fragments of pteropods also are present. Their origin (disintegration by solution, predation, breakage during handling) is not known.

Foraminiferal shells are abundant and generally show excellent preservation. Etching and some fragmentation also was observed, especially on small, delicate, slowly settling tests in the deepest tow (Tow 5, 4,000 m). The faunal composition differs considerably within various size fractions. In the very fine net (53  $\mu$  mesh), the bulk of the tests is provided by *Turborotalita humilis*, *Globigerinita iota*, *G. glutinata*, *Globigerinoides sacculifer*, *Globigerina rubescens*, and

TABLE 1

Percentage abundances of the greater than 149  $\mu$  fraction of foraminifera species from the shallow vertical tows and the deep Bongo tows.

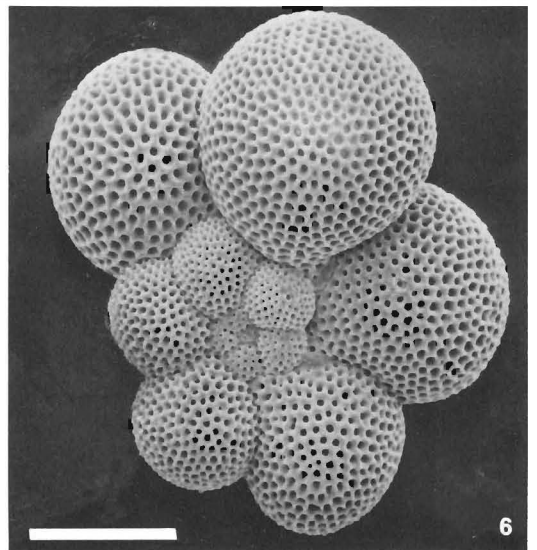
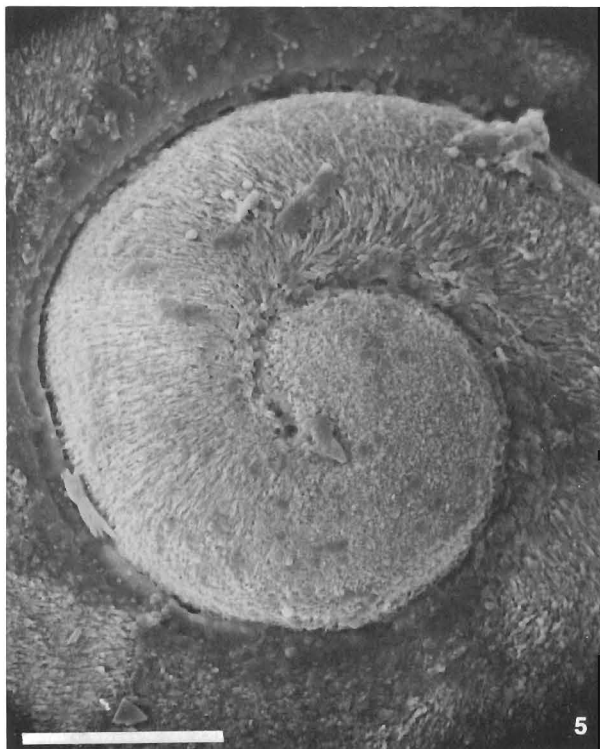
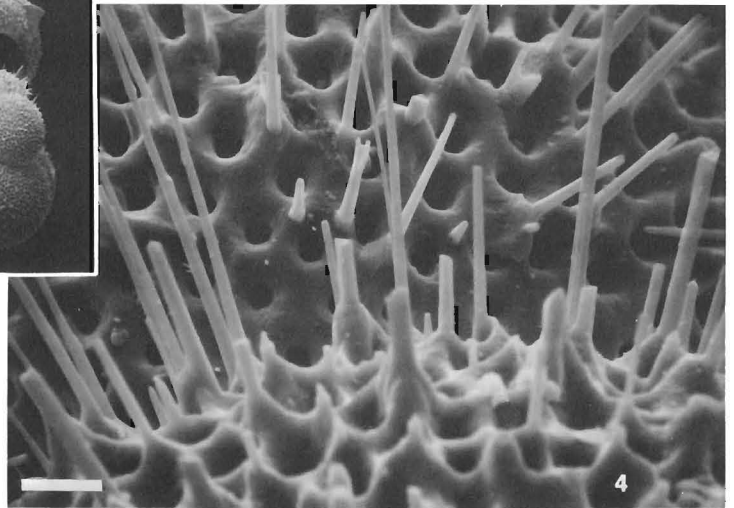
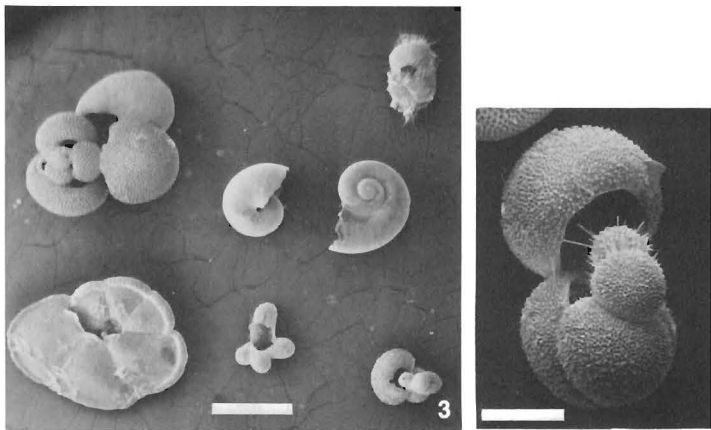
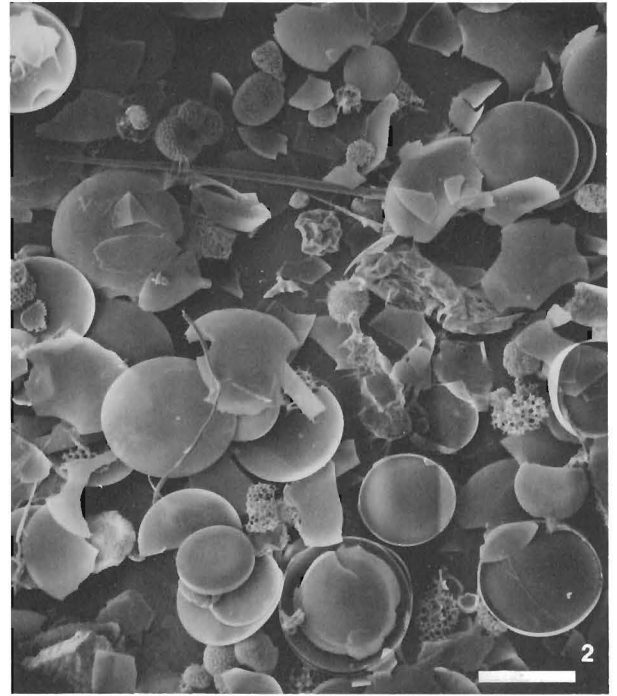
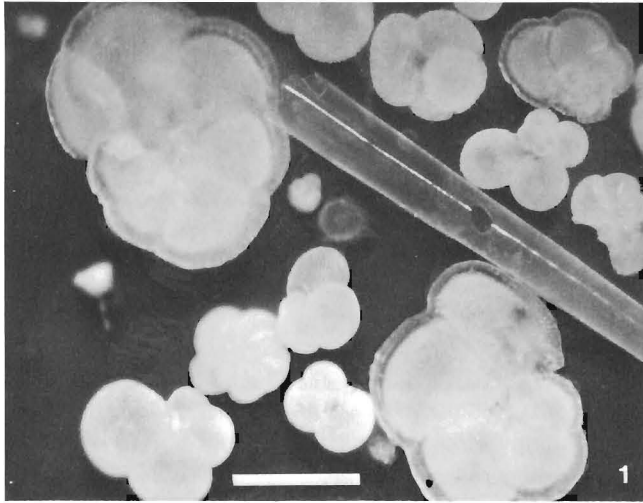
	Clipperton Fracture Zone Area			Intermediate	Western Working Area		
	Vert. Tow 3 0-200 m	Bongo Tow 1 3000 m	Bongo Tow 2 3000 m		Vert. Tow 6 0-200 m	Vert. Tow 7 0-200 m	Bongo Tow 4 300 m
<i>Globorotalia tumida</i> (Brady)				P	P		
<i>Pulleniatina obliquiloculata</i> (Parker and Jones)						P*	
<i>Globoquadrina conglomerata</i> (Schwager)	5						
<i>Globorotalia inflata</i> (d'Orbigny)	P					P	P
<i>Globoquadrina dutertrei</i> (d'Orbigny)	7	P		2	2	4	2
<i>Globigerinoides conglobatus</i> (Brady)	3	P	P	1		4	2
<i>Globorotalia cultrata</i> (d'Orbigny)	4	9*	2	25	63	2	2
<i>Globorotalia truncatulinoides</i> (d'Orbigny)		P*		P			
<i>Globorotalia hirsuta</i> (d'Orbigny)	5	4		6	2		
<i>Globigerinoides tenellus</i> Parker	1	3	3	P	P	1	P
<i>Globigerinoides sacculifer</i> (Brady)	22	7	21	11	10	22*	28
<i>Globigerinoides ruber</i> d'Orbigny	28	50	46	14	2	20	26
<i>Globigerinella siphonifera</i> d'Orbigny	3	5	9	10	7	9	9
<i>Globigerina calida</i> Parker	P	1	2	P	2	2	1
<i>Globigerina bulloides</i> d'Orbigny	P	1	P	1		P	1
<i>Globigerina rubescens</i> Hofker	P	3	1	P	2	3	2
<i>Globoquadrina hexagona</i> (Natland)	9	4*	6	22	6	1	1
<i>Globigerinita iota</i> Parker		P					
<i>Globigerinita glutinata</i> (Egger)	7	8	7	4	3	12	10
<i>Orbulina universa</i> d'Orbigny	2			2	1	19	13
<i>Globigerina digitata</i> Brady	P					1	
<i>Candeina nitida</i> d'Orbigny		P*					
<i>Hastigerina pelagica</i> d'Orbigny	P			P	P		
<i>Globigerinita uvula</i> (Ehrenberg)			P				
<i>Globigerinella adamsi</i> (Banner and Blow)		1			P	P	
TOTAL COUNTED	257	281	176	250	263	368	211

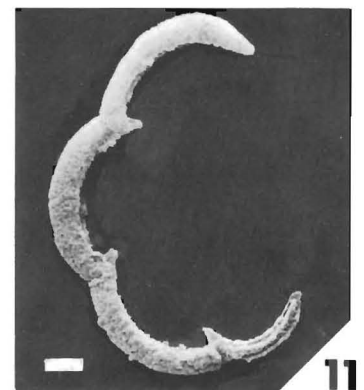
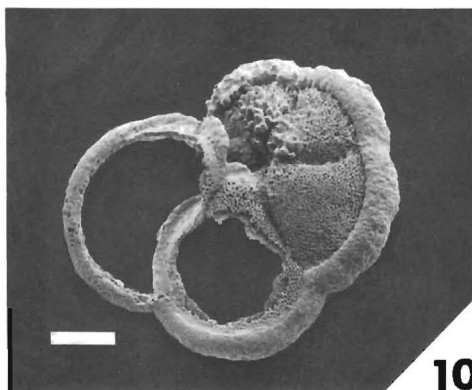
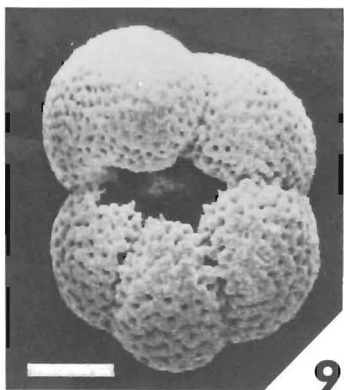
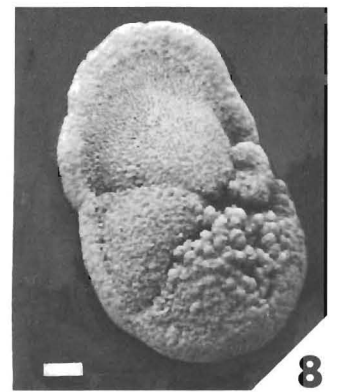
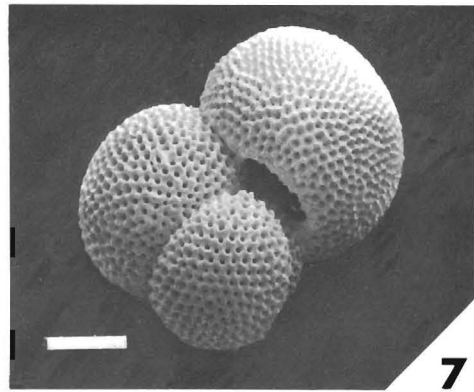
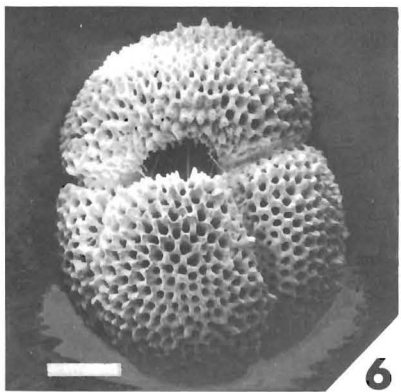
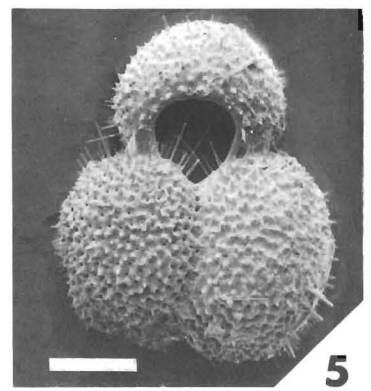
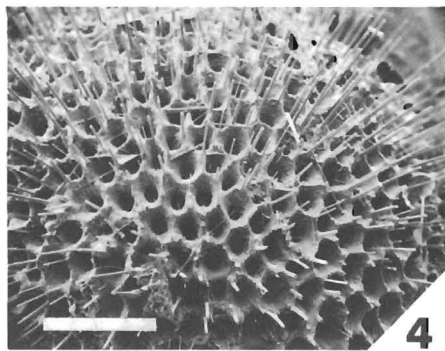
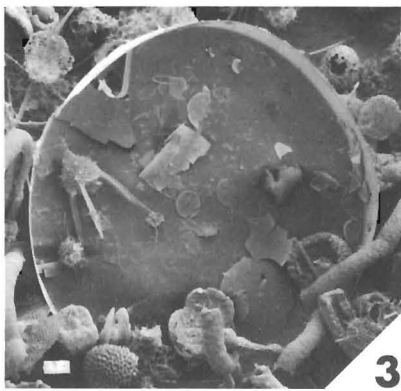
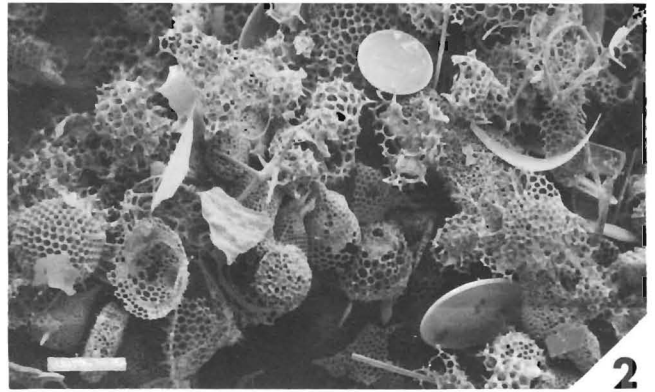
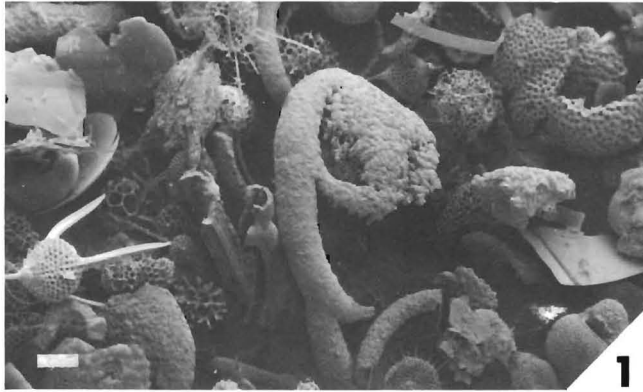
\* Living specimens from the deep Bongo tows

## PLATE 1

## Results from the deep Bongo net tows

- 1 Large foraminifera and a pteropod (*Creseis* sp.) from Bongo Tow 1 (3,000 m), showing clear, unetched shells, and suggesting enrichment with the more slowly settling forms (very thin *Globorotalia cultrata*, bulbous *Globigerinoides sacculifer*). Bar equals 500  $\mu$ .
- 2 Typical view of shell assemblage in Bongo Tow 2 (3,000 m), showing centric diatoms, *Coscinodiscus* sp., largely preserved with two halves, and without signs of etching. Bar equals 250  $\mu$ .
- 3 Foraminifera and pteropods (*Limacina* sp.) from Bongo Tow 4 (3,000 m), showing spiny *Globigerinoides ruber*, slightly damaged *Globigerina digitata* and a slightly etched *Limacina* shell (see fig. 5 for close-up). Bar equals 500  $\mu$ .
- 4 Well-preserved *Globigerinella siphonifera*, with spines (Bongo Tow 4, 3,000 m). Inset shows the complete test. Note that a small terminal chamber apparently broke off, but that no obvious signs of etching are seen. Bars are equal to 200  $\mu$  and 10  $\mu$ .
- 5 Close-up of *Limacina* shown in figure 3, illustrating incipient etching. Bar equals 50  $\mu$ .
- 6 A living *Globoquadrina hexagona* from 3,000 meters depth (Bongo Tow 1). This foram appears to be able to survive at great depths, better than other species. Note absence of any tendency for encrustation in this species. Bar equals 100  $\mu$ .





*Globigerinoides tenellus*. The *G. sacculifer* show the typical juvenile form figured by Parker (1973), but commonly have a smaller than normal final chamber ("kummerform"), indicating termination of growth in these juveniles. Termination of growth also is indicated in most other tests, presumably due to reproduction or stress, or both. Predation apparently can be excluded as an important shell-producing mechanism in the sand-sized foraminifera as was suggested previously (Berger, 1971).

Absolute numbers are greatly dependent on the mesh size used. With the 53  $\mu$  mesh net, 14,000 to 20,000 specimens were caught per haul, corresponding to 10–15 forams/m<sup>3</sup>. The 153  $\mu$  mesh nets caught about 1,000 specimens per haul, for a concentration of 0.7 forams/m<sup>3</sup>. In Tow 2 (3,000 m) less than 3 percent of the foraminifera are larger than 100  $\mu$ , and in Tow 4 (3,000 m) the medium-sized forams (150  $\mu$ –200  $\mu$ ) outnumbered the large ones (250  $\mu$ –600  $\mu$ ) by five to one.

Small tests are enriched through differential settling in the net tows. Differential enrichment of slowly settling species is indicated by the relatively great abundances of *Orbulina*, *Globigerinoides ruber*, *G. sacculifer*, and *Globigerinella siphonifera* in the large sizes (table 1). Slowly settling variants within species are expected to be similarly enriched. Upon arrival at the sea floor, these slowly settling shells will have experienced a greater amount of solution than the rest. This is seen in the decrease in abundance and poorer preservation of the fine fraction from the deepest Bongo tow (Tow 5, 4,000 m, see table 2).

TABLE 2

The preservation and relative abundances of the microfossil assemblages in the deep bongo net tows. The ratio shows the relative abundance compared to the state of preservation (D = Dominant; A = Abundant; C = Common; R = Rare; G = Good; F = Fair; P = Poor).

	Bongo Tow 1 3000 m	Bongo Tow 2 3000 m	Bongo Tow 4 3000 m	Bongo Tow 5 4000 m
Coarse Fraction 149 $\mu$ –1000 $\mu$ 153 $\mu$ Mesh Net				
Diatoms	D/G	D/G	C/G-F	C/G-F
Phaeodarians	R/G-F	C/G	A/G	C/G-F
Polycystine Radiolarians	A/G	A/G	A/G-F	D/G-F
Copepod Carapaces	A/F-P	A/F-P	D/F-P	A/F-P
Pteropods	C/G-F	C/G-F	C/G-F	C/G-F
Foraminifera	A/G	A/G	A/G	A/G
Fine Fraction (43 $\mu$ –149 $\mu$ ) 53 $\mu$ Mesh Net				
Diatoms	D/G	D/G	A/G-F	C/G-F
Phaeodarians	C/F-P	C/F-P	A/F-P	A/F-P
Polycystine Radiolarians	A/G	A/G	D/G	D/G-F
Copepod Carapaces	—	—	—	—
Pteropods	—	—	—	—
Foraminifera	A/G	A/G	C/G	R/F-P

#### BOX CORES

Seven box cores were taken from near and below the CCD. The greater than 62  $\mu$  fractions were initially scanned wet. Fine fraction forams (62  $\mu$ –149  $\mu$ ) were extremely rare. Although fecal pellets were abundant, they are believed to originate entirely from benthic

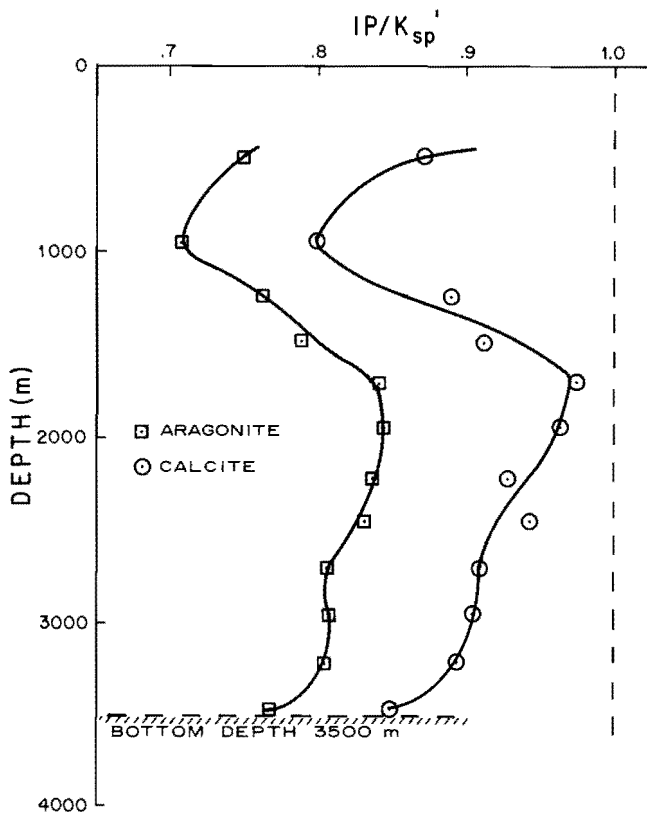
←

#### PLATE 2

Results from the sediment-seawater interface, sampled by box core

All bar scales equal 100  $\mu$

- 1 Appearance of the coarse fraction (> 149  $\mu$ ) from the interface of Box Core 50 (3,655 m). Fragments are dominant in the foram fraction especially the keels of *Globorotalia tumida*-*G. cultrata* which represent the most resistant part of the entire foram assemblage.
- 2 Appearance of the coarse fraction (> 149  $\mu$ ) from the interface of Box Core 74 (3,980 m). The entire assemblage is composed of diatoms and radiolarians. Forams and foram fragments are extremely rare.
- 3 An entire valve of *Ethmodiscus rex*, from the interface of Box Core 50, showing the excellent preservation of the siliceous assemblage.
- 4 Spined *Globigerinoides* sp. from the interface of Box Core 82 (4,258 m).
- 5 Spined *Globigerinoides ruber* from the interface of Box Core 56 (4,158 m).
- 6 Well-preserved *Globigerinoides conglobatus*, from the interface of Box Core 83 (4,226 m), showing the preservation of a few spines around the aperture.
- 7 Well-preserved *Globigerinoides sacculifer* from the interface of Box Core 74 (3,980 m).
- 8 Etched *Globorotalia tumida* from the interface of Box Core 83 (4,226 m).
- 9 Partially dissolved *Globoquadrina dutertrei*, from the interface of Box Core 56 (4,158 m), showing partial destruction of the apertural area.
- 10 Partially dissolved *Globorotalia cultrata* from the interface of Box Core 83 (4,226 m).
- 11 *Globorotalia cultrata* from the interface of Box Core 56 (4,158 m) dissolved except for the highly resistant keel.



TEXT FIGURE 4

Results of carbonate saturation, Benthiface Cruise, 11°10' N, 109°37' W, UCLA casts numbers 79 and 80. Unpublished data from S. Ben-Yaakov, I. Kaplan, and E. Ruth.

organisms judging from the high percentage of clays found in them. None were found that were of obvious planktonic origin, so that the idea that fecal pellets may be important in transporting well-preserved microfossils from the euphotic zone to the sea floor could not be verified in these samples.

Microfossil assemblages in the box cores were mainly from one of two distinct depositional regimes. Box cores 10 and 50 were located at the bases of major slopes having over 3,000 meters of relative relief. Their sediments showed significant downslope redeposition of microfossils. The interface samples from these cores did not show a distinct foram assemblage characterized by well-preserved recent arrivals. The sediment in the two cores is a typical deep sea brown clay with 5 to 10 percent carbonate and abundant siliceous microfossils. Plate 2, figure 1 shows a typical assemblage from the greater than 149  $\mu$  fraction. Radiolarians, diatoms, and foraminiferal fragments are abundant. Whole

specimens of foraminifera are rare, and pteropod fragments are extremely rare but are present. The overall preservation of the foraminiferal assemblage is poor. *Globorotalia tumida*-*G. cultrata* keel fragments are the dominant component and solution-resistant species are selectively enriched. The presence of some spined non-resistant species and of pteropod fragments indicates that the sediment is a mixture of components in various states of preservation, interpreted as mainly reflecting downslope redeposition of sediment. This mechanism is also apparent from the presence of *Höglundina elegans* at the depth of the CCD. Bandy (1954) found this benthonic foraminifera to be aragonitic. Analysis of data in Phleger, Parker, and Peirson (1953) by J. Yount (personal communication) has shown this species to be restricted to slopes above the lysocline. This is generally confirmed off Peru and Chile in the data from Bandy and Rodolfo (1964).

The preservation of the siliceous microfossils is extremely good as evidenced by the presence of the diatom genera *Asteromphalus* and *Ethmodiscus* (Johnson, in press). Plate 2, figure 3 shows the excellent preservation of one valve of the diatom *Ethmodiscus rex* which is rarely found intact in the sediments (Belyayeva, 1968). This large diatom can sink at a rate of 500m/day (Smayda, 1970) thus increasing its chance to reach the sea floor.

The depths of the CCD and lysocline were remarkably shallow in the area near Clipperton Island. As evidenced by the low carbonate content in the two box cores, the CCD resides at 3,400 meters or slightly shallower. Gravity cores from the surrounding topographic highs revealed highly dissolved assemblages as shallow as 1,163 m. Dissolution at these shallow depths may in part be due to current action. Calcite saturation suggests that waters should be highly corrosive toward calcareous fossils on the sea floor at relatively shallow depth (text fig. 4).

The second depositional regime, found in Box Cores 56, 63, 74, 82, and 83, reflects normal pelagic sedimentation to the sea floor below the CCD, well removed from large-scale redeposition (text fig. 1). In all the cores, the sediment is a uniform brown clay with less than 5 percent carbonate. Smear slides reveal the fine fraction to be virtually free of carbonate fragments and coccoliths, including the interface samples. The coarse fraction (> 149  $\mu$ ) is dominated by well-preserved radiolarians and diatoms. Foraminifera and their fragments are extremely rare (pl. 2, fig. 2). No evidence was found bearing on the idea that coccoliths are more resistant to dissolution than foraminifera.

TABLE 3  
The interface assemblage of whole foram tests from the box cores.

		DELICATE						RESISTANT			TOTAL	Fragments of Planktonic Foraminifera Present
		<i>Globigerinoides ruber</i>	<i>Globigerinoides sacculifer</i>	<i>Globigerinoides conglobatus</i>	<i>Globigerinita iota</i>	" <i>Orbulina universa</i> "	<i>Globorotalia cultrata</i>	<i>Globoquadrina dutertrei</i>	<i>Pulleniatina obliquiloculata</i>	<i>Globorotalia tumida</i>		
BNFC 56 Box 4158 m	Interface	1*	1	1	—	—	—	4	1	—	8	Yes
	3-5 cm	—	—	—	—	—	—	—	—	—	0	No
	12-14 cm	—	—	—	—	—	—	—	—	—	0	No
BNFC 63 Box 4045 m	Interface	1*	2	1	—	—	1	—	—	—	5	Yes
	3-5 cm	—	—	—	—	—	—	—	—	—	0	No
BNFC 74 Box 3980 m	Interface	2*	2	—	1	—	4	2	—	—	11	Yes
	5-7 cm	—	—	—	—	—	—	—	—	—	0	No
	12-14 cm	—	—	—	—	—	—	—	—	—	0	No
BNFC 82 Box 4258 m	Interface	—	1	—	—	—	1	1	1	—	4	Yes*
	3-5 cm	—	—	—	—	—	—	—	—	—	0	No
BNFC 83 Box 4226 m	Interface	2	3	2*	—	1	2	19	—	1	30	Yes
	3-5 cm	—	—	—	—	—	—	—	—	—	0	No

\* Contains at least one spined test.

Table 3 shows the distribution of whole foraminifera in the box cores. No traces of foraminifera are present in samples from below the surface, yet the interface contains a small assemblage of forams. In each box core, there is a complete range of solution preservation in the interface foram assemblage (pl. 2, figs. 4-11). Fragments, dominated by *Globoquadrina dutertrei* and *Globorotalia cultrata*, are more abundant than whole tests (pl. 2, figs. 9-11). This assemblage of diverse stages of dissolution is as expected for an interface with concomitant deposition and dissolution of forams. The excellent preservation of the spined individuals (pl. 2, figs. 4-6) indicates that little solution occurs during the settling of these forams to the sea floor. For a medium-size foram (~ 177-250  $\mu$ ), it takes 6 to 10 days to settle through the water column (Berger and Piper, 1972).

The average residence time for whole foraminifera (> 150  $\mu$ ) at the interface can be roughly estimated. Because of dissolution effects, the rate of supply of calcareous ooze at the equator is greater than the maximum accumulation rate of 2.4 cm/1,000 yrs (Deep Sea Drilling Project, Leg 9, Site 82). The standing stock at lat 15° N. is roughly one-fourth the standing stock at the equator (Bradshaw, 1959), so that the supply

rate at lat 15° N. should be correspondingly lower, a minimum of 0.6 cm/1000 yrs. Assuming a reasonable value of 1 cm/1,000 yrs., about 10 forams/cm<sup>2</sup>yr is the expected delivery rate (calculated from data in Arrhenius, 1952). For the 40 cm<sup>2</sup> of interface sampled, this yields an annual supply rate of roughly 400 forams. Undoubtedly some of the interface assemblage was lost during sampling. Thus the 30 forams found in Box Core 83 are assumed to be the most nearly intact assemblage. Comparing it to the annual supply rate yields a minimum residence time of between three and four weeks.

If the estimate of a residence time of about one month is roughly correct, the settling time in undersaturated waters (below 90 m, Pytkowitz, 1970) for a medium-size foram (~ 177-250  $\mu$ ) represents one-quarter to one-sixth of the total dissolution time. Why then are no solution effects seen in the recent arrivals to the interface? The tests could be protected by organic coatings (Chave, 1965; Suess, 1970) during settling, or the bottom waters are significantly more corrosive to calcite, or both. Supporting the short residence time is the fact that the fine fraction forams, which take longer than three weeks to settle to the sea floor, show solution effects and a decrease in abun-

dance in the deepest Bongo net tow, number 5 (table 2). This fraction ( $< 149 \mu$ ) comprises about 40 percent by weight of the total foraminiferal assemblage (Revelle, 1944).

### CONCLUSIONS

We conclude that for all but very small foram tests most dissolution takes place on the sea floor rather than during settling through the water column. Since our study area has an unusually shallow CCD, this conclusion should be true for most other oceanic regions as well. The flux of tests to the sea floor should constitute an important input of food for benthonic organisms. The organic carbon associated with the tests is found as exterior coatings, as layers within the tests, and as matrix material surrounding the individual crystals which make up the tests (Bé and Hemleben, 1970; Towe, 1971). The predominant dissolution of forams at and near the bottom means that their main input of alkalinity is to the bottom waters. The effects of pteropod and of coccolith dissolution are not well understood; and depending upon where most of the dissolution occurs, the overall profile of alkalinity input due to carbonate dissolution may differ significantly from the one based on foram tests alone.

Geologically, our observations imply that the preservation state of the foraminiferal assemblage mainly records the conditions on the sea floor. Inferences cannot be made about the state of saturation of the overlying waters from preservation aspects alone. Thus, an assemblage of forams recovered from the sediments records the conditions for growth in the euphotic zone and the solution-preservation conditions on the sea floor.

### ACKNOWLEDGMENTS

We thank F. B. Phleger, F. L. Parker, P. H. Roth, J. C. Yount, and T. C. Johnson for their criticism and suggestions. We are grateful for the assistance of P. H. Roth at the Scanning Electron Microscope and to T. C. Johnson for help during the field work. We are indebted to Capt. A. W. Finney and the crew of the R/V MELVILLE for their cooperation and work during the "Benthiface Cruise" on which the samples were collected. This research was supported by the National Science Foundation grants GA 41078 and 36697.

### REFERENCES

- ARRHENIUS, G., 1952, Sediment cores from the East Pacific: Swedish Deep-Sea Exped. (1947-1948) Repts., v. 7, no. 1, p. 1-228.
- BACON, M. P., and EDMOND, J. M., 1972, Barium at Geosecs III in the Southwest Pacific: Earth and Planetary Sci. Letters, v. 16, no. 1, p. 66-74.
- BANDY, O. L., 1954, Aragonitic Tests among the foraminifera: Jour. Sed. Petrology, v. 24, no. 1, p. 60-61.
- BANDY, O. L., and RODOLFO, K. S., 1964, Distribution of foraminifera and sediments, Peru-Chile Trench area: Deep-Sea Research., v. 11, no. 5, p. 817-837.
- BÉ, A. W. H., and HEMLEBEN, C., 1970, Calcification in a living planktonic foraminifera, *Globorotalia menardii* (D'Orbigny): Eclogae Geol. Helvetiae, v. 59, p. 885-896.
- BELYAYEVA, T. V., 1968, Range and numbers of diatoms of the genus *Ethmodiscus* Cast. in Pacific Plankton and sediments: Oceanology, v. 8, p. 79-85.
- BEN-YAAKOV, S., and KAPLAN, I., 1971, Deep Sea *in situ* calcium carbonate saturation: Jour. Geophys. Research, v. 76, p. 722-731.
- BEN-YAAKOV, S., RUTH, E., and KAPLAN, I., 1974, Calcium carbonate saturation in northeastern Pacific: *in situ* determination and geochemical implications: Deep-Sea Research, v. 21, p. 229-243.
- BERGER, W. H., 1967, Foraminiferal ooze: solution at depths: Science, v. 156, no. 3773, p. 383-385.
- , 1971, Planktonic foraminifera: sediment production in an oceanic front: Jour. Foram. Research, v. 1, no. 3, p. 95-118.
- , 1974, Seven Lectures on Deep-Sea Deposits, in Burk, C. A., and Drake, C. P., eds., The geology of continental margins: New York, Springer Verlag.
- BERGER, W. H., and PIPER, D. J. W., 1972, Planktonic foraminifera: differential settling, dissolution, and redeposition: Limnology and Oceanology, v. 17, no. 2, p. 275-287.
- BOUMA, A. H., and MARSHALL, N. F., 1964, A method for obtaining and analysing undisturbed oceanic sediment samples: Marine Geology, v. 2, no. 1/2, p. 81-89.
- BRADSHAW, J. S., 1959, Ecology of living planktonic foraminifera in the north and equatorial Pacific Ocean: Cushman Found. Foram. Research Contr., v. 10, no. 2, p. 25-64.
- BRAMLETTE, M. N., 1961, Pelagic Sediments, in Sears, M., ed., Oceanography: Washington, D. C., Am. Assoc. Adv. Sci., p. 345-366.
- CHASE, T. E., MENARD, H. W., and MAMMERICKX, J., 1971, Topography of the North Pacific: IMR Tech. Rept. Series TR-17.
- CHAVE, K. E., 1965, Carbonates: association with organic matter in surface seawater: Science, v. 148, no. 3678, p. 1723-1724.
- GIESKES, J. M., 1974, The alkalinity-total carbon dioxide system in sea water, in Goldberg, E. D., ed., The sea, v. 5: John Wiley and Sons, p. 123-151.
- JOHNSON, T. C., in press, The dissolution of siliceous microfossils in surface sediments of the eastern tropical Pacific: Deep-Sea Research.

- KUENEN, PH. H., 1950, *Marine Geology*: New York, John Wiley, 568 p.
- LAL, D., and LERMAN, A., 1973, Dissolution and behavior of particulate biogenic matter in the ocean: some theoretical considerations: *Jour. Geophys. Research*, v. 78, no. 30, p. 7100-7111.
- MURRAY, J. and RENARD, A. F., 1891, Report on deep-sea deposits based on the specimens collected during the voyage of H.M.S. Challenger in the years 1872 to 1876: Rept. Voyage Challenger, London, Longmans, 525 p. (Reprinted by Johnson Reprint Corp., New York, 1965).
- PARKER, F. L., 1973, Living planktonic foraminifera from the Gulf of California: *Jour. Foram. Research*, v. 3, no. 2, p. 70-77.
- PETERSON, M. N. A., 1966, Calcite: rates of dissolution in a vertical profile in the central Pacific: *Science*, v. 154, no. 3756, p. 1542-1544.
- PHLEGER, F. B, PARKER, F. L., and PEIRSON, J. F., 1953, North Atlantic Foraminifera: Swedish Deep-Sea Exped. (1947-1948) Repts., v. 7, no. 1, p. 1-122.
- POND, S., PYTKOWITZ, R. M., and HAWLEY, J. E., 1969, Particle dissolution during settling in the oceans: *Deep-Sea Research*, v. 18, no. 11, p. 1135-1139.
- PYTKOWITZ, R. M., 1970, On the carbonate compensation depth in the Pacific Ocean: *Geochem. et Cosmochim. Acta*, v. 34, no. 7, p. 836-839.
- REVELLE, R. R., 1944, Marine bottom samples collected in the Pacific Ocean by the Carnegie on its seventh cruise: Carnegie Inst. Washington Pub. 556, p. 1-180.
- SAIDOVA, KH. M., 1968, Condition of foraminifera in water, ground and intestines of mud eaters: *Akad. Nauk SSSR, Doklady*, v. 182, no. 2, p. 453-455.
- SCHRADER, H. J., 1971, Fecal pellets: role in sedimentation of pelagic diatoms: *Science*, v. 174, p. 55-57.
- SMAYDA, T. J., 1970, The suspension and sinking of phytoplankton in the sea: *Oceanog. Marine Biol. Ann. Rev.*, v. 8, p. 353-414.
- SUESS, E., 1970, Interaction of organic compounds with calcium carbonate: *Geochim. et Cosmochim. Acta*, v. 34, p. 157-168.
- TOWE, K. M., 1971, Lamellar wall construction in planktonic foraminifera: *Planktonic Conf.*, 2d, Rome (1970), Proc., Farinacci, A., ed., p. 1213-1224.

# DEEP-SEA CARBONATES: DISSOLUTION PROFILES FROM FORAMINIFERAL PRESERVATION

WOLFGANG H. BERGER

Scripps Institution of Oceanography, University of California, San Diego  
La Jolla, California 92037

---

## ABSTRACT

The foraminiferal lysocline, defined as the boundary zone between well-preserved and poorly preserved foraminiferal assemblages on the sea floor, is not by necessity a level of accelerated dissolution or "lysocline" in a general sense, such as found by Peterson (1966). The foram lysocline has the properties of a compensation depth, in that it can exist independently of the particular shape of a dissolution profile as long as rates increase with depth. There is considerable evidence

for pronounced dissolution above the foram lysocline in the area just south of Peterson's experiment. Detailed stratigraphic work and quantitative modeling of progressive dissolution of foram assemblages is necessary to establish to what degree the hydrographic lysocline (Peterson's level) leaves a trace on the sea floor, in the form of a sedimentary lysocline; that is, a marked decrease in the rate of sedimentation.

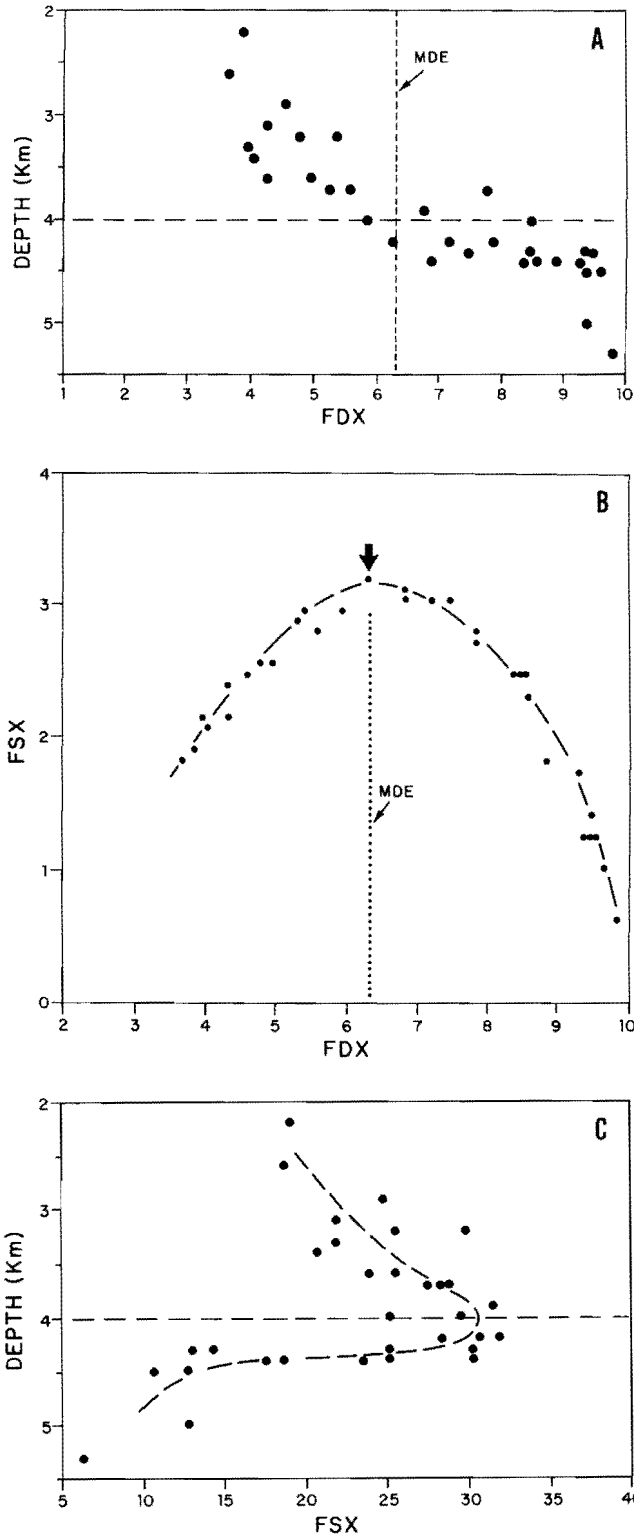
---

## INTRODUCTION

As a result of Peterson's field experiment (Peterson, 1966; Berger, 1967), it was established that in the central Pacific dissolution of calcite in the deep ocean begins at a depth well above the calcite compensation depth (CCD) mapped by Bramlette (1961), and that there is a level somewhat above the regional CCD where dissolution rates increase drastically. These findings imply that calcareous fossil assemblages are poorly preserved when approaching the CCD. This is indeed the case as recognized by the enrichment of solution-resistant species through differential removal of the more solution-susceptible forms (Ruddiman and Heezen, 1967; McIntyre and McIntyre, 1971). By ranking the species with respect to their susceptibility to dissolution and calculating the average weighed rank for an assemblage, the preservation state of a sample from the sea floor can be assessed. In the central Atlantic, it was found that there is a depth where the preservation state changes rather drastically from well

preserved to poorly preserved. This level has been termed "lysocline" (Berger, 1968) and is more specifically referred to as "foraminiferal lysocline" or "foram lysocline." The foram lysocline has been mapped in various parts of the ocean (Berger, 1968; Parker and Berger, 1971).

The term "lysocline" has also been used in a fundamentally different sense, as a depth where dissolution rates of calcite greatly accelerate (Berger, 1970; Morse and Berner, 1972). While this usage is entirely proper and reflects the intent of the term, it does imply a correlation between the level found by Peterson (1966) and the foram lysocline as defined on the basis of preservation profiles. Indeed, the term "lysocline" was originally coined in the belief that the striking change in foraminiferal composition at the interface of Antarctic Bottom Water and North Atlantic Deep Water constitutes a trace of accelerated dissolution in the water column; that is, a Peterson level. Furthermore, it appears that a correspondence between foram lysocline



TEXT FIGURE 1

Relationships between foraminiferal indices and depth. FDX is the average weighted rank of samples, based on species susceptibility to dissolution, on a scale from 1 to 10. FSX is the standard deviation of this average rank. 1A, the FDX

and hydrographic lysocline in this area is supported by the evidence available (Berger, in press). However, a general equivalence of the (foram) lysocline as mapped on the sea floor and any dissolution rate levels measured in the field (Peterson, 1966; Ben-Yaakov and others, 1974) or calculated on the basis of laboratory experiments (Morse and Berner, 1972) is by no means established, since the degree to which foraminifera dissolve above their lysocline has received little attention.

Here I present evidence that the foram lysocline does not necessarily represent a trace on the sea floor of Peterson's level (hydrographic lysocline), but that it could result from internal statistical properties of more or less uniformly dissolving assemblages. In particular, considerable dissolution takes place above the foram lysocline (and also above the hydrographic lysocline), in the area south of Peterson's experiment.

#### LYSOCLINE POSITION FROM SOLUTION INDICES

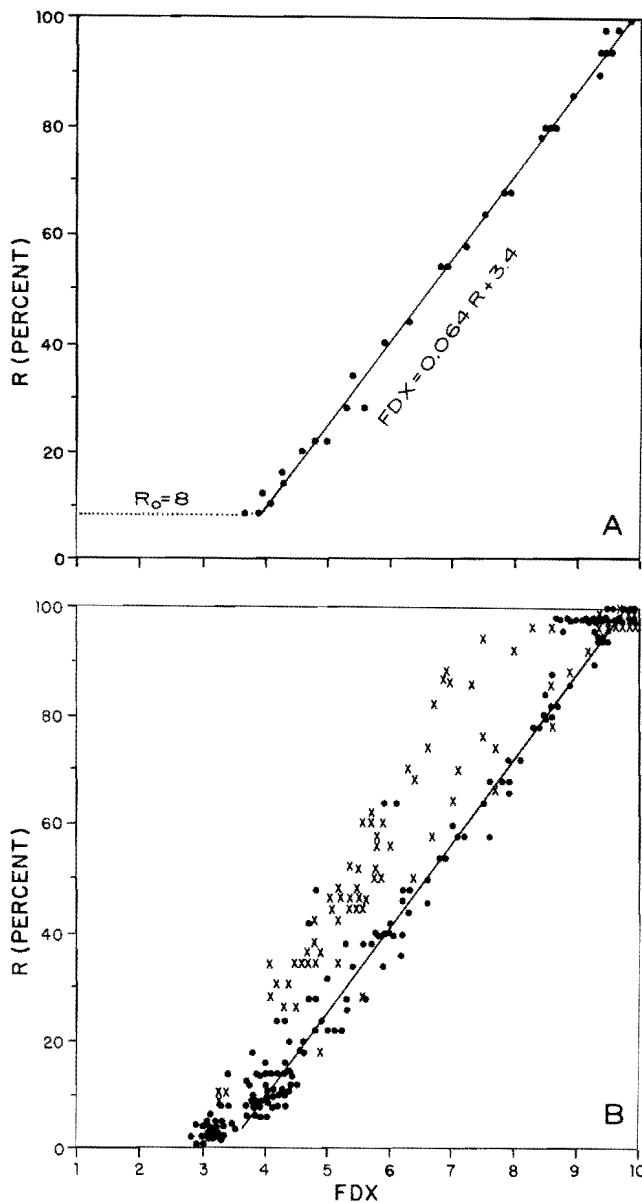
The preservation aspect of foram assemblages is described by a foraminiferal dissolution index (FDX). The FDX is a weighted average of nine dissolution groups to which the 37 foraminiferal species are assigned, normalized to a scale from 1 to 10:

$$FDX = \frac{\sum_{i=1}^9 i P_i}{9} \times 10/9$$

where  $i$  is the group number and  $P_i$  is the proportion of the assemblage assigned to the group  $i$ . The FSX is the standard deviation of this weighted average. The groups to which the 37 foraminiferal species are as follows: 1. *H. pelagica*; 2. *G. anfracta*, *G. ruber*, *G. rubescens*, *G. tenellus*, *G. quinqueloba*, *G. bulloides*; 3. *G. siphonifera*, *G. adamsi*, *G. sacculifer*, *G. conglobatus*, *G. falconensis*, *C. nitida*, *O. universa*; 4. *G. calida*, *G. fimbriata*, *G. uvula*, *G. glutinata*, *G. iota*; 5. *G. scitula*, *G. hexagona*, *G. digitata*; 6. *G. conglomerata*, *G. hirsuta*, *G. crassaformis*; 7. *G. truncatulinoides*, *G. inflata*; 8. *G. menardii*, *G. dutertrei*; 9. *G. pachyderma*, *G. pumilio*, *P. obliquiloculata*, *S. dehiscescens*, *G. tumida*, *T. humilis*.

←

increases markedly between 3.5 and 4 km depth. MDE (maximum dissolution equitability) is taken from 1B, which shows how the FSX varies systematically with the FDX. 1C, the FSX profile allows an improved definition of the foraminiferal lysocline.



TEXT FIGURE 2

Relationship between foraminiferal dissolution index FDX and the percentage of resistant species, R. 1A, the relationship is linear in the area considered. 1B, there is considerable scatter when several areas are combined. Dots: tropical samples. Crosses: extratropical samples. Line fitted by eye.

The basis for this study are 32 foraminiferal analyses from the equatorial Pacific, between lat 10°N. and 10°S. and west of long 155°W. (Parker and Berger, 1971). The depth of the foraminiferal lysocline in this area is given as 3,500 to 4,000 m (Parker and Berger, 1971; Valencia, 1973), the same as the hydrographic lysocline

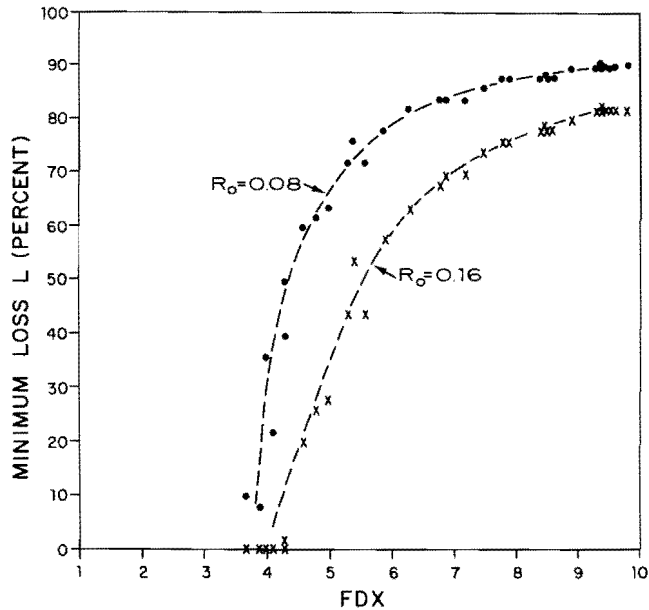
to the north (Peterson, 1966). A plot of foraminiferal dissolution index values (FDX) against depth (text fig. 1A) confirms this assessment in a general way, although it is difficult to identify a critical value for FDX which will separate "well preserved" and "poorly preserved" assemblages. To aid in the definition of such a value, the standard deviation of FDX can be employed. This index (FSX) reaches a maximum when solution-susceptible and solution-resistant species reach equal proportions (Maximum Dissolution Equitability, MDE, see text fig. 1B). In a plot of FSX versus depth, this maximum is reached near 4 km (text fig. 1C).

#### RELATIONSHIPS BETWEEN INDICES AND SOLUTION LOSSES

While these statistical exercises confirm and refine the previously mapped lysocline position, they do not answer the question of whether this position marks a level of increased dissolution rate. A minimum loss of foraminifera by dissolution can be estimated according to

$$L = 1 - R_0/R \quad [1]$$

where L is the proportion lost,  $R_0$  is the initial proportion of resistant species, and R the final one (Berger, 1971). The formula assumes that the resistant species are not dissolving at all. The resistant species are *G. truncatulinoides*, *G. inflata*, *G. crassaformis*, *G. menardii*, *G. dutertrei*, *G. pachyderma*, *P. obliquiloculata*, *S. dehiscens*, *G. tumida*, *T. humilis*. Before this formula can be used to estimate minimum dissolution, samples must be shown to be homogeneous as concerns their dissolution behavior, and  $R_0$  must be defined. A plot of R versus FDX (text fig. 2A) establishes that these two measures are linearly correlated for the 32 samples considered; that is, there is no reason to suspect that R is influenced by variations in  $R_0$  or by mechanical processes. A similar plot for all samples from the various regions studied by Parker and Berger shows that marked heterogeneity in initial compositions and in dissolution behavior introduces considerable scatter into the relationship (text fig. 2B). It must be emphasized that some variation in  $R_0$  may nevertheless exist for the 32 samples here analyzed. In the equatorial Atlantic, for example,  $R_0$  values increase from 8 percent to twice this value when going from lat 10°N. to the equator (Berger, in press). As I will show, the main conclusions presented are not affected by this complication.

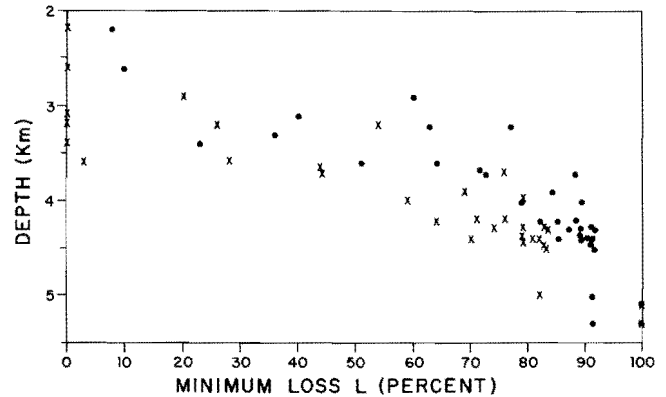


TEXT FIGURE 3

Relationships between the minimum losses  $L = 1 - R_0/R$  and the foram dissolution indices FDX. The FDX is not very sensitive for losses below 70%, especially if the initial proportion of resistant species ( $R_0$ ) is small.

For the present set of samples,  $R_0$  may initially be taken as equal to 0.08 (text fig. 3). It is immediately obvious that the FDX is rather insensitive for minimum losses of less than 70 percent and closely monitors only the losses greater than that. Assuming  $R_0$  equal to 0.16 does not change the nature of this result. This behavior is exactly analogous to that of carbonate percentages in surface sediments, which also are related to dissolution profiles in a non-linear fashion (Heath and Culberson, 1970; Berger, 1971; Ellis and Moore, 1973).

The fact that both foram dissolution indices and carbonate percentages are difficult to use in establishing profiles of actual dissolution does not, of course, invalidate either as useful tools of facies description. In fact, the very non-linearity of the response of foram assemblages to progressive dissolution makes it plausible that different workers on foraminifera come to the same conclusion about the approximate position of the lysocline without recourse to counting. Thus, references to samples "above" or "below" the lysocline are numerous in the appropriate chapters of the Initial Reports of the Deep Sea Drilling Project. Such assessments are possible because the initially small value of  $R$  en-



TEXT FIGURE 4

Depth profile of the minimum loss  $L = 1 - R_0/R$ . There is evidence for considerable loss of foraminifera above 3.5 km depth, especially if  $R_0 = 0.08$  (dots), but also for  $R_0 = 0.16$  (crosses).

ures that poorly preserved samples with high  $R$  values are easily recognized. In essence, the foram lysocline is the level where the more susceptible species, initially very much in the majority, cease to be dominant. It is noteworthy that the same is not true for coccoliths, because unlike in foraminiferal assemblages, resistant forms are dominant to begin with (see Roth and Berger, this volume). Thus, the foram lysocline has properties of a compensation depth, which may or may not be associated with accelerated dissolution on a regional basis. In the western central South Pacific, for example, the lysocline apparently does coincide with accelerated dissolution, since there is no indication whatever of a systematic increase of dissolution indices down to 4 km depth (see in Parker and Berger, 1971, fig. 14, area B). Also, in the central Atlantic where the lysocline was originally defined, there is evidence for an acceleration in dissolution rate, as mentioned before.

#### SOLUTION LOSSES VERSUS DEPTH

To obtain the best minimum estimate of actual loss through dissolution,  $L$  is plotted versus depth (text fig. 4), assuming  $R_0 = 0.08$  (dots). Considerable loss is indicated at 3 km depth, even when  $R_0$  is doubled (crosses). Does this preclude losses at even shallower depths? Not so, because all losses are calculated with respect to the foram composition at somewhat below 2 km. Only if the actual  $R_0$ , that is, the percentage

of resistant species in the assemblage originally supplied to the sea floor, is not smaller than the value assumed, can losses at shallower depths be excluded. Does the L value directly reflect the weight loss in carbonate? Not necessarily, since it only refers to proportions of numbers of foraminifera, the lightweight representatives of which are more easily dissolved than the heavyweights. For the same reason, the foraminiferal shells increasingly resist being dissolved as dissolution proceeds and eliminates the more susceptible forms. Thus, the faunal dissolution profile does not directly reflect the "aggressiveness" of the water, which is a function of degree of undersaturation, water motion, and other factors (for review see Gieskes, 1974; Edmond, 1974).

The obvious next step is to compare the foraminiferal loss L with a similar loss L for carbonate, calculated by substituting clay proportions for  $R_0$  and R. The chief difficulty in such a study are the small values of  $R_0$  and R at the depths of interest in both sets of data, which introduce large instabilities in the transformation  $[1 - R_0/R]$  due to measurement errors and interference from processes other than dissolution. It will be necessary, therefore, to combine detailed stratigraphic control—for sedimentation rates—with detailed preservational analysis, including quantitative modeling, in order to calibrate this micropaleontological technique for geochemical processes of dissolution.

### CONCLUSION

Preservation facies of foraminiferal assemblages on the sea floor, as presently mapped, reflect both inherent statistical properties of the assemblages and processes of dissolution operating on these properties. With regard to the concept of the lysocline, it is advisable to clearly distinguish a level of accelerated dissolution in the water column (Peterson's level, or "hydrographic lysocline") from any level of accelerated dissolution on the sea floor ("sedimentary lysocline") from any level of maximum change in foraminiferal (or coccolith) assemblages ("foram lysocline" and "coccolith lysocline").

Much confusion can be avoided in the communication between chemists, sedimentologists, and paleontologists if these distinctions are kept in mind. The term "lysocline" by itself and without qualifier, should be reserved for the concept of a level of accelerated dissolution, while observed depth-dependent inflections in properties of calcareous sediments should bear the

appropriate operational prefix, unless the meaning is clear from the context.

### REFERENCES

- BEN-YAAKOV, S, RUTH, E., and KAPLAN, I. R., 1974, Carbonate compensation depth: relation to carbonate solubility in ocean waters: *Science*, v. 184, p. 982-984.
- BERGER, W. H., 1967, Foraminiferal ooze: solution at depth: *Science*, v. 156, p. 383-385.
- , 1968, Planktonic foraminifera: selective solution and paleoclimatic interpretation: *Deep-Sea Research*, v. 15, p. 31-43.
- , 1970, Planktonic foraminifera: selective solution and the lysocline: *Marine Geology*, v. 8, p. 111-138.
- , 1971, Sedimentation of planktonic foraminifera: *Marine Geology*, v. 11, p. 325-358.
- , (in press), Sedimentation of deep-sea carbonate: maps and models of variations and fluctuations: Symposium on marine plankton and sediments, Kiel, 1974, Micropaleontology Press.
- BRAMLETTE, M. N., 1961, Pelagic sediments, *in* Sears, M., ed., *Oceanography: Am. Assoc. Adv. Sci. Pub.*, v. 67, p. 345-366.
- EDMOND, J. M., 1974, On the dissolution of silicate and carbonate in the deep sea: *Deep-Sea Research*, v. 21, p. 455-480.
- ELLIS, D. B., and MOORE, T. C., JR., 1973, Calcium carbonate, opal, and quartz in Holocene pelagic sediments and the calcite compensation level in the South Atlantic Ocean: *Jour. Marine Research*, v. 31, no. 3, p. 210-227.
- GIESKES, J. M., 1974, The alkalinity-total carbon dioxide system in seawater, *in* Goldberg, E. D., ed., *The sea*, v. 5: New York, Interscience, p. 123-151.
- HEATH, G. R., and CULBERSON, C., 1970, Calcite: degree of saturation, rate of dissolution, and the compensation depth in the deep oceans: *Geol. Soc. America Bull.*, v. 81, p. 3157-3160.
- MCINTYRE, A. and MCINTYRE, R., 1971, Coccolith concentration and differential solution in oceanic sediments, *in* Funnell, B. M., and Riedel, W. R., eds., *The micropaleontology of oceans*: Cambridge Univ. Press, p. 253-261.
- MORSE, J. W., and BERNER, R. A., 1972, Dissolution kinetics of calcium carbonate in sea water: II. A kinetic origin for the lysocline: *Am. Jour. Sci.*, v. 272, p. 840-851.
- PARKER, F. L., and BERGER, W. H., 1971, Faunal and solution patterns of planktonic foraminifera in surface sediments of the South Pacific: *Deep-Sea Research*, v. 18, p. 73-107.
- PETERSON, M. N. A., 1966, Calcite: rates of dissolution in a vertical profile in the central Pacific: *Science*, v. 154, p. 1542-1544.
- RUDDIMAN, W. F. and HEEZEN, B. C., 1967, Differential solution of planktonic foraminifera: *Deep-Sea Research*, v. 14, no. 6, p. 801-808.
- VALENCIA, M. J., 1973, Calcium carbonate and gross-size analysis of surface sediments, western equatorial Pacific: *Pacific Science*, v. 27, no. 3, p. 290-303.

*Research supported by the Oceanography Section, National Science Foundation, NSF Grant GA-41078.*

# DISTRIBUTION AND DISSOLUTION OF COCCOLITHS IN THE SOUTH AND CENTRAL PACIFIC

PETER H. ROTH AND WOLFGANG H. BERGER

Scripps Institution of Oceanography, University of California, San Diego  
La Jolla, California 92037

---

## ABSTRACT

The distribution of coccoliths in surface sediments of the Pacific is greatly influenced by dissolution processes. Etching, fragmentation, and differential removal are obvious from about 3 km depth downward, and increase rapidly below about 4 km depth. Overgrowth is observed on some placoliths in samples at intermediate stages of dissolution. Cluster analysis defines groups of varying preservation aspects in tropical waters, in the central gyre, and at high latitudes. Dissolution rankings

for tropical and extratropical regions are established using pairing analysis. The coccolith lysocline is difficult to define, but can be recognized near 4,000 m depth as a considerable drop in diversity of assemblages with respect to the solution resistance of their members. A comparison of dissolution aspects of coccoliths and forams shows that coccolith dissolution indices are sensitive above the lysocline and foram dissolution indices are sensitive below the lysocline.

---

## INTRODUCTION

Recent calcareous oozes contain up to 30 percent coccoliths, fossil deep-sea carbonates up to 60 percent (Bramlette, 1958). The dissolution characteristics of planktonic foraminifera, which make up the coarse fraction of calcareous oozes, have been studied for some time and in some detail (reviewed by Berger, 1971). Recently, the differential dissolution of coccoliths also has received increasing attention (Bramlette and Sullivan, 1961; Hay, 1970; Hsü and Andrews, 1970; Cita, 1971; McIntyre and McIntyre, 1971; Bukry, 1971, 1973; Roth and Thierstein, 1972; Schneidermann, 1972, 1973; Berger, 1973).

Here we report on the differential dissolution of coccoliths in surface sediments of the South and Central Pacific, roughly following the general format of a similar study on planktonic foraminifera in the same area, by Parker and Berger (1971). In this manner we hope to lay the groundwork for a comparative investigation of the dissolution behavior of the two major

carbonate components in the deep sea. Such study of similarities and differences in preservation patterns should materially improve understanding of both coccolith and foram distributions.

Samples are the same as those studied by Parker and Berger (1971); they are from near tops of cores. Treatment of samples was kept to a minimum to avoid damage of coccoliths. Slides were prepared of all samples for study in the light microscope (LM). The following species or groups of species were counted in the light microscope:

*Gephyrocapsa* sp.  
*Coccolithus pelagicus*  
*Cyclococcolithina leptopora*  
*Umbilicosphaera sibogae*  
*Cyclolithella annula*  
*Helicopontosphaera kamptneri*  
*Umbellosphaera* sp.  
*Discosphaera tubifera*  
*Rhabdosphaera clavigera*

*Syracosphaera pulchra*  
*Syracosphaera histricea*  
*Syracosphaera* sp.  
*Pontosphaera discopora*  
*Pontosphaera scutellum*  
*Scapholithus*  
*Scyphosphaera* sp.  
*Ceratolithus cristatus*  
*Thoracosphaera* sp.

At least 400 specimens were counted in each sample containing a sufficient number of coccoliths. Because many of the smaller forms cannot be identified with certainty in the light microscope, all samples were also studied in the scanning electron microscope (SEM). An untreated suspension of the sample in distilled water was spread on a piece of cover glass which was attached to a SEM specimen stub. The suspension was dried and coated with gold-palladium. The following specimens were counted in the SEM:

*Emiliana huxleyi*  
*Gephyrocapsa oceanica*  
*G. caribbeanica*  
*G. ericsonii*  
*Cyclococcolithina fragilis*  
*Umbellosphaera hulburtiana*  
*Umbellosphaera tenuis*  
*U. irregularis*  
*Syracosphaera* sp.

The ratios of these species to the total number of *Gephyrocapsa* were determined, which allowed calcula-

tion of the percentages of these species with respect to the light microscope counts. Solution and overgrowth effects on the ultrastructure were noted and some typical specimens were photographed (see pls. 1-3). The following species are easily recognized even after partial destruction:

*Emiliana huxleyi*  
*Cyclococcolithina leptopora*  
*Coccolithus pelagicus*  
*Helicopontosphaera kamptneri*  
*Umbellosphaera tenuis*  
*Rhabdosphaera clavigera*  
*Ceratolithus cristatus*  
*Scapholithus*

The fact that some species are readily recognized after partial destruction, while others become unidentifiable can introduce bias into counts. Unrecognizable fragments were not counted.

Data will be published in full upon completion of a study of coccolith distributions in the entire Pacific.

#### IDENTIFICATION OF COCCOLITHS

*Emiliana huxleyi*: Can only be identified in the SEM with certainty. Strongly dissolved rims are difficult to distinguish from rims of *Gephyrocapsa*. There are two ecophenotypic variants, a cold-water form with fused elements in the proximal shield and a warm water form with T-shaped elements in both shields. These two forms were not separated in the present study.

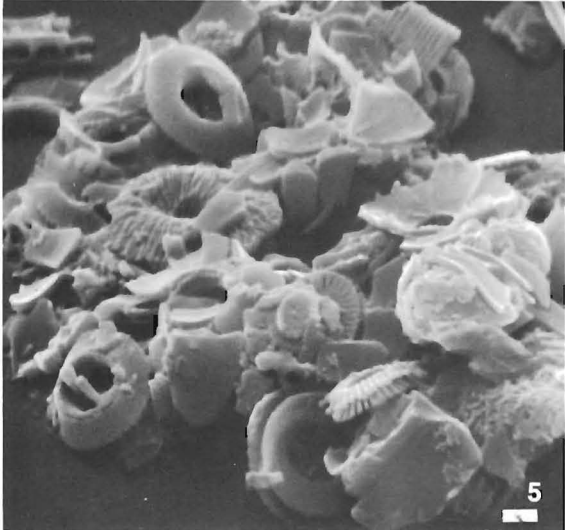
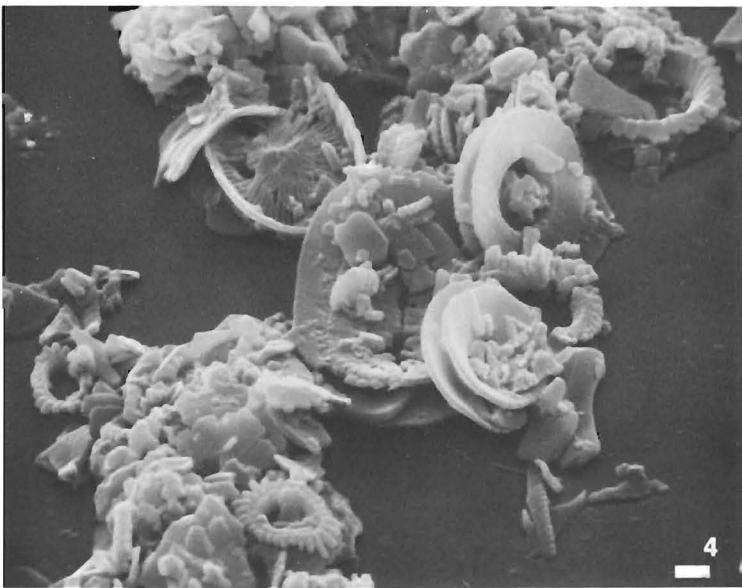
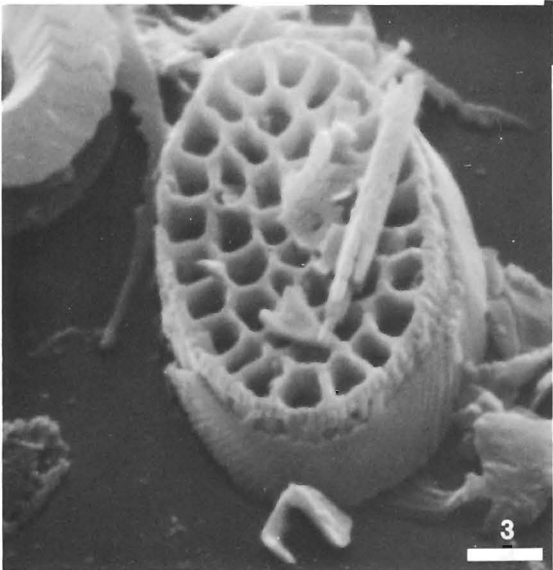
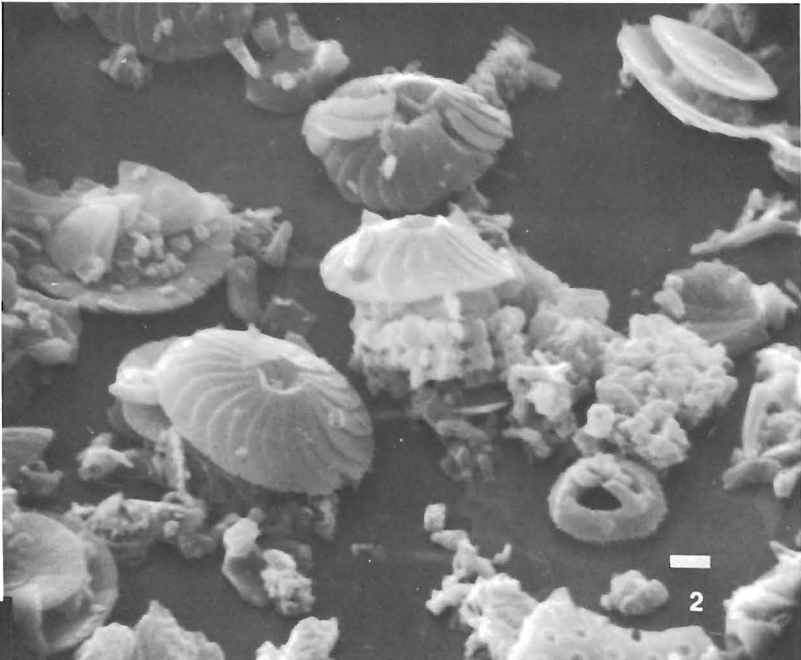
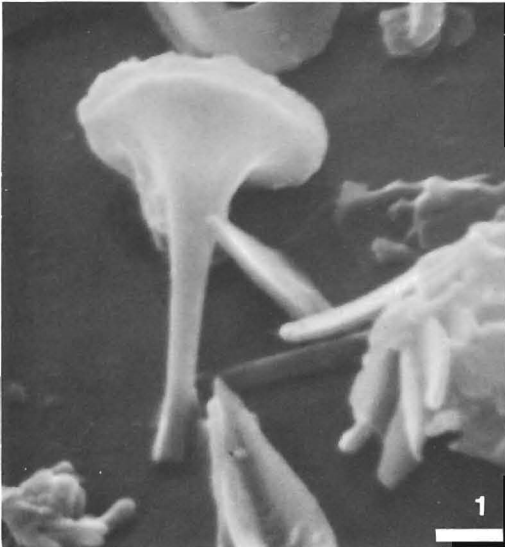
#### PLATE 1

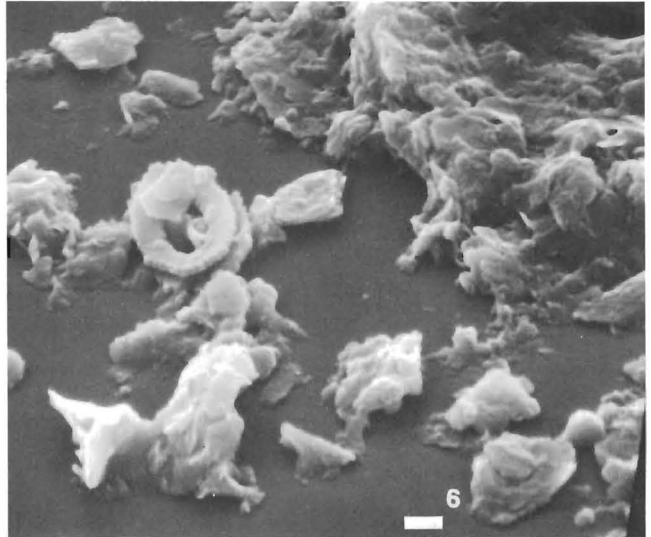
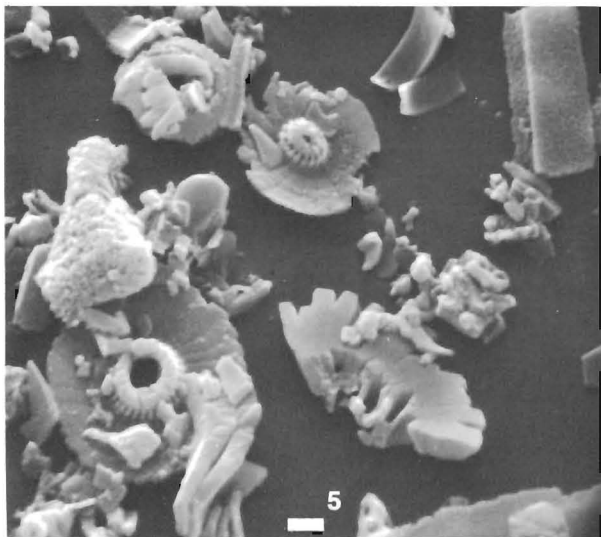
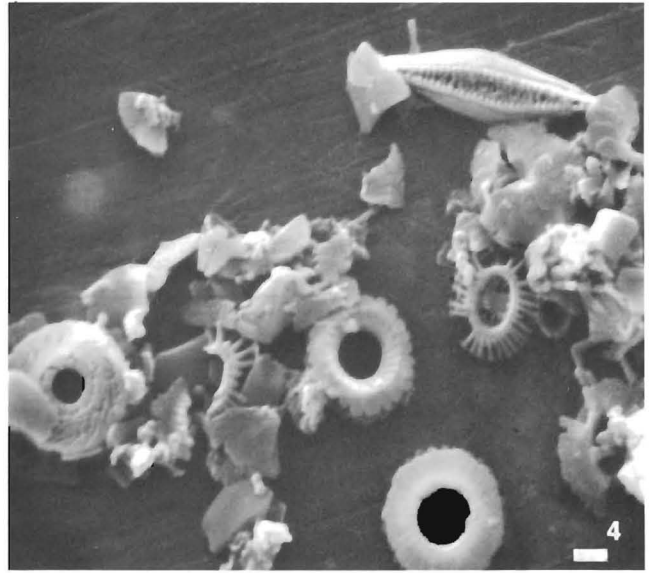
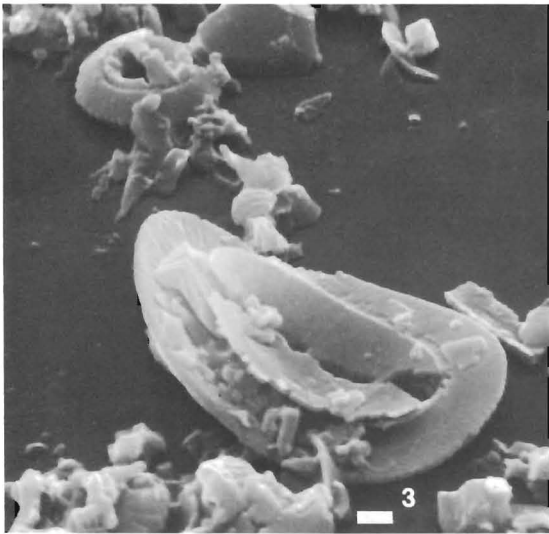
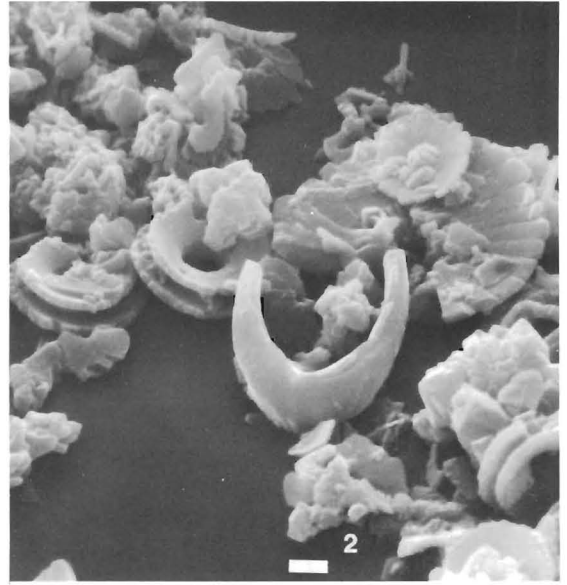
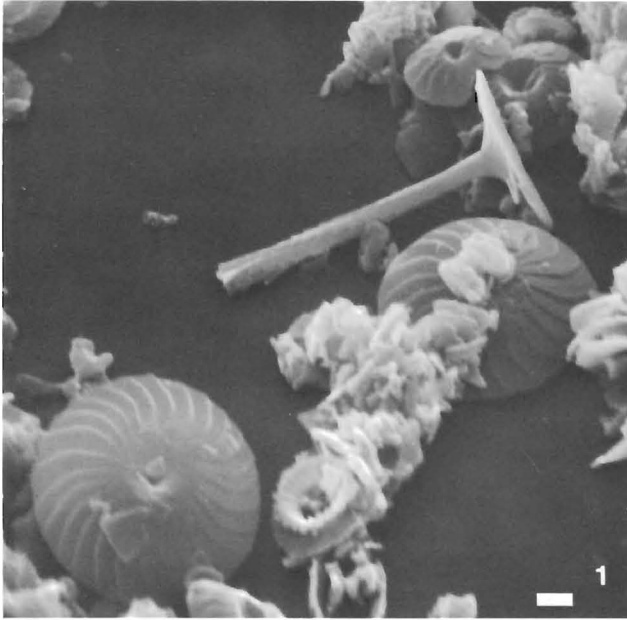
Length of bar is 1  $\mu$ m in all figures.

- 1 Central process of *Discosphaera tubifera*, one of the least-resistant coccoliths. The basal plate which would be attached to the narrow end of the central process is missing. Core RIS 87, S16°30', W145°7', water depth 1,443 m.
- 2 Characteristic mid-latitude assemblage with small *Cyclococcolithina leptopora* (cold-water form) and *Gephyrocapsa caribbeanica* (lower right). The high percentage of resistant forms makes this sample look more dissolved. Core DWD 36HG, S45°30', W119°50', water depth 3,770 m.
- 3 *Pontosphaera discopora*, a delicate species composed of thin laths. This species is rare and usually found only in samples from above the lysocline. Core MP 33L, N17°51', W174°17', water depth 1,750 m.
- 4 Assemblage with *Syracosphaera pulchra* (upper left) with slightly damaged central grill, *Helicopontosphaera kampt-*

*neri* with a partially dissolved center, two well-preserved specimens of *Gephyrocapsa oceanica* (to the right of *H. kamptneri*) and strongly corroded specimens of *Emiliana huxleyi* (lower left). Core LSDH-79, S3°23', E170°2', water depth 3,600 m.

- 5 Well preserved assemblage with *Umbellosphaera tenuis* (center), *Emiliana huxleyi* with T-shaped elements in both shields (lower right), *Gephyrocapsa caribbeanica* (lower left), and *G. oceanica* (upper left). Core CAP 24BG, S19°29', W137°44' water depth 2,780 m.
- 6 Slightly corroded specimen of *Cyclolithella annula* with some slits between the elements due to dissolution. *Gephyrocapsa oceanica* (lower right) shows hardly any corrosion. Core CAP 4BG, S4°8', E171°46', water depth 3,670 m.





*Gephyrocapsa oceanica*: The bridge forms a low angle of 20° or less with the short axis of the ellipse. Forms described as *Gephyrocapsa omega* Bukry, 1973 (= *G. parallela* Hay and Beaudry, 1973, p. 672, pl. 1, figs. 10–12) are considered variants of *Gephyrocapsa oceanica*.

*Gephyrocapsa caribbeanica*: This species is characterized by a relatively small central area with a bridge forming an angle of about 40°–50° with the small axis of the ellipse. *Gephyrocapsa lumina* Bukry, 1973 is included in this species.

*Gephyrocapsa ericsonii*: A highly arched bridge forms an angle of about 60° with the short axis of the ellipse. This species is also the smallest of the three species of *Gephyrocapsa*.

*Cyclococcolithina leptopora*: The two shields often separate in highly dissolved samples. Only proximal shields (bright under crossed nicols) and whole specimens were counted. Varieties used by McIntyre and Bé (1967) were not distinguished because intergradations occur commonly. However, a trend of decreasing size with increasing latitude was also observed in the samples studied.

*Cyclococcolithina fragilis*: Only symmetrical forms as illustrated by Deflandre and Fert (1954) and Okada and Honjo (1973) were found in the Pacific. Asymmetrical forms (= *Discolithus antillarum* Cohen = *Oolithotus antillarum* Cohen) were not encountered in any sample from the Pacific.

*Umbilicosphaera sibogae* (= *Umbilicosphaera mirabilis*): Two forms were observed. The warm-water

form has a large central hole and a distal shield smaller than the proximal shield. The cold-water form is more robust, shows a well-developed inner cycle (called overgrowth by McIntyre and Bé, 1967) and a crater-like depression in the center. In the LM these specimens are often difficult to distinguish from small and poorly preserved specimens of *Cyclococcolithina leptopora*.

*Cyclolithella annula*: The species concept of McIntyre and Bé (1967) is followed. Slightly etched specimens develop slits between the elements (pl. 1, fig. 6). The more robust cold-water form was not distinguished from the more delicate warm-water forms.

*Umbellosphaera irregularis* and *U. tenuis*: Only the distal side of *U. tenuis* shows ridges and is readily distinguishable from *U. irregularis*. The proximal sides of the two species are almost identical.

*Rhabdosphaera clavigera*: This species is considered to include forms assigned to *Rhabdosphaera stylifera* by some authors.

*Syracosphaera* sp.: In the LM it is possible to distinguish *S. hystrica* from *S. pulchra* by the hourglass-shaped extinction figures under crossed nicols of the formal species. In dissolved samples, usually only the rim remains. These rims, together with other rare specimens of other species of *Syracosphaera*, were listed as *Syracosphaera* sp.

*Syracosphaera ribosa* (Kamptner) n. comb. (= *Discolithus ribosus* Kamptner, 1967, p. 136, pl. 5, figs. 30–31) occurs in some samples, but is always rare.

*Pontosphaera*: Besides *Pontosphaera discopora* (with

←

## PLATE 2

Length of bar is 1  $\mu$ m in all figures

- 1 *Rhabdosphaera clavigera* (upper half). *Cyclococcolithina leptopora* (lower half) and *Umbilicosphaera sibogae* (two well-preserved specimens upper right, above *Rhabdosphaera*, a strongly etched specimen to the right of the lower *C. leptopora*), Core RIS 76G, S13°54', W125°21', water depth 3,800 m.
- 2 Assemblage dominated by dissolution resistant species. In the center the horseshoe-shaped *Ceratolithus cristatus*, to the right of it *Gephyrocapsa* sp. with jagged outlines, in the upper right two isolated distal shields of *Cyclococcolithina leptopora*. Core CAO 12HG, S20°25', E178°14', water depth 3,600 m.
- 3 Beginning fragmentation of coccoliths. *Helicopontosphaera kamptneri* with corroded center and *Gephyrocapsa oceanica* (upper left) with part of the shield broken out. Many coccolith fragments. Core MP-10-1, N40°35', W139°58', water depth 4,451 m.
- 4 Etching and first signs of fragmentation of more delicate coccoliths. Well-preserved *Scapholithus* (upper right), *Umbilicosphaera sibogae* (specimen with secondary cycle and small central depression below scapholith, two specimens without inner cycle in center and lower right) and *Emiliana huxleyi* with some missing elements. Many fragments of coccoliths. Core R1S84, S15°15', W142°27', water depth 3,675 m.
- 5 Assemblage consisting almost completely of fragments and isolated shields. Isolated distal shields of *Cyclococcolithina leptopora* (lower left and above center). Fairly well-preserved *Gephyrocapsa caribbeanica* (the upper left) and many coccolith fragments. Core MNS-135, S4°26', W149°24', water depth 4,600 m.
- 6 Almost completely dissolved assemblage with *Gephyrocapsa* sp. and some fragments, but dominated by clay minerals. Core LSDH-61, S13°7', E152°24', water depth 4,610 m.

many relatively large pores visible in the LM) and *P. scutellum* (no pores visible), some other rare species occur like *P. syracusana* (= *P. alboraenis* Bartolini, 1970, p. 148–150, pl. 6, figs. 6–7) with a high wall and numerous small pores, and *P. messinae* with small pores only in the central part.

*Scyphosphaera*: All specimens observed belong to *Scyphosphaera apsteinii*.

*Thoracosphaera*: Most specimens observed can be assigned to *Thoracosphaera heimi* or *T. saxea*, but no attempt was made to list them as species because they are only a minor component of the coccolith fraction in most samples.

*Scapholithus*: The genera *Anoplosolenia* and *Calciosolenia* are based on the morphology of the living cell. Therefore, the organ genus *Scapholithus* was used for these scapholiths.

#### OBSERVATIONS ON ETCHING, FRAGMENTATION, AND OVERGROWTH

Partial dissolution in its early stages leads to etching of coccoliths producing rounded corners of crystallites (pl. 3, fig. 2) and serrate margins (pl. 2, fig. 4; pl. 1, fig. 6). Generally, the smaller the crystallites a coccolith is composed of, the more easily it is destroyed (Roth and Adelseck, unpublished observations). As dissolution advances more delicate parts of the coccoliths, like central grills and loosely attached plates, are destroyed (pl. 1, fig. 4). Finally breakup begins (pl. 2, fig. 3) and results in an ever-increasing amount of coccolith fragments (pl. 2, figs. 4–6). Similar observations have been made by earlier workers.

Bukry (1971) discussed the dissolution resistance of various fossil nanoplankton genera and indicated some of the factors responsible for the relatively high resistance of nanofossils, such as incorporation of cellulose-like material within the skeletal calcite, organic coatings

on the surface of coccoliths and relative position of the optic axis in the elements of the coccoliths. McIntyre and McIntyre (1971) and Scheidemann (1972, 1973) discussed the selective removal of coccoliths from sediment assemblages and the destruction of ultrastructural elements of various species as dissolution proceeds.

Overgrowth, that is the deposition of secondary calcite on fossil coccoliths, gives important clues for precipitation-dissolution reactions of carbonate in interstitial waters. Overgrowth on Cenozoic and Cretaceous nanofossils has been amply demonstrated (Bukry and others 1971; Roth, 1973; Schlanger and others, 1973). Experimental evidence provided by Adelseck and others (1973) shows that discoasters and large coccoliths grow at the expense of small coccoliths under simulated diagenetic conditions. Burns (1972) described overgrown discoasters from recent sediment. They are obviously reworked from older sediments and most probably had acquired secondary overgrowth before they were redeposited in recent biogenous oozes. Thus, the question whether overgrowth can occur near the sea floor remained open.

Secondary calcite deposits were observed in a large number of our samples, although *Cyclococcolithina leptopora* (pl. 3, fig. 3) and *Umbilicosphaera sibogae* (pl. 3, fig. 4) are the only two species that show secondary overgrowth, usually restricted to the distal shield. Significantly, overgrowth is most prevalent in samples ranging in depth from about 3,500 m to 4,800 m and which show considerable dissolution effects with increased numbers of solution-resistant species and fragments of coccoliths. Reworked Tertiary nanofossils were not observed in the samples showing secondary overgrowth. This is a clear indication that dissolution and reprecipitation of calcite on nanofossils can occur within centimeters of the sediment-water interface and does not require much overburden nor geologically long time.

---

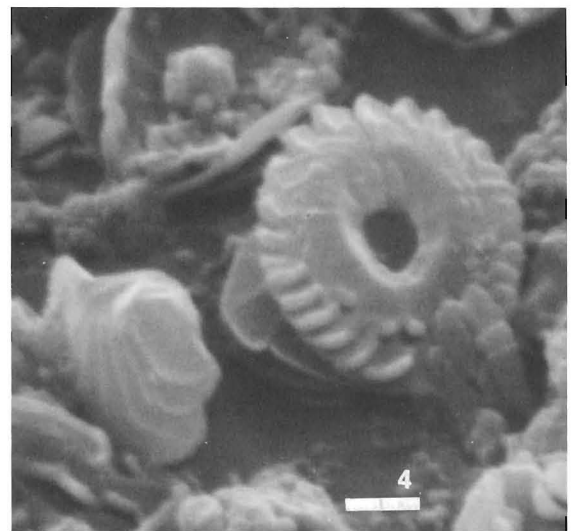
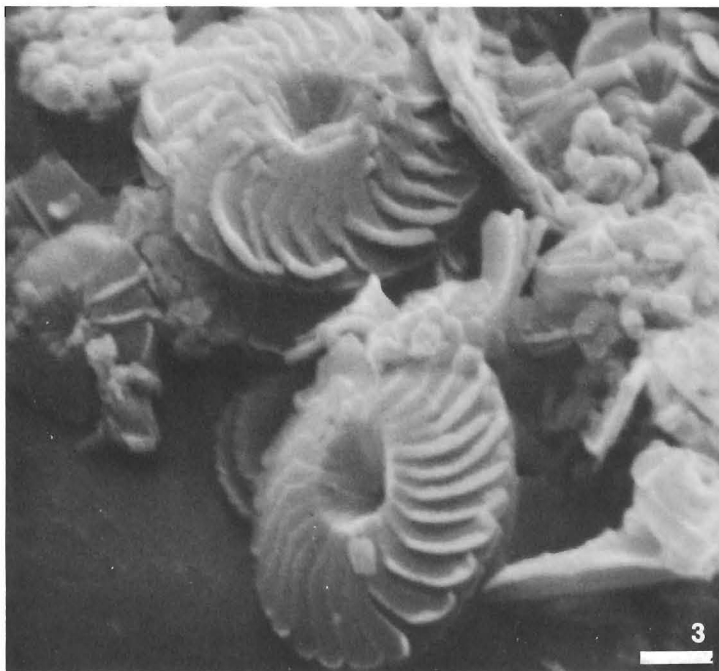
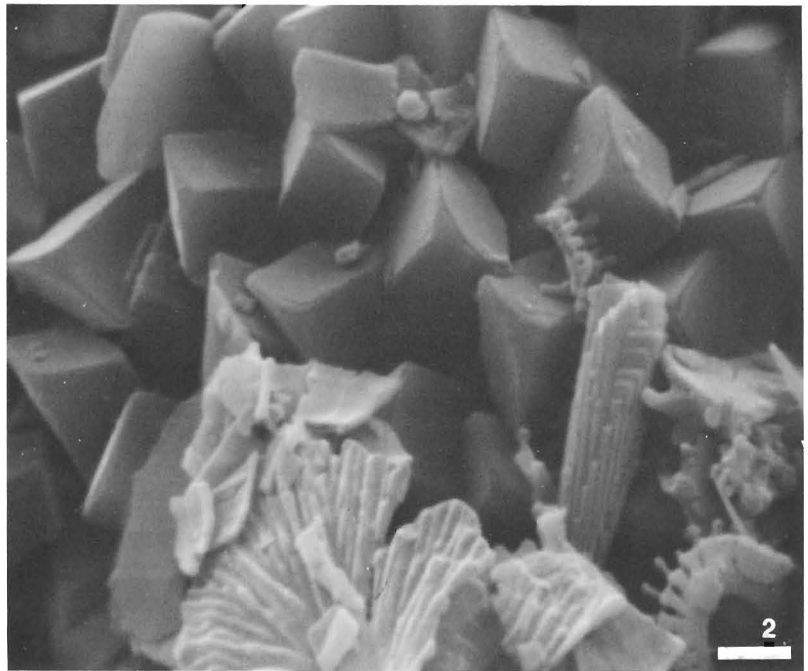
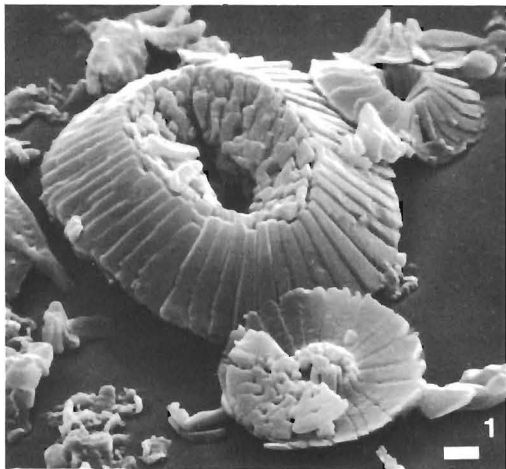
#### PLATE 3

Length of bar is 1  $\mu\text{m}$  in all figures

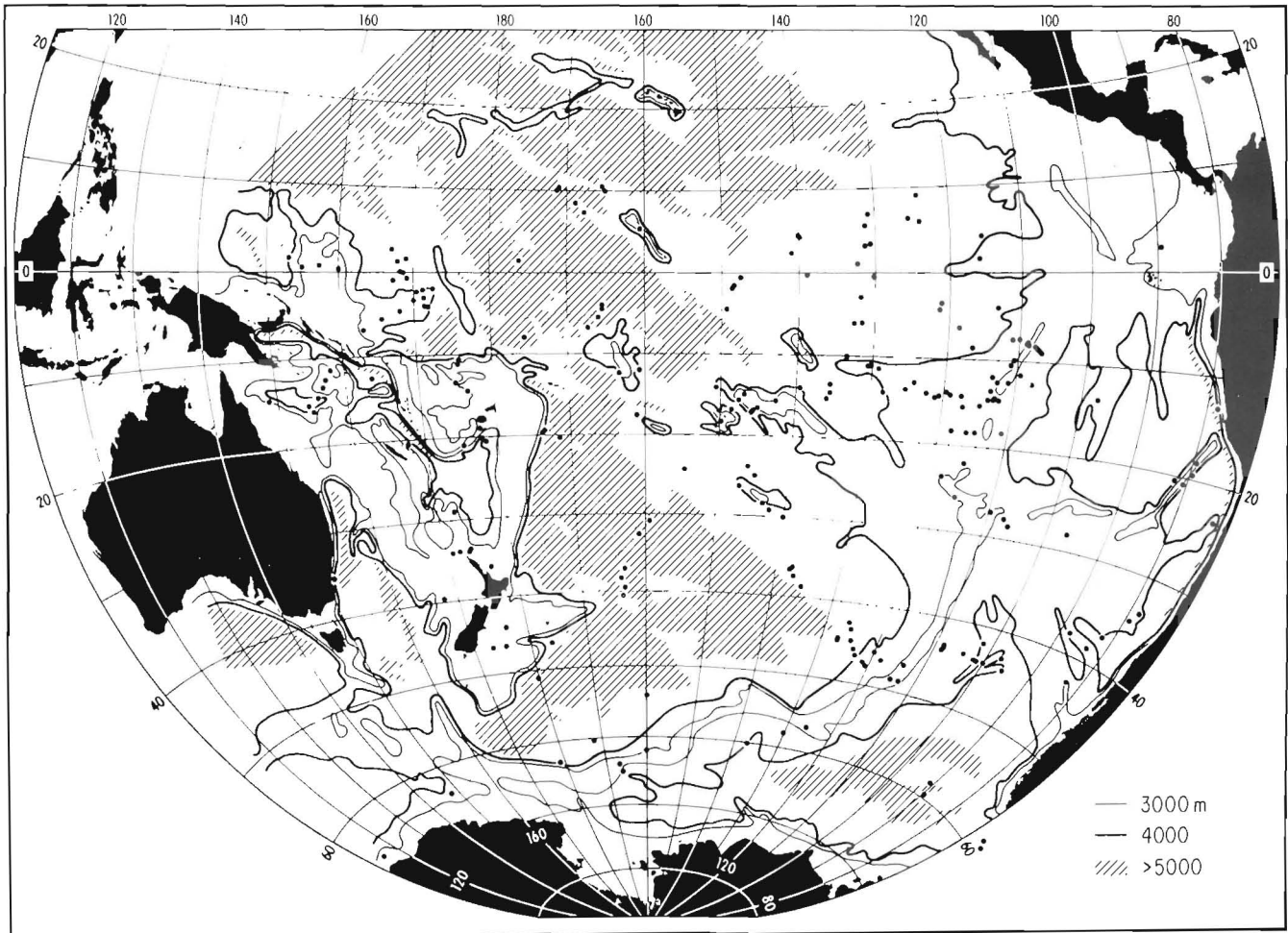
- 1 Cold-water assemblage with *Coccolithus pelagicus* and small *Cyclococcolithina leptopora*. Core DWD-35-HG, S44°21', W127°14', water depth 4,675 m.
- 2 Wall of *Thoracosphaera* sp. composed of calcite rhombs. Slight dissolution resulted in rounded corners and edges of the rhombs. The damaged specimen of *Umbellosphaera tenuis* also shows dissolution effects. Core MP33L, N17°51', W174°17', water depth 1,750 m.
- 3 Secondary calcite overgrowth on the distal shields of

*Cyclococcolithina leptopora* resulting in ridges along the edges of the elements. Coccoliths are of latest Pleistocene to Holocene age. Core CAO 14 HG, S14°43', W121°1', water depth 3,660 m.

- 4 Secondary overgrowth on the distal shield of *Umbilicosphaera sibogae*. The ridges of secondary calcite along the edges of the elements seem to be restricted to the outer cycle of the shield. Core CAP 46 HG, S12°3', W113°24', water depth 3,276 m.







TEXT FIGURE 1

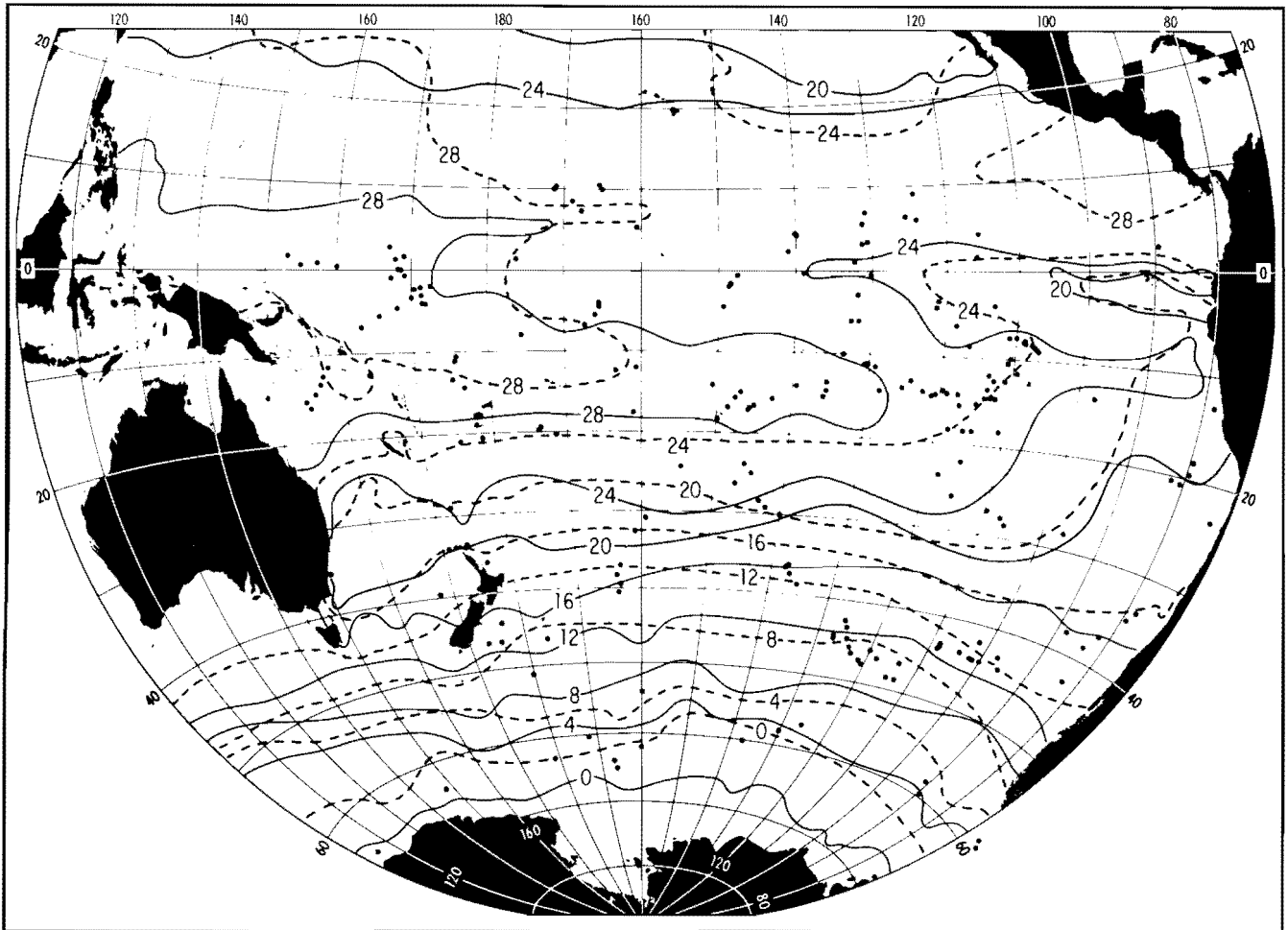
Bathymetry of the South Pacific (after Menard, 1964; from Parker and Berger, 1971).

## GEOGRAPHY AND OCEANOGRAPHY

The main features of the geography and oceanography of the area under study are evident in text figures 1 to 3. The South Pacific floor is divided into several major basins by the north-south-trending East Pacific Rise, the east-west-trending Pacific-Antarctic Ridge, and the Sala y Gomez-Chile Rise complex. Calcareous sediments rich in coccoliths are generally restricted to depths shallower than 4.5 km (see calcium compensation depth map in the introduction to this volume).

Surface temperature distributions result from the upper water circulation pattern and from warming in low latitudes. In general, the isotherms trend east-west

parallel to the prevailing currents, and fluctuate north and south according to season. A major deflection of isotherms is evident in the eastern south Pacific where the north-flowing Peru-Chile Current carries cold waters toward the tropics. Equatorial upwelling also results in a distinct temperature anomaly, with isotherms indicating a ribbon of relatively cooler water within several degrees of the equator. Phosphate distributions reflect the general circulation patterns and show that there are essentially two high fertility provinces from which considerable coccolith production may be expected, that is, the equatorial tropics and the west-wind drift region. The tropical and the extratropical supply centers are separated by the subtropical gyre center which forms a low fertility boundary zone.



TEXT FIGURE 2

Temperature of the sea surface (after Reid, 1969; from Parker and Berger, 1971). Solid line, southern summer; dashed line, southern winter.

### GEOGRAPHIC SPECIES DISTRIBUTIONS

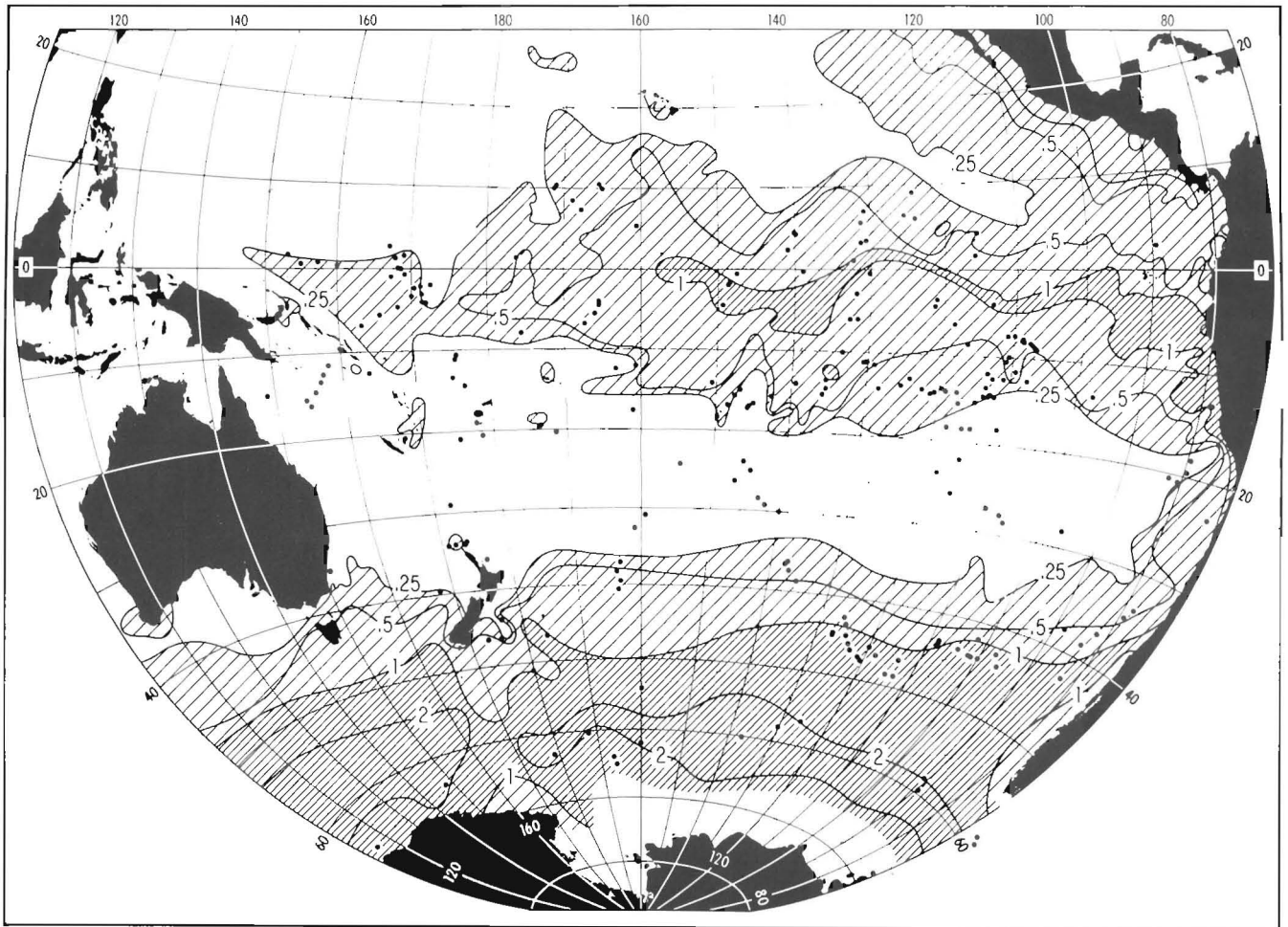
Longitude-latitude and latitude-depth plots for each important coccolith species (text figs. 4, 5, 6, 7) provide a ready reference to their geographic distributions. These reflect (1) the overall relative abundance of a species, (2) its preference as to tropical, extratropical, or cosmopolitan habitat, and (3) its resistance to dissolution.

The various distributions may be briefly characterized as follows:

*Emiliania huxleyi* is present in almost all samples, except for very deep ones. It is most abundant (40–60 percent) in areas shallower than 3,000 m, but occurs from 500–4,600 m. Samples in the equatorial

region (lat 10°N. to 10°S.) generally contain fewer specimens of *E. huxleyi* than the area between 10°S. and 30°S. and 40°S. and 50°S. There seems to be no trend with respect to phosphate distributions.

The highest percentages of *Gephyrocapsa oceanica* are found in the tropics, in the deeper parts of the ocean (4,000–4,900 m). There is no evidence of any fertility control on the distributions of either *Gephyrocapsa oceanica* or *G. caribbeanica*. The cold-water species, *G. caribbeanica*, also increases proportionally at greater depth, although this trend is less pronounced in this species than in *G. oceanica*. Highest concentrations occur between 3,700 m and 4,900 m, south of lat 25°S. and in the area of the cold Humboldt Current.



TEXT FIGURE 3

Distribution of  $\text{PO}_4\text{-P}$  at the surface in  $\mu\text{g-at./l}$  (after Reid, 1962; from Parker and Berger, 1971). Blank area:  $\text{PO}_4\text{-P}$  less than  $0.25 \mu\text{g-at./l}$ . Widely hachured:  $\text{PO}_4\text{-P} = 0.25$  to  $1 \mu\text{g-at./l}$ . Narrowly hachured:  $\text{PO}_4\text{-P}$  more than  $1 \mu\text{g-at./l}$ .

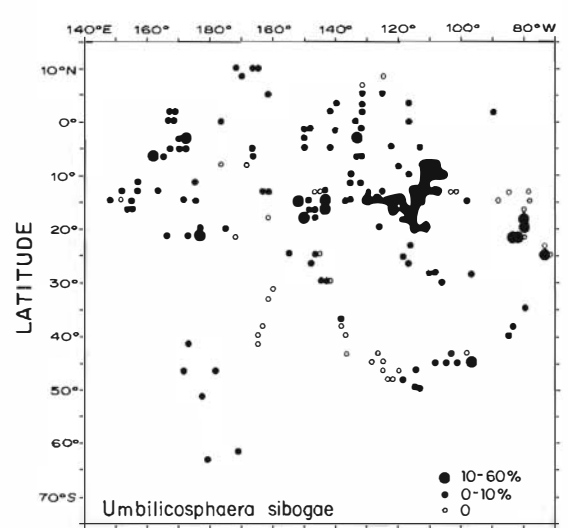
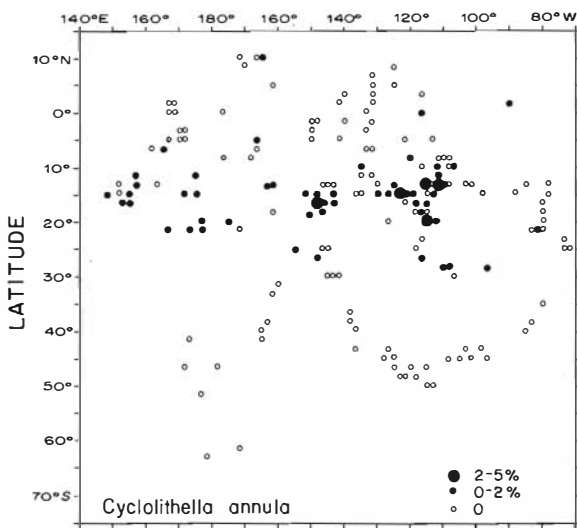
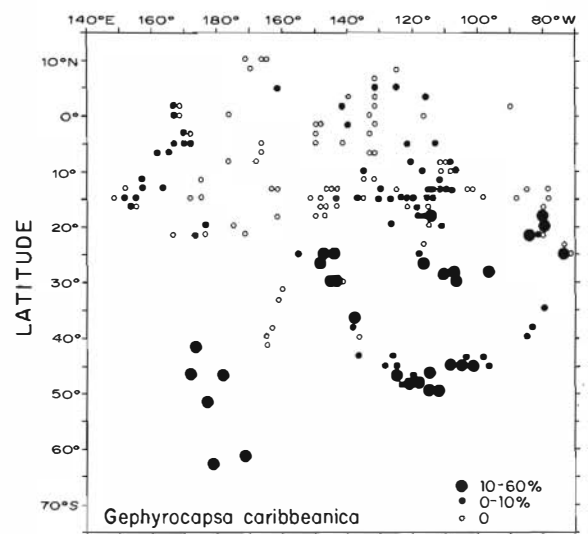
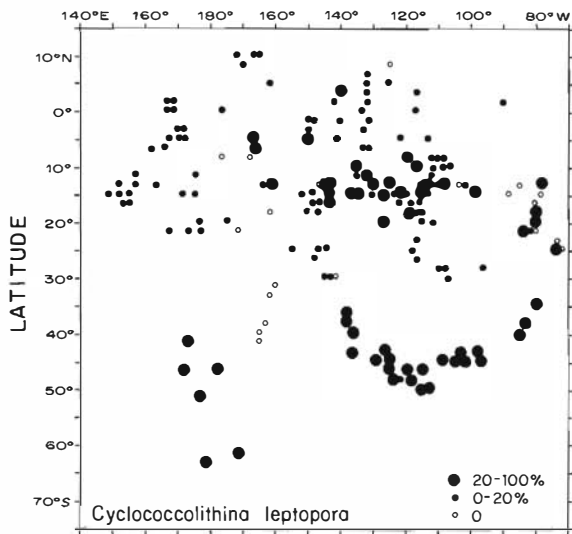
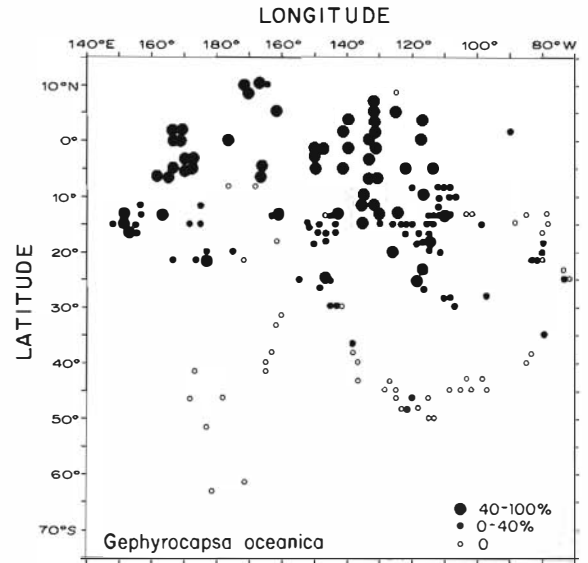
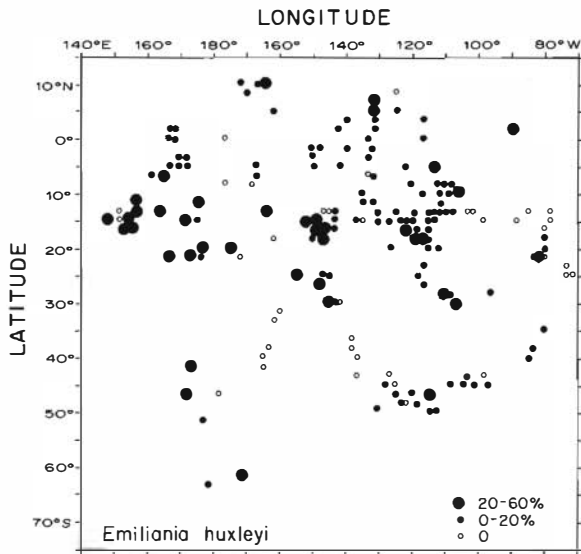
*Cyclocolithina leptopora* is most abundant in the high-fertility areas between the equator and lat  $20^\circ\text{S}$ . and between lat  $35^\circ\text{S}$ .– $60^\circ\text{S}$ ., but it is never abundant in the central gyre. In low latitudes, a pronounced increase of this solution-resistant species with depth results in high percentages between 3,500 m and 5,000 m.

*Umbilicosphaera sibogae* occurs in great numbers, between lat  $8^\circ\text{S}$ . and  $20^\circ\text{S}$ ., along the East Pacific Rise and the Nazca Rise, around the Society Islands, and less commonly on the tropical West Pacific Plateaus. This species is generally more abundant in the eastern part of the South Pacific. Fairly high values are also observed on the East Pacific Rise between lat  $40^\circ\text{S}$ . and  $50^\circ\text{S}$ .. *Umbili-*

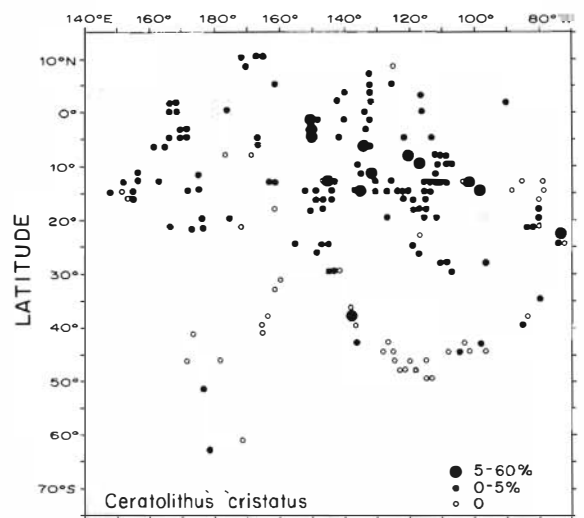
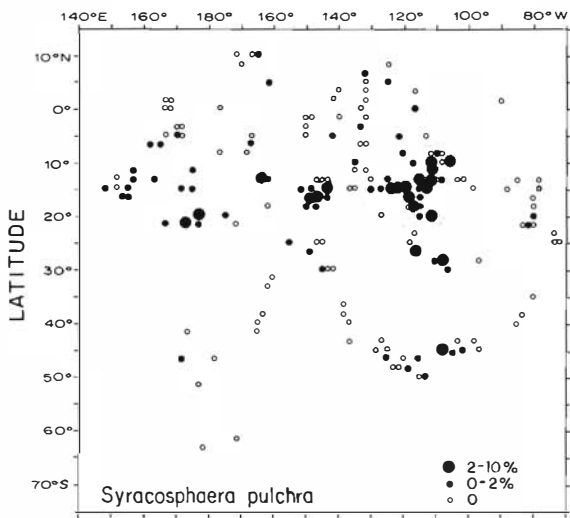
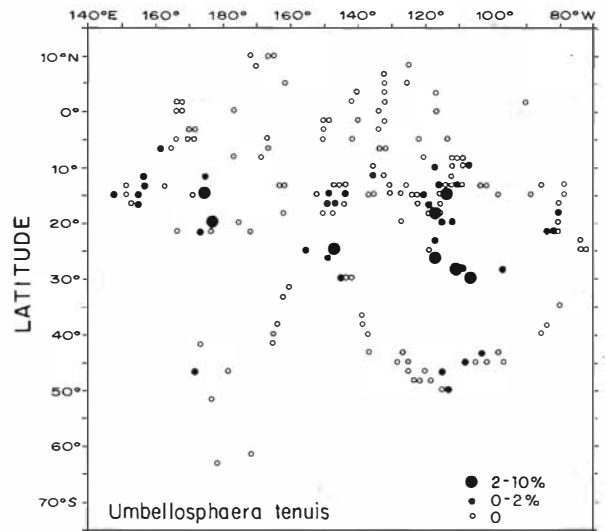
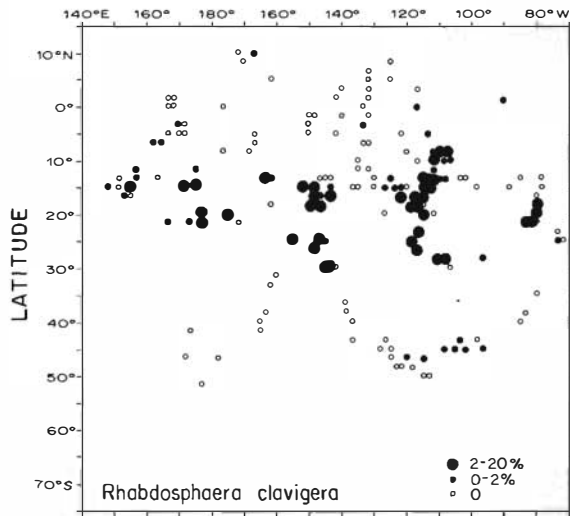
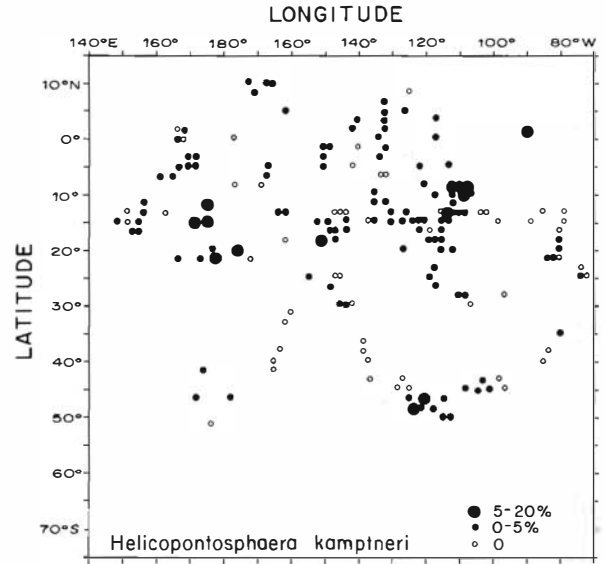
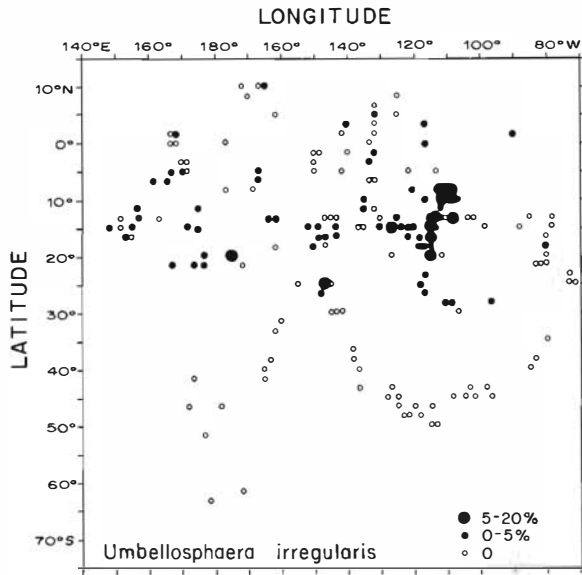
*cosphaera sibogae* is never very abundant in the central gyre and seems to be best developed in medium-to high-fertility regions. It is medium resistant and is most abundant between 3,000 m and 4,300 m.

*Cyclolithella annula*, a tropical species avoiding the equator proper, is rather delicate and is never very abundant. Its highest proportions (2–5 percent) occur between 2,500 m and 3,800 m, and between lat  $10^\circ\text{S}$ . and  $20^\circ\text{S}$ .. As *U. sibogae* it is most abundant in areas with medium  $\text{PO}_4\text{-P}$  values in the water.

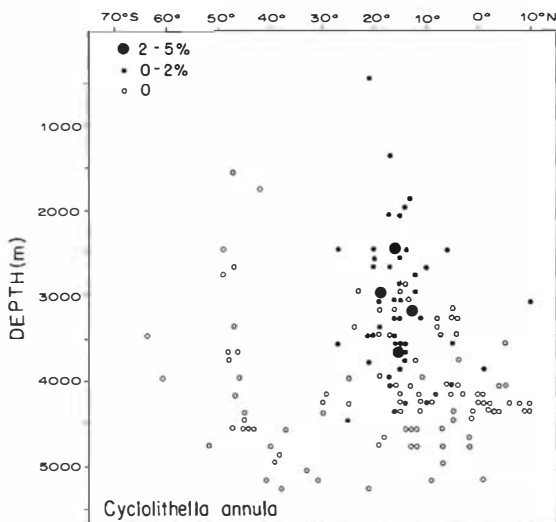
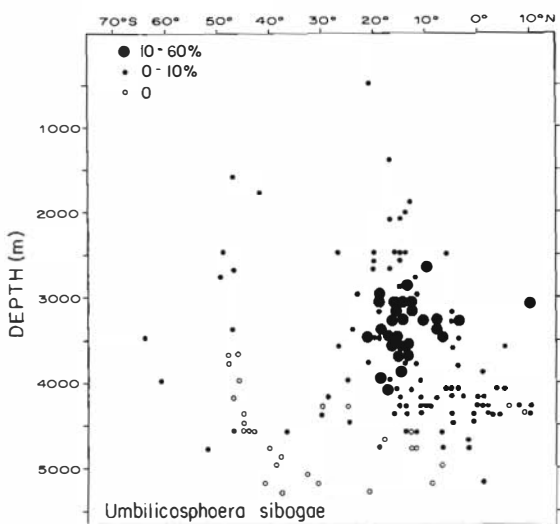
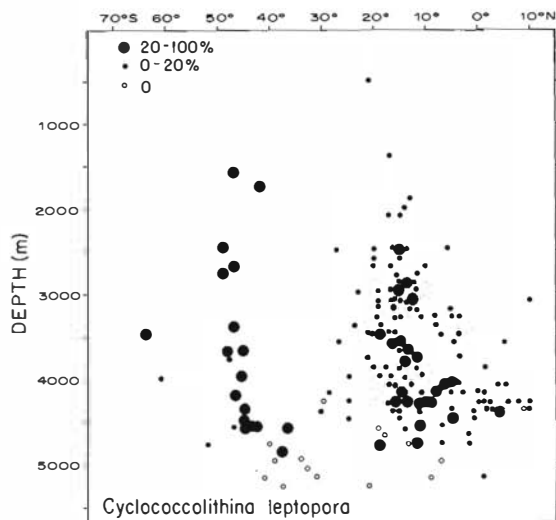
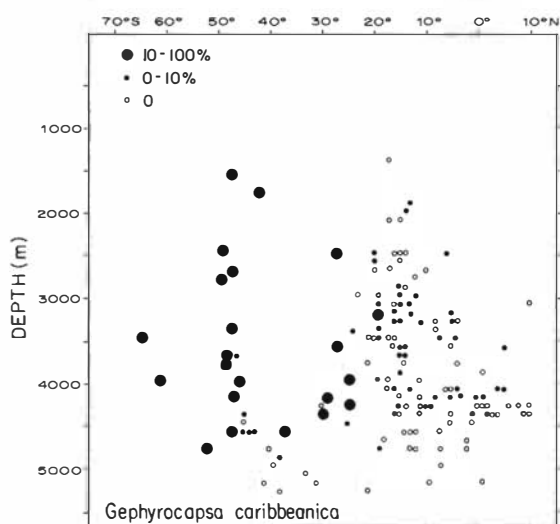
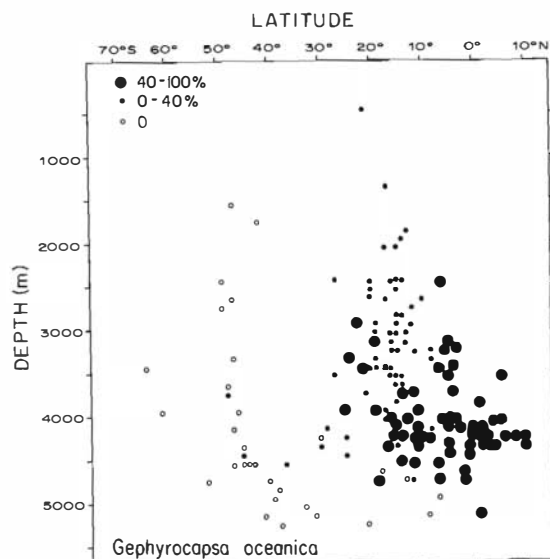
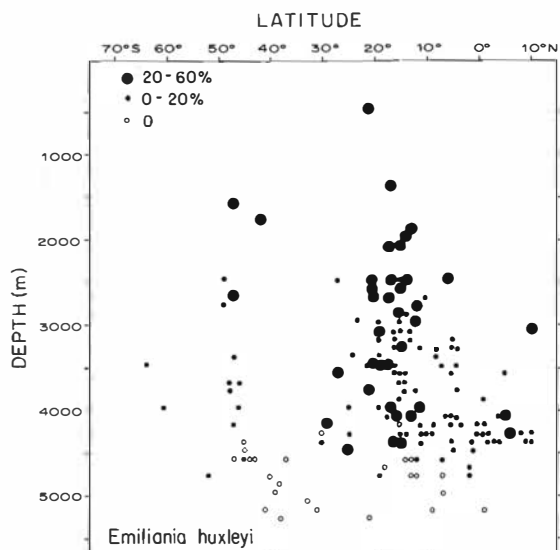
*Helicopontosphaera kamptneri* usually is a minor constituent of the coccolith assemblages. It was observed in greatest relative abundance (5–20 percent) between lat  $8^\circ\text{S}$ . and  $20^\circ\text{S}$ . and between  $45^\circ\text{S}$ . and



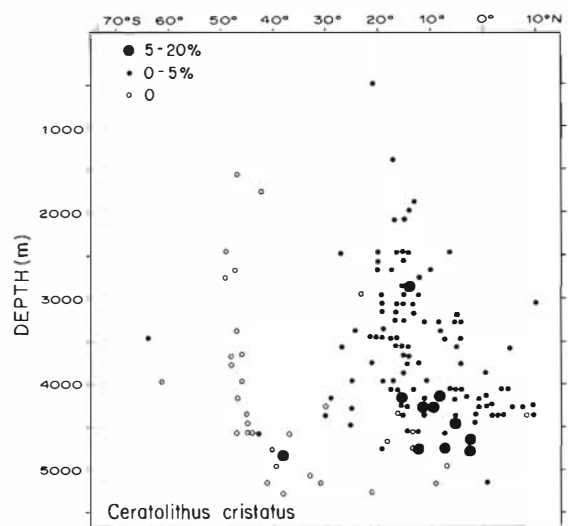
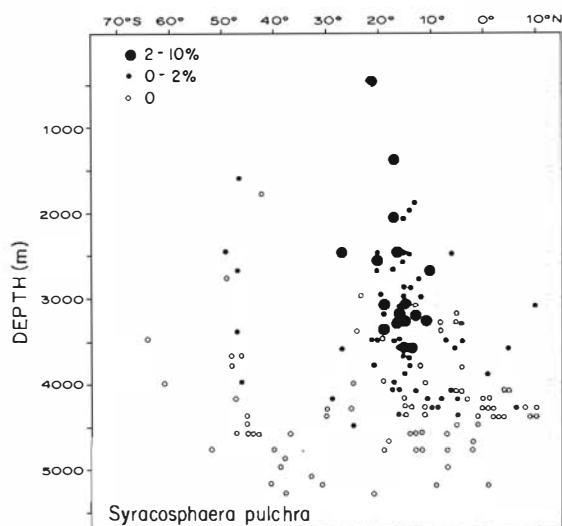
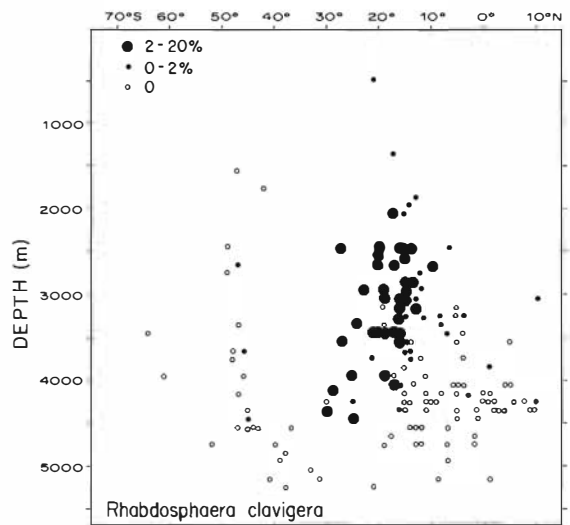
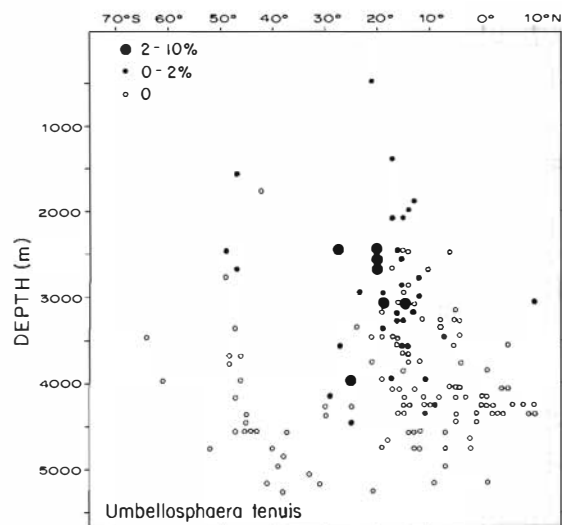
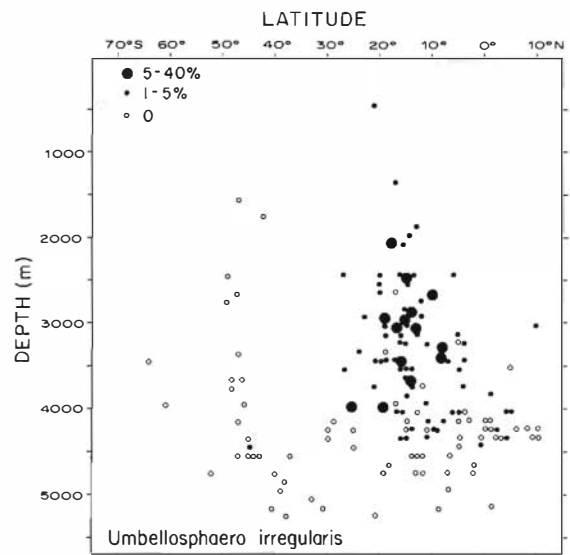
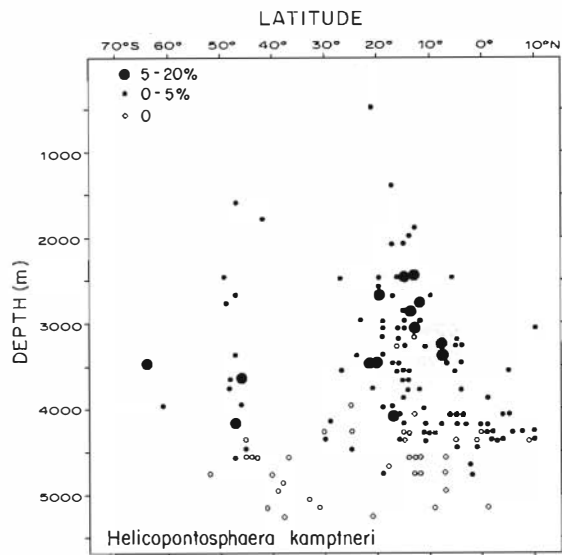
TEXT FIGURES 4 AND 5



Geographic distribution of important coccolith species in surface sediments of the Central and South Pacific.



TEXT FIGURES 6 AND 7



Depth-latitude distribution of important coccolith species in surface sediments of the Central and South Pacific.

TABLE 1

Distribution of important coccolith species with respect to depth, latitude, temperature, and phosphate in surface waters.

Species	Highest Percentage of Total	Depth	Latitude	Temperature	PO <sub>4</sub> -P
<i>E. huxleyi</i>	60%	shallow < 3000 m	10°S–20°S 40°S–50°S	24°–28° 8°–16°	medium–low
<i>G. oceanica</i>	> 80%	deep (4000–5000 m)	10°N–15°S	26°–28°	high to low
<i>G. caribbeanica</i>	> 80%	deep (3700–4900 m)	25°S–65°S	20°–4°	high to low
<i>C. leptopora</i>	> 80%	deep (3000–5000 m)	0°S–20°S 40°S–50°S	24°–28° 8°–16°	high
<i>U. sibogae</i>	60%	intermediate (3000–4000 m)	0°S–20°S	24°–28°	medium–high
<i>C. annula</i>	5%	shallow (2500–3500 m)	10°S–20°S	26°–28°	medium
<i>H. kamptneri</i>	20%	intermediate (2500–3500 m)	8°S–22°S 45°S–65°S	26°–28° 4°–12°	high
<i>U. irregularis</i>	40%	shallow to intermediate (2000–4000 m)	8°S–20°S	26°–28°	high
<i>U. tenuis</i>	10%	shallow to intermediate (2000–3800 m)	10°S–20°S	24°–28°	medium–low
<i>R. clavigera</i>	20%	shallow to intermediate (2000–4600 m)	9°S–30°S	24°–28°	low
<i>S. pulchra</i>	10%	shallow to intermediate (2000–3800 m)	10°S–20°S	24°–28°	medium–low
<i>C. cristatus</i>	20%	deep (4000–5000 m)	0°S–15°S	26°–28°	high

65°S., at depths ranging from 2,500 m and 3,600 m. At the equator and in the central gyre, abundances are distinctly lower, indicating a preference for gyre margin waters of medium to high fertility.

*Umbellosphaera irregularis*, a delicate species, never comprises more than 20 percent of the coccolith assemblages. It is most abundant in samples from between lat 5°S. and 25°S., at 2,000 m to 4,000 m depth, mostly along the East Pacific Rise and near large island chains. It tends to prefer fertile waters. *Umbellosphaera tenuis* is generally even less abundant and never exceeds 10 percent of sediment assemblages. It seems most common in samples from 2,500 m to 3,000 m in a band between lat 15°S. and 30°S. and is thus relatively abundant in low-fertility waters of the central gyre.

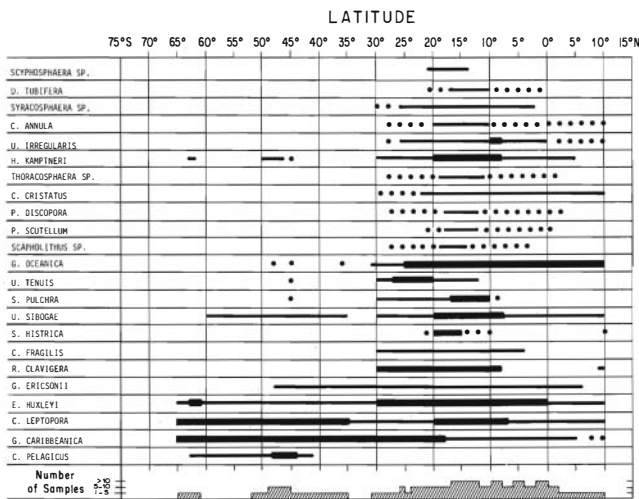
*Rhabdosphaera clavigera* usually is a minor constituent of sediment assemblages. It is most abundant in samples from 2,000 m–3,700 m, somewhat less

abundant between 4,000 m and 4,600 m. It reaches the highest values below the low-fertility waters of the central gyre (lat 15°S.–30°S.). It is mostly absent from the equator.

*Syracosphaera pulchra* is most common in samples from 2,000 m–3,000 m and between lat 10°S. and 20°S. It occurs at the equator and is also quite common below the less fertile waters of the central gyre.

*Ceratolithus cristatus* is always rare. It has its highest concentrations in sediments from close to the CCD (4,000 m–5,000 m) near the equator (lat 0°–15°S.). It seems to be more abundant in fertile waters, but it is also present in the central gyre.

A summary of this distributional information is given in table 1. Agreement with previously published information on temperature and fertility habitat is very good (McIntyre and others, 1970, and other authors; see Berger, in press, table 6).



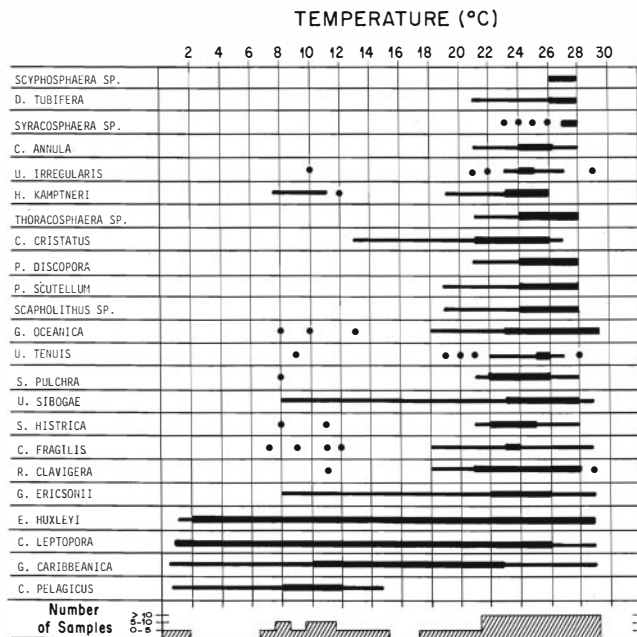
TEXT FIGURE 8

Latitudinal distribution of coccolith species. Thick bars indicate abundant, thin bars common, and dots rare occurrences. The number of samples is shown at the bottom of the graph.

Distributions of all species considered in this report are summarized in text figures 8, 9, and 10, with respect to latitude, temperature, and depth. The number of samples on the bottom of the graphs provides a guide to the trustworthiness of the ranges.

The equatorial region between lat 10°N. and 8°S. is dominated by *G. oceanica*, *E. huxleyi*, *C. leptopora*, and *C. cristatus* with smaller numbers of *U. sibogae* and *H. kamptneri*. We find the greatest number of species in the region between lat 10°S. and 30°S. Characteristic forms for this area are *Scyphosphaera*, *D. tubifera*, *C. annula*, *U. irregularis*, *U. tenuis*, *Pontosphaera* spp., *Scapholithus*, *G. oceanica*, *C. fragilis*, *H. kamptneri*, *R. clavigera*, together with more cosmopolitan forms (*E. huxleyi*, *C. leptopora*, *U. sibogae*). South of lat 30°, the assemblages are greatly reduced in the number of species with *E. huxleyi*, *G. caribbeanica*, *C. leptopora* as the dominant forms and *U. sibogae*, *G. ericsonii*, and *H. kamptneri* as minor components of the assemblages. The only high-latitude species is *C. pelagicus*, which occurs between lat 41°S. and 63°S.

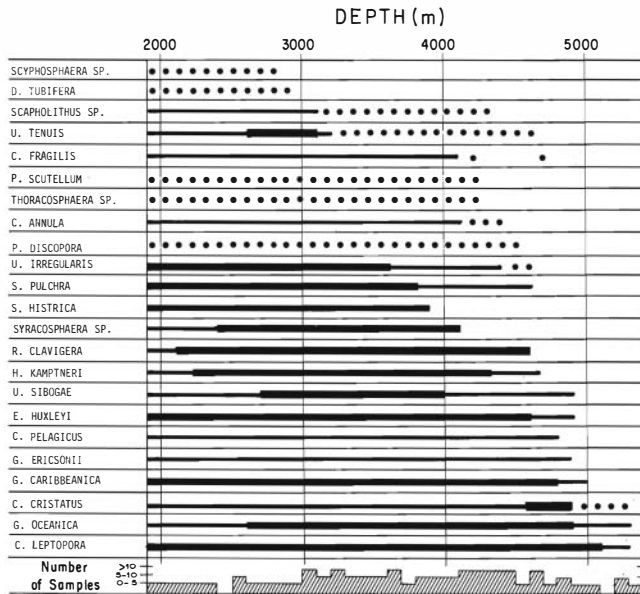
The plot of species versus average temperature (mean of summer and winter temperature) shows a similar picture (text fig 9). The majority of species are most common in or restricted to warm waters of temperatures ranging from 18°C to 28°C. Only one species (*C. pelagicus*) occurs only in cold water, and three species (*E. huxleyi*, *C. leptopora*, and *G. caribbeanica*) occur in waters ranging from 2°C to 28°C.



TEXT FIGURE 9

Temperature ranges of coccolith species. Thick bars indicate optimal temperature ranges, thin bars common and dots rare to occasional occurrences. The number of samples is shown at the bottom of the graph.

The species versus depth plot (text fig. 10) largely reflects the resistance of coccoliths to dissolution, as previously noted (McIntyre and McIntyre, 1971; Schneidermann, 1973). The distribution of the coccolith species in text figure 10 was averaged over all the geographical areas between lat 10°N. and 65°S., which introduced other variables besides differential dissolution. Nevertheless, the major trends are recognizable. At roughly 3,000 m, *Scyphosphaera* and *Discosphaera tubifera* disappear and *U. tenuis* becomes rare. Few changes occur between 3,000 m and 4,000 m. Close to 4,000 m, members of the genus *Syracosphaera* become rare. Between 4,200 m and 4,500 m, *Scapholithus* sp., *Pontosphaera* sp., *Thoracosphaera* sp., and *C. annula* disappear. *Umbellosphaera irregularis*, *U. tenuis*, *R. clavigera*, *S. pulchra*, and *H. kamptneri* were not found below 4,600 m. At 4,800 m–4,900 m, *U. sibogae*, *E. huxleyi*, *C. pelagicus*, *G. ericsonii* drop out. Below 5,000 m, coccolith assemblages are composed only of *C. cristatus*, *G. oceanica*, *C. leptopora*. They disappear completely, as do the most resistant foraminifera, at 5,300 m. There does not seem to be a clear indication of a coccolith lysocline, but rather a series of



TEXT FIGURE 10

Depth ranges of coccolith species. Thick bars indicate abundant, thin bars common, and dots rare occurrences. The number of samples is shown at the bottom of the graph.

changes in the composition of the assemblages between 3,000 m and 5,000 m, as Schneidermann (1973) found in the Atlantic.

### CLUSTER ANALYSIS

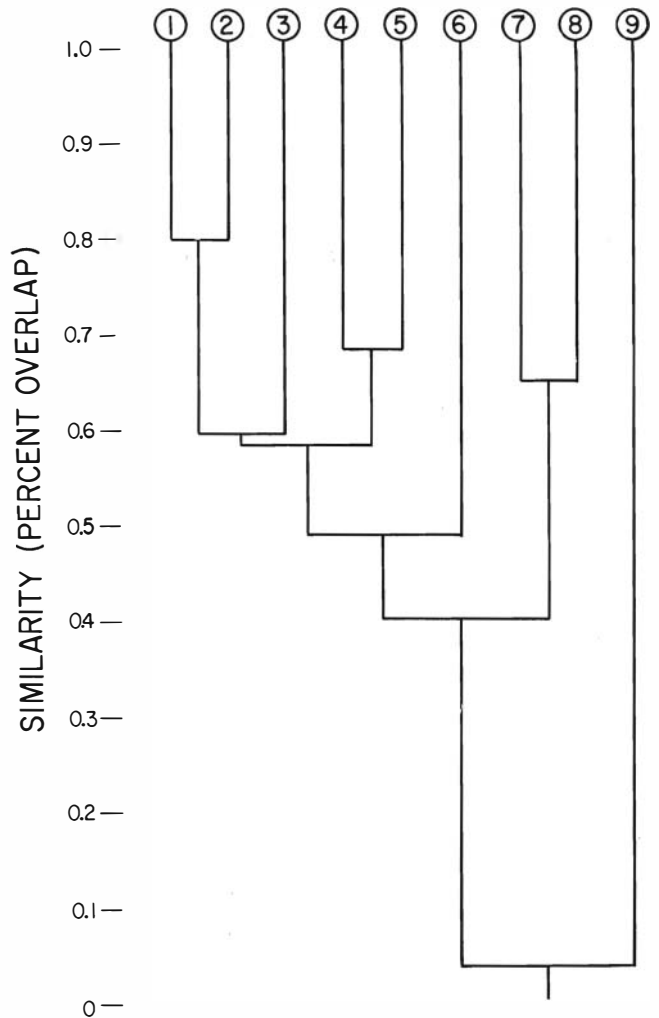
Samples were clustered according to the following procedure:

1. Find the similarity of each sample with each other one by adding up the smaller of the two percentages of each species in the samples (Sanders, 1958):

$$\text{Similarity} = \text{Sum} [\min (P_i, P_j)]$$

This similarity may be visualized as the overlapping area resulting from superposing two percentage histograms for species composition (Ruddiman and others, 1970).

2. Determine the closest neighbor for each sample that is down from it on the list of all samples.
3. Combine neighbors into the first of the two neighbor samples, if their similarity exceeds a specified minimum. Add the weights of the two samples (initially each sample has the weight one). Assign the new weight to the sample containing the new combined composition and assign zero weight to the



TEXT FIGURE 11

Relationships between clusters.

other sample. Samples with zero weight are ignored subsequently.

4. Relax the minimum similarity requirement and start with Step 1.

The procedure is exactly analogous to considering the samples as containers holding 100 numbered markers corresponding to the species percentages, and emptying the containers successively into the ones with the most similar contents. At some point the procedure is interrupted, lest all markers end up in the same container.

Clustering was terminated when the minimum overlap requirement dropped below 0.6. The nine resulting clusters (table 2) differ greatly in size and

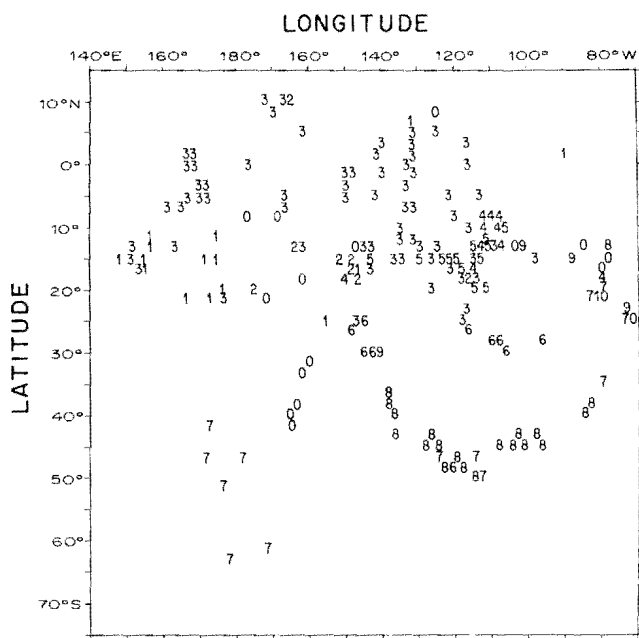
TABLE 2  
Average composition of clusters.

Species	Clusters								
	1	2	3	4	5	6	7	8	9
1. <i>E. huxleyi</i>	41.7	27.7	9.5	9.3	14.7	20.9	15.9	3.1	0
2. <i>G. oceanica</i>	30.0	27.0	58.6	13.5	17.0	9.5	4.1	0.3	0
3. <i>G. caribbeanica</i>	1.5	0.9	1.6	1.2	1.1	48.4	20.8	8.6	0
4. <i>G. ericsonii</i>	0.4	0	0.2	0	0.3	0.8	0.6	0.2	0
5. <i>C. pelagicus</i>	0	0	0	0	0	0.1	1.1	0.7	0
6. <i>C. leptopora</i>	4.9	12.4	16.3	19.1	12.6	5.2	47.1	79.3	1.8
7. <i>C. fragilis</i>	0.7	0.1	0.3	2.8	0.7	0.9	0.8	0.4	0
8. <i>U. sibogae</i>	5.5	9.4	4.9	21.1	37.9	3.0	5.4	2.4	0
9. <i>C. annula</i>	0.5	1.5	0.2	0.1	1.5	0.3	0	0	0
10. <i>H. kamptneri</i>	4.0	2.5	1.3	7.1	1.9	0.9	1.9	1.1	0
11. <i>U. irregularis</i>	2.1	2.9	0.9	12.8	1.4	0.5	0.2	0.1	0
12. <i>U. tenuis</i>	1.4	0.9	0.2	0.1	0.7	1.2	0.3	0	0
13. <i>D. tubifera</i>	0.2	0.2	0	0	0	0	0	0	0
14. <i>R. clavigera</i>	1.7	4.3	0.9	2.9	1.9	5.2	0.6	0.2	0
15. <i>S. pulchra</i>	1.1	1.7	0.2	0.8	3.4	0.9	0.5	0.1	0
16. <i>S. histrica</i>	0.6	3.7	0.1	0.5	0.4	0.1	0	0	0
17. <i>Syracosphaera</i> sp.	0.8	1.3	0.8	4.9	1.0	0.5	0.3	0	0
18. <i>P. discopora</i>	0.1	0.1	0	0.1	0	0.1	0	0.3	0
19. <i>P. scutellum</i>	0.2	0.1	0	0	0	0	0	0	0
20. <i>Scapholithus</i>	0.6	0.8	0	0.5	0.3	0.2	0	0	0
21. <i>Scyphosphaera</i>	0.1	0.1	0	0	0	0	0	0	0
22. <i>C. cristatus</i>	0.6	1.1	2.8	3.0	1.2	0.9	0.3	0.5	17.9
23. <i>Thoracosphaera</i>	0.4	0.6	0.1	0.2	0.2	0.2	0	0	0
24. Others Quaternary	0.7	0.5	0.3	0.1	1.7	0.2	0	0	0
25. Others Pre-Quaternary	0.3	0.2	0.9	0	0.2	0.1	0.3	2.6	80.4
Number of Samples in Clusters	21	11	78	17	17	10	15	25	4

show various degrees of interrelationship (text fig. 11). Clusters 1, 2, 3, 4, and 5 are similar and differ mainly in the relative proportions of the various species. Clusters 7 and 8 are also much alike, whereas cluster 6 does not pair with any individual cluster. Cluster 9 is different from all the others because it is dominated by reworked forms.

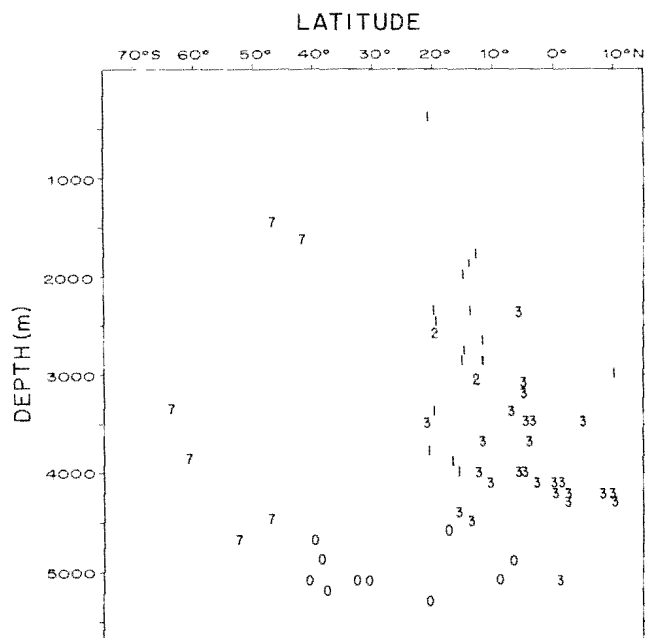
The chief characteristics and the distributions of the clusters may be summarized as follows (see text figs. 12–15): Cluster 1 (west tropical, shallow) is dominated by *Emiliania huxleyi* and *Gephyrocapsa oceanica*. It is virtually restricted to the shallow plateaus of the Western Pacific west of long 155°W., between lat 10°S. and 30°S. and shallower than 3,000 m, with some occurrences as deep as 4,000 m. The PO<sub>4</sub>-P content of the water in areas where Cluster 1 dominates is medium to low. Cluster 2 (central tropical, shallow) in which *E. huxleyi* and *G. oceanica* are almost equally abundant and *C. leptopora* is common, is found in a belt between lat 10°S. and 30°S and long 110°W. and

180°W. at a depth of 2,000–3,500 m on plateaus or near island chains. The fertility, as measured by the PO<sub>4</sub>-P content is usually medium to high. Cluster 3 (tropical deep) contains large numbers of *G. oceanica* and fairly high numbers of *C. leptopora*, but *E. huxleyi* is considerably less abundant. This cluster covers the equatorial belt between lat 10°N. and 15°S., mostly between long 150° E. and 110°W., at depths ranging from 3,000 m to 5,000 m, with a high number of samples between 4,000 and 5,000 m. PO<sub>4</sub>-P values are high in the area covered by Cluster 3. This cluster seems to be a more dissolved equivalent of Clusters 1 and 2. Cluster 4 (east-central tropical, shallow) with *U. sibogae*, *C. leptopora*, *G. oceanica*, and *U. irregularis* as the most abundant species, covers the area between long 155°W. and 80°W., lat 5°S. and 20°S. and has a depth range from 2,500–3,500 m. Most members of this cluster occur on the East Pacific Rise, the Nazca Rise, or near the Society Islands. Fertility (PO<sub>4</sub>-P) of the water is generally medium to high. Cluster 5 is dominated by *U. sibogae*, *G. oceanica*, *E. huxleyi* and *C. leptopora*. It is



TEXT FIGURE 12

Geographic distribution of clusters. Zero denotes coccolith-free samples.



TEXT FIGURE 13

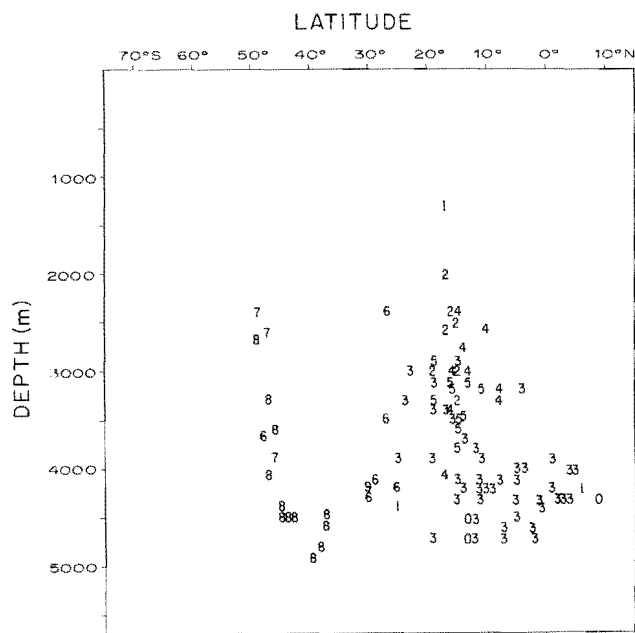
Depth-latitude distribution of clusters for area west of long 155° W.

very similar to Cluster 4 and occurs almost in the same region, i.e., between long 100°W. and 155°W and lat 0°–20°S. but tends toward somewhat greater depths (3,000 m–4,000 m). Cluster 6 (subtropic-temperate) with a high percentage of *G. caribbeanica* and *C. leptopora* is mostly restricted to the low-fertility region of the central gyre between long 90°W. and 155°W., lat 20° and 30°S. over a wide depth range (3,000–4,500 m). Cluster 7 (cold, shallow) contains high percentages of *C. leptopora*, *G. caribbeanica* and *E. huxleyi*. It is found at the southern margin of the central gyre and in the area of the Humboldt Current between long 160°E. and 75°W., lat 35°S. and 65°S. and mostly between 3,000 m and 4,000 m but as deep as 4,800 m. Cluster 8 (cold, deep) with mostly *G. caribbeanica* and *E. huxleyi* covers a similar area as the previous cluster but is concentrated at somewhat greater depths. PO<sub>4</sub>-P values are medium to high in the region where Clusters 7 and 8 are found. Cluster 9 (reworked) is dominated by *C. cristatus* and reworked pre-Quaternary. It is usually found in regions below 4,000 m between lat 10° and 30°S. all across the Central Pacific. Cluster 0 consists of all samples barren of coccoliths.

#### TEMPERATURE-SOLUTION ANALYSIS

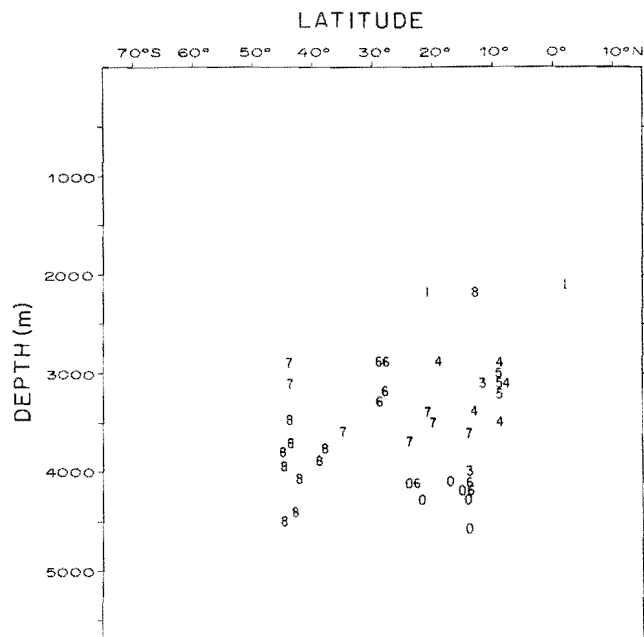
From the foregoing descriptions of species and cluster distributions it is clear that several factors may be invoked as controlling processes, of these, temperature of surface waters is a convenient parameter because of its correlation with other hydrographic factors such as vertical mixing and nutrient supply, its correlation with irradiation, and its own direct effects on growth of algal species. Modification of assemblages at depth by differential dissolution is the other important parameter.

To assess the "aspect" of a sample with respect to temperature we use an indexing system modified from Berger (1968). Each species is given a "grade" on a scale from 1 to 10, with respect to the parameter in question. For temperature, the values are as follows: *E. huxleyi* 5.5 (1/9), *G. oceanica* 8.3 (1/2), *G. caribbeanica* 5.0 (1/4), *G. ericsonii* 7.3 (1), *C. pelagicus* 1.0 (1), *C. leptopora* 5.5 (1/8), *C. fragilis* 8.3 (1), *U. sibogae* 8.3 (1/2), *C. annula* 9.0 (1), *H. kamptneri* 8.3 (1), *U. irregularis* 9.5 (1), *U. tenuis* 8.3 (1), *D. tubifera* 9.0 (1), *R. clavigera* 8.3 (1/2), *S. pulchra* 8.3 (1), *S. histrica* 8.0 (1), *Syracosphaera* 9.5 (1), *P. discopora* 9.0 (1), *P. scutellum* 9.0 (1), *Scapholithus* 9.0 (1), *Scyphosphaera* 9.5 (1), *C. cristatus*



TEXT FIGURE 14

Depth-latitude distribution of clusters between long 155° W and 110° W.



TEXT FIGURE 15

Depth-latitude distribution of clusters east of 110° W.

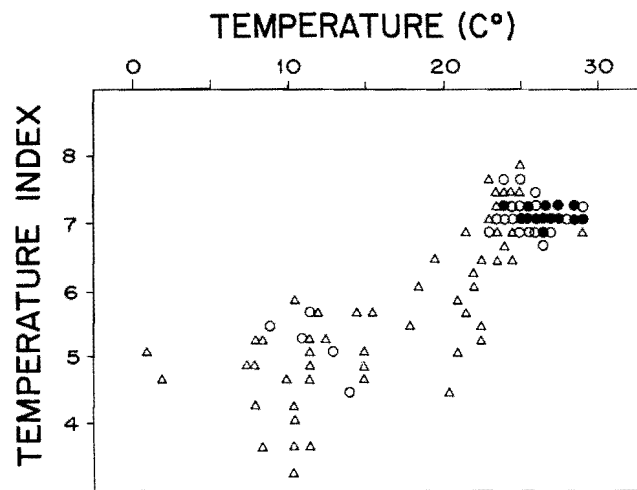
9.0 (1), *Thoracosphaera* 9.0 (1). The numbers in parentheses are a measure of the reliability of the "grade." The grades and the reliability are based on modal temperature and temperature range, respectively. The temperature aspect of a sample is calculated as the weighted mean of all grades (adjusted for reliability), as follows:

$$T_x = \text{Sum} (P_i \cdot G_i/R_i) / \text{Sum} (P_i/R_i)$$

The temperature indices ( $T_x$ ) thus derived correspond in a general way to the temperatures in the euphotic zone overlying the samples (text fig. 16). The correspondence between indices and actual temperatures could be improved by force-fitting the index, but this has certain undesirable features and is not necessary for the present analysis.

To determine the solution (or preservation) aspect of a sample a similar grading (or ranking) of the species with respect to resistance to dissolution is required. Derivation of a rank list rests on the proposition that, given two samples, the deeper one is depleted in delicate species and enriched in resistant ones, all other things being equal. To keep "all other things equal," and to maximize the depth effect, each sample was paired with other ones if and only if

the other ones were within 5° latitude, no further away than 10 degrees and had a minimum depth difference of 500 meters. In all pairs thus formed it was noted which species increased, which decreased, and which



TEXT FIGURE 16

Plot of coccolith temperature indices versus average sea surface temperatures. Triangles indicate 1 sample, open circles 2-3 samples, and dots more than 3 samples occupying the same position.

TABLE 3

Ranking of coccolith species in the order of increasing resistance to dissolution, for various geographic regions. The rank correlations of these lists with the generalized lists in Table 4 is given in the upper right corner.

<p><b>A</b> C. ANNULA <math>r_d = 0.6</math>          U. IRREGULARIS          H. KAMPTNERI          S. PULCHRA          C. FRAGILIS          R. CLAVIGERA          E. HUXLEYI          U. SIBOGAE          C. CRISTATUS          G. CARIBBEANICA          C. LEPTOPORA          G. OCEANICA</p>	<p><b>B</b> C. FRAGILIS <math>r_d = 0.9</math>          R. CLAVIGERA          U. SIBOGAE          H. KAMPTNERI          U. IRREGULARIS          S. PULCHRA          C. ANNULA          E. HUXLEYI          U. TENJIS          C. LEPTOPORA          C. CRISTATUS          G. CARIBBEANICA          G. OCEANICA</p>	<p><b>C</b> D. TUBIFERA <math>r_d = 0.8</math>          S. PULCHRA          C. FRAGILIS          U. TENJIS          R. CLAVIGERA          U. IRREGULARIS          E. HUXLEYI          U. SIBOGAE          C. ANNULA          H. KAMPTNERI          G. CARIBBEANICA          C. CRISTATUS          G. OCEANICA          C. LEPTOPORA</p>									
<p><b>D</b> R. CLAVIGERA <math>r_d = 0.8</math>          C. ANNULA          C. FRAGILIS          U. IRREGULARIS          U. SIBOGAE          H. KAMPTNERI          S. PULCHRA          E. HUXLEYI          G. OCEANICA          G. CARIBBEANICA          C. LEPTOPORA          U. TENJIS          C. CRISTATUS</p>	<p><b>E</b> D. TUBIFERA <math>r_d = 0.9</math>          C. FRAGILIS          R. CLAVIGERA          U. IRREGULARIS          H. KAMPTNERI          U. TENJIS          C. ANNULA          E. HUXLEYI          S. PULCHRA          U. SIBOGAE          C. LEPTOPORA          C. CRISTATUS          C. PELAGICUS          G. OCEANICA          T. CARIBBEANICA</p>	<p><b>F</b> E. HUXLEYI <math>r_d = 0.9</math>          C. ANNULA          R. CLAVIGERA          U. TENJIS          S. PULCHRA          C. FRAGILIS          H. KAMPTNERI          U. SIBOGAE          C. LEPTOPORA          G. OCEANICA          G. CARIBBEANICA          U. IRREGULARIS          C. PELAGICUS          C. CRISTATUS</p>									
<p>155°W 110°W          10°N  <table border="1" style="display: inline-table;"> <tr><td>A</td><td>B</td><td>C</td></tr> <tr><td>D</td><td>E</td><td>F</td></tr> <tr><td></td><td>G</td><td>H</td></tr> </table>         10°S          30°S          50°S</p>	A	B	C	D	E	F		G	H	<p><b>G</b> E. HUXLEYI <math>r_d = 0.8</math>          U. SIBOGAE          C. FRAGILIS          S. PULCHRA          U. TENJIS          G. CARIBBEANICA          H. KAMPTNERI          R. CLAVIGERA          C. PELAGICUS          G. OCEANICA          C. LEPTOPORA</p>	<p><b>H</b> S. PULCHRA <math>r_d = 0.7</math>          U. TENJIS          E. HUXLEYI          C. PELAGICUS          H. KAMPTNERI          C. FRAGILIS          G. CARIBBEANICA          R. CLAVIGERA          U. SIBOGAE          C. LEPTOPORA</p>
A	B	C									
D	E	F									
	G	H									

stayed the same when going from the shallower to the deeper sample. Adding the scores based on these changes, a ranking is readily obtained. As some species showed considerable variation in their position within such a rank list, depending on whether tropical or extratropical samples were considered, we applied the scoring procedure to 9 different regions of the study area (table 3).

The results show a reasonable degree of coherence between the rank lists, but also emphasize the variability of certain species with respect to dissolution resistance, and the dependence of the rank list obtained on the sampling space employed. Since the rankings for areas

A, B, C, D, and E are very similar an overall tropical ranking was calculated by averaging the normalized ranks. The same was done for areas F, G, and H to obtain an overall extratropical ranking (table 4). In both overall rankings, the average rank of *Umbellosphaera irregularis* and *Umbellosphaera tenuis* are used and listed as *Umbellosphaera* sp. because the position of these species in the regional rankings is quite variable. The two overall rankings are similar, with a rank correlation coefficient  $r_d = 0.66$ . Noteworthy is the relatively low rank of *Rhabdosphaera clavigera* in the tropical ranking and the relatively low rank of *Emiliania huxleyi* in the extratropical ranking.

The ranking obtained for the Pacific agrees reasonably well with the ranking for the Atlantic as calculated by Berger (1973). The rank correlation coefficients between the Atlantic ranking and each of the Pacific rankings are both  $r_d = 0.8$ .

In all subsequent analysis either the tropical or the extratropical rankings were used, as appropriate for each sample. Ranks were converted to "grades" by normalizing to a scale from 1 to 100. Reliability factors were not used in this case, although such factors could be extracted from comparing the rank lists in table 3.

The solution aspect for each sample can now be calculated as the weighted mean of all species "grades" in a sample:

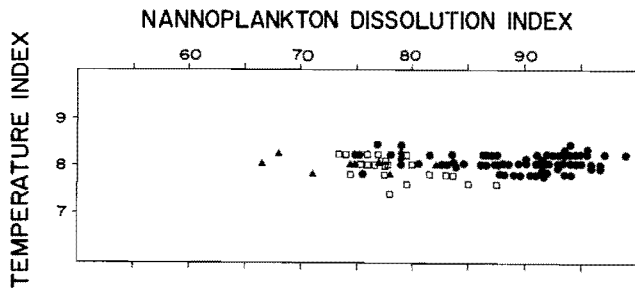
$$S_x = \text{Sum } (P_i \cdot G_i) / \text{Sum } (P_i).$$

Temperature-solution plots for the various clusters were generated using the T and S indices, in order to explore further the relationships between the clusters.

### CLUSTER RELATIONSHIPS

On plots of dissolution index versus temperature index (text figs. 17, 18, and 19) the low-latitude clusters (1, 2, 3, 4, 5) show little spread of temperature indices but considerable spread of solution indices. Clusters 4 and 5 have the lowest solution indices. Clusters 1 and 2 are intermediate, and cluster 3, which is most likely a more dissolved equivalent of clusters 1 and 2, has the highest dissolution indices. Cluster 6 has intermediate temperature indices and a considerable scatter of the dissolution index values. Cluster 7 has lower solution index values than cluster 8, but similar temperature indices.

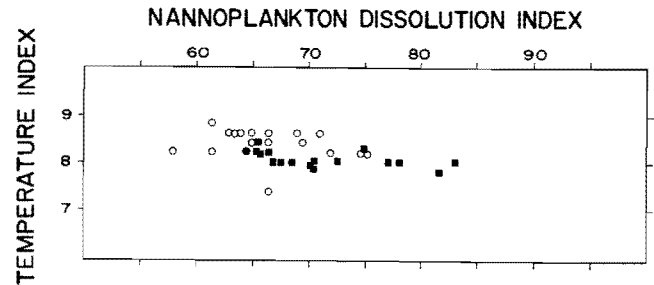
If we compare these nannoplankton temperature index vs. dissolution index plots with a similar plot for planktonic foraminifera (Parker and Berger, 1971, fig. 10), we can see that there are considerable differences.



TEXT FIGURE 17

Nannoplankton dissolution indices *versus* temperature indices for clusters 1, 2 and 3.

- Cluster 1: open squares
- Cluster 2: filled triangles
- Cluster 3: dots



TEXT FIGURE 18

Nannoplankton dissolution indices *versus* temperature indices for clusters 4 and 5.

- Cluster 4: circles
- Cluster 5: filled squares

For planktonic foraminifera, the spread of the temperature indices increases as dissolution progresses, whereas for coccoliths the spread of the temperature indices is about the same for low and high dissolution indices. The reason that dissolution of coccolith assemblages changes the temperature index very little is that the solution-resistant forms, which are also good temperature indicators (*G. oceanica*, *G. caribbeanica*) are dominant even in well-preserved sediment assemblages.

Other good temperature indicators (see table 1) are usually such minor constituents that their presence or absence has little influence on the temperature aspect of a sample.

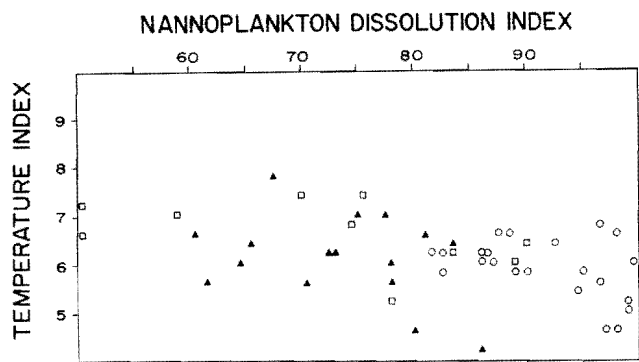
#### SEARCH FOR A COCCOLITH LYSOCLINE

The difference in the dominance patterns between foram and coccolith assemblages which is evident in the temperature-solution plots also affects the recognition

TABLE 4  
Overall tropical and extratropical dissolution ranking.

Tropical area (A,B,C,D,E)	Extratropical area (F,G,H)
1. <i>Scyphosphaera</i> sp.	1. <i>Emiliana huxleyi</i>
2. <i>Discosphaera tubifera</i>	2. <i>Cyclolithella annula</i> *
3. <i>Scapholithus</i> sp.	3. <i>Syracosphaera pulchra</i>
4. <i>Cyclococcolithina fragilis</i>	4. <i>Cyclococcolithina fragilis</i>
5. <i>Rhabdosphaera clavigera</i>	5. <i>Helicopontosphaera kamptneri</i>
6. <i>Pontosphaera scutellum</i>	6. <i>Syracosphaera</i> sp.
7. <i>Cyclolithella annula</i>	7. <i>Umbellosphaera sibogae</i>
8. <i>Pontosphaera discopora</i>	8. <i>Umbellosphaera</i> sp.
9. <i>Syracosphaera</i> sp.	9. <i>Rhabdosphaera clavigera</i>
10. <i>Syracosphaera pulchra</i>	10. <i>Gephyrocapsa ericsonii</i>
11. <i>Helicopontosphaera kamptneri</i>	11. <i>Gephyrocapsa caribbeanica</i>
12. <i>Umbellosphaera</i> sp.	12. <i>Coccolithus pelagicus</i>
13. <i>Syracosphaera histrica</i>	13. <i>Gephyrocapsa oceanica</i>
14. <i>Umbellosphaera sibogae</i>	14. <i>Cyclococcolithina leptopora</i>
15. <i>Thoracosphaera</i> sp.	15. <i>Ceratolithus cristatus</i> *
16. <i>Gephyrocapsa ericsonii</i>	
17. <i>Emiliana huxleyi</i>	
18. <i>Ceratolithus cristatus</i>	
19. <i>Cyclococcolithina leptopora</i>	
20. <i>Coccolithus pelagicus</i>	
21. <i>Gephyrocapsa caribbeanica</i>	
22. <i>Gephyrocapsa oceanica</i>	

\* Only in Area F.



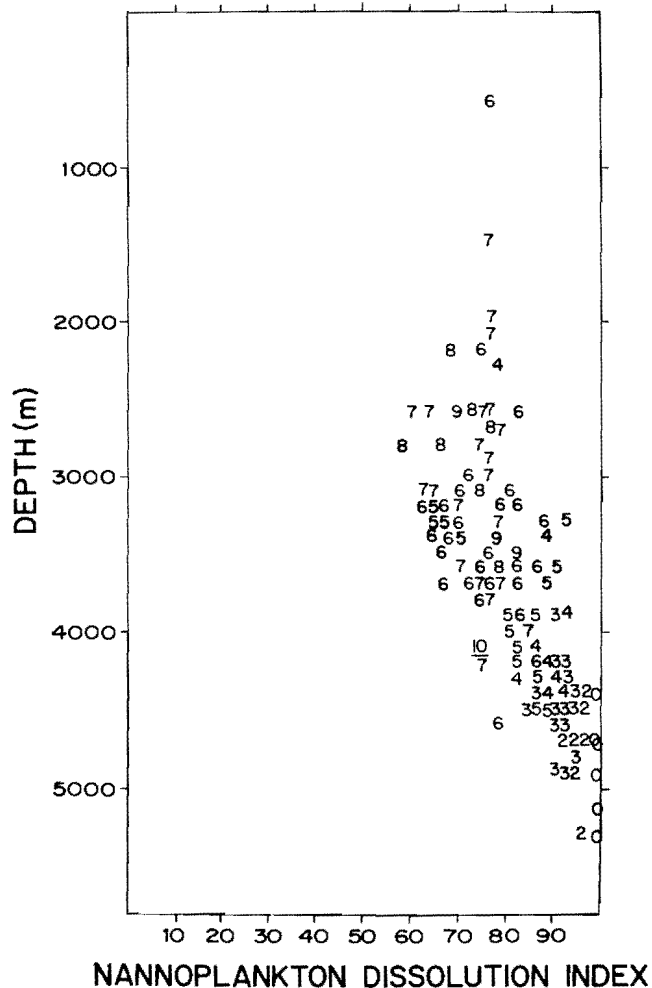
TEXT FIGURE 19

Nannoplankton dissolution index *versus* temperature index plot for clusters 6, 7 and 8.

- Cluster 6: open squares
- Cluster 7: filled triangles
- Cluster 8: circles.

of a coccolith lysocline. In foraminifera, the change-over from well-preserved to poorly preserved assemblages—which marks the lysocline—is well defined, because the more delicate forms are dominant to begin with and the resistant forms become dominant as a result of partial dissolution. Thus, a typical foram assemblage completely changes its character due to differential dissolution. In contrast, no such pronounced change in character occurs in coccolith assemblages, because the highly resistant forms are dominant at the outset. Selection for hardy forms by the various processes involved in transferring the particles to the sea floor may play a role in providing this particular dominance structure. Such transfer processes are expected to be completely different for coccoliths and for foraminifera.

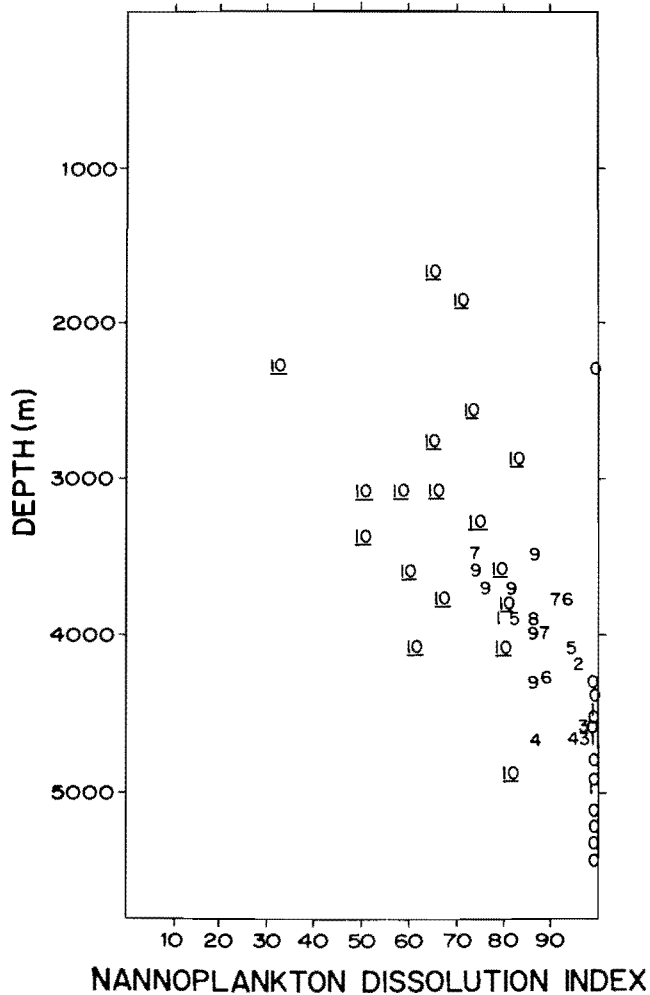
Plots of nannoplankton dissolution indices (NDX) versus depth clearly demonstrate this lack of drastic change through partial dissolution (text figs. 20 and 21). Nevertheless, as in foraminifera, the rate of change in the assemblages is seen to reach a maximum at depths near 4 km, close to the lysocline identified by Parker and Berger (1971). However, this change is somewhat more difficult to measure than in the foraminifera, and we have to take recourse to the internal dispersion of the solution indices. This dispersion is calculated as the standard deviation of the solution index (which in turn is a weighted average). It is a measure of the diversity of an assemblage with respect to the dissolution resistance of its members. Such deviation



TEXT FIGURE 20

Nannoplankton dissolution indices *versus* depth for the tropical region (areas A to E). The numbers 0 to 10 indicate the normalized standard deviation of each nannoplankton dissolution index. Note the considerable drop in the standard deviations at 4,000 m.

indices had been calculated routinely for foraminifera also (Berger, unpublished) but since the changes in the foram solution indices were so obvious, the application of internal index deviations seemed unnecessary. It will be noted that there is a maximum change in the solution deviation indices with depth near the lysocline zone (text figs. 20 and 21). The reason is that the more solution susceptible species are removed mainly at this depth. This does not preclude, of course, removal at shallower depths than the lysocline, for which evidence was presented earlier (text fig. 10).

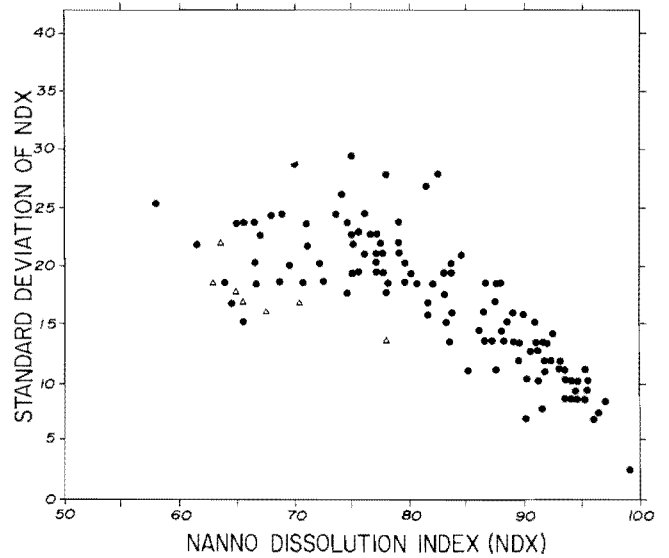


TEXT FIGURE 21

Nannoplankton dissolution indices *versus* depth for the extratropical region (areas F to H). The numbers 0 to 10 indicate the normalized standard deviation of each coccolith dissolution index. Note maximum change in the standard deviations occurs around 4,000 m.

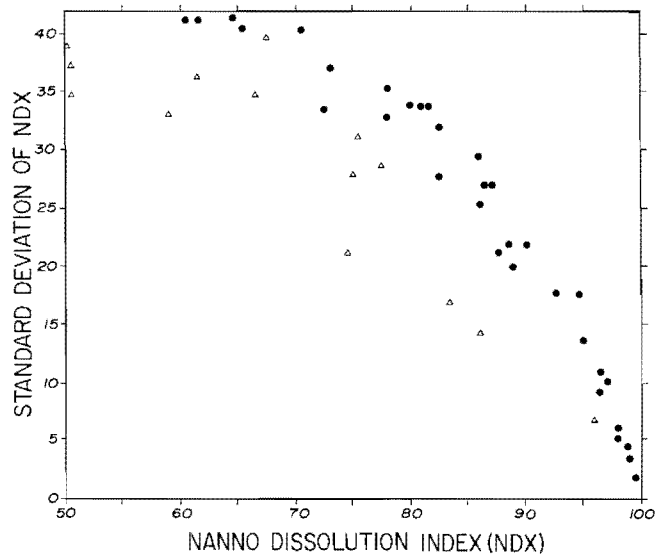
In foraminifera also, removal of the most fragile form (*Hastigerina pelagica*) starts some thousand meters above the lysocline, as pointed out previously (Berger, 1971).

The relationship between the nannoplankton dissolution index and its internal standard deviation is further explored in text figures 22 and 23. In the region of little or moderate dissolution, say  $NDX < 80$ , the two variables appear quite independent, but when the more susceptible species begin to be markedly removed, a definite correlation develops exactly as expected for the decrease in diversity that dissolution provides.



TEXT FIGURE 22

Plot of nannoplankton dissolution indices (NDX) *versus* standard deviations of the NDX for the tropical region. Dots indicate samples from areas A, B, D, E; triangles indicate samples from area C.

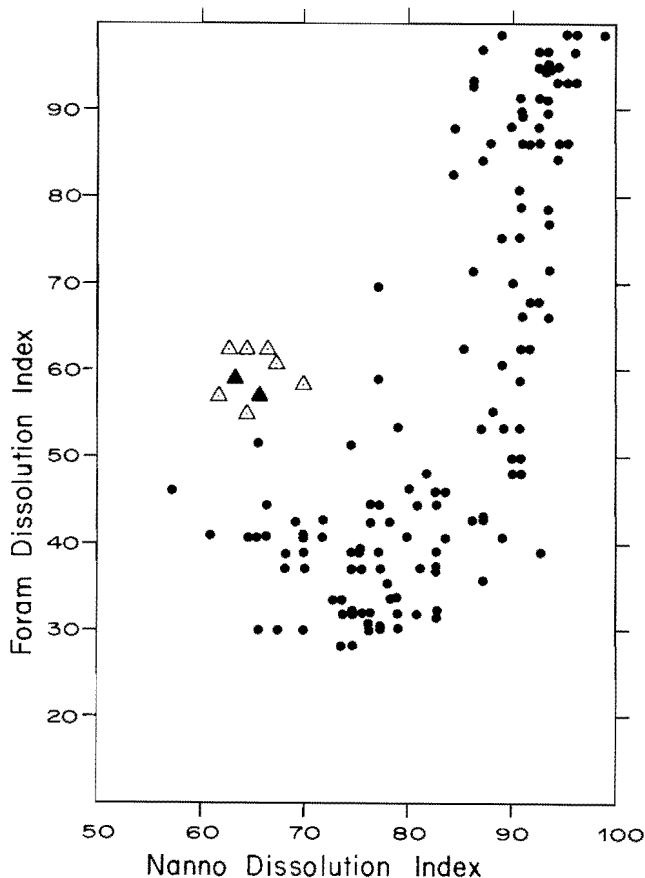


TEXT FIGURE 23

Plot of nannoplankton dissolution indices (NDX) *versus* standard deviations of the NDX for extratropical regions. Dots indicate samples from areas G & H; triangles indicate samples from area F.

#### FURTHER COMPARISON OF COCCOLITH AND FORAM DISSOLUTION

The differences in dissolution aspects of coccolith and foram assemblages, which are a liability when at-



TEXT FIGURE 24

Plot of foraminiferal dissolution indices *versus* nannoplankton dissolution indices. Empty triangles indicate samples from area C, filled triangles show samples from the same general region on the East Pacific Rise which are in area B. These samples are remarkable for their high initial proportions of of *G. dutertrei*, a resistant foram species.

tempting to define a coccolith lysocline, also are an asset in that the information obtained is complementary rather than redundant.

In tropical regions (area A to E; text fig. 24), we observe a fairly large spread of the nannoplankton dissolution index values at foraminiferal dissolution index values below 60. This means that the nannoplankton dissolution index is a much more sensitive measure of the degree of dissolution in shallower regions (above the foraminiferal lysocline). On the other hand, at high values of the nannoplankton dissolution index there is quite a range of values for the foraminiferal dissolution index, which indicates that the planktonic foraminiferal dissolution index allows us to determine the state of dissolution more accurately than the nanno-

plankton dissolution index below the planktonic foraminiferal lysocline. The points indicated by triangles on text figure 24 are from a shallow area on the East Pacific Rise at about lat 80°S. and long 110°W. They have an unusually high foraminiferal dissolution index, which is due to a great abundance of *Globoquadrina dutertrei* (a resistant species) in these samples. Thus, the coccolith preservation in these samples indicates that the percentage of resistant forams is anomalously high initially, and prevents us from falsely ascribing these high proportions to differential dissolution. At high latitudes the plot of nannoplankton dissolution index versus foraminiferal dissolution index shows almost random distribution, and has been omitted, therefore.

#### SUMMARY AND CONCLUSIONS

An average coccolith assemblage from the sediment differs from the nannoplankton in the water column by an almost complete lack of holococcoliths, which comprise 2–5 percent of the living coccolithophorids. Deep-living forms like *Florisphaera profunda* and *Thorosphaera flabellata* (see Okada and Honjo, 1973) and some delicate cancoliths are either missing or very rare in sediment assemblages. However, the majority of coccoliths in both the plankton and in well-preserved sediment are solution resistant. This is in contrast to planktonic foraminifera, where well-preserved assemblages contain a high percentage of delicate forms. Consequently, dissolution patterns of the two groups are quite dissimilar. The foraminifera dissolution index has a greater range than the nannoplankton dissolution index. Coccolith assemblages start showing signs of dissolution above 3,000 m, and there are a series of changes in the composition of the assemblages between 3,000 m and 5,000 m, leading to less and less diverse nannofloras and finally to the disappearance of coccoliths at 5,300 m. Any indication of a coccolith lysocline in the South Pacific rests on a change in the depth gradient of preservational diversity, somewhere within a dissolution zone of about 2,000 m thickness above the CCD. Planktonic foraminifera, on the other hand, show few changes in the composition of the assemblages above the foraminiferal lysocline, but are very sensitive indicators of the state of dissolution below that level. On the whole, they are as solution resistant as coccoliths in Recent sediments.

These contrasting dissolution characteristics of coccolith and planktonic foraminifera assemblages allow us to evaluate the influence of other factors than dissolution on the composition of calcareous assemblages and

to determine the degree of dissolution well above the foraminiferal lysocline.

The use of coccoliths as temperature indicators is less promising than that of forams because most coccolith species are tropical or cosmopolitan, and only one form is a cold-water indicator.

This work was supported by the National Science Foundation, Oceanography Section, Submarine Geology and Geophysics, NSF Grant-GA-36697. We thank David Bukry, U.S. Geological Survey, for his helpful comments on this paper.

## REFERENCES

- ADELSECK, C. G., GEEHAN, G. W., and ROTH, P. H., 1973, Experimental evidence for the selective dissolution and overgrowth of calcareous nannofossils during diagenesis: *Geol. Soc. America Bull.*, v. 84, p. 2755-2762.
- BARTOLINI, C., 1970, Coccoliths from sediments of the western Mediterranean: *Micropaleontology*, v. 16, p. 129-154.
- BERGER, W. H., 1968, Planktonic Foraminifera: selective solution and paleoclimatic interpretation: *Deep-Sea Research*, v. 15, p. 31-43.
- , 1971, Sedimentation of planktonic foraminifera: *Marine Geology*, v. 11, p. 325-358.
- , 1973, Deep-sea carbonates: evidence for a coccolith lysocline: *Deep-Sea Research*, v. 20, p. 917-921.
- , (in press), Biogenous deep sea sediments: production, preservation, and interpretation. *in* Riley, J. P., and Chester, R., eds., *Treatise on chemical oceanography*. London, Academic Press, v. 3.
- BRAMLETTE, M. N., 1958, Significance of coccolithophorids in calcium-carbonate deposition: *Geol. Soc. America Bull.*, v. 69, p. 121-126.
- BRAMLETTE, M. N., and SULLIVAN, F. R., 1961, Coccolithophorids and related nannoplankton of the early Tertiary in California: *Micropaleontology*, v. 7, p. 129-188.
- BUKRY, D., 1971, Cenozoic calcareous nannofossils from the Pacific Ocean: *San Diego Soc. Nat. History Trans.*, v. 16, p. 303-327.
- , 1973, Coccolith stratigraphy, eastern equatorial Pacific, Leg 16 Deep Sea Drilling Project: *Deep Sea Drilling Proj. Initial Repts.*, v. 16, p. 653-711.
- BUKRY, D., DOUGLAS, R. G., KLING, S. A., and KRASHENINNIKOV, V., 1971, Planktonic microfossil biostratigraphy of the northwestern Pacific Ocean: *Deep Sea Drilling Proj. Initial Repts.*, v. 6, p. 1253-1300.
- BURNS, D. A., 1972, Discoasters in Holocene sediments: Southwest Pacific Ocean: *Marine Geology*, v. 12, p. 301-306.
- CITA, M. B., 1971, Paleoenvironmental aspects of DSDP legs I-IV: *Planktonic Conf.*, 2d, Rome (1970), *Proc.*, v. 1, p. 251-285.
- DEFLANDRE, G., and FERT, C., 1954, Observations sur les coccolithophoridés actuels et fossiles en microscopie ordinaire et électronique: *Annales de Paléontologie*, v. 40, p. 115-176.
- HAY, W. W., 1970, Calcium carbonate compensation: *Deep Sea Drilling Proj. Initial Repts.*, v. 4, p. 672.
- HAY, W. W., and BEAUDRY, F. M., 1973, Calcareous nannofossils—Leg 15, Deep Sea Drilling Project: *Deep Sea Drilling Proj. Initial Repts.*, v. 15, p. 625-683.
- HSÜ, K. J., and ANDREWS, J. E., 1970, Lithology: *Deep Sea Drilling Proj. Initial Repts.*, v. 3, p. 445-453.
- KAMPTNER, E., 1967, Kalkflagellaten—Skelettreste aus Tiefseeschlamm des Südatlantischen Ozeans: *Ann. Naturhist. Mus. Wien*, v. 66, p. 139-204.
- MCINTYRE, A., and BÉ, A. W. H., 1967, Modern Coccolithophoridae of the Atlantic Ocean—I. Placoliths and cyrtoliths: *Deep-Sea Research*, v. 14, p. 561-597.
- MCINTYRE, A., BÉ, A. W. H., and ROCHE, M. B., 1970, Modern Pacific Coccolithophorida: a paleontological thermometer: *New York Acad. Sci. Trans., Ser. II*, v. 32, p. 720-731.
- MCINTYRE, A., and MCINTYRE, R., 1971, Coccolith concentration and differential solution in oceanic sediments, in Funnel, B. M., and Riedel, W. R., eds., *The micropaleontology of oceans*: Cambridge University Press, p. 253-261.
- MENARD, H. W., 1964, *Marine geology of the Pacific*: New York, McGraw-Hill, p. 1-271.
- OKADA, H., and HONJO, S., 1973, The distribution of oceanic coccolithophorids in the Pacific: *Deep-Sea Research*, v. 20, p. 355-374.
- PARKER, F. L., and BERGER, W. H., 1971, Faunal and solution patterns of planktonic Foraminifera in surface sediments of the South Pacific: *Deep-Sea Research*, v. 18, p. 73-107.
- REID, J. L., JR., 1962, On circulation, phosphate-phosphorus content, and zooplankton volumes in the upper part of the Pacific Ocean: *Limnology and Oceanography*, v. 7, p. 287-306.
- REID, J. L., 1969, Sea surface temperature, salinity and density of the Pacific Ocean in summer and winter: *Deep-Sea Research, Suppl. 1.*, v. 16, p. 215-224.
- RUDDIMAN, W. F., TOLDERLUND, D. S., and BÉ, A. W. H., 1970, Foraminiferal evidence of a modern warming of the North Atlantic Ocean: *Deep-Sea Research*, v. 17, p. 141-155.
- ROTH, P. H., 1973, Calcareous nannofossils—Leg 17, Deep Sea Drilling Project: *Deep Sea Drilling Proj. Initial Repts.*, v. 17, p. 695-795.
- ROTH, P. H., and THIERSTEIN, H., 1972, Calcareous nannoplankton: Leg 14 of the Deep Sea Drilling Project: *Deep Sea Drilling Proj. Initial Repts.*, v. 14, p. 421-485.
- SANDERS, H. L., 1958, Benthic studies in Buzzards Bay—I. Animal-sediment relationships: *Limnology and Oceanography*, v. 3, p. 245-258.
- SCHLANGER, S. O., DOUGLAS, R. G., LANCELOT, Y., MOORE, T. C., and ROTH, P. H., 1973, Fossil preservation and diagenesis of pelagic carbonates from the Magellan Rise, Central North Pacific Ocean: *Deep Sea Drilling Proj. Initial Repts.*, v. 17, p. 407-427.
- SCHNEIDERMAN, N., 1972, Selective dissolution of Recent coccoliths in the Atlantic Ocean: Univ. Illinois at Urbana-Champaign, Ph.D. dissertation, (No. 73-17, 403, University Microfilms, Ann Arbor, Michigan).
- , 1973, Deposition of coccoliths in the compensation zone of the Atlantic Ocean, in Smith, L. A., and Hardenbol, J., eds., *Proc. symposium calcareous nannofossils, Gulf Coast Sec., Soc. Econ. Paleontologists and Mineralogists, Houston, Texas*, p. 140-151.

# DISSOLUTION OF SUSPENDED COCCOLITHS IN THE DEEP-SEA WATER COLUMN AND SEDIMENTATION OF COCCOLITH OOZE

SUSUMU HONJO

Woods Hole Oceanographic Institution, Woods Hole, Massachusetts 02543

---

## ABSTRACT

Suspended coccoliths are abundantly distributed throughout the water column down to 5 km along a meridional aphotic water profile of the central North Pacific Ocean. Their state of preservation varies from unaltered to slightly etched at all depths. This observation contradicts the expectation that coccoliths falling from the photic layer should dissolve and disappear in the calcite-undersaturated part of the water column. The species composition of coccolithophore assemblages in the overlying productive layer was reflected throughout the aphotic water column with no significant change. Electron microscopic study of fecal pellets from grazers collected at depth by a sediment trap as well as laboratory experiments feeding cultured coccolithophores to small zooplankton suggest that fecal transport is an efficient process removing the coccoliths produced in surface waters directly to the deep-sea floor. The sus-

pended coccoliths can be classified into two categories; the free-falling coccoliths from the surface productive layer which are the result of shedding from host coccolithophores while they are living, and the suspended coccoliths replenished at any depth by spilling out from the host fecal pellets while they descend. The type 1 coccoliths probably will be dissolved as soon as they pass the calcite saturation depth. The majority of the type 2 coccoliths may eventually dissolve at undersaturated depths before descending very far, but are widely distributed throughout the deep-sea column at least temporarily. Thus the suspended coccoliths may play a very small role but the direct and rapid transport of coccoliths via fecal pellets appears to be the main channel in carbonate ooze sedimentation on the deep sea floor.

---

## INTRODUCTION

The pathway and the fate of a typical small calcium carbonate particle migrating through the deep-water column toward the sea floor is poorly understood. There is no guarantee that the thanatocoenoses of microorganisms replicate the living communities in the overlying productive layer (Berger, 1971). However, a knowledge of the oceanographic transfer mechanisms and the extent of modification of settling assemblages expected in the water column is indispensable for accurate paleoceanographic reconstruction.

Contribution No. 3436 of the Woods Hole Oceanographic Institution

A coccolith is small but provides a relatively large surface area. The residence time of a coccolith suspended in the deep sea column may be considerably longer than the other geologically and paleontologically important particles such as planktonic foraminiferan tests. Therefore, coccolith communities may suffer severe physical screenings before they reach the bottom. The lateral shifting and winnowing by the surface and deep water current system may result in serious disruption of the relation between the original community produced in the productive layer and the corresponding thanatocoenosis.

The sea water is undersaturated in calcite at relatively

shallow depth and throughout the deeper water column below that depth, the calcite saturation depth (Takahashi and others, 1970; Takahashi, this volume). If the rate of the calcite dissolution in the deep sea measured on calcite crystals (Peterson, 1966) and planktonic foraminiferan tests (Berger, 1967) is pertinent to free-falling coccoliths (whose chemical composition is close to planktonic foraminiferan tests, i.e., low magnesium calcite, Thompson and Bowen, 1969), and their rate of descent is in the order of a hundred meters per year, they may disappear soon after they cross the saturation depth. In reality, however, coccolith ooze ranges widely over the ocean floor where depths exceed the saturation depth. Suspended coccoliths in deep-sea columns may provide a useful natural laboratory to solve such confusing problems on the carbonate solution chemistry in the deep sea.

This report consists of three parts. First, the distribution of suspended coccoliths along the 155° W profile is described, based upon systematically collected samples. Well-preserved suspended coccoliths were recovered throughout the water column, contrary to expectation. Detailed electron microscopy was conducted to investigate the records of dissolution on the surface architecture of suspended coccoliths. Suspended coccolith species were analyzed using a variety of community analysis techniques to test if there was any geographical provincialism in terms of depth and latitude.

Second, the suspended coccoliths communities were compared to the directly overlying living coccolithophore communities along the same transect described earlier (Honjo and Okada, 1974). The samples of deep-sea suspended coccoliths for this study were collected by extending the water casting to 4.0 km or 5.0 km beneath the photic substations. The suspended coccolith communities were more or less identical to the overlying "source" community showing no taxonomical screening during sinking. However, the amount of suspended coccoliths immediately below the productive layer was considerably less than anticipated if these coccoliths are to provide the flux in a steady state relationship.

Third, a model is given that explains the presence of slowly settling coccoliths in undersaturated waters and the discrepancy between the number of coccoliths found in the aphotic layers and the expected flux by rapid transportation via fecal pellets. The great majority of suspended coccoliths, even apparently well preserved at great depths, does not reach the deep-sea floor. The coccolith population produced in the surface

is transported almost instantaneously by fecal pellets of grazers, bypassing the aphotic water column. The laboratory culture/feeding experiment of coccolithophores and electron microscopic observation of fecal pellets collected on a deep-sea sediment trap support this view. This model enhances the reliable correspondence between the living community of coccoliths and the thanatocoenosis and avoid the complex physical and chemical screening expected during long-term suspension in the water column.

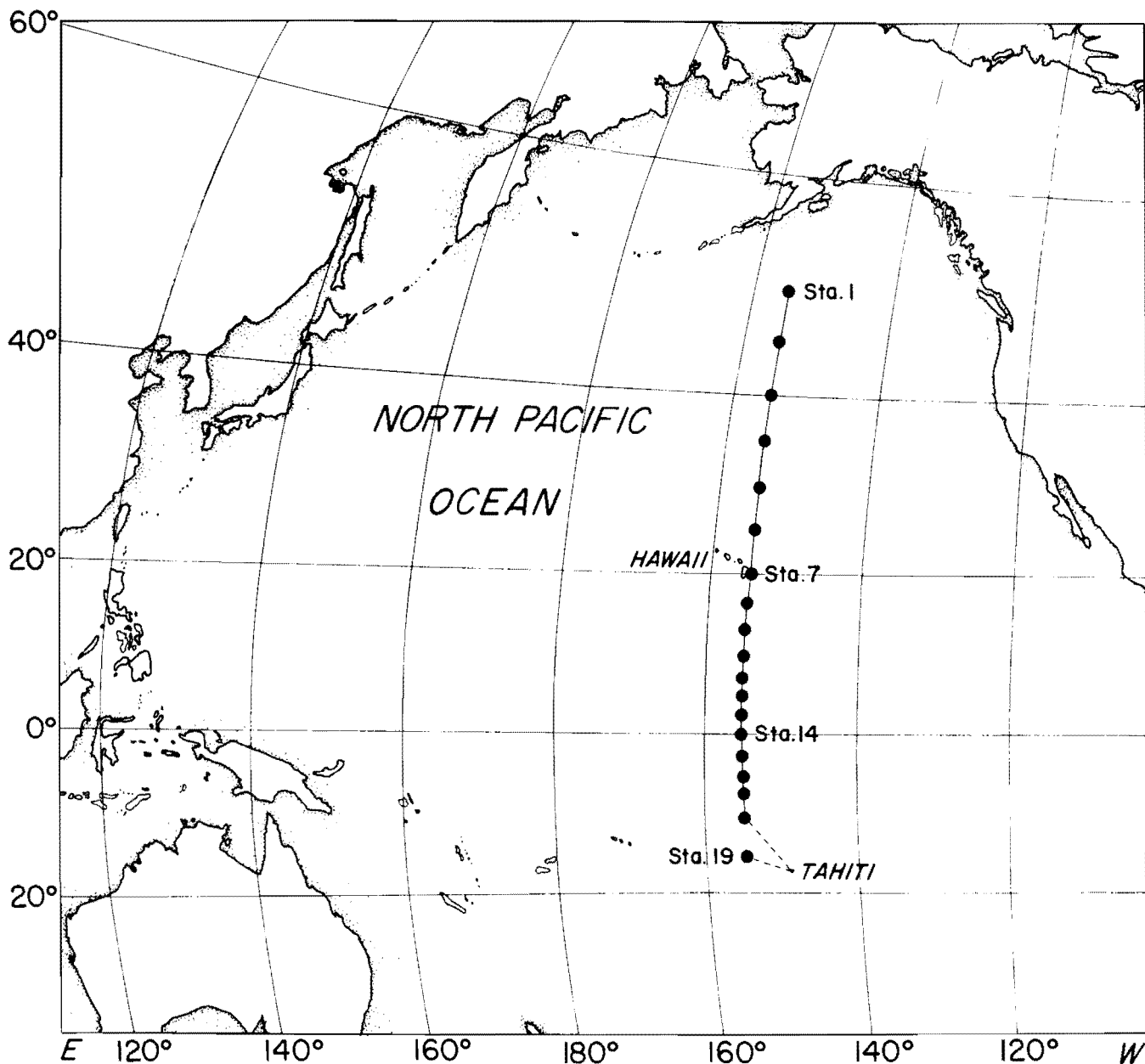
This paper is mainly concerned with the preservation, dissolution and transportation of coccoliths while they are suspended or sinking in the deep-sea column; the fate of coccoliths after arriving at the water-sediment interface (McIntyre and McIntyre, 1971; Berger, 1973; Schneidermann, 1973) is not discussed (See Roth and Berger, this volume).

## SAMPLES AND METHODS

Nintey-three water samples were collected by 30-liter van Dorn-type water samples from 14 stations along 155° W meridian (text fig. 1) from 0.4, 0.6, 1.0, 1.5, 2.0, 3.0, 4.0, and 5.0 km depth during the HAKUHO MARU cruise HK69-4 in the summer and fall of 1969 (Ocean Research Institute, 1970). The aphotic water samples were always collected at the same stations where the living community of coccolithophores was investigated (Honjo and Okada, 1974).

Water samples were filtered immediately on board ship with Millipore<sup>(1)</sup> filters of 47 mm diameter (McIntyre and Bé, 1967) with a nominal pore size of 0.45  $\mu\text{m}$ , applying a constant and gentle negative pressure (less than 3 psi). Ten to twenty liters of water usually yielded a satisfactory number of coccoliths for statistic analysis and electron microscopy. The filters were rinsed with approximately 20 ml of prefiltered distilled water while the filters were wet, placed in an oven at 50° C for a few hours, then stored in plastic containers. The above-mentioned procedure was repeatedly tested on fresh laboratory-cultured coccolithophore specimens and was found to cause no significant damage to coccoliths and coccospheres.

A piece of filtered sample was placed on a glass slide and rendered transparent with a few drops of synthetic immersion oil and sealed by cover glass with cellulose solution for preservation. A high magnification polarizing and phase contrast microscope was utilized for counting the standing stocks. A video-matic computer system (Honjo, Emery, and Yamamoto,



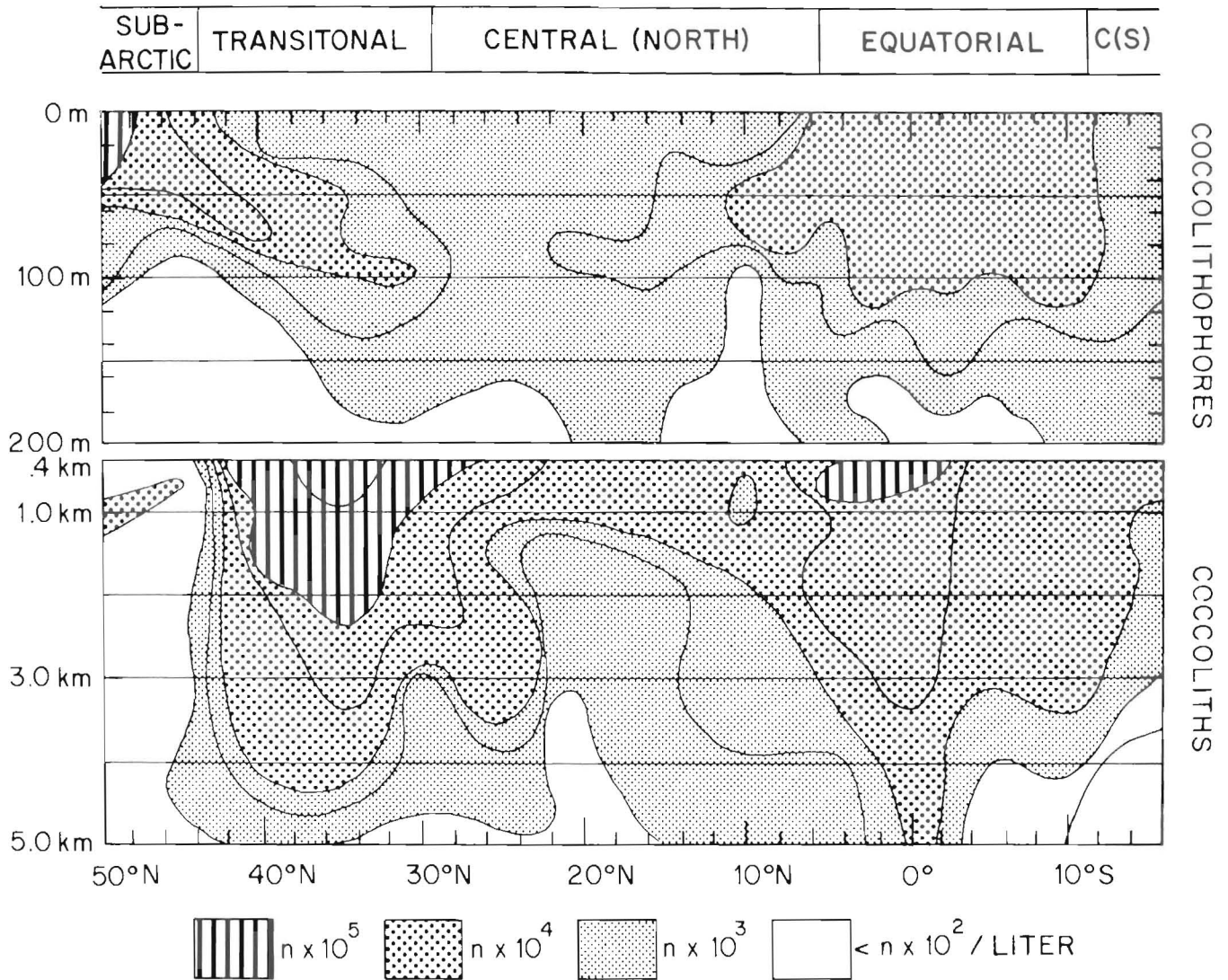
TEXT FIGURE 1

Location of the stations. The water samples were collected from station 1 (Aug. 23) to station 19 (Oct. 14), during the HK 69-4, R/V HAKUHO MARU. The detailed information of location and casting date is available in Okada and Honjo, 1973b.

in press) was used for statistical tests for randomness of the coccolith distribution on filter samples.

The identification of coccolith species and the detailed observation of the dissolution of suspended coccoliths was conducted under transmission and scanning electron microscopes using different pieces cut from the same filter used for the standing stock counting.

The same preparation procedure used for the transmission electron microscopy of living coccolithophores (Okada and Honjo, 1973b) was applied for the suspended coccolith study. A piece of filter was coated by thin platinum/palladium film for the scanning microscope observation. The detailed reports on the counting data, lists of species, statistical analysis, and electron



TEXT FIGURE 2

Distribution of standing stock of suspended coccoliths in the 155° W aphotic profile (lower figure) and living cells (coccospheres) in the overlying photic profile. All coccoliths (or coccospheres) in the view field of optical microscope was counted by traversing microscopic stage for 8 mm in X-direction and this was repeated 10 times to cover 3.6 mm<sup>2</sup>. Then the obtained was calibrated to per liter concentration. Fragments of less than a third were not counted.

micrographs on which this paper is partially based, are available in a separate technical report (Honjo, 1974).

### SUSPENDED COCCOLITH COMMUNITIES IN THE APHOTIC LAYER: OBSERVATIONS

#### DISTRIBUTION OF SUSPENDED COCCOLITHS IN THE DEEP WATER COLUMN

Suspended coccoliths abundance was usually on the order of 10<sup>3</sup> to 10<sup>4</sup> individuals per liter throughout

the profile along the 155° W meridian, except for the northern part of the transect. The water samples from greater depths such as 5.0 km also yielded significant numbers of suspended coccoliths (text fig. 2). They were far less dense in the aphotic Subarctic zone<sup>1</sup> than in other parts of the profile and concentrations were generally several hundreds per liter. A few substations

<sup>1</sup>The term "aphotic Subarctic Zone" in this paper means "the layer of aphotic water underneath the sub-Arctic Zone" (Compare Okada and Honjo 1973, for zonations).

yielded higher concentrations, 0.6 km and 1.0 km deep, with interesting specific contents which will be discussed below. Concentrations were particularly high in two areas between 4.0 km and 2.0 km of the Transitional Zone and the uppermost aphotic layer of the Equatorial Zone. The highest concentrations of suspended coccoliths which was recorded during this cruise was  $9.1 \times 10^5$  per liter of water collected from lat  $35^\circ$  N, long  $155^\circ$  W, 0.4 km deep. The photic water column of the Central zone yielded a relatively small number of suspended coccoliths. The number of suspended coccoliths generally decreased rapidly with depth at all stations except for the Subarctic Zone. The rate of decrease was not consistent. Concentrations at 4.0 km were between 1/100 to 1/1,000 of those in the uppermost aphotic layer.

#### STATE OF PRESERVATION

The suspended coccoliths were well preserved at all depths throughout the aphotic layer. Under the electron microscope, many coccoliths showed slight etching on the surface but never severe dissolution. Broken specimens were also found occasionally (pl. 1). At 0.4 km the evidence of etching on coccoliths was hard to recognize. At 0.6 and 1.0 km, more obviously etched samples were found but the majority were complete and intact coccoliths. In samples collected deeper than 1.5 km, etching was observed. More progressively etched coccoliths, usually found at 5 km depth, were limited to large, rigid placoliths, such as *Cylococcolithina leptopus* (Murray and Blackman) Wilcoxon. However, the complete specimens of fragile-looking

species of coccoliths were still commonly found at this depth. Fresh-looking, complete coccoliths were distributed ubiquitously in the aphotic profile. No evidence of progressive dissolution with depth was found.

Etching and dissolution of palacoliths at great depths usually progressed by numerous curving of small "steps" (0.1 to 0.3  $\mu$ m) around the edge of unit crystals (pl. 1, fig. 3). Rounding of edges was observed on slightly dissolved coccoliths of the *Emiliana* and *Geophyrocapsa* groups (pl. 1, figs. 4, 5).

The coccoliths of *Umbellosphaera* were most easily disintegrated into unit crystals along the seams of their unit crystal, particularly in water deeper than 0.6 km (pl. 2, fig. 2). However, intact specimens of this species, with no sign of damage, were often found at greater depth, 4.0 km. Coccoliths of *Florisphaera* and *Thorosphaera* were excellently preserved throughout the profile (pl. 2, fig. 1b). No preferential progress of etching was found on the distal or proximal discs of placoliths. At deeper stations, the distal parts of *Helicopontosphaera* were more severely etched while the proximal part was intact.

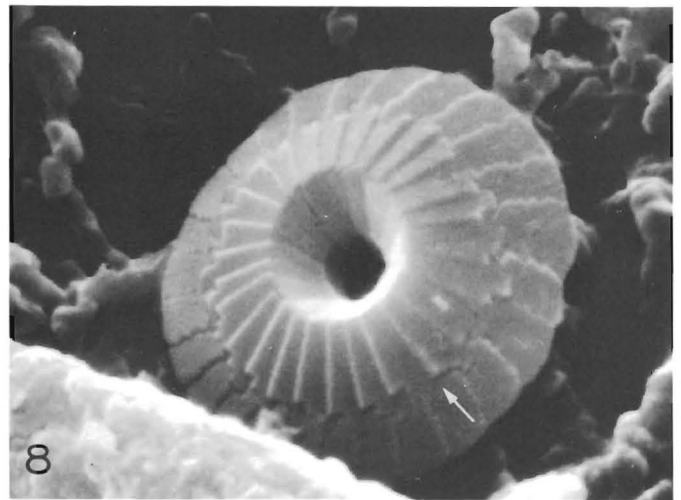
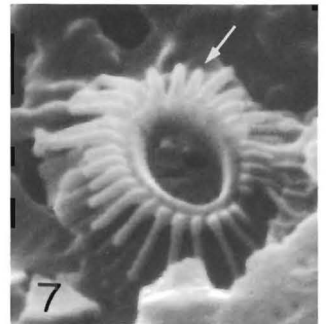
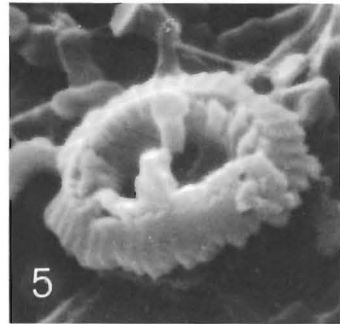
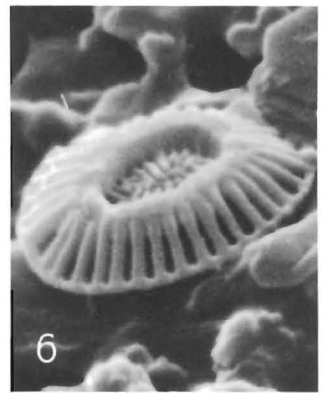
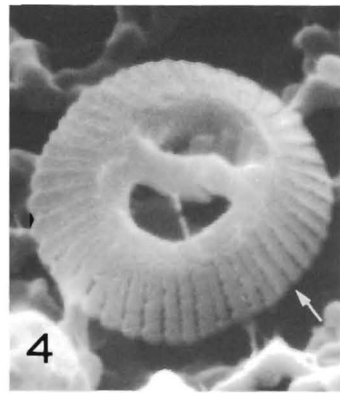
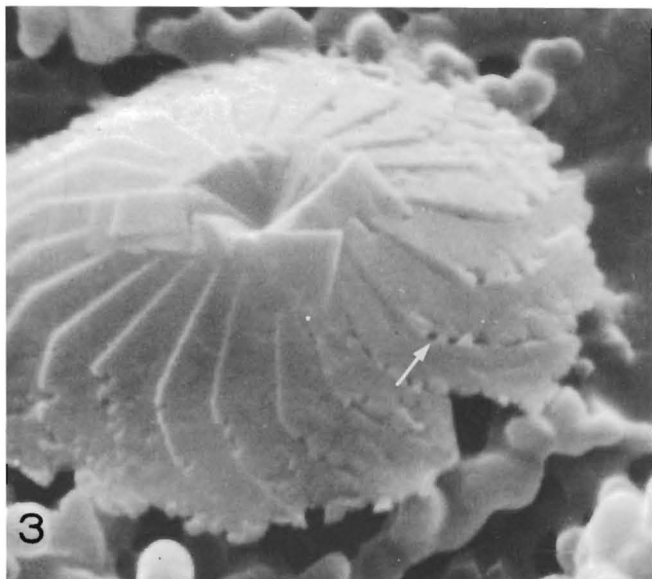
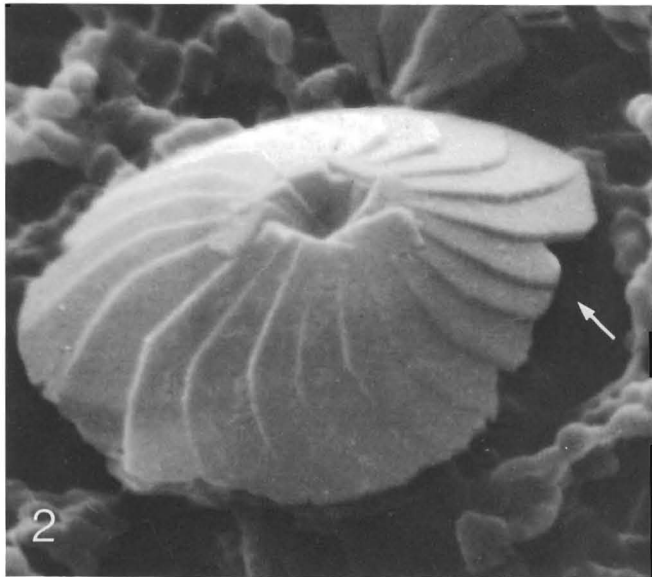
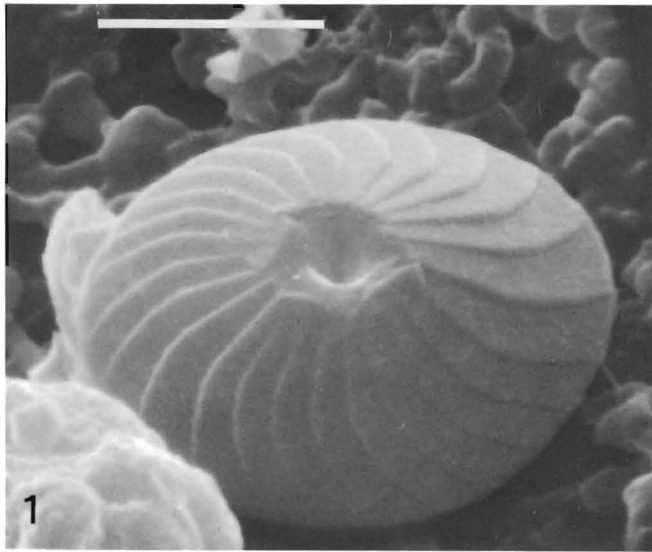
#### SPECIES ASSEMBLAGES OF SUSPENDED COCCOLITHS

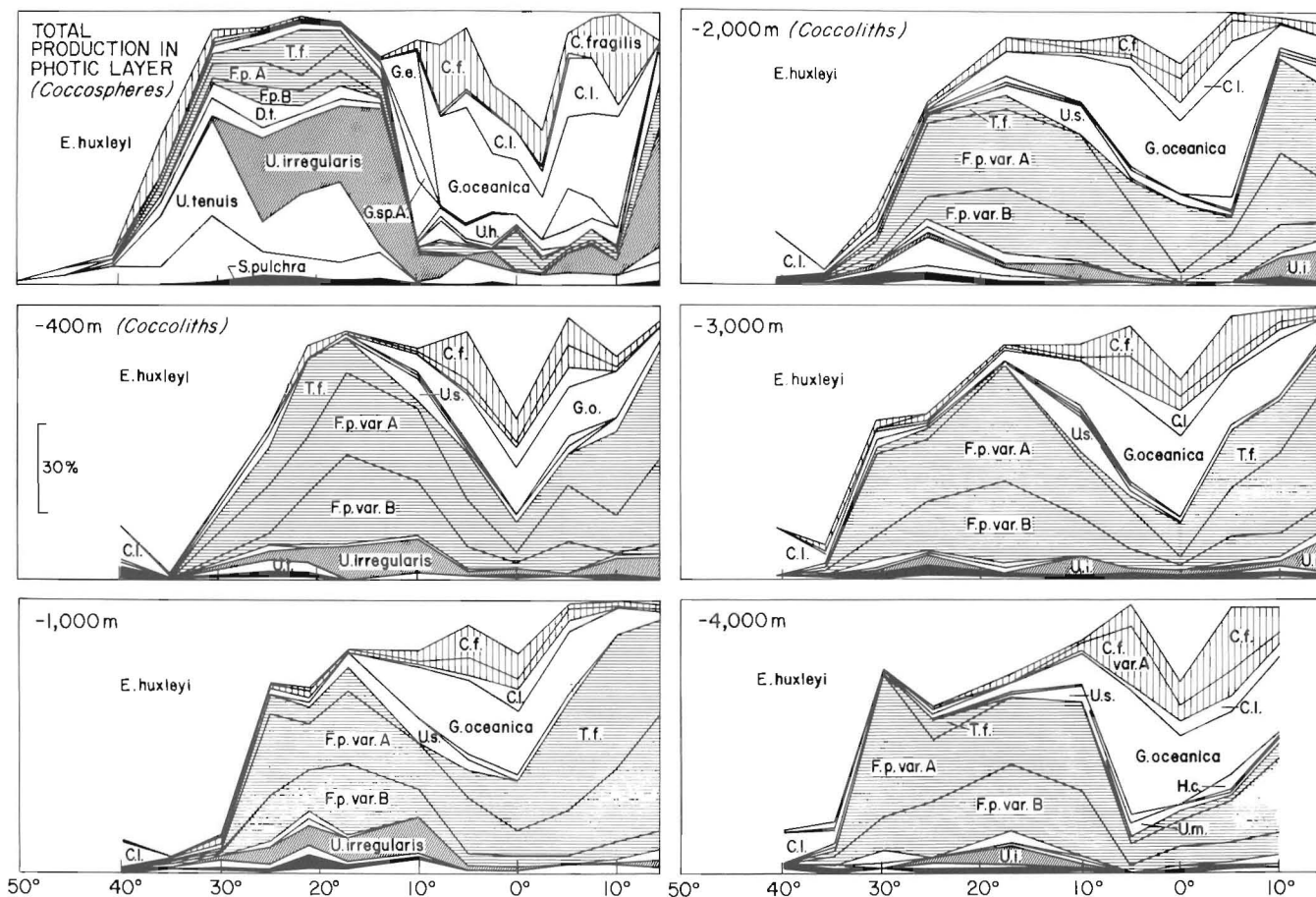
As we reported previously, coccolithophore assemblages in the surface water were zonally arranged in distinct zones. Vertical provincialism was also developed in the photic layer. The total species assemblage (text fig. 3, uppermost left figure) integrated from 0 to 200 m, was somewhat different from that obtained from the surface water (0–50 cm) (Okada and Honjo, 1974; Honjo and Okada, 1974).

### PLATE 1

Scanning micrographs of suspended coccoliths. Scale bar approximately 3  $\mu$ m.

- 1 A well preserved coccolith of *Cylococcolithina leptopora*. No etching is observed on the surface. 0.4 km,  $0^\circ$ ,  $155^\circ$  W.
- 2 A cracked (arrow mark) specimen of the same species showing slight etching along the seams of the unit crystals. 3.0 km,  $35^\circ$  N,  $155^\circ$  W.
- 3 Extensively etched coccoliths like this specimen are found rarely and only at greater depth such as 5.0 km. Better preserved specimens like figures 1 and 2 are also usually found on the same filter sample.
- 4 Slightly etched coccoliths of *Geophyrocapsa oceanica*; the seams between the unit crystals (arrow mark) are separated by dissolution. They will be disintegrated into the smaller units and may disappear during filtering. 3.0 km/ $0^\circ$ ,  $155^\circ$  W.
- 5 Sometimes *G. oceanica* is extensively dissolved, yet keeps the basic configuration while other species are disintegrated in the earlier stage of dissolution. 4.0 km,  $0^\circ$ ,  $155^\circ$  W.
- 6 Coccoliths of *Emiliana huxleyi* are fragile but many are found in excellent condition at the greater depths. 4.0 km,  $0^\circ$ ,  $155^\circ$  W.
- 7 Incomplete coccoliths of *E. huxleyi* are often found in the photic layer, probably by shedding while the host is alive. Short end and rounded ray without the peripheral bars (arrow mark) are not always the result of dissolution, particularly in case of *E. huxleyi*. 0.4 km,  $0^\circ$ ,  $155^\circ$  W.
- 8 Slightly etched coccolith of *Umbilicosphaera sibogae*. Etching proceeds along the edge of inner rim. 4.0 km,  $0^\circ$ ,  $155^\circ$  W.
- 9 Disintegration of this species usually starts along the inner rim (arrow mark, also pl. 2, fig. 1d). 3.0 km,  $0^\circ$ ,  $155^\circ$  W.





TEXT FIGURE 3

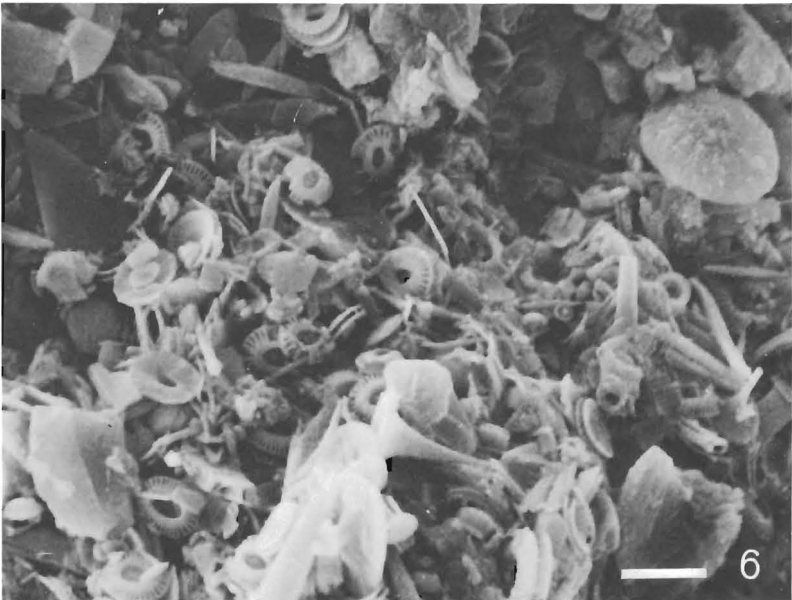
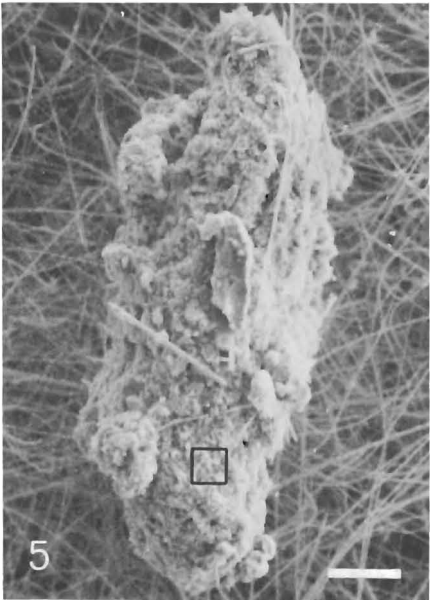
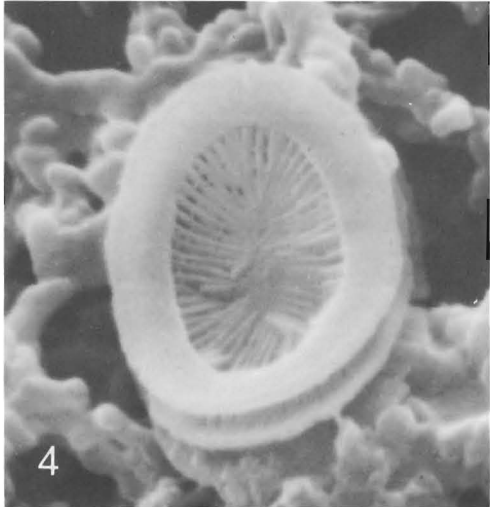
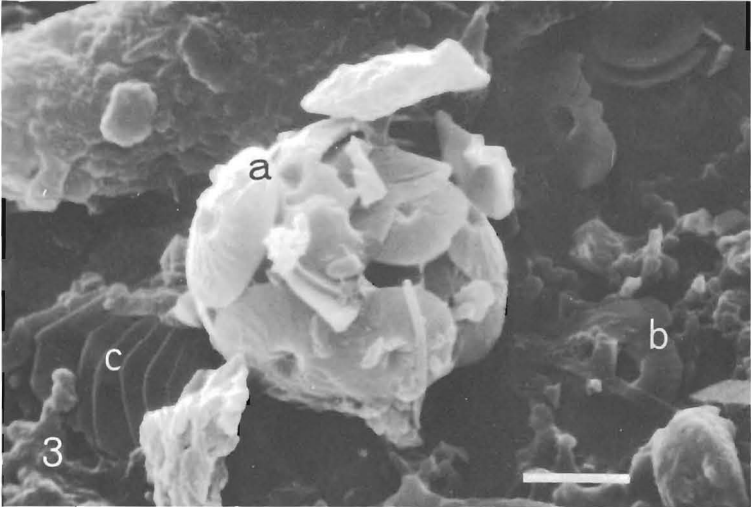
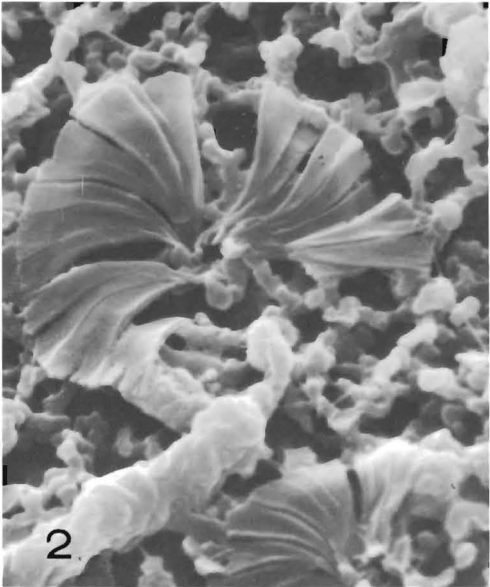
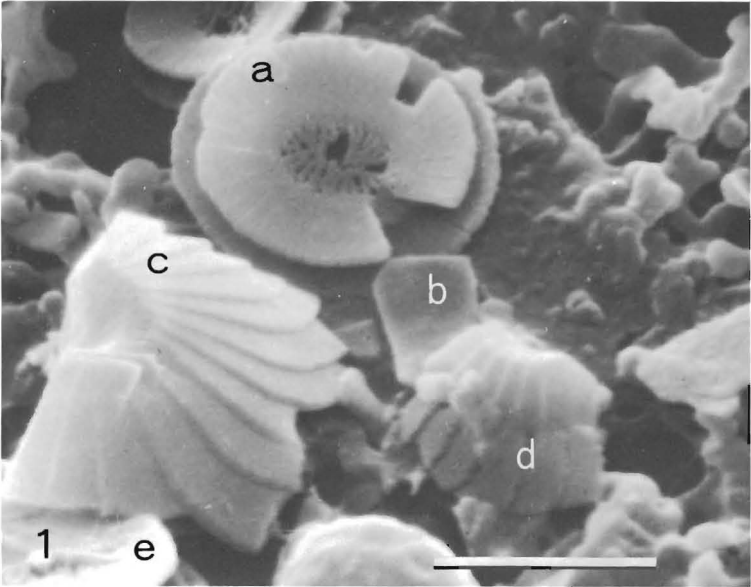
Species assemblage of suspended coccoliths at five levels through the 155° W meridian. The left uppermost figure is the total species assemblage of living coccospheres for the total photic-water column (Okada and Honjo, 1973a; Honjo and Okada, 1974). C.f. *Cycloccolithus fragilis*, C.I. *Cycloccolithina leptoporus*, D.t. *Discosphaera tubifera*, G.o. *Gephyrocapsa oceanica*, G.e. *G. ericsoni*, F.p. var. A or B, *Florisphaera profunda*, var. A or B, T.f. *Thorsphaera flabellata*, U.i. *Umbellosphaera irregularis*, U.t. *Umbe. tenuis*, U.h. *Umbellosphaera hulburiana*, U.s. *Umbi. sibogae*.

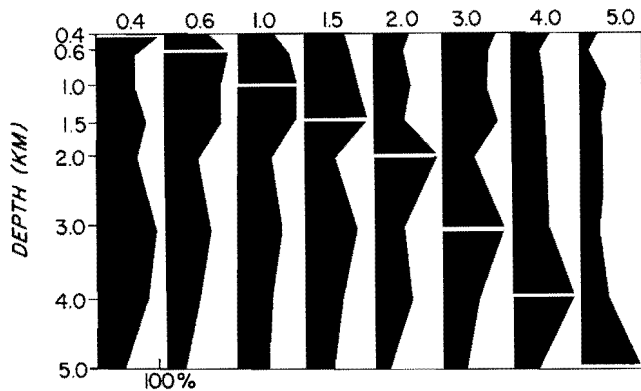
←

## PLATE 2

Scanning micrographs of suspended coccoliths and fecal pellets.

- 1 A typical view of a filter sample. Some are intact and the the others are etched in different extents.
  - a. almost intact coccoliths of *G. oceanica*, proximal view;
  - b. *Florisphaera profunda*, no etching is observed;
  - c. A half fragment of *C. leptoporus*, broken but no etching is observed on the surface nor along the fracture.
  - d. An eighth fragment of *Umbellosphaera sibogae*;
  - e. Strongly dissolved *Helicopontosphaera kamptneri*, proximal view. 0°, 155° W. Scale bar, 3 μm, common for figures 1, 2 and 4.
- 2 *Umbellosphaera irregularis* are disintegrated easily along the seams of the unit crystals. 4.0 km, 0°, 155° W.
- 3 Part of a probable fecal pellet. A coccosphere of *C. leptoporus* is intact (a) and coccoliths of *G. oceanica*, (b) and *C. leptoporus* (variety with large coccoliths) are excellently preserved and show no effects of etching. 4.0 km, 0°, 155° W. Scale bar; 3 μm.
- 4 Coccoliths with delicate architecture such as *Syracosphaera pulchra* Lohmann are usually found intact at greater depths. 4.0 km, 0°, 155° W.
- 5 A "green fecal pellet" collected by the Wiebe-type sediment trap at the equatorial Atlantic. Scale bar; 50 μm.
- 6 Enlargement of figure 5 indicated by the square showing fecal pellets made of coccolith (and coccospheres). Several species of coccoliths are observed in this photomicrograph. Scale bar; 5 μm.





TEXT FIGURE 4

An example of per cent similarity curves for depth levels. Similarity is computed (Honjo and Okada, 1974) between the sample indicated by a white bar and all other samples in the same column. No conspicuous structure was found at this station nor any other.

Provincialism observed in the photic layer was vaguely replicated in suspended coccolith assemblages in the aphotic layer. *Emiliania huxleyi* increased at the expense of *Umbellosphaera* in the aphotic Transitional Zone. Two deep photic genera *Florisphaera* and *Thorosphaera* were particularly abundant in the Central and Equatorial Zones. Those two genera exceeded 50 percent of all other suspended coccoliths at many stations. *Gephyrocapsa oceanica* (Kamptner), *Cyclococcolithus fragilis* (Lohmann) Wilcoxson, and *C. leptoporus* were more abundant in the Equatorial zone. They gradually increased from the Central zone toward the south. The percentages of *Umbellosphaera tenuis* (Kamptner) Paasche and *U. irregularis* (Paasche) slightly decreased in the layer deeper than 1,500 m; the latter was usually the more abundant except in the northern part of the Central zone, somewhat reflecting its distribution in the photic total assemblage.

The percentage of *G. oceanica* increased with depth at the Equatorial zone. However, the species assemblage profiles at different depths through 40° N to 15° S (text fig. 3) in the aphotic layer, were generally quite similar to each other, indicating no vertically developed structures and this will be further tested by similarity analysis in the following section.

#### SIMILARITY OF SUSPENDED COCCOLITH COMMUNITIES

Quantitative analysis of similarity-dissimilarity between communities in each substation using Whittaker's percent similarity index has been a useful method

to clarify the large-scale provincialism of pelagic planktonic communities (Honjo and Okada, 1974). Lateral comparison was made between all possible combinations of substations at the same aphotic depth level. Vertical comparison was also made between communities at different depths at the same station. Tabulation of computation results and similarity curves in lateral and vertical comparisons of the aphotic suspended coccolith communities are available in a separate report (Honjo, 1974).

The lateral similarity comparison showed the community between lat 40° and 30° N (Transitional zone) was unique to other areas throughout the water column. This was simply due to the dominance of *E. huxleyi*. The boundary between the Central and Equatorial zones was not clearly shown. The Southern Hemispheric Central zone at 15° S was also not distinguished from the Equatorial zone by this method.

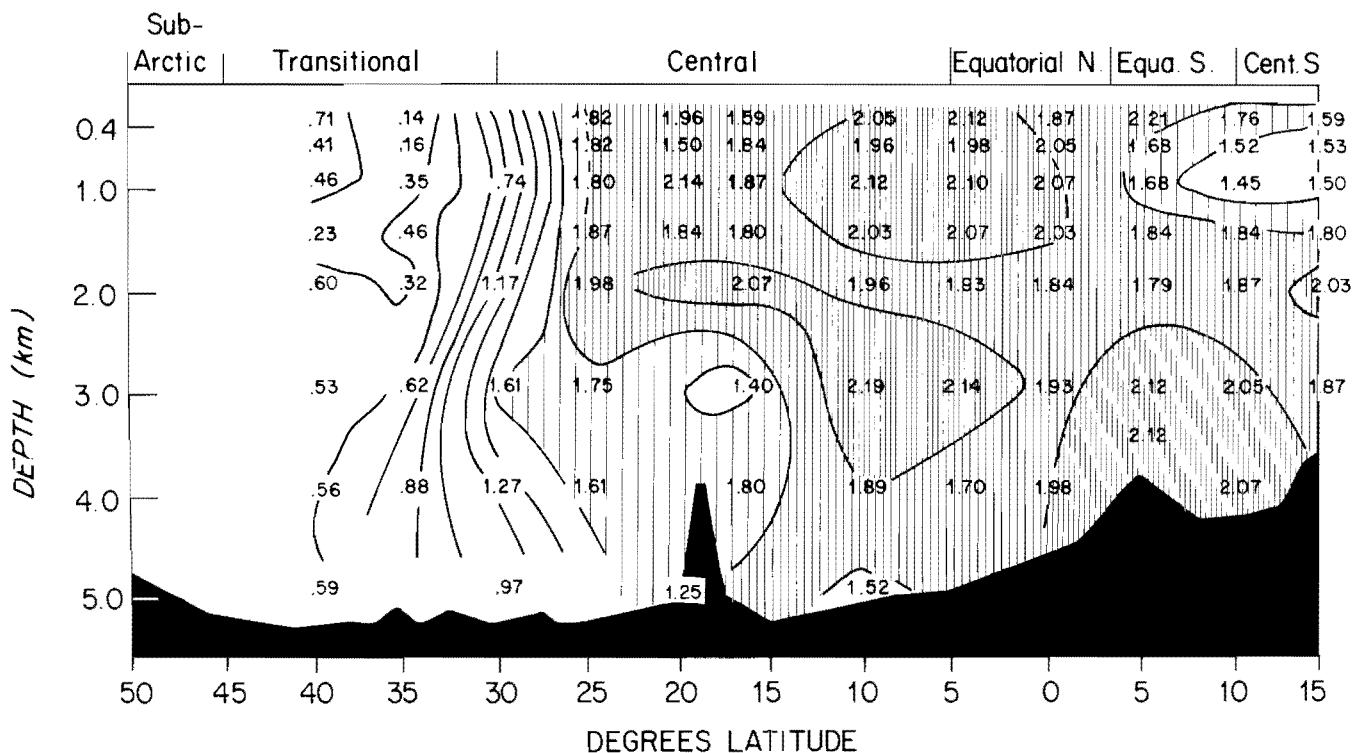
Downward comparison within the same stations showed that the suspended coccolith communities at different depths were dissimilar in cases (text fig. 4, for an example). The community at 5.0 km showed marked dissimilarity to the ones in the overlying water column in our limited number of stations (4 stations); more samples are required to generalize this observation. Generally speaking, similarities between suspended coccolith assemblages were poorly developed at the same depth levels and little grouping was observed.

#### DIVERSITY OF SUSPENDED COCCOLITHS IN THE APHOTIC LAYER

Species diversity indices ( $H'$ ) of suspended coccolith assemblages were computed using Shannon-Weaver's formula (Pielou, 1966) on 200 randomly sampled individuals from each substation (text fig. 5). Diversity was generally low at all depths and somewhat variable in the north. Indices increased rapidly toward the south at all depths. In the southern part of the Central Zone and the Equatorial Zone, diversity was consistently high at all depths exceeding 2.0  $H'$  units in many substations. It was relatively low at the station in the Southern Hemispheric Central zone.

No systematic change of diversity was observed with depth (through 0.4 km to 4.0 km) except it increased somewhat at middle depths (such as between 1.5 km to 3.0 km) in many stations. Diversity indices at 5.0 km were only available at four stations; they were always smaller than diversity at 400 m levels of the same water columns.

## DIVERSITY OF SUSPENDED COCCOLITHS, ALONG 155° W



TEXT FIGURE 5

The distribution of the species diversity ( $H'$ ) of suspended coccoliths throughout the aphotic profile of the 155° W meridian during the Leg 69-4. The contour lines were produced by computer linear interpolation.

### SUSPENDED COCCOLITHS IN DEEP SEA AS CALCITE

Text figure 6 shows the distribution of the total weight of the suspended coccoliths as calcite in a liter of sea water at each substation. Weights were calculated from the average volume of coccoliths per species as estimated from scanning micrographs and the specific gravity of calcite. The effects of etching on the surface was ignored. This method is somewhat crude considering the complicated morphology of coccoliths and their variable size. The error is estimated to be more than 50 percent in the Central and Equatorial Zones.

### COMPARISON OF COCCOLITH COMMUNITY BETWEEN THE SURFACE PRODUCTIVE LAYER AND NON-PRODUCTIVE LAYER

#### STANDING STOCK

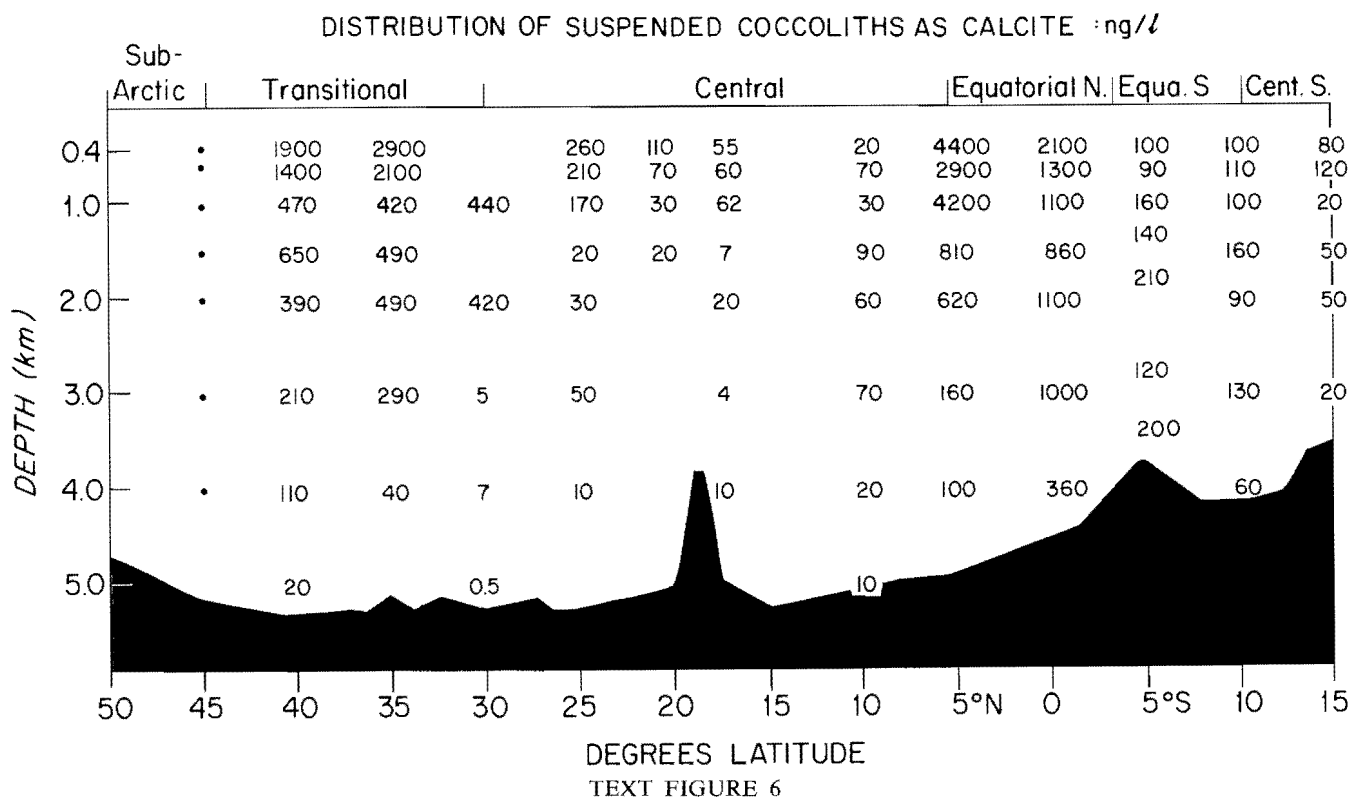
A numerical relation may exist between the production of coccoliths in the photic layer and the standing

stock of suspended coccoliths in the immediately underlying layer assuming they are under steady state condition. Suppose the only source of the suspended coccoliths is the disintegration of coccospheres in the overlying productive layer, the following should be observed; the yearly production of coccoliths in photic unit column is equal the number of suspended coccoliths in the aphotic extension of the same column with the length of the yearly rate of descent of coccoliths.

Therefore,

$$S \cdot t \cdot n = s \cdot D \quad (1)$$

where,  $S$  = the total standing stock of coccospheres in the productive layer, in number per  $m^2$ ,  
 $t$  = yearly turn-over rate of coccospheres, in times per year,  
 $n$  = average number of coccoliths on a coccosphere,  
 $s$  = concentration of coccoliths in the uppermost aphotic layer, in number per  $m^3$ ,  
 $D$  = yearly rate of descent of an average coccolith, in m per year.



The distribution of the estimated total weight of the suspended coccoliths per liter of sea water.

This hypothesis was tested in several tropical stations between 17° N and 15° S where the seasonal fluctuation of total standing crop in the productive layer is reasonably small. The field turnover rate in such an area is not measured as yet but estimated *in vitro* and at least more than once every ten days (36 times per year). The average number of coccoliths on each coccosphere of dominant species was obtained from a large number of electron micrographs and is roughly 20. The total standing stock in a unit water column during Leg 69-4, HAKUHO MARU, is available (Honjo and Okada, 1974). The productive layer of certain coccospheres such as *Thorosphaera* and *Florisphaera* sometimes extends to as deep as 300 m (Okada and Honjo, 1973). Therefore, the standing stocks of suspended coccoliths at 400 m level measured during the same leg were applied to the value of (s). Sea water below several hundred meters is undersaturated in terms of calcite in the tropical central North Pacific (Takahashi and others, 1970; Ben-Yaakov and others, 1974) and data on the standing crop of suspended coccoliths obtained below the saturation depth should not be used for estimation.

At the 10° N, 155° W (Station 10), for example, the total standing crop of coccospheres in the unit photic water column was  $2.2 \times 10^9$  per m<sup>2</sup>. The yearly production of coccoliths in the water column (S·t·n) is thus estimated as  $1.6 \times 10^{12}$  per m<sup>2</sup> per year. The standing stock of suspended coccoliths at 0.4 km was  $2.9 \times 10^3$  per liter during Leg 69-4. Suppose Stoke's law is applicable to coccoliths and considering its shape factor (A. Lerman, personal communication, 1974), an average size coccolith (a placolith of 3 μm × 5 μm) descends approximately one hundred meters in a year. Coccoliths produced during a year and subsequently suspended in the underlying aphotic layer (s·D) is estimated at  $3 \times 10^7$ . This implies that only a few coccoliths in every 10<sup>5</sup> coccoliths that were produced in the photic layer, arrived at the 400 m level. Assuming a turnover rate t of 36 per year and solving equation (1) in terms of D, the rate of descent of coccoliths becomes  $1.7 \times 10^6$  m per year of  $4.7 \times 10^2$  m per day, and such a high estimate of rate of descent is unacceptable.

## COMPARISON OF PHOTIC AND APHOTIC COMMUNITY

The total number of coccolith species in the aphotic layer were more or less constant and did not show significant correlation with the total species number of coccospheres in the overlying photic column. The former was always smaller than the latter. Approximately 95 living coccolithophore species were found in the photic layer of the transect (Honjo and Okada, 1974) and approximately 75 species of coccoliths were identified from the aphotic profile. The majority of the species distributed in an aphotic water column were also observed in the directly overlying photic layer but sometimes this rule was not followed. The discrepancy between the number of species between the aphotic layer and photic layer was mostly attributed to rare or very rare species which consist of less than a half percent (in photic layer) of the coccolithophore (coccosphere) population. During this study, 200 suspended coccoliths from each substation were identified and counted; also 200 coccospheres, each of which carried 15 to more than 100 coccoliths. Therefore, the chances of overlooking the rare species of suspended coccoliths are much larger than missing the rare coccosphere species unless one counts 20 times (the average number of coccoliths in coccospheres) more suspended coccoliths for a direct comparison of the aphotic and photic species lists. An exception was the relation between the living coccospheres and the suspended coccoliths of *Coccolithus pelagicus* (Wallich) Schiller. Only a few specimens of the coccospheres of this species were found during this cruise (47° N, 155° W, 0–50 cm) although they were reported in more abundance from the sub-arctic zone of the Pacific Ocean by other investigators (McIntyre and others, 1970). On the other hand, suspended coccoliths of *C. pelagicus* were frequently found at 0.6 km and 1.0 km depth between 55° N and 50° N. They occupied more than 60 percent of the suspended coccoliths' population in such substations.

For the same reason mentioned in the last paragraph, photic coccosphere diversity data cannot be compared to the underlying aphotic coccoliths' diversity except for a crude estimate. The diversity of suspended coccolith communities at any aphotic substation was smaller than the total diversity of coccospheres in the overlying photic column [the  $H'$  value computed on the hypothetical coccosphere community of 0 m to 200 m (Honjo and Okada, 1974)]. They were closer in the

Equatorial zone where the number of rare or very rare species was reduced in the photic column.

The relation of the photic and aphotic diversity of coccospheres and coccoliths are more unrelated at the Transitional zone. The total species number and diversity in the photic water column rapidly increased toward the south. At the boundary of the Transitional and the Central zones (30° N, 155° W) the number of species at this station was 52 and this was the largest throughout the transect. While in the underlying aphotic layer, only 13, 14, and 10 species were found at 0.4 km, 3 km, and 5 km deep, respectively, in the same station. The total number of species for the aphotic water column was 19. The total diversity of the aphotic coccolith species at this station was significantly smaller than the one on the total photic coccosphere which was also the largest along the transect. Such a large discrepancy between the photic and aphotic community is hard to explain by the difference of statistics between the photic coccolithophore and aphotic coccolith communities.

## DISCUSSION

### DISSOLUTION OF SUSPENDED COCCOLITHS IN THE DEEP SEA

Recent estimates of calcite saturation in the North Central Pacific Ocean suggests that the transition from calcite supersaturation to undersaturation occurs within several hundred meters of the surface (Takahashi, and others, 1970; Morse and Berner, 1972); sea water is undersaturated at all depths beneath this. Spar-calcite spheres (Peterson, 1966) or planktonic foraminiferan tests (Berger, 1967) dissolve slowly in such undersaturated water until the lysocline (Berger, 1970) where planktonic foraminiferan tests in the sediment first show significant dissolution. The planktonic foraminiferal lysocline in the North Pacific is significantly deeper than the saturation depth.

An average size coccolith (a placolith of  $3\mu\text{m} \times 5\mu\text{m}$ ) weighs approximately  $22 \times 10^{-12}\text{g}$ . The area exposed to the sea water is approximately  $0.8 \times 10^{-6}\text{cm}^2$ . (The total surface area in a gram of such placoliths is estimated as at least  $1 \times 10^5\text{cm}^2$ .) The rate of dissolution of a calcite sphere obtained from the Peterson's exposure experiment (Fig. 2, p. 1543 in Peterson, 1966) is approximately  $0.3 \text{ mg cm}^{-2}\text{yr}^{-1}$  between 0.7 km and 1.5 km deep. If we assume this is also applicable to coccoliths, the maximum time to completely dissolve a coccolith at such a rate of dissolution is approximately 0.9 years. Berger's experiments (1970)

indicate planktonic foraminiferan tests dissolve at a rate of approximately 0.2 percent day<sup>-1</sup> at such depth. If this rate is pertinent to coccoliths, they should disappear within 1.5 years. As long as the rate of descent of a coccolith is as slow as 100 meters per year, free-falling coccoliths can remain only in the uppermost layer of the undersaturated water and should disappear long before reaching greater depth. This estimate contradicts present observations on the distribution of abundant and well-preserved coccoliths in the deep sea of the central North Pacific Ocean.

One explanation is that the dissolution rate of coccoliths is much slower than the ones measured on the spar-calcite or foraminifera samples. It has been suggested that fossil coccoliths are more resistant (McIntyre and McIntyre, 1971) to the dissolution than the other calcareous microfossils. They are relatively more abundant than planktonic foraminiferan tests close to the carbonate compensation depth (Hsü and Andrews, 1970; Hay, 1970). However, Berger (1973) observed that the dissolution behavior of coccoliths and planktonic foraminiferan tests are similar in deep-sea sediment. Chemosorptive organic coatings (Chave and Suess, 1970) or organic coatings of a biological origin (McIntyre and McIntyre, 1971) can also be considered an efficient protection. However, Morse (1973) did not find significant inhibition of carbonate dissolution in a large selection of organic and biochemical sea-water solutions. In situ saturation experiments on deep-sea carbonate sediment near Hawaii, which is mainly composed of coccoliths and planktonic foraminiferan tests, showed no significant difference from pure calcite (Ben-Yaakov, and others, 1974). The dissolution experiments at constant disequilibrium on the calcite powder and coccoliths bearing fine calcareous sediment in the pH-stat, did not show a significant difference (Berner, personal communication, 1974). Dissolution inhibition models do not explain why fresh-looking and slightly etched coccolith specimens coexist at great depths.

#### RAPID TRANSPORTATION BY FECAL PELLETS

A large number of fecal pellets of zooplankton, probably copepods, were collected by a sediment trap settled for two months at the Tongue of the Ocean at 2,200 m depth (P. H. Wiebe, S. H. Boyd and C. Winget, unpublished). They were a few hundred microns long and several tens of microns wide (pl. 2, fig. 5). Two types of fecal pellets were identified under the binocular microscope: greenish-colored, less consolidated pellets and darker, consolidated pellets with

more consistent configuration than the other. Under the electron microscope, greenish-colored fecal pellets consist almost exclusively of coccoliths (pl. 2, fig. 6). Sometimes, intact coccospheres were found in them. An average green fecal pellet weighed approximately 0.8  $\mu\text{g}$  (as  $\text{CaCO}_3$ , estimated by atomic adsorption analysis) and contains approximately  $4 \times 10^4$  coccoliths. By virtue of the elongated cylindrical shape, they descend rapidly at the rate of approximately 200 m/day. They were estimated to arrive at the sea floor at the rate of approximately 250/m<sup>2</sup>/day. The detailed microscopic study of fecal pellets collected by the sediment trap will be published elsewhere by S. Honjo and P. H. Wiebe. Several species of calanoid copepods collected near Woods Hole were successfully maintained by feeding pure-cultured *E. huxleyi* with the cooperation of Dr. Thomas Lawson, Woods Hole Oceanographic Institution. They produced fecal pellets which consisted of near 100 percent of the coccoliths with similar configuration to the greenish fecal pellets collected by the trap. No dissolution of coccoliths was observed either in the natural or laboratory produced fecal pellets.

The above observations suggest that fecal pellets of the grazers can transport coccoliths and coccosphere population from the surface productive layer to the deep-sea floor with great efficiency. Similar observation was made on the vertical transportation of pelagic diatoms (Schrader, 1971) or radionuclides (Osterberg and others, 1963).

There might be many other marine organisms who graze coccolithophores. For example, Lohmann (1902) found a large number of coccoliths in salp guts. Mauchline and Fisher (1969) reported that a euphausiid eats anything from detritus to other euphausiids. Therefore, some of the coccoliths may be transported indirectly by the larger fecal pellets as far as the guts of the hosts are not acidic.

#### THE ORIGIN AND FATE OF SUSPENDED COCCOLITHS

The coccolithophore population is presumed to be under high grazing pressure from small zooplanktons such as copepods in the oligotrophic open sea and the majority of coccolithophores is taken up by such grazers before it completes the life cycle. Therefore, the chances of shedding the free coccoliths from the "dead coccospheres" might be small.

Coccospheres of *E. huxleyi* in our laboratory culture shedded a number of coccoliths during growth under

slightly stressed condition particularly when a "stimulant" such as a small amount of methyl alcohol was dropped into the media, hundreds of extra coccoliths were produced by a coccolithophore and they were shed into the media. If this observation is applicable to the natural photic ecosystem, the majority of free-falling coccoliths are shed individuals while they are productive. Shedding is inconsistent and probably has little quantitative relation with the host community. Such free-falling coccoliths may disappear by dissolution shortly after they come across the saturation depth and are removed from the water column.

The abundant suspended coccoliths distributed in greater depth is presumed to have spilled out from fecal pellets. The green fecal pellets mentioned before were not strongly consolidated and after they were passed by gravity through 3-foot-long, 4° C sea-water columns a few times in the laboratory, a substantial number of coccoliths were left in water in suspension. Fresh coccoliths or coccospheres may thus be replenished at all depths by rapidly descending fecal pellets. After coccoliths are released from the host fecal pellets, the rate of descent decreases a thousandfold and they are fully exposed to the undersaturated deep water. At the depth deeper than the calcite saturation depth, dissolution proceeds immediately, and the structure of a coccolith is weakened by loss of adhesion which keeps its unit crystals intact. As a consequence, the coccolith decomposes into a smaller unit and is lost during filtration. This explains the reason why no strongly dissolved coccoliths are left on the filter residue. The decrease of the standing crop (text fig. 2) and the weight as calcite in a unit volume (text fig. 6) with depth may reflect the rate of such decomposition with depth (rather than dissolution) in the progressively undersaturated sea water.

The suspended coccolith populations in the upper aphotic layer which is shallower than the saturation depth are a mixture of coccoliths with two different origins; 1) the falling coccoliths from the photic layer possibly originated by shedding, and 2) the coccoliths and coccospheres "spilled out" freshly from fast descending fecal pellets. Therefore, the balance of the standing crops of coccoliths between the productive and aphotic layers cannot be of steady state. The yearly yields of the suspended coccoliths in a unit column must be significantly smaller, under the circumstances where the majority of coccoliths produced in the photic layer is removed by grazing activity bypassing the aphotic water column.

#### PALEO-OCEANOGRAPHIC IMPLICATIONS OF THE RAPID FECAL PELLET TRANSPORT MODEL

If the above-mentioned model on coccoliths, coccospheres, and fecal pellets is pertinent in pelagic water column, free-falling coccoliths from the productive layer and suspended coccoliths resulting from dispersion from fecal pellets are all dissolved before reaching the sea floor where the depth exceeds the saturation depth. The majority of coccoliths produced in the photic layer is sealed in fecal pellets and transported to the underlying sea floor almost instantaneously. Therefore, oceanographic filters expected during the free fall of minute calcareous particles, such as selective dissolution, lateral transport by current, or winnowing of coccolith species by size, will give no effect on the deep-sea coccolith-ooze formation. The majority of the coccolith population is continually transported to the underlying sea floor, regardless of the depth, maintaining its original community structure (if no selective grazing occurs at the species level). Selective dissolution of coccoliths (McIntyre and McIntyre, 1971; Schneidermann, 1973; Roth and Berger, this volume) may occur after arrival at the sediment-water interface. The contribution of coccoliths to controlling the alkalinity of deep-sea water columns is mainly achieved by the diffusion from the sea floor, and the role of dissolving coccoliths suspended throughout the water column would be minor.

#### ACKNOWLEDGMENTS

My special thanks are due to Dr. Hisataka Okada, Lamont-Doherty Geological Observatory, for his thorough work on the water sample collection and counting of standing stocks of suspended coccoliths for this investigation. I am grateful to Drs. P. H. Wiebe and K. O. Emery for valuable discussions throughout the course of this investigation. I also wish to thank Dr. G. P. Lohmann for his critical reading of the manuscript; Dr. T. Lawson for cooperation on the feeding experiments. Particular thanks go to Dr. W. A. Berggren and Mr. T. Goreau. Without their valuable suggestions this work could not have been completed.

This investigation was made possible through financial support by the Oceanographic Section of the National Science Foundation under grant GA-30996.02.

#### REFERENCES

- BEN-YAAKOV, S., RUTH, E., and KAPLAN, I. R., 1974, Carbonate compensation depth: Relation to carbonate solubility in ocean waters: *Science*, v. 184, p. 982-984.

- BERGER, W. H., 1967, Foraminiferal ooze: solution at depth: *Science*, v. 156, p. 383-385.
- , 1970, Planktonic foraminifera: selective solution and lysocline: *Marine Geology*, v. 8, p. 111-138.
- , 1971, Sedimentation of planktonic foraminifera: *Marine Geology*, v. 11, p. 325-358.
- , 1973, Deep sea carbonate, evidence for a coccolith lysocline: *Deep-Sea Research*, v. 20, p. 917-921.
- CHAVE, K. E., and SUESS, E., 1970, Calcium carbonate saturation in sea water: Effects of dissolved organic matter: *Limnology and Oceanography*, v. 15, p. 633-637.
- HAY, W. W., 1970, Calcareous nannofossils from cores recovered on Leg 4, Deep Sea Drilling Project: Initial Rept. Deep Sea Drilling Proj., v. 4, p. 455-540.
- HONJO, S., 1974, Suspended coccoliths in deep-sea layers; raw data and photomicrographs: Woods Hole Oceanogr. Inst. Tech. Rept.
- HONJO, S., and OKADA, H., 1974, Community structure of coccolithophorids in the photic layer of the mid-Pacific Ocean: *Micropaleontology*, v. 20, p. 209-230.
- HONJO, S., EMERY, K. O., and YAMAMOTO, S., 1974, Suspended mineral particles in Asian marginal seas of the Pacific. *Sedimentology*, in press.
- HSÜ, K. J., and ANDREWS, J. E., 1970, Lithology: Initial Repts. of the Deep Sea Drilling Proj., v. 3, p. 445-453.
- LOHMANN, H., 1902, Die coccolithophoridae: *Arch. protistenk.*, v. 2, p. 89-165.
- MAUCLINE, J., and FISHER, L. R., 1969, The biology of euphausiids: *Advan. Marine Biology*, v. 7, p. 1-454.
- MCINTYRE, A., and MCINTYRE, R., 1971, Coccolith concentrations and differential solution in oceanic sediments, in Funnell, B. M., and Riedel, W. R., eds., *The Micropaleontology of Oceans*: Cambridge Univ. Press, p. 253-262.
- MCINTYRE, A., and BÉ, A. W. H., 1967, Modern coccolithophoridae of the Atlantic Ocean—I, placoliths and cryoliths: *Deep-Sea Research*, v. 14, p. 561-597.
- MCINTYRE, A., BÉ, A. W. H., and ROCHE, M. B., 1970, Modern Pacific Coccolithophorida: a paleontological thermometer: *New York Acad. Sci. Trans.*, Ser. 2, v. 32, p. 720-731.
- MORSE, J. W., 1973, The dissolution kinetics of calcite: a kinetic origin for the lysocline: Yale Univ., Ph.D. dissertation, 118 p. (Univ. Microfilms, Ann Arbor, Mich.).
- MORSE, J. W., and BERNER, R. A., 1972, Dissolution kinetics of calcium carbonate in sea water, II. A kinetic origin for the lysocline: *Am. Jour. Sci.*, v. 272, p. 840-851.
- OKADA, H., and HONJO, S., 1973a, The distribution of oceanic coccolithophorids in the Pacific: *Deep-Sea Research*, v. 20, p. 355-374.
- , 1973b, Distribution of coccolithophorids in the North and Equatorial Pacific Ocean: Quantitative data and samples collected during Leg 30, OSHRO MARU, 1968 and Leg HK 69-4, HAKUHO MARU, 1969: Woods Hole Oceanogr. Inst. Tech. Rept., WHOI-73-8.
- OSTERBERG, C., CAREY, A. G., and CURL, H., 1963, Acceleration of sinking rates of radionuclides in the ocean: *Nature*, v. 200, p. 1276-1277.
- PETERSON, M. N. A., 1966, Calcite: rate of dissolution in a vertical profile in the Central Pacific: *Science*, v. 154, p. 1542-1544.
- PIELOU, E. C., 1966, The measurement of diversity in different types of biological collections: *Jour. Theoret. Biology*, v. 13, p. 131-144.
- SCHNEIDERMANN, N., 1973, Deposition of coccoliths in the compensation zone of the Atlantic Ocean: Gulf Coast Sec., Soc. Econ. Paleontologists and Mineralogists Proc., Symposium on Calcareous Nannofossils, p. 140-151.
- SCHRADER, T. J., 1971, Fecal pellets: role in sedimentation of pelagic diatoms: *Science*, v. 174, p. 55-57.
- TAKAHASHI, T., WEISS, R. F., CULBERSON, C. H., EDMOND, J. M., HAMMOND, D. E., WONG, C. S., LI, Y-H, and BRAINBRIDGE, A. E., 1970, A carbonate chemistry profile at the 1969 GEOSECS intercalibration station in the eastern Pacific Ocean: *Jour. Geophys. Research*, v. 75, p. 7648-7666.
- THOMPSON, G., and BOWEN, V. T., 1969, Analysis of coccoliths ooze from the deep tropical Atlantic: *Jour. Marine Research*, v. 27, p. 32-41.
- TOKYO UNIV. OCEAN RESEARCH INST., 1970, Preliminary Report of HAKUHO MARU Cruise HK-69-4, Marumo, R., ed., Tokyo Univ. Ocean Research Inst., p. 68.

# LATE PLEISTOCENE CARBONATE DISSOLUTION CYCLES IN THE EASTERN EQUATORIAL ATLANTIC

JAMES V. GARDNER<sup>1</sup>

CLIMAP, Lamont-Doherty Geological Observatory  
Palisades, New York 10964

---

## ABSTRACT

Deep-sea sediments from the eastern equatorial Atlantic indicate that dissolution of carbonate was greater during the late Pleistocene glacial stages than at present or during the last interglacial stage. Surface (Holocene) carbonate distribution shows a correlation with the 1.9°C potential temperature isotherm which represents the top of Antarctic Bottom Water. A comparison of the surface versus glacial Pleistocene (18,000 YBP) carbonate distribution indicates that the effects of Antarctic Bottom Water were felt 200 to 700 meters shallower during glacial than interglacial conditions.

Records of carbonate composition for the past 200,000 years show increases in both carbonate dissolution and terrigenous noncarbonate dilution during

glacial stages. Likewise, microscopic examination of the planktonic foraminiferal faunas indicates much greater test fragmentation and destruction and higher percentages of benthonic forams per total foram populations during glacial conditions. The available evidence suggests that Antarctic Bottom Water was the mechanism that produced the increased carbonate dissolution. Therefore, probably either an increase in the production and circulation of Antarctic Bottom Water during glacial stages or the production of a glacial North Atlantic Bottom Water occurred. Regardless of the model used to explain the observations, all of these data suggest that the eastern equatorial Atlantic experienced greater carbonate dissolution during late Pleistocene glacial stages.

---

## INTRODUCTION

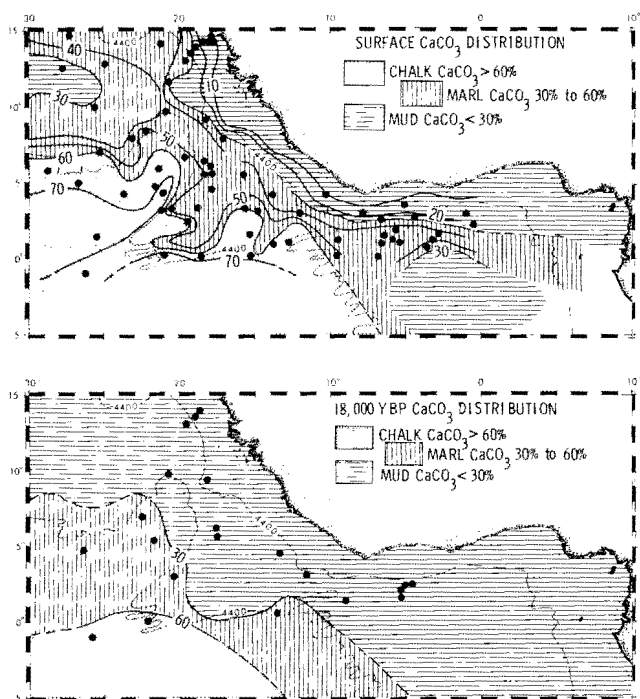
There has been a debate for more than 20 years over whether Pleistocene climatic changes caused increased or decreased dissolution of the carbonate component of marine sediments. Arrhenius (1952), working in the Pacific, was the first to suggest carbonate dissolution as the control of carbonate content in Pleistocene sediments. His work was later confirmed by Olausson (1965, 1967), Berger (1968, 1973), and Hays and others (1969). Many of these researchers supported Arrhenius who suggested decreased carbon-

ate dissolution during the glacial stages for Pacific sediments. The controversy has developed over whether the same sense of carbonate dissolution has occurred in Atlantic sediments (Broecker and others, 1958; Broecker, 1971; Berger, 1973) or the reverse, that is, greater carbonate dissolution in glacial stages (Phleger and others, 1953; Olausson, 1967, 1971). The present discussion attempts to demonstrate increased dissolution of carbonate during glacial stages in the equatorial Atlantic.

During the course of an examination of equatorial Atlantic sediments (Gardner, 1973) 15 piston cores were analyzed gasimetrically for total carbonate using the technique of Hülsemann (1966), and zoned biostratigraphically using the scheme of Ericson and others

---

<sup>1</sup> Present Address: University of California, San Diego, Scripps Institution of Oceanography, P.O. Box 1529, La Jolla, California 92037.



TEXT FIGURE 1

- A. Distribution of total carbonate in trigger-weight core tops. Solid points represent data points.  
 B. Distribution of total carbonate at 18,000 YBP. The 4,400-meter isobath is used to show general bathymetric provinces.

(1961). The total carbonate content represents the amount of biogenic carbonate contributed by coccoliths and forams which has accumulated on the ocean floor (detrital carbonate is negligible or absent in the study region). Whether or not the resulting carbonate content is a function only of carbonate production (biological productivity) or a combination of carbonate production, carbonate dissolution, and noncarbonate dilution is the heart of the matter.

This problem, as it applies to the eastern equatorial Atlantic, will be attacked in three phases: (1) a comparison of Holocene to glacial Pleistocene distribution of carbonate; (2) an analysis of the sedimentologic effects of dissolution versus noncalcareous dilution compared to the observed sediment record for the past 200,000 years; and (3) foraminiferal evidence from the 200,000-year record.

#### DISSOLUTION EVIDENCE FROM $\text{CaCO}_3$ DATA

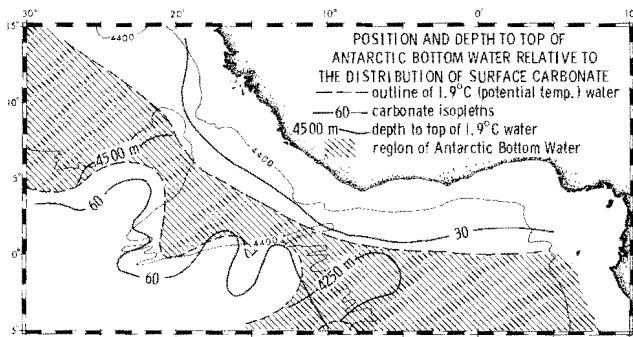
The distribution of  $\text{CaCO}_3$  in surface (Holocene) sediments is shown in text figure 1A. These data are

taken from the tops of trigger-weight cores and represent the Holocene distribution of carbonate. The carbonate isopleths were drawn using as guides both chemical analyses and bathymetric data. Because the present lysocline in the eastern equatorial Atlantic lies at a depth somewhere around 4,500 meters (Berger, 1968), the use of bathymetric data as a partial guide seemed justified.

A three-part division of the carbonate values into chalk ( $\text{CaCO}_3 > 60\%$ ), marl ( $\text{CaCO}_3 > 30$  to  $60\%$ ), and mud ( $\text{CaCO}_3 < 30\%$ ) is used to show trends. The Holocene distribution map (text fig. 1A) clearly shows a band of noncalcareous terrigenous mud along the continental shelf which represents high dilution of the carbonate material. Farther seaward and deeper these muds give way to marls which blanket most of the area. The marls form a thick wedge of sediments extending from the continental margin out to the lower flanks of the Mid-Atlantic Ridge. Farther from the continent and deeper yet, in the basins deeper than 5,500 meters, muds appear again.

The large area covered by chalks represents regions separated from the continent by basins. The basins can act as traps for much of the terrigenous sediments, thus the sediments beyond the basins would be diluted by only minor amounts of noncalcareous sediment. Alternately, the deep basins could be regions of carbonate dissolution and the shallower areas could be above the calcite compensation depth (CCD). The areas coated by biogenic chalks, the Sierra Leone Rise, Liberia Rise, and the flanks of the Mid-Atlantic Ridge, all lay at depths shallower than 4,800 meters. A map of the depth of the  $1.9^\circ\text{C}$  potential temperature isotherm superimposed on the carbonate-distribution map (text fig. 2) shows a close correspondence between the zones of marls and  $1.9^\circ\text{C}$  Antarctic Bottom Water (AABW). The presence of marl rather than mud under AABW suggests the accumulation rate of carbonate exceeds the rate of dissolution in this region.

A comparison can be made of the surface distribution of carbonate with the carbonate distribution during a glacial time. Work by the CLIMAP group (McIntyre and others, in press; Gardner and Hays, in press; Prell and Hays, in press; Prell and others, in press) has defined a chronostratigraphic horizon representing severe Wisconsin glacial conditions which can be confidently correlated over almost all of the temperate and tropical North Atlantic. This datum, representing 18,000 YBP, was chosen in 21 cores from the study area and the sediments were analyzed for total carbonate. Text figure 1B shows that extensive areas



TEXT FIGURE 2

Plot of the position and depth to the top of 1.9°C potential temperature bottom water relative to the distribution of surface total carbonate. The temperature data is from Worthington and Wright (1970).

where Holocene sediments are marls contain primarily muds at 18,000 YBP. In a similar manner, late Holocene chalks were preceded by marls. This can be interpreted as the effects of carbonate dissolution which would require a significant rise in the lysocline during the glacial stage, thereby indicating increased circulation of AABW.

The above data and interpretation, taken alone, would not be totally convincing because several alternate explanations could be equally as plausible. Two other interpretations might be: (1) AABW will naturally seek the deepest basins and fill upward to accommodate its volume because it is the densest of the water masses in the equatorial Atlantic. Terrigenous sediments shed off Africa would also find these same deep basin areas diluting the pelagic carbonate rain. Therefore the correlation between AABW and marls could be nothing more than the end product of gravity. The decrease in carbonate content during the glacial datum could be reflecting the increased terrigenous output caused by denudation of the continental shelves during lowered sea level. (2) The well-known Harmaton Winds (Radczewski, 1939; Folger and others, 1967; Carlson and Prospero, 1972) shed clay-sized noncalcareous material into the eastern equatorial Atlantic. The correlation between AABW and marls could be only by chance, actually resulting from the fallout zone of these windborne clays over the ocean. Hays and Perruzza (1972) contend that the observed decrease in carbonate during glacial stages in the eastern equatorial Atlantic is the result of increased Trade Wind activity thereby diluting pelagic sediments with eolian material. Consequently, additional data must be used

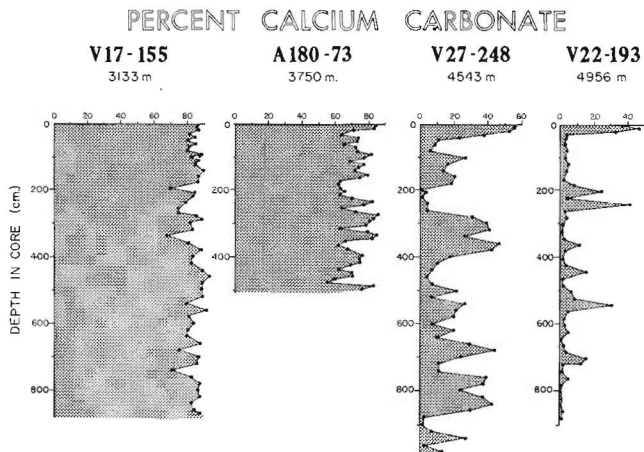
to shed more light on the problem. Carbonate curves representing complete climatic cycles can be used to compare complete glacial-stage carbonate deposition with interglacial carbonate accumulations.

## INTERPRETATION OF CALCIUM CARBONATE ANALYSES

The character of a carbonate curve can reflect any one or a combination of: (1) carbonate productivity changes, (2) carbonate dissolution, and (3) dilution by noncarbonate material, both terrigenous sediments and siliceous organisms. Obviously, carbonate productivity, the production of Coccolithophoridae, and planktonic foraminifers, in the surface- and near-surface waters, play a role in regulating the amount of carbonate material accumulating on the ocean floor. Likewise, siliceous productivity will ultimately affect sediment composition, as will noncarbonate sedimentation.

Arrhenius (1952), Olausson (1965), and Berger (1970, 1971) all suggested that dissolution can result from the bacterial reduction of organic material deposited on the ocean floor. This process liberates CO<sub>2</sub> into the bottom waters making the waters more corrosive to carbonate. This mechanism should act both penecontemporaneously and post-depositionally. Therefore, the preservation of carbonate may be a function of the amounts of organic material originally deposited and the amount of benthic activity on and within the sediments. Also, bottom waters charged with CO<sub>2</sub> collected along its journey, together with very cold temperatures and high hydrostatic pressures, can cause both penecontemporaneous and post-depositional dissolution of carbonate material (Olausson, 1965; Berger, 1970).

Calculations can be made of the amount of time a planktonic foraminiferal test spends in the water column versus the time spent resting on the bottom directly exposed to bottom water. Estimates have been made varying from a few days to a few months (Langhus, 1970; Berger and Piper, 1972) for the time it takes a planktonic foraminiferal test to free-fall without interruption to the ocean floor once the organism discards its test or dies. If the test is 0.1 mm thick, for instance, and the accumulation rate is 3 cm/10<sup>3</sup> yrs., that test will rest on the sea floor exposed directly to bottom water for more than 3 years before it is covered completely. This would suggest that the time a test is in direct contact with bottom water is essentially all spent resting on the bottom. Consequently, post-depositional dissolution could be the important carbonate-reducing mechanism. Of course once covered, the tests would



TEXT FIGURE 3

Carbonate curves from cores of progressively deeper depths showing the changing character of the carbonate.

still be susceptible to dissolution related to decay of organic matter, to corrosive interstitial waters, and sediment overturn by bioturbation.

By looking at cores from increasingly deeper water depths and comparing their carbonate concentration, it is seen that the relative importance of productivity, dissolution, and dilution must vary (text fig. 3). Shallow cores, such as V17-155, have very high carbonate values (80 percent) with very small variations. The character of the curve is rather nondescript; no easily recognizable zones are present. The planktonic forams show no signs of dissolution (test fragmentation, lack of spines on spinose species, concentration of dissolution-resistant species at the expense of dissolution-susceptible species, high percentage of benthic forams). Deeper in a basin, but still above the abyssal plain level, the carbonate curves begin to look like that represented by A180-73 in text figure 3. The amplitude of the carbonate cycles increases but the average carbonate value decreases. Microscopically, there is still very little evidence of dissolution. Deeper yet, the curves begin to show zones with carbonate values below 10 percent, but the maximum values still approach 50 percent. Cores such as V27-248 show evidence of moderate to severe dissolution in the low-carbonate zones but only slight to moderate dissolution in high-carbonate zones. Still deeper, curves of the type represented by V22-193 are found. This type shows very little high-frequency oscillation in the low-carbonate areas, which are consistently below 10 percent. The higher carbonate zones are narrow spikes which

approach 40 percent carbonate. The low-carbonate zones show massive planktonic foram test fragmentation, to the point where it is difficult to find 50 complete specimens in a standard 2-gm sample. This gradation of carbonate with depth must be in part the result of increasing dissolution.

Cores from the basins, such as V27-248 and V22-193, show the effects of dilution by terrigenous material and dissolution of the carbonate components. Dissolution is much stronger in the low-carbonate zones, as shown by extensive fragmentation of foraminiferal tests. These two factors work together to accentuate the carbonate highs and lows. The very deep cores, represented by V22-193 at 4,956 meters, show the effects of severe dissolution (almost total test fragmentation and concentration of only a few of the most dissolution-resistant species) in the low-carbonate zones and strong dissolution (abundant test fragmentation) in the carbonate highs. Dilution also affects these very deep cores, but, because they lie far out in the basin, the terrigenous component is very fine grained and thus seems to preclude thick accumulations; the average accumulation rates are only around 4 cm/10<sup>3</sup> years.

Twenty-one carbonate curves are shown in text figures 4A to F, grouped together according to physiographic provinces (see text fig. 5). The cores have been zoned biostratigraphically using the planktonic foram zonation of Ericson and others (1961). Immediately it can be seen that all of the cores taken from depths below 4,000 meters show quite similar carbonate responses; generally less than 10 percent carbonate in the glacial stages and 30–40 percent carbonate in the interglacial stages. Cores taken above 4,000 meters depth also show somewhat similar carbonate patterns to each other, but with a more uniform 60–80 percent carbonate.

Each of the carbonate curves represents at least the last 200,000 years of continuous depositional history, with the one exception of V26-46, the core with a hiatus in the Y zone, and each curve can be correlated in detail with other curves in its bathymetric province, as well as correlated from one province to another. Correlations of the finer details with Pleistocene climatic events has been demonstrated in another paper (Gardner, 1973).

#### SEDIMENTATION IMPLICATIONS

In order to analyze the influence of the sediment components that result in a carbonate value for any given point on a carbonate curve at least three variables

A.

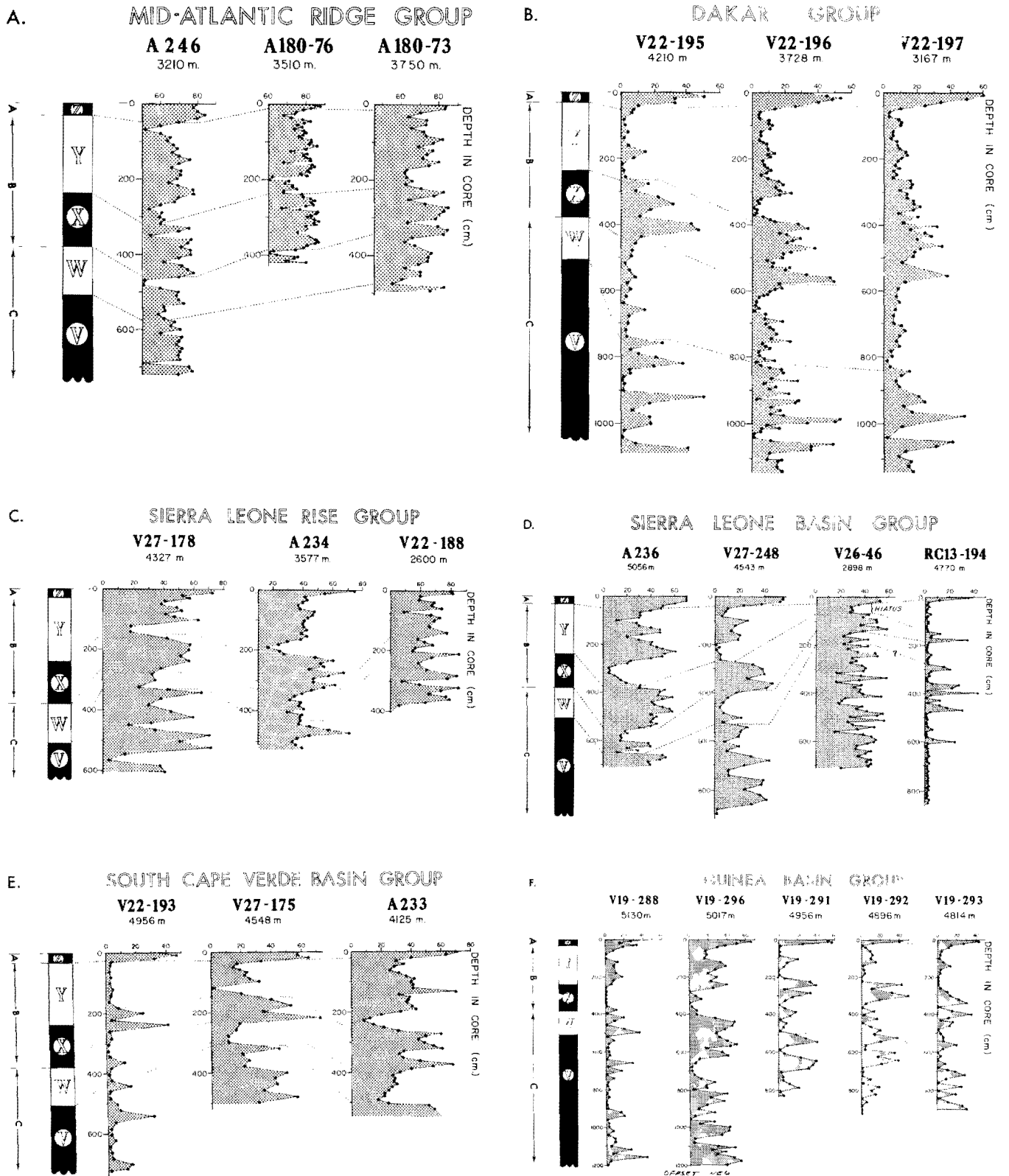


C.



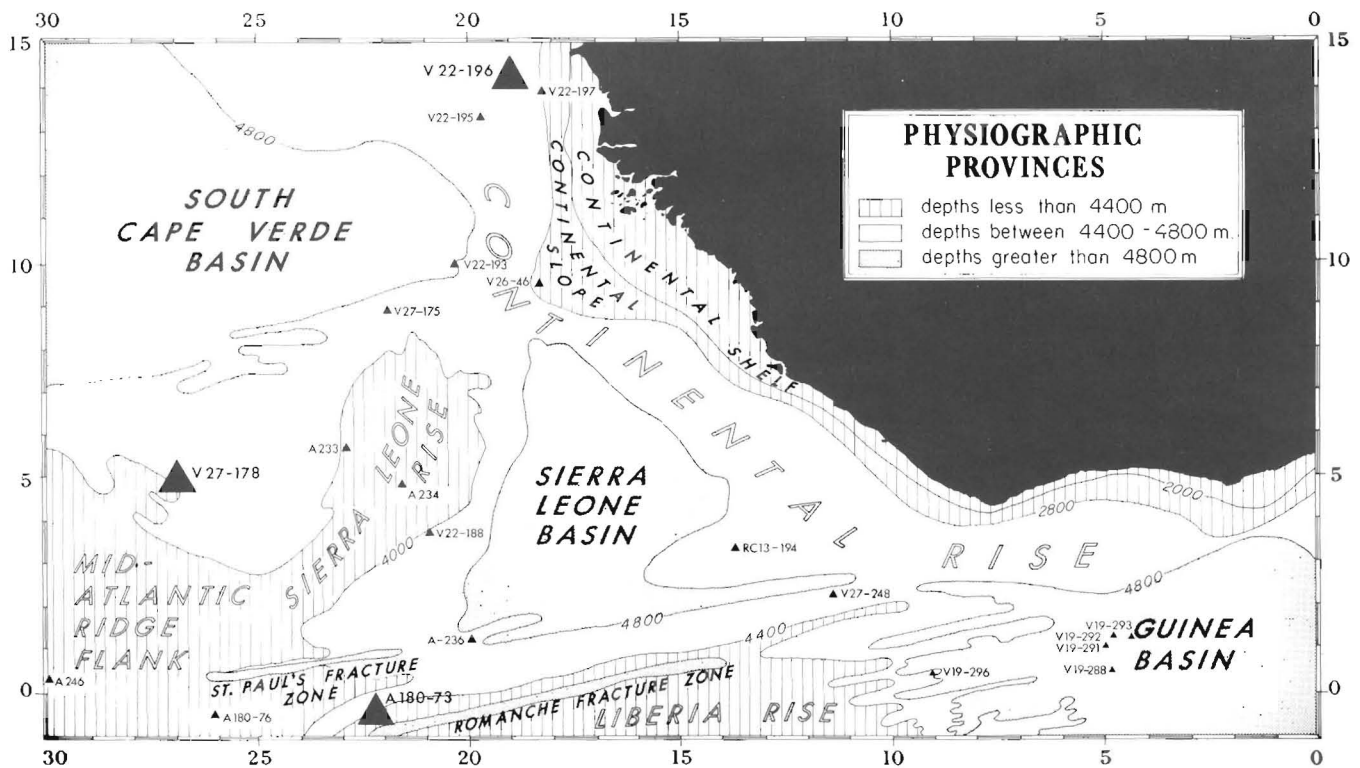
E.





TEXT FIGURE 4

Carbonate curves from selected physiographic provinces in the eastern equatorial Atlantic. For core locations see text figure 5.



TEXT FIGURE 5

Location of the three cores used for the 200,000-year record.

must be considered: (1) noncalcareous dilution, (2) carbonate dissolution, and (3) biogenic productivity. All three could have varied independently with time. Because there is no a priori reason to hold any one of these three constant, a quantitative determination of the effects of each variable is not possible with the present data available. However, a qualitative indication of whether one of two extremes can account for the reduced glacial carbonate values is possible. If productivity changes are considered negligible (only for simplification), carbonate reduction is possible through increased noncarbonate material (dilution) or by loss of carbonate material (dissolution). If these two methods are looked at as end-member extremes, they can each be analyzed independently.

In order to establish a framework for reference, the ratio of the time duration represented by the climatic zones is used. The value  $Y:X$  (time) is 1.23 and that for the  $W:X$  (time) is 0.91. If the carbonate values of the glacials were reduced only by input of noncalcareous material, the ratio of the core length of the

$Y$  zone relative to the  $X$  should exceed 1.23 and the  $W:X$  (length) should be greater than 0.91. If dissolution was the sole process, the ratios should be less than 1.23 and 0.91, respectively. Table 1 shows the results of this comparison. These results show that only four cores have shortened  $Y$  sections, i.e., only four cores could possibly be explained by dissolution alone. The remaining cores have glacial sections longer than a 1:1 relationship to the  $X$  zone. These could possibly be explained by dilution alone.

To investigate these two extremes further, quantitative determinations can be made on the amount of carbonate loss or noncarbonate gain necessary to reduce the carbonate by the observed amount. Dilution has been suggested as the major contributor to the carbonate character in equatorial Atlantic cores (Ruddiman, 1971; Hays and Perruzza, 1972). If the assumption is made that all the variations in calcium carbonate content in a core are the results of dilution of a uniform supply of carbonate by a noncalcareous material, a calculation can be made as to the amount of additional

TABLE 1

A and B: Comparisons of the ratios of the lengths of the Y and W glacial zones to the X interglacial zone. If  $A > 1.23$ , then dilution > dissolution (\* indicates these cores); if  $A < 1.23$  then dissolution > dilution. For the W zone  $B = 0.91$  and the same balance between dissolution and dilution holds as for A;  $B > 0.91$  the W zone accumulation rate exceeds the X zones. C and E: the percent gain of noncarbonate material necessary to account for the observed carbonate curve for Y and W zones and, D and F: the percent loss of original carbonate to account for observed carbonate curve for Y and W zones.

Depth Corrected	Core	A	B	C	D	E	F
		Ratios of Lengths of Y and W to X zone		Y-X % Addition	Y-X % Loss	W-X % Addition	W-X % Loss
		Y:X	W:X				
5130 m	V19-288	1.94	0.88*	547	83.4	970	91.7
4956 m	V19-291	1.95	2.21	1112	93.5	635	87.1
4896 m	V19-292	2.39	1.67	1800	96.0	1050	92.0
4814 m	V19-293	2.25	2.42	879	97.1	879	91.1
5017 m	V19-296	1.84	0.88	156	62.0	800	88.0
4770 m	V22-195	1.23*	1.77	1521	93.5	1521	93.5
4819 m	V22-196	1.84	1.26	800	90.0	800	90.0
4890 m	V22-197	1.88	1.55	451	81.6	451	81.6
3750 m	A180-73	1.71	1.16	123	55.2	262	72.5
3510 m	A180-76	1.53	—	183	45.5	—	—
3210 m	A246	1.21*	0.86*	150	34.6	113	53.8
5065 m	A236	1.88	0.62*	207	51.7	314	76.0
4543 m	V27-248	1.92	1.16	423	81.2	924	87.5
4770 m	RC13-194	2.60	1.80	2540	97.1	2540	97.1
2898 m	V26-46	—	0.45*	—	—	250	97.6
4327 m	V27-178	1.00*	0.64*	162	38.0	221	69.0
2600 m	V22-188	0.75*	0.62	191	47.5	136	57.7
3577 m	A234	1.91	0.91	194	66.2	244	70.7
4548 m	V27-175	1.50	1.00	867	89.0	1431	93.2
4125 m	A233	1.84	0.85*	839	34.0	200	68.0
4956 m	V22-193	2.22	2.58	3150	97.6	3150	97.6

noncarbonate material necessary to reduce the carbonate percentages. The formula:

$$A = [(C_i/C_f) - 1]/N_i$$

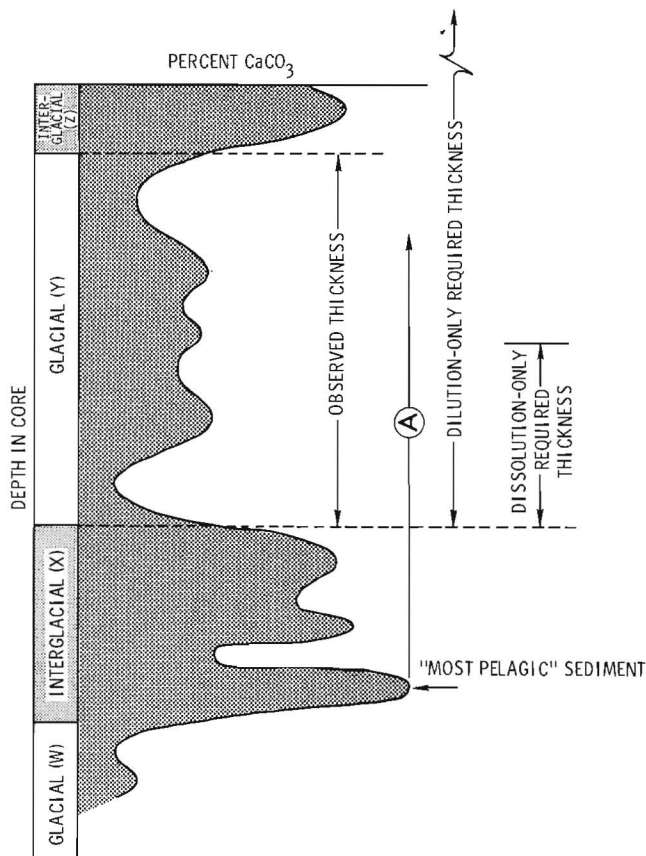
calculates A, the additional percentage increase of noncarbonate material necessary to reduce the initial carbonate value  $C_i$  to the final value  $C_f$ .  $N_i$  is the initial noncarbonate percentage. The initial carbonate value was always taken as the highest value obtained in the X zone. The rationalization for this is that the highest carbonate value must represent the most pelagic condition with the least amount of nonbiogenic input. Therefore, decreases from this "most pelagic condition" (text fig. 6) represents some modification of this sediment. The results (columns C and E in table 1) show that from as little as 1.23 to 31 times more noncarbonate is needed than is found to account for the fluctuations. Although most of the cores shows an addition to the sediment (column  $A > 1.23$ ;  $B > 0.91$ ), in only a few cases is the Y zone twice the normalized thickness ( $A > 2.46$ ;  $B > 1.82$ ). Therefore, although noncal-

careous dilution undoubtedly increased, a model using only dilution predicts glacial sections much larger than those observed (columns C and E).

The opposite extreme is a model using only calcareous dissolution, with no dilution. For these calculations a formula suggested by Berger (1971) can be used

$$L = [1 - (N_i/N_f)]/C_i$$

where the loss of initial carbonate, L, necessary to increase the initial noncarbonate value  $N_i$  to  $N_f$  is calculated. Columns D and F in table 1 shows that a range of from 34 percent to more than 97 percent of the original carbonate must be dissolved to account for the carbonate decreases. Several cores show a ratio of Y:X indicating a shortened glacial section ( $A < 1.23$ ;  $B < 0.91$ ) but the values of the ratios are not less than half of the time ratio. Therefore, although dissolution is indicated, it cannot account for all the variations in carbonate. The two factors, dilution and dissolution, must have worked together. The two end member models are summarized in text figure 6.



TEXT FIGURE 6

Generalized equatorial Atlantic carbonate curve showing graphically the dilution-only and dissolution-only models to explain observed carbonate. The line A represents carbonate content expected if sediments would have accumulated unchanged from the "most pelagic" time.

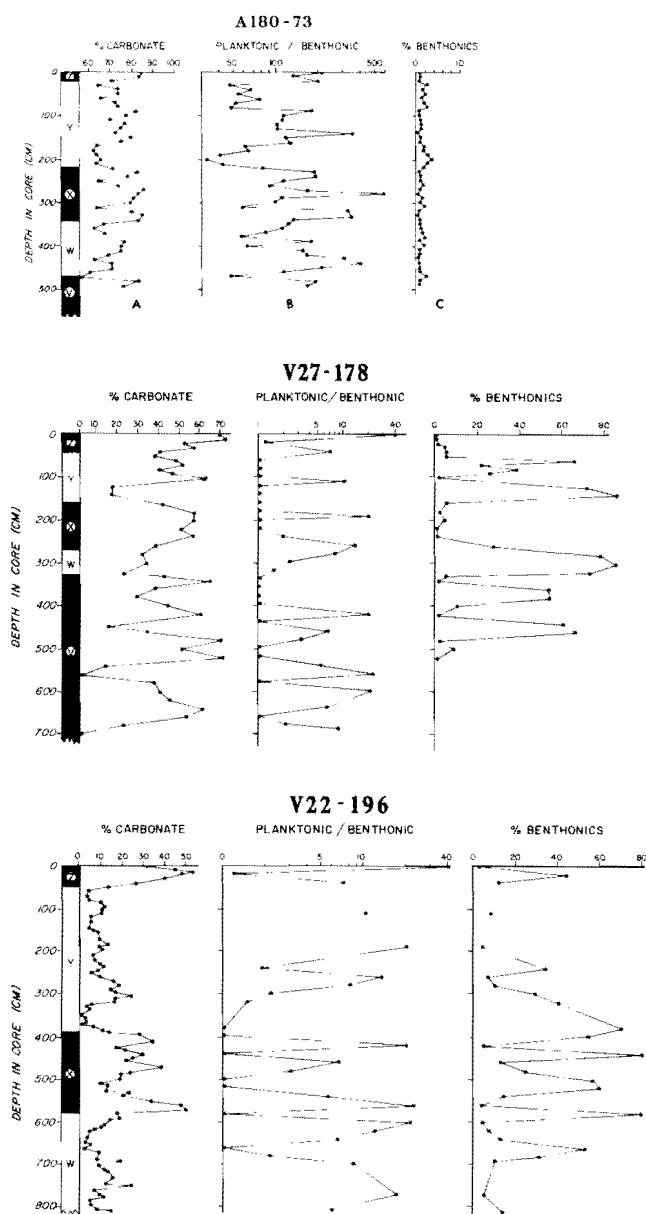
Additional information on dissolution was found when the foraminiferal faunas were analyzed. The initial indications of dissolution in any sample are found while the foraminifers are being identified. Test fragmentation and corrosion are readily apparent at this time. Qualitatively, test fragmentation appears as separate individual chambers, such as those of *Globigerinoides sacculifer*, loose in the sample, broken individuals of the *Globigerinoides* genera, and as only keels or as holes in the tests of globorotalids. With increased dissolution the fragments become smaller, much more numerous, and increasingly difficult to assign to a species. Any quantification of fragmentation is hampered because the number of fragments an individual breaks into is, of course, quite variable. Dissolution also appears as an increase in the benthonic foraminifers

in any given sample. Two or three benthonics are typical for analyses of the very well-preserved trigger-weight core tops within the region of the study, but in the dissolved samples this number increases by at least an order of magnitude. These three indications, test corrosion, fragmentation, and increased benthonic foraminifers, seem to be the most reliable qualitative indices for dissolution.

Attempts have been made to quantify the effects of dissolution. Planktonic-to-benthonic ratios have been used to indicate the degree of dissolution in any given sample (Oba, 1969; Parker and Berger, 1971). Test fragmentation by dissolution reduced the numbers of the more fragile planktonic foraminifers retained on a given sieve size. The tests of benthonic foraminifers, being much more compact and robust than the tests of planktonic foraminifers are less susceptible to fragmentation. This difference results in the increased proportion of benthonic foraminifers relative to planktonic foraminifers in samples which have been subjected to dissolution.

Other parameters have been suggested, notably by Berger (1971), which include ratios of spinose to non-spinose species and enrichment of resistant species relative to a nondissolved standard fauna. These may be good indices for studying surface faunas in an oceanographically stable area such as a central gyre but difficulties arise as different water masses move into an area with time. These water masses bring in new faunas whose ratio of spinose to nonspinose or resistant to non-resistant species differ from those occurring there today (see, for example, Bé and others, 1971). To further complicate the picture, these new faunas can be a combination of those found today, such as a transitional and a tropical fauna mixed, as might be found in an area with seasonal differences or a submerged assemblage (Gardner, 1973). Thus, through vertical stratification or seasonal fluctuations of faunas, these indices can change considerably even in the absence of any dissolution. Water masses did fluctuate with time in the tropical Atlantic (Gardner, 1973; Gardner and Hays, in press; Prell and others, in press), consequently Berger's methods are not applicable to this region.

The dissolution indicators used in this study, ratios of planktonic to benthonic foraminifers and the percentage of benthonics to the total foraminifer count, are used together. To demonstrate these relationships, the results from three cores are presented here. Plots of these two ratios, the carbonate curve and stratigraphic zonation are shown in text figures 7A to C. Although the planktonic-to-benthonic ratio for A180-73 shows



TEXT FIGURE 7

The carbonate, planktonic-to-benthonic ratio, and percent benthonics curves for cores A180-73, V27-178, and V22-196.

high-amplitude oscillations the actual values are more important. Out of an average total count of 385 (high of 856 and low of 305) the highest benthonic count was 13 in a count of 429, the lowest was 0 from a count of 344, and the average was 4 per sample. The paucity of benthonics means that an increase of only one or two individuals greatly reduces the ratio. This is the reason for the high-amplitude oscillations in text figure

7A. A clearer picture of dissolution is seen in the plot of percent benthonics per total foraminifers. The highest value is 3 percent which represents the 13 benthonics in a count of 429. When these two indices are compared to the carbonate curve there is a good correlation with planktonic-to-benthonic ratio but only a hint of a correlation with the percent benthonics. In the glacial portions of this core very minor dissolution could well have occurred. Alternate explanations for the small variations in the number of benthonics encountered are differences in the splits made from the bulk sample or productivity changes in planktonic and/or benthonic foraminifers with time. Indeed, if the increase in benthonics from a nondissolved count of 1 or 2 individuals per 300 counts to 13 was the result of dissolution, 85 to 92 percent of the total foraminifers would have been dissolved. This clearly is not the case with the sample at 200 cm. The drop in abundances of *G. ruber* and *G. sacculifer* is more likely an actual ecological response. I conclude, therefore, that any dissolution effects in this core were slight.

Compare these above results with text figures 7B and 7C; plots of the same indices for cores V27-178 and V22-196. First, notice the change in scales. In A180-73 the range of the ratio of planktonic to benthonic foraminifers is 30 to 500 whereas in these other cores the range is from less than 1 to only 40. Likewise, the percent benthonic scale for A180-73 goes from 0 to 3 percent but for V27-178 and V22-196 it is from 0 to more than 80 percent. These data must also be looked at in light of the total counts made for each sample (table 2). The benthonic counts in cores V27-178 and V22-196 exceed that of A180-73. Cores V27-178 and V22-196 show evidence for much greater dissolution, but only in certain zones. It is readily apparent that those zones with planktonic counts less than 200 have very low planktonic to benthonic ratios and very high percent benthonics. The zones with indications of low dissolution correlate with the interglacial sediments (Z, X and V zones) and the zones showing high effects of dissolution correlate with the glacial zones (Y and W).

Almost all of the 16 cores examined showed extensive fragmentation of planktonic foraminiferal tests in the glacial zones but in many cores the interglacial zones were relatively well preserved. For instance, in those cores in table 1 which show shortened glacial sections (V22-195, V27-178, V22-188, and V27-175) all but V22-188 showed effects of dissolution. Taking V27-178 as an example of the others the effects of dissolution are especially evident in the carbonate depressions

TABLE 2

Counts of total planktonic and total benthonic foraminifers for cores A180-73, V27-178, and V22-196. Missed intervals in core V22-196 represent samples which contained no whole planktonic foram tests in the  $> 149\mu$  size fraction of a standard 2-gm bulk sediment sample.

Sample	Total Planktonic	Total Benthonic	Sample	Total Planktonic	Total Benthonic
A180-73					
0	856	4	250	352	3
10	407	3	260	368	4
20	401	2	270	315	2
30	382	8	280	599	1
40	469	7	290	342	4
50	333	6	300	420	4
60	467	6	310	358	6
70	312	6	320	359	1
80	439	9	330	351	0
90	362	2	340	396	3
100	461	4	350	367	3
110	333	3	360	332	3
120	514	5	370	346	4
130	314	3	380	341	6
140	359	1	390	364	2
150	353	3	400	311	5
160	380	3	410	313	2
170	484	8	420	338	2
180	321	5	430	310	1
190	324	7	440	404	1
200	416	13	450	432	2
210	337	8	460	339	3
220	568	7	470	338	7
230	380	2	480	584	3
240	387	2	490	340	2
V27-178					
0	310	1	238	386	5
12	442	4	262	244	94
22	323	4	282	51	182
32	281	15	302	11	67
42	466	23	325	46	128
55	430	25	332	550	29
62	116	223	342	399	9
72	431	124	362	60	69
82	327	212	382	83	99
92	315	112	402	452	51
102	345	9	422	322	6
125	42	106	442	130	197
142	8	51	462	69	130
162	358	19	482	389	8
183	422	10	502	443	41
202	487	25	522	376	6
222	313	3			
V22-196					
0	364	9	480	336	102
20	138	117	500	224	294
40	429	59	520	317	462
110	678	63	540	364	64
190	308	15	560	351	15

TABLE 2 (Continued)

Sample	Total Planktonic	Total Benthonic	Sample	Total Planktonic	Total Benthonic
240	44	23	580	44	171
260	695	50	600	661	30
280	503	61	620	391	32
300	211	89	640	339	51
320	194	131	660	226	255
380	49	118	680	174	79
400	233	275	690	342	39
420	384	19	770	303	17
440	52	216	810	471	78
460	366	54			

(text fig. 7B) at 50–100 cm; 120–150 cm; 260–340 cm. These zones correlate with intense glacial climates of 18,000, 73,000, and 135,000 YBP using the correlations and dates of Broecker and van Donk (1970). The lack of the very resistant *Globorotalia tumida* and *G. menardii*, among others, confirms these zones as glacial rather than interglacial. The other cores showing the effects of dissolution (V22-195 and V27-175) show the same pattern but the effects of dissolution are even more intense.

Throughout V22-188 however, almost no effects of dissolution appear. Foraminiferal tests show no evidence of fragmentation, benthonic foraminifers show no increases, and no increases occur in dissolution-resistant foraminiferal species at the expense of fragile forms. The only other cores that show minimal effects of dissolution are A180-73 and A180-76. The locations of the cores reveal that V22-188 was taken from water 2,600 meters deep, A180-73 from 3,750 meters and A180-76 from 3,510 meters. The remainder of the cores are all from depths in excess of 4,327 meters, the depth of V27-178.

As is shown in text figure 2, Antarctic Bottom Water today floods the entire eastern equatorial Atlantic below 4,250 meters at the equator and gradually dips to below 4,700 meters at lat 15°N. The top of this bottom-water mass can be traced by following the 1.9°C potential-temperature isotherm. During the glacial stages the dissolution level in the eastern equatorial Atlantic must have shoaled from its present depth (and presumably the X zone level as well) to somewhere between 3,750 meters and 4,327 meters. The most reasonable explanations are either that during the glacial stages the corrosive Antarctic Bottom Water mass thickened a few hundred meters to reach these shallower depths or that North Atlantic Deep Water was either altered or replaced by a lens of more corrosive waters, or possibly both.

The first model, increased production and circulation of Antarctic Bottom Water, has been suggested by numerous workers (Arrhenius, 1952; Olausson, 1960; Berger, 1968; Johnson, 1973; among others). With a global cooling it is probable that larger volumes of Antarctic Bottom Water were formed around Antarctica. Increased production would allow colder Antarctic Bottom Water to penetrate farther north than is found today. Indirect evidence for this is the discovery of Antarctic diatoms as far north as lat 10°N. in samples from the Y zone in cores from the Brazil Basin (L. H. Burckle, personal commun.). By contrast, Antarctic diatoms in Holocene sediments can be traced only to about lat 10°S. This indicates a glacial strengthening of the circulation of Antarctic Bottom Water which would allow colder waters to penetrate farther north. A portion of this colder water would funnel through the Romanche Fracture Zone as it does today, and possibly other fracture zones as well, and would flood the eastern basins. Not only might this glacial bottom water be colder than today's, but the increased generation of bottom water would cause the watermass to thicken. Thus, its corrosive effects would be more intense than during interglacial conditions and felt at shallower depths during glacial conditions.

An alternate model would involve generation of glacial North Atlantic Bottom Water such as proposed by Weyl (1968) and Olausson (1971). Evidence suggests that 17,000 YBP the sea-ice margin in the North Atlantic was situated at about lat 60° N. (McIntyre and others, 1972). If during glacial cooling a large proportion of the Norwegian Sea and northernmost North Atlantic became ice covered, then glacial-North Atlantic Bottom Water could form. This watermass would form much farther south than the present-day North Atlantic Deep Water and probably would be confined mostly to the eastern basins. The Azores Ridge is the only barrier that exists between lat 60°N. and the eastern equatorial Atlantic which could block a southward flow of deep water. Several narrow channels 4,400 meters deep through the Azores Ridge could have allowed some flow of deep water to reach into the eastern equatorial region. But at some point this glacial-age North Atlantic Bottom Water would meet glacial-age Antarctic Bottom Water. Two possible circumstances could result: either (1) the glacial-age North Atlantic Bottom Water flowed up over Antarctic Bottom Water or (2) under it. In either case the corrosive nature of the watermasses must have in-

creased which would increase carbonate dissolution at the shallower depths indicated by the sediments. Streeter (1973) and Schnitker (1974) presented data from North Atlantic benthonic foraminifers which suggest that in the North Atlantic a glacial-age bottom water mass, different in physical character from that of the interglacials, replaced the present-day bottom water. This replacement phenomenon was found as far south as lat 40° N. in the northeastern Pacific but no samples farther south were examined. Either an increased Antarctic Bottom Water or a glacial-age North Atlantic Bottom Water could have caused the dissolution effects found in the sediments and nothing in the data from this study indicates a preferred watermass.

## CONCLUSIONS

Carbonate analyses and sedimentological considerations, as well as faunal data from the eastern equatorial Atlantic, indicate:

1. Contrary to some reports, data from the eastern equatorial Atlantic suggest that carbonate dissolution is an active process today but that it was even more effective during the Pleistocene glacial stages.
2. Corrosive Antarctic Bottom Water is the agent causing carbonate dissolution today.
3. Stratigraphic sequences indicate that both dilution of carbonate sediments with noncalcareous terrigenous material and carbonate dissolution occurred but the relative proportion of each process is unknown.
4. The glacial-aged lysocline in the eastern equatorial Atlantic stood between 4,327 and 3,750 meters rather than the 4,500- to 4,750-meter depth found today.
5. The most reasonable models to explain increased carbonate dissolution during the Pleistocene glacial stages involves either increased production of northward-flowing AABW or the generation of a southward-flowing glacial-age North Atlantic Deep Water.

## ACKNOWLEDGMENTS

I wish to thank J. D. Hays and Andrew McIntyre who carefully reviewed and improved on an earlier portion of this manuscript, and Ansis Kaneps for discussions and a review of this manuscript.

This research was supported by: The CLIMAP Program, N.S.F. GX28671; core curating contracts, N.S.F. GA35454; and office of Naval Research, N00014-67-A-0108-6004. LDGO contribution no. 2132.

## REFERENCES CITED

- ARRHENIUS, G., 1952, Sediment cores from the East Pacific: Swedish Deep-Sea Exped. (1947-1948) Repts., v. 5, fasc. I, 89 p.
- BÉ, A. W. H., VILKS, G., and LOTT, L., 1971, Winter distribution of planktonic foraminifera between Grand Banks and the Caribbean: *Micropaleontology*, v. 17, no. 1, p. 31-92.
- BERGER, W. H., 1968, Planktonic foraminifera: selective solution and paleoclimatic interpretation: *Deep-Sea Research*, v. 15, no. 1, p. 31-43.
- , 1970, Planktonic foraminifera: selective solution and the lysocline: *Marine Geology*, v. 8, p. 111-138.
- , 1971, Sedimentation of planktonic foraminifera: *Marine Geology*, v. 11, p. 325-358.
- , 1973, Deep-sea carbonates: Pleistocene dissolution cycles: *Jour. Foram Research*, v. 3, no. 4, p. 187-195.
- BERGER, W. H., and PARKER, F. L., 1970, Diversity of planktonic foraminifera in deep-sea sediments: *Science*, v. 168, p. 1345-1347.
- BERGER, W. H., and PIPER, D. J. W., 1972, Planktonic foraminifera: differential setting, dissolution, and redeposition: *Limnology and Oceanography*, v. 17, no. 2, p. 275-287.
- BROECKER, W. S., 1971, Calcite accumulation rates and glacial to interglacial changes in oceanic mixing, *in* Turekian, K. K., ed., *Late Cenozoic glacial ages*: New Haven, Yale Univ. Press, p. 239-265.
- BROECKER, W. S., TUREKIAN, K. K., and HEEZEN, B. C., 1958, The relation of deep-sea sedimentation rates to variations in climate: *Am. Jour. Sci.*, v. 256, p. 503-517.
- BROECKER, W. S., and VAN DONK, J., 1970, Insolation changes, ice volumes, and the O<sup>18</sup> record in deep-sea cores: *Rev. Geophysics*, v. 8, no. 1, p. 169-198.
- CARLSON, T. N., and PROSPERO, J. M., 1972, The large-scale movement of Saharan air outbreaks over the northern equatorial Atlantic: *Jour. Appl. Meteorology*, v. 11, no. 2, p. 283-297.
- ERICSON, D. B., EWING, M., WOLLIN, G., and HEEZEN, B. C., 1961, Atlantic deep-sea sediment cores: *Geol. Soc. America Bull.*, v. 72, no. 2, p. 193-286.
- FOLGER, D. W., BURCKLE, L. H., and HEEZEN, B. C., 1967, Opal phytoliths in a North Atlantic dust fall: *Science*, v. 155, p. 1243-1244.
- GARDNER, J. V., 1973, The eastern equatorial Atlantic: sedimentation, faunal, and sea-surface temperature responses to global climatic changes during the past 200,000 years: Columbia Univ., Ph.D. Dissertation, 387 p.
- GARDNER, J. V., and HAYS, J. D., in press, The eastern equatorial Atlantic: sea-surface temperature and circulation responses to global climatic change during the past 200,000 years: *Geol. Soc. America Mem.*
- HAYS, J. D., and PERRUZZA, A., 1972, The significance of calcium carbonate oscillations in eastern equatorial Atlantic deep-sea sediments for the end of the Holocene warm interval: *Quaternary Research*, v. 2, no. 3, p. 355-362.
- HAYS, J. D., SAITO, T., OPDYKE, N. D., and BURCKLE, L. H., 1969, Plio-Pleistocene sediments of the equatorial Pacific: their paleomagnetic, biostratigraphic, and climatic record: *Geol. Soc. America Bull.*, v. 80, p. 1481-1514.
- HÜLSEMANN, J., 1966, On the routine analysis of carbonates in unconsolidated sediments: *Jour. Sed. Petrology*, v. 36, p. 622-625.
- JOHNSON, D. A., 1972, Ocean-floor erosion in the equatorial Pacific: *Geol. Soc. America Bull.*, v. 83, no. 10, p. 3121-3144.
- LANGHUS, B. G., 1970, Foraminiferal tests as sedimentary particles [abs.]: *Geol. Soc. America Abs. Ann. Mtg.*, p. 601.
- MCINTYRE, A., BÉ, A., BISCAYE, P., BURCKLE, L., GARDNER, J., GEITZENQUER, K., GOLL, R., KELLOGG, T., PRELL, W., ROCHE, M., IMBRIE, J., KIPP, N., RUDDIMAN, W., and MOORE, T., 1972, The glacial North Atlantic 17,000 years ago: Paleoisotherm and oceanographic maps derived from floral-faunal parameters by CLIMAP: *Geol. Soc. America Abs. Ann. Mtg.*, p. 590-591.
- MCINTYRE, A., KIPP, N., BÉ, A. W. H., CROWLEY, T., GARDNER, J. V., KELLOGG, T., PRELL, W. L., and RUDDIMAN, W. F., in press, The glacial North Atlantic 18,000 years ago: A CLIMAP reconstruction: *Geol. Soc. America Mem.*
- OBA, T., 1969, Biostratigraphy and isotopic paleotemperature of some deep-sea cores from the Indian Ocean: *Tohoku Univ. Sci. Repts.*, 2nd ser. (Geol.), v. 41, no. 2, p. 129-195.
- OLAUSSON, E., 1960, Description of sediment cores from the North Atlantic: *Swedish Deep-Sea Exped. (1947-1948) Rept.*, v. 7, no. 5, p. 229-286.
- , 1965, Evidence of climatic changes in North Atlantic deep-sea cores with remarks on isotopic paleotemperature analysis, *in* Sears, M., ed., *Progress in oceanography*: Pergamon Press, v. 3, p. 221-252.
- , 1967, Climatological, geochemical, and paleo-oceanographical aspects of carbonate deposition, *in* Sears, M., ed., *Progress in oceanography*: Pergamon Press, v. 4, p. 245-265.
- , 1971, Quaternary correlations and the geochemistry of oozes, *in* Funnell, B. M., and Riedel, W. R., eds., *The micropalaeontology of oceans*: Cambridge Univ. Press, p. 375-398.
- PARKER, F. L., and BERGER, W. H., 1971, Faunal and solution patterns of planktonic foraminifera in surface sediments of the South Pacific: *Deep-Sea Research*, v. 18, no. 1, p. 73-107.
- PHLEGER, F. B., PARKER, F. L., and PIERSON, J. F., 1953, North Atlantic foraminifera: *Swedish Deep-Sea Exped. (1947-1948) Repts.*, v. 7, fasc. 1, 122 p.
- PRELL, W. L., and HAYS, J. D., in press, Late Pleistocene faunal and temperature patterns of the Colombia Basin, Caribbean Sea: *Geol. Soc. America Mem.*
- PRELL, W. L., GARDNER, J. V., BÉ, A. W. H., and HAYS, J. D., in press, Late Pleistocene circulation and seasonality

- in the equatorial Atlantic and Caribbean Sea: Geol. Soc. America Mem.
- RADCZEWSKI, O. E., 1939, Eolian deposits in marine sediments, *in* Trask, P. ed., Recent marine sediments: Am. Assoc. Petroleum Geologists, p. 496–502.
- RUDDIMAN, W. F., 1971, Pleistocene sedimentation in the equatorial Atlantic: Stratigraphy and faunal paleoclimatology: Geol. Soc. America Bull., v. 82, no. 2, p. 283–302.
- SCHNITKER, D., 1974, West Atlantic abyssal circulation during the past 120,000 years: Nature, v. 248, p. 385–387.
- STREETER, S. S., 1973, Bottom water and benthonic foraminifera in the North Atlantic—glacial-interglacial contrasts: Quaternary Research, v. 3, p. 131–141.
- WEYL, P. K., 1968, The role of the oceans in climatic change: A theory of the ice ages: Meteorol. Mons., v. 8, no. 30, p. 37–62.
- WORTHINGTON, L. V., and WRIGHT, W. R., 1970, North Atlantic oceanographic atlas of potential temperatures and salinities in the deep water: Woods Hole Oceanog. Inst. Atlas Ser., v. II, p. 1–24.

# CaCO<sub>3</sub> SOLUTION IN THE TROPICAL EAST PACIFIC DURING THE PAST 130,000 YEARS

BOAZ LUZ<sup>1</sup> AND NICHOLAS J. SHACKLETON<sup>2</sup>

---

## ABSTRACT

Application of various micropaleontological techniques and  $\delta^{18}\text{O}$  stratigraphy to cores from the tropical east Pacific reveals the record of temporal variations in CaCO<sub>3</sub> solution intensity in the area. In general, the solution intensity increased approximately 115,000–65,000 years BP, but according to the location with respect to the lysocline the information registered in the cores varies. Below the lysocline the magnitude of the fluctuations in the solution intensity is large. Near the lysocline the changes are relatively small. The increased solution intensity results in higher relative abundance of resistant planktonic foraminifera, but does not have an apparent effect on the percent CaCO<sub>3</sub>. Above the lysocline effects of increased solution are evident only at the end of the high solution period, and as in the previous case, the magnitude of the fluctuations is small and the percent of CaCO<sub>3</sub> is not affected.

Comparison of the solution record of the equatorial Pacific with the record of CaCO<sub>3</sub> accumulation in high latitudes reveals that in general the solution intensity increases when more carbonate is deposited. There are some discrepancies however. The major changes in the solution occur several thousand years after the major changes in accumulation. It is theorized that the solution changes are driven by the variations in accumulation in the high latitudes, produced by climatic change. Since the amount of carbonate available for deposition in the ocean is limited, fluctuations in carbonate accumulation in the high latitudes are compensated by changes in the solution intensity. The timing discrepancy between the cause, climatic change, and the resulting solution may be due to the slow response time of the oceanic carbonate system.

---

## INTRODUCTION

During the last 130,000 years the earth's climate went from full glacial conditions to full interglacial and back again. Effects of the climatic fluctuations are evident in variations of the oceanic surface circulation as well as in changes of deep-sea circulation and chemistry. To shed light on the nature of climatic fluctuations, it is useful to compare variations in the deep

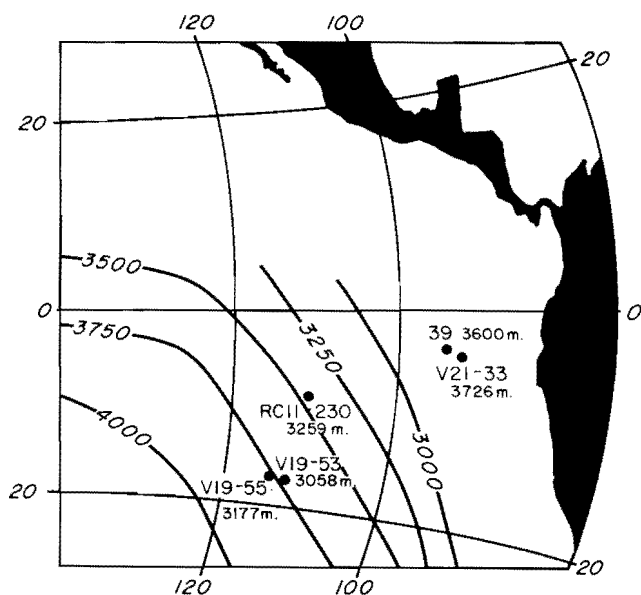
ocean to changes in climate. One of the most valuable records of changes in the deep ocean is found in calcareous sediments. Variations in the degree of carbonate dissolution are recorded in these sediments and reflect climatic-induced fluctuations of the oceanic carbonate system.

Variations in rates of CaCO<sub>3</sub> accumulation in Pleistocene sediments of the east equatorial Pacific were reported by Arrhenius (1952) and Hays and others (1969). The origin of these fluctuations was subject to different interpretations. Arrhenius suggested surface water productivity as a primary control over accumulation rates. High rates of accumulation were correlated with increased productivity during glacial times. However, his hypothesis was challenged by Broecker

---

<sup>1</sup>CLIMAP, Department of Geological Sciences, Brown University, Providence, Rhode Island 02912. Present address: Department of Geology, The Hebrew University of Jerusalem, Jerusalem, Israel.

<sup>2</sup>Sub-Department of Quaternary Research, University of Cambridge, Cambridge, England (International Corresponding Member, CLIMAP).



TEXT FIGURE 1

Depth of the lysocline map (after Parker and Berger, 1971) and core locations.

(1971), who suggested variations in rates of dissolution as an interpretation. Hays and others (1969) correlated the  $\text{CaCO}_3$  record with the climatic record of Atlantic cores and suggested as did Arrhenius (1952) that times of high  $\text{CaCO}_3$  accumulation are approximately in phase with glacial periods. The exact correlation, however, was yet to be documented.

The development of oxygen isotope stratigraphy has made it possible to obtain fine stratigraphic zonation within the Pleistocene, and we feel that the time is ripe for another attack on the problem of  $\text{CaCO}_3$  sedimentation in the equatorial Pacific. In the present study we aim at the following: (1) understanding the processes which control rates of carbonate accumulation; (2) timing the major changes in rates of accumulation and dissolution; and (3) placing some limits on magnitude of variations in rates of dissolution.

#### MATERIAL AND DATA

Core material analyzed by us is from the Lamont-Doherty Geological Observatory collection. Core locations and data sources are given in table 1. Locations of cores from the east equatorial Pacific are shown in text figure 1.

Counts of biogenic constituents were made on samples which contained more than 300 specimens greater

TABLE 1  
Core locations and data sources.

Core	Lat.	Long.	Depth (m)	Reference
V19-53	17°01'S	113°31'W	3058	This paper, Luz (1973)
V19-55	17°00'S	114°11'W	3177	This paper, Luz (1973)
V21-33	3°48'S	92°05'W	3726	This paper
RC11-230	8°48'S	110°48'W	3259	This paper, Luz (1973)
39	2°44'S	92°45'W	3600	Arrhenius (1952)

than  $250\mu$ .  $\text{CaCO}_3$  content was determined gasometrically by a technique described by Lohmann (1974). Oxygen isotope analysis was performed on *Globigerinoides sacculifera* in the case of V19-55 and RC11-230, and on *Globoquadrina dutertrei* in the case of V21-33.

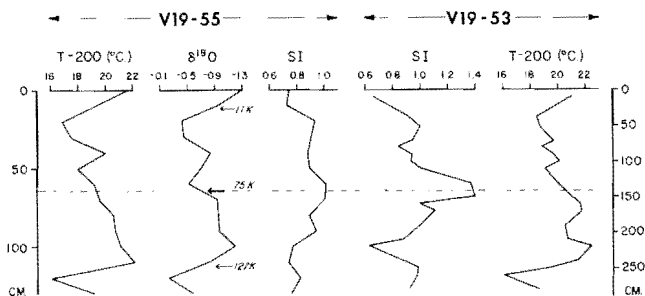
#### METHODS OF THE STUDY

Our chief objective is to obtain the record of dissolution variations in the tropical east Pacific during the past 130,000 years. In order to achieve this purpose it is necessary to have the following: (1) a means to evaluate the intensity of the  $\text{CaCO}_3$  dissolution process; and (2) a time scale down the cores studied.

#### DISSOLUTION INDICATORS

Parker and Berger (1971) have shown the usefulness of solution indexing in studying dissolution patterns on the floor of the South Pacific Ocean. A similar method can be applied in down-core study in order to obtain the record of dissolution variations. In calculating the solution index (SI), the solution ranking of Parker and Berger (1971) was used, and SI was calculated as described by Berger (1968). The solution indexing is based on the proportions of the different species in a planktonic foraminiferal assemblage. High values of SI indicate relative enrichment of an assemblage with solution resistant species. Where it is reasonable to assume that ecology is not the cause for down-core variations, SI indicates fluctuations in the intensity of  $\text{CaCO}_3$  dissolution.

SI is sensitive to variations in dissolution only where the down-core assemblages contain a mixture of solution resistant and solution susceptible species. Once that carbonate dissolution proceeds to a degree where all the solution susceptible species are eliminated, SI is no longer sensitive to any further change in dissolution. In this case the relative abundance of resistant faunal elements such as radiolarians and benthonic foraminifers are better indicators of the dissolution intensity.



TEXT FIGURE 2

Plots of SI (solution index), T-200 (an estimate of the paleotemperature at 200 m) and  $\delta^{18}\text{O}$  (with respect to Emiliani B1 standard) for cores V19-53 and V19-55. The cores are located several hundred meters above the lysocline (see text fig. 1). In both cores high SI values indicate increased solution around 75,000 years B.P.

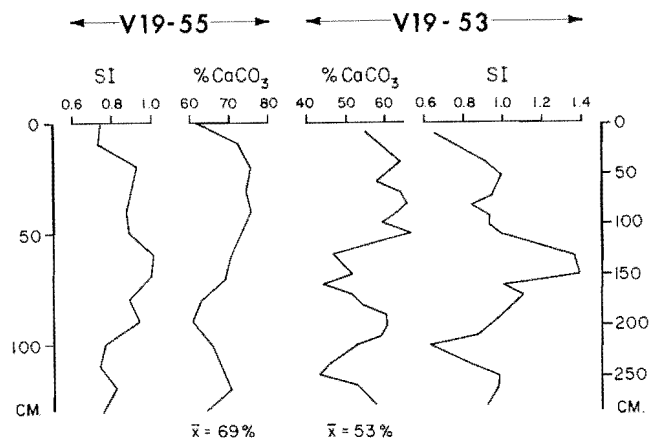
#### TIME SCALE

Our basis for correlation of the cores and timing of the changes in solution intensity is matching of  $\delta^{18}\text{O}$  curves. It has been shown that the primary control over  $\delta^{18}\text{O}$  fluctuations are global changes in glacial ice volume (Broecker and van Donk, 1970; Shackleton, 1967; Shackleton and Opdyke, 1973). In this case, the major fluctuations in isotopic composition took place simultaneously in various cores, and the  $\delta^{18}\text{O}$  curves provide a precise stratigraphic tool.

The time scale of Broecker and van Donk (1970) is adopted in this paper. According to this time scale the last interglacial began 127,000 years BP and ended 75,000 years BP. The termination of the last glacial occurred 11,000 years BP. These three events are easy to recognize in most  $\delta^{18}\text{O}$  curves produced for deep-sea cores. The events are indicated by arrows in text figures 2, 4, and 5, and are used in estimation of the age of the major changes in the solution intensity. If the time scale of Emiliani (1966) is chosen, it would be necessary to change the age estimates of the solution events and to correct the calculated rates of accumulation (text figs. 9 and 10) accordingly. It should be noted, however, that the correlation of the solution and the climatic changes would not be affected.

#### TEMPORAL AND SPATIAL VARIATIONS IN CARBONATE DISSOLUTION IN THE TROPICAL EAST PACIFIC

The cores selected for the present study (see text fig. 1) belong to three different categories. Cores which are located well above the lysocline (as mapped by



TEXT FIGURE 3

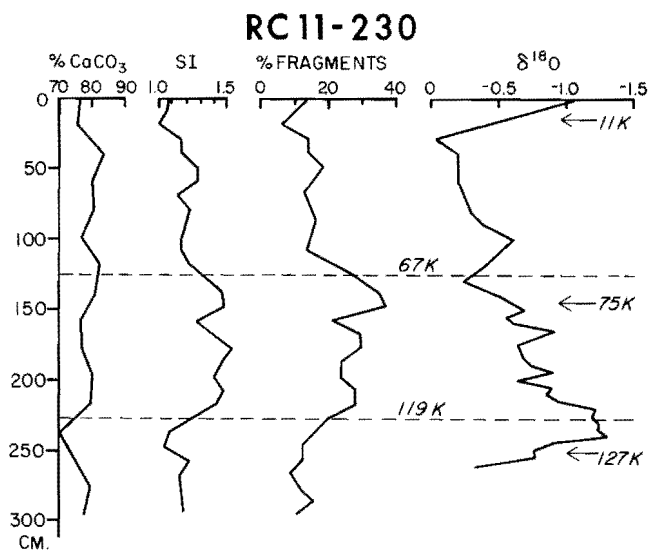
Plots of SI (solution index) and percent  $\text{CaCO}_3$  in V19-53 and V19-55. The cores are located several hundred meters above the lysocline (text fig. 1). Note the lack of correspondence between the carbonate content and the solution intensity.

Parker and Berger, 1971), near the lysocline, and well below the lysocline. The shape of the solution record and the effect of the solution on the sediment, depend on the location with respect to the lysocline.

#### THE CORES ABOVE THE LYSOCLINE

Two cores (V19-53 and V19-55) are located several hundred meters above the lysocline (text fig. 1).  $\delta^{18}\text{O}$  was determined only on V19-55, and correlation between the two cores is done by means of the foraminiferal index T-200 (from Luz, 1973). SI curves are plotted in text figure 2. These curves register considerable noise, but both show an indication for increased solution intensity around 75,000 years BP.

It is interesting to find out to what extent the concentration of calcium carbonate in the cores, is controlled by the changing solution intensity. SI and percent  $\text{CaCO}_3$  curves for V19-53 and V19-55 are plotted in text figure 3. Comparison of the curves reveals little or no correspondence between  $\text{CaCO}_3$  content and solution intensity. The cores V19-53 and V19-55 were raised from near the crest of the East Pacific Rise and the carbonate in this area is diluted by material derived from local volcanism (Bender and others, 1971; Bostrom and others, 1973). It seems that local sedimentary conditions and perhaps variations in the activity of the ridge account for most of the changes observed. In any case, dissolution variations seem to play only a minor role in shaping the percent  $\text{CaCO}_3$  curves.



TEXT FIGURE 4

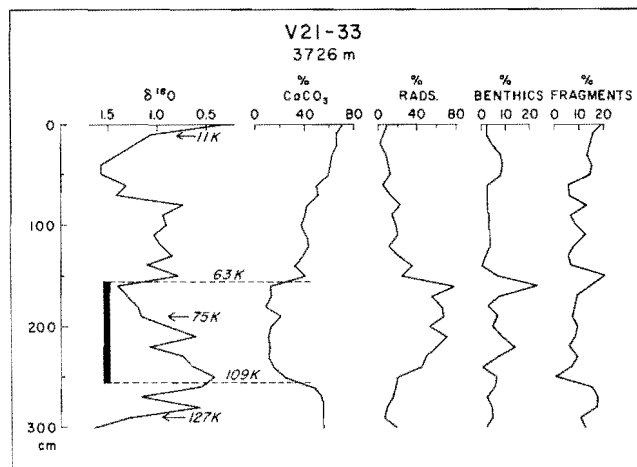
Plots of percent  $\text{CaCO}_3$ , SI (solution index), percent fragments, and  $\delta^{18}\text{O}$  with respect to the PDB standard in RC11-230. The core is located near the lysocline (text fig. 1). Note that the carbonate content is not affected by the changes in the solution intensity.

#### THE CORE NEAR THE LYSOCLINE

Plots of  $\delta^{18}\text{O}$  and SI for core RC11-230 are shown in text figure 4. Comparison of the curves shows that dissolution peaked up in intensity about 119,000 years BP, after the beginning of the last interglacial. The dissolution decreased in intensity about 67,000 years BP, after the end of the last interglacial. Comparison of the solution record with the percent  $\text{CaCO}_3$  curve (text fig. 4) does not reveal any correspondence. The percent  $\text{CaCO}_3$  is very uniform all the way down the core. The increased solution results in the destruction of fragile planktonic foraminifers, but the change in the amount of carbonate removed to solution is small, and not sufficient to cause the percent  $\text{CaCO}_3$  curve to fluctuate. It is worthwhile emphasizing that it is unlikely that the change in the foraminiferal assemblage reflects a change in the ecology. Luz (1973) has shown that only small variations in upper water conditions are registered in RC11-230, and those variations that are recorded do not correlate with the changes in carbonate solution intensity.

#### THE CORES BELOW THE LYSOCLINE

Core V21-33 is located several hundred meters below the lysocline (text fig. 1), and throughout its length it

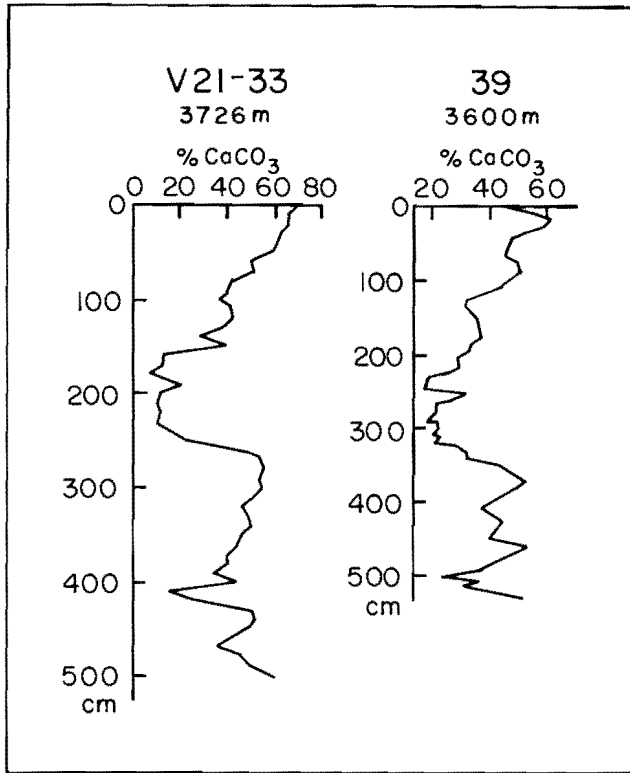


TEXT FIGURE 5

Plots of  $\delta^{18}\text{O}$  (with respect to PDB), percent  $\text{CaCO}_3$ , percent radiolarians, percent benthonic foraminifers and percent fragments in V21-33. The core is located below the lysocline (text fig. 1). Increased solution intensity is indicated in the carbonate-low interval, by relatively high abundance of radiolarians and benthonic foraminifers. The abundance of fragments in this core does not correspond to other dissolution indicators.

shows considerable dissolution effects. The planktonic foraminiferal assemblage consists almost entirely of one resistant species (*Globoquadrina dutertrei*) and its fragments. Since we are dealing with monospecific assemblage, SI is not sensitive to solution variations, and is not useful in this case. Radiolarians and benthonic foraminifers—both less affected by solution than planktonic foraminifers—fluctuate in abundance down the core. Their high abundance in the  $\text{CaCO}_3$ -low interval (text fig. 5) is judged to indicate increased solution. It seems that in this case the variations in solution intensity are large, and play an important role in shaping the percent  $\text{CaCO}_3$  curve. The abundance of fragments of planktonic foraminifers does not correspond to the solution intensity. It seems that in this core the rate at which whole shells fall apart into fragments is close to the rate at which other fragments are eliminated. Comparison of the percent  $\text{CaCO}_3$  curve with the  $\delta^{18}\text{O}$  curve shows that the reduction in carbonate content due to the increased solution occurred approximately between 109,000 and 63,000 years BP.

In several equatorial Pacific cores which have a complete record of the last 11,000 years, percent  $\text{CaCO}_3$  decreases near the top (Arrhenius, 1952; Hays and others, 1969). Such a decrease does not occur in V21-33, but is found in the nearby core 39 (text fig. 6).

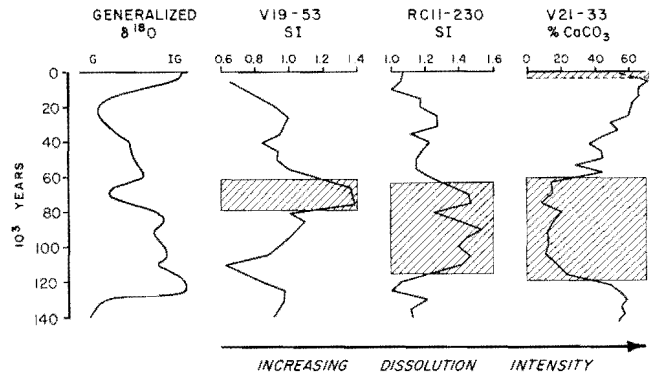


TEXT FIGURE 6

Plots of percent  $\text{CaCO}_3$  in cores V21-33 and 39 (after Arrhenius, 1952). Note that percent  $\text{CaCO}_3$  does not drop at the top of V21-33. It seems that the upper-most part of this core is truncated.

It seems that the top of V21-33 is truncated, but correlation with the  $\delta^{18}\text{O}$  curve (text fig. 5) indicated that the early part of the Holocene section is present, and that the decrease in percent  $\text{CaCO}_3$  occurs at the later part of the Holocene. It is possible that the late Holocene decrease in percent  $\text{CaCO}_3$  is a result of increased solution. However, more evidence has to be found before this matter can be decided.

To summarize, effects of changing carbonate dissolution are recorded in all the cores studied (text fig. 7). Dissolution increased during the period from about 115,000–65,000 years BP (based on information from both RC11-230 and V21-33). The change in solution intensity is significant in the cores below the lysocline, and produces percent  $\text{CaCO}_3$  fluctuations. Near the lysocline the same dissolution period is recorded, but the percent  $\text{CaCO}_3$  curve is not affected. Above the lysocline the effects are small, and increased solution is noticed only at the end of the period.



TEXT FIGURE 7

Correlation of the carbonate-solution record of three tropical east Pacific cores with a generalized  $\delta^{18}\text{O}$  curve. From left to right the cores are located progressively deeper with respect to the lysocline (see text fig. 1). The shading indicates zones of increased solution intensity. In general the solution increased approximately 115,000–65,000 years BP (based on information from RC11-230 and V21-33), but above the lysocline (V19-53) the effects of the increased solution were felt only at the end of this period. Carbonate solution plays an important role in shaping percent  $\text{CaCO}_3$  curves only below the lysocline (V21-33, and see text figs. 3–5).

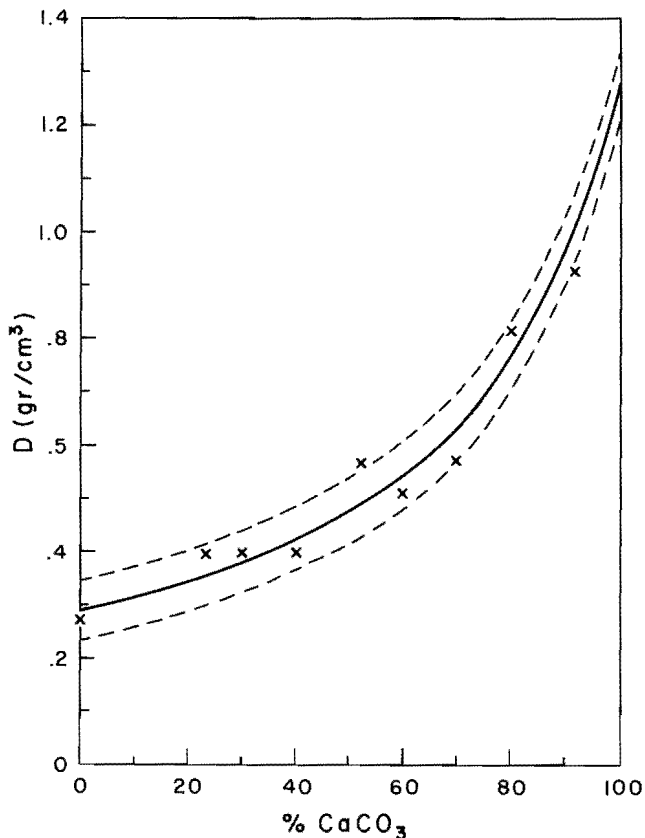
## RATES OF ACCUMULATION

Although solution indices can be used to indicate time intervals in which dissolution increased, these indices do not measure the actual change in the amount of material removed. In order to obtain some estimate of the magnitude of the change, it is useful to calculate absolute rates of accumulation for the time of high and the time of low solution intensity.

In order to calculate meaningful rates of accumulation of different sediment components, it is necessary to know the density of sediment. However, direct density measurements were not available, and for that reason we used estimates in the calculations. The following regression equation can be used to estimate the density from percent  $\text{CaCO}_3$ :

$$\hat{D} = \frac{1}{3.379 - 0.026 (\% \text{CaCO}_3)}$$

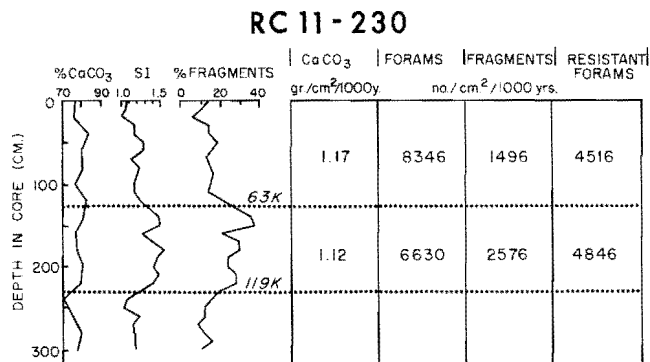
where  $\hat{D}$  is estimated dry weight (in gr) of one  $\text{cm}^3$  wet sediment. The equation is derived from data on equatorial Pacific sediments (from Arrhenius, 1952). A plot of density versus percent  $\text{CaCO}_3$  is shown in text figure 8. The linear correlation coefficient between the estimated density ( $\hat{D}$ ) and the observed density ( $D$ ) is  $R_{\hat{D},D} = 0.9723$ , and the standard error of estimate is  $SE = 0.0581 \text{ gr/cm}^3$ .



TEXT FIGURE 8

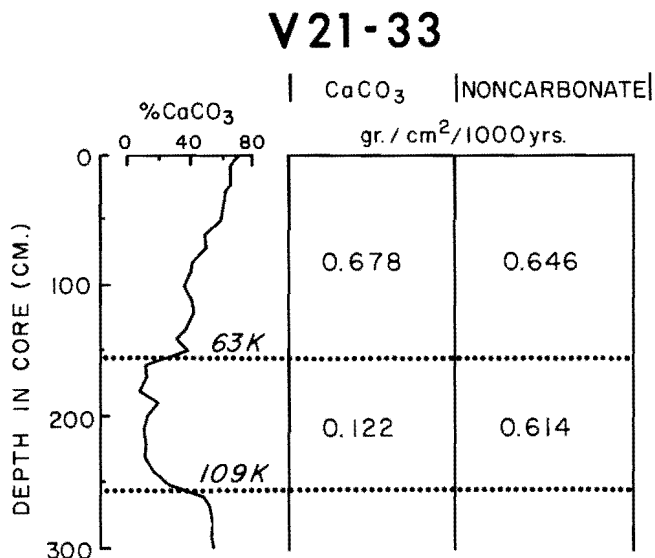
Sediment density (in gr dry sediment per cm<sup>3</sup> wet sediment) versus percent CaCO<sub>3</sub>. The solid curve is a plot of  $\hat{D} = \frac{1}{3.379 - 0.026 (\%CaCO_3)}$ . The dashed curves mark the 68 percent confidence interval. The data are from Arrhenius (1952).

The average rates of accumulation of calcium carbonate were determined in RC11-230 and V21-33 (text figs. 9 and 10). Assuming no change in the rate of shell output, the change in the rate of solution in RC11-230 was 0.05 gr/cm<sup>2</sup>/1000 years or about 4 percent. Calcium carbonate content is not sensitive to such a small change (Berger, 1971), and for that reason the percent CaCO<sub>3</sub> remains essentially uniform. While carbonate content does not change, the shells of fragile planktonic foraminifers are affected. It appears that the increased solution weakened the shells, which then fell apart and the absolute number of fragments increased. Note that the absolute abundance of the resistant foraminifers does not change significantly (text fig. 9).



TEXT FIGURE 9

Plots of percent CaCO<sub>3</sub>, SI (solution intensity), percent fragments and calculated accumulation rates for the low- and the high-solution periods in RC11-230. The core is located near the lysocline (text fig. 1) and the change in the rate of CaCO<sub>3</sub> solution is small. The increased solution approximately 119,000–67,000 years BP weakened the shells of fragile planktonic foraminifers and they fell apart into fragments (the accumulation of planktonic foraminifers decreased and the accumulation of fragments increased). Resistant planktonic foraminifers were not affected.



TEXT FIGURE 10

Percent CaCO<sub>3</sub> plot and calculated rates of accumulation for the low- and the high-solution periods in V21-33. The change in the rate of accumulation of CaCO<sub>3</sub> is large, while the change in the noncarbonate is relatively small. The core is located below the lysocline (text fig. 1) and the changes in the carbonate content and accumulation result from the variations in the solution intensity.

Arrhenius (1952) attributed the variations in carbonate accumulation in the equatorial Pacific to oscillations in carbonate production. However, in the light of the data from RC11-230, it seems that the rate of shell production is fairly uniform. As mentioned above, the rate of accumulation of the resistant foraminifers, which in this core are relatively unaffected by the solution variations, is close to uniform. If the rate of production did change, then the absolute abundance of the resistant shells would have shown variations.

Considerable change in dissolution rate is registered in V21-33, which is located several hundred meters below the lysocline. The change in this core was 0.556 gr/cm<sup>3</sup>/1000 years or 82 percent, enough to cause large fluctuations in the percent CaCO<sub>3</sub> curve. The change in carbonate content would have been even greater, but as shown in text figure 10, there is more dilution by noncarbonate material in the interval of low dissolution.

In conclusion, cores which are located deep enough are subjected to large fluctuations in dissolution intensity. On the other hand, shallow cores are subjected to relatively minor changes in CaCO<sub>3</sub> removal to solution.

## DISCUSSION

In the previous sections we have demonstrated that CaCO<sub>3</sub> dissolution intensity fluctuated in the tropical east Pacific; that large changes in rates of dissolution are registered only in cores located below the lysocline; and that the period from approximately 115,000 through 65,000 years BP saw increased solution intensity. Broecker (1971) and Berger (1973) have shown that the well-known carbonate cycles of the equatorial Pacific (Arrhenius, 1952; Hays and others, 1969) are controlled by solution variations. Peter Thompson (personal communication) finds that the relationships between  $\delta^{18}\text{O}$  and SI in west equatorial Pacific cores are similar to those found in RC11-230. Thus vast areas in the tropical Pacific were subjected to solution variations, and increased intensity occurred 115,000–65,000 years BP.

So far we have been concerned with documentation of the variations in the dissolution process. At this point we may ask why dissolution variations occur at all. Before trying to answer this question, it will be helpful to examine other parts of the world ocean where carbonate deposition occurs. It is widely known that the North Atlantic is a major trap of carbonate sediments, and it is reasonable to assume that variations in CaCO<sub>3</sub> sedimentation there would have significant effects on

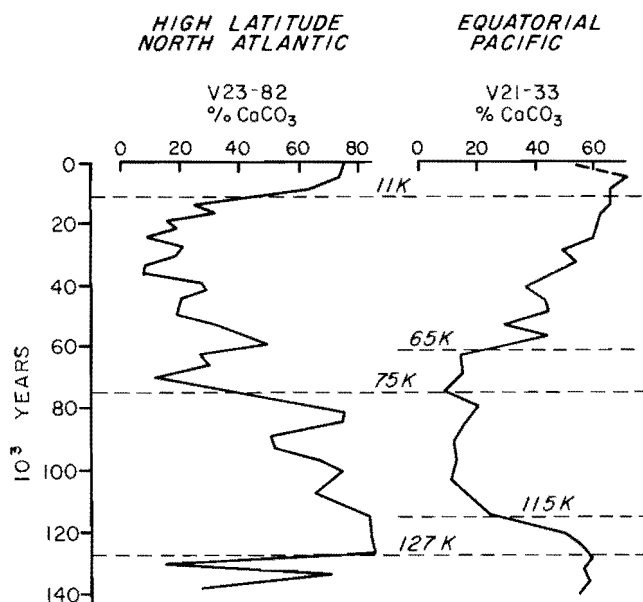
carbonate deposition elsewhere. Fluctuations in percent CaCO<sub>3</sub> are found in many North Atlantic cores, but the cause of the fluctuations is not always clear. Reading the literature on the North Atlantic (Berger, 1973; Broecker, 1971; Thiede, 1973; McIntyre and others, 1972; Olausson, 1971; Ruddiman, 1971; to mention only a few) results in much confusion. There is no agreement between the various authors about the mechanism that accounts for the changes in carbonate content, and about the timing of intensified solution.

Gardner (1974) shows that at least in some Atlantic cores there is strong evidence for increased carbonate solution during glacial maxima. He links high solution intensity to increased production of the Antarctic Bottom Water (AABW). As we have shown above, increased solution intensity in the Pacific occurred at different times, and thus it is not likely to be driven by the same cause. It seems that the Atlantic is favorably located to receive influence from past variations in AABW production, while the Pacific is not.

Broecker (1971) compiled data on various low- and mid-latitude North Atlantic cores. He has demonstrated that the accumulation rates of CaCO<sub>3</sub> do not change considerably from glacial to interglacial. This is judged to indicate that carbonate production rate there is relatively stable, and in this discussion we assume that production in the low- and mid-latitudes does not have much effect on global variations in CaCO<sub>3</sub> budget. In the high latitudes the pattern is different. Recent studies (Ku and others, 1972; McIntyre and others, 1972; Sancetta and others, 1972, 1973) have shown that large fluctuations occurred in the rate of production of CaCO<sub>3</sub>, in the high latitudes of the North Atlantic, and that production and climatic fluctuations are closely related. During times of relatively warm sea surface, production was high, and during the cold production was low. From 127,000 to 75,000 years BP CaCO<sub>3</sub> production was high, 75,000–11,000 years BP the production was low, and high production started 11,000 years BP and it continues today.

Another area of high calcium carbonate production—the Sub-Antarctic—seems to work in a much similar fashion. Hays and others (in press) have shown that large fluctuations in CaCO<sub>3</sub> accumulation occur in a belt to the north of the present position of the Antarctic Convergence. As in the high latitudes of the North Atlantic, these fluctuations are in step with the climatic changes. North of the belt of large fluctuations the rate of accumulation is relatively uniform.

In searching for an explanation for the variations in the solution intensity in the tropical Pacific, it is im-



TEXT FIGURE 11

Typical percent  $\text{CaCO}_3$  curves of the high-latitude North Atlantic (after McIntyre and others, 1972) and of the equatorial Pacific. In the North Atlantic the variations indicate primarily climatic induced changes in the production of  $\text{CaCO}_3$ . In the equatorial Pacific the variations result primarily from fluctuations in the carbonate solution intensity. Note that the changes in the solution occur after the changes in production. The ages of the solution changes are approximate and based on information from V21-33 and RC11-230.

portant to consider the total amount of carbonate available for deposition in the ocean. With limited carbonate supply, the variations in the accumulation rates in high latitudes, and perhaps solution variations in the Atlantic, are likely to have significant effects on the rate of  $\text{CaCO}_3$  dissolution in the deep Pacific. Comparison of percent  $\text{CaCO}_3$  curves from the high-latitude North Atlantic and from the equatorial Pacific is shown in text figure 11. As discussed above, the North Atlantic core records climatic-induced variations in calcium carbonate production, while the equatorial Pacific core records variations in solution intensity. In general, the two records correspond in such a way that increased high-latitude production matches with increased dissolution intensity, and vice versa. There are some discrepancies, however. The major changes in solution intensity at 115,000 and 65,000 years BP occur after the major changes in production (at 127,000 and 75,000 years BP). It appears then, that when more  $\text{CaCO}_3$  accumulates in the high latitudes, less is available for deposition in the equatorial Pacific, and since

$\text{CaCO}_3$  production rate in the equatorial Pacific remains essentially unchanged, compensation is achieved by increased solution rate. The response of the solution to the production changes is not instantaneous, and the solution lags several thousand years behind production.

In order to check whether the lag is a reasonable explanation, the response time of the oceanic carbonate system has to be known. Determination of the response time would involve fluxes and relaxation times of different components of the carbonate system, but this information is not yet available. Based on  $\text{CO}_3^{2-}$  content of sea water and the rate of  $\text{CaCO}_3$  accumulation, Broecker (1971) estimates 20,000 years as the response time of the carbonate ion in the ocean. If Broecker's estimate approaches reality, then the lag in the dissolution response to the driving production change would be reasonable.

## CONCLUSIONS

The duration and the intensity of calcium carbonate solution on the floor of the tropical east Pacific depend on the location with respect to the lysocline. Significant changes in the solution rate occur only below the lysocline. Above the lysocline, effects of increased solution are evident, but the changes in solution rate are minor and the duration of the high solution period shorter. Approximately 115,000–65,000 years BP the rate of solution increased, and the percent  $\text{CaCO}_3$  in deep cores was reduced.

$\text{CaCO}_3$  budget considerations suggest that the solution cycles of the equatorial Pacific are driven by climatic-induced fluctuations of the rate of  $\text{CaCO}_3$  accumulation in the high latitudes of the North Atlantic and in the Sub-Antarctic. However, it seems that the solution response to the fluctuations in the high latitudes is not instantaneous. The changes in carbonate solution occur several thousand years after the changes in carbonate accumulation, and it is possible that this timing discrepancy results from relatively slow response time of the oceanic carbonate system.

## ACKNOWLEDGMENTS

We thank W. S. Broecker and A. McIntyre for critically reading the manuscript and for helpful suggestions. Discussions with J. Imbrie, J. D. Hays, and T. J. Crowley were very stimulating. We also thank Peter Thompson for allowing us to quote his unpublished results. This research has been supported by NSF/IDOE grants GX-28671 (LDGO), GX-28672

(Brown), and GX-28673 (OSU). All the samples used in this study are from the Lamont-Doherty Geological Observatory collection, whose curatorial services and collection are funded by the Office of Naval Research and by the NSF contracts ONR (N00014-67-A-0108-0004) and NSF-GA-29460.

## REFERENCES

- ARRHENIUS, G., 1952, Sediment cores from the East Pacific: Swedish Deep-Sea Exped. (1947-1948) Repts., v. 5, p. 6-227.
- BENDER, M., BROECKER, W., GORNITZ, V., MIDDEL, U., KAY, R., SUN, S., and BISCAYE, P., 1971, Geochemistry of three cores from the East Pacific Rise: *Earth and Planetary Sci. Letters*, v. 12, p. 425-433.
- BERGER, W. H., 1968, Planktonic foraminifera: Selective solution and paleoclimatic interpretations: *Deep-Sea Research*, v. 15, p. 31-43.
- , 1971, Sedimentation of planktonic foraminifera: *Marine Geology*, v. 11, p. 325-358.
- , 1973, Deep-sea carbonates: Pleistocene dissolution cycles: *Jour. Foram. Research*, v. 3, p. 187-195.
- BOSTROM, K., KRAEMER, T., and GARTNER, S., 1973, Provenance and accumulation rates of opaline silica, Al, Ti, Fe, Mn, Cu, Ni, and Co in Pacific pelagic sediments: *Chem. Geology*, v. 11, p. 123-149.
- BROECKER, W. S., 1971, Calcite accumulation rates and glacial to interglacial changes in oceanic mixing, *in* Turekian, K. K., ed., *The late Cenozoic glacial ages*: New Haven, Yale University Press, p. 239-265.
- BROECKER, W. S., and VAN DONK, J., 1970, Insolation changes, ice volumes, and the O<sup>18</sup> record in deep-sea cores: *Rev. Geophysics Space Physics*, v. 8, p. 169-198.
- EMILIANI, C., 1966, Paleotemperature analysis of Caribbean Cores P 6304-8 and 6304-9 and a generalized temperature curve for the past 425,000 years: *Jour. Geology*, v. 74, p. 109-126.
- GARDNER, J. V., 1974, Late Pleistocene carbonate dissolution cycles in the eastern equatorial Atlantic *in* Sliter, W. V., Bé, A. W. H., and Berger, W. H., eds., *Dissolution of deep-sea carbonates*: Cushman Found. Foram. Research Spec. Pub. No. 13, p. 129-141.
- HAYS, J. D., SAITO, T., OPDYKE, N. D., and BURCKLE, L. H., 1969, Pliocene-Pleistocene sediments of the Equatorial Pacific: their paleomagnetic, biostratigraphic, and climatic record: *Geol. Soc. America Bull.*, v. 80, p. 1481-1514.
- HAYS, J. D., LOZANO, J., SHACKLETON, N. J., and IRVING, G., in press, An 18,000 years B.P. reconstruction of the Atlantic and Western Indian Sectors of the Antarctic Ocean, *in* Cline, R. M., and Hays, J. D., eds., *First CLIMAP*, *Geol. Soc. America Memoir*.
- KU, T. L., BISCHOFF, J. L., and BOERSMA, A., 1972, Age studies of Mid-Atlantic Ridge sediments near 42°N and 20°N: *Deep-Sea Research*, v. 19, p. 233-247.
- LOHMANN, G. P., 1974, Paleo-oceanography of the Oceanic Formation, Barbados, West Indies: Ph.D. dissertation, Brown University, Providence, R.I.
- LUZ, B., 1973, Stratigraphic and paleoclimatic analysis of late Pleistocene tropical southeast Pacific Cores (with an Appendix by N. J. Shackleton): *Quaternary Research*, v. 3, p. 56-72.
- MCINTYRE, A., RUDDIMAN, W. F., and JANZEN, R., 1972, Southward penetrations of the North Atlantic Polar Front; faunal and floral evidence of large-scale surface water mass movements over the last 225,000 years: *Deep-Sea Research*, v. 19, p. 61-77.
- OLAUSSON, E., 1971, Quaternary correlations and the geochemistry of oozes, *in* Funnell, B. M., and Riedel, W. R., eds., *Micropaleontology of the oceans*: Cambridge University Press, p. 375-398.
- PARKER, F. L., and BERGER, W. H., 1971, Faunal and solution patterns of planktonic foraminifera in surface sediments of the South Pacific: *Deep-Sea Research*, v. 18, p. 73-107.
- RUDDIMAN, W. F., 1971, Pleistocene sediments in the equatorial Atlantic; stratigraphy and faunal paleoclimatology: *Geol. Soc. America Bull.*, v. 82, p. 283-302.
- SANCETTA, C., IMBRIE, J., KIPP, N. G., MCINTYRE, A., and RUDDIMAN, W. F., 1972, Climatic record in North Atlantic Deep-Sea Core V23-82: Comparison of the last and present interglacials based on quantitative time series: *Quaternary Research*, v. 2, p. 363-367.
- SANCETTA, C., IMBRIE, J., and KIPP, N. G., 1973, Climatic record of the past 130,000 years in North Atlantic deep-sea core V23-82 with the terrestrial record: *Quaternary Research*, v. 3, p. 110-116.
- SHACKLETON, N. J., 1967, Oxygen isotopic analyses and Pleistocene temperature reassessed: *Nature*, v. 215, p. 15-17.
- SHACKLETON, N. J., and OPDYKE, N. D., 1973, Oxygen isotope and paleomagnetic stratigraphy of equatorial Pacific core V28-238: oxygen isotope temperatures and ice volumes on a 10<sup>5</sup> and 10<sup>6</sup> year scale: *Quaternary Research*, v. 3, p. 39-55.
- THIEDE, J., 1973, Planktonic foraminifera in hemipelagic sediments: shell preservation off Portugal and Morocco: *Geol. Soc. America Bull.*, v. 84, p. 2749-2754.

# DIFFERENTIATING DISSOLUTION AND TRANSPORT EFFECTS IN FORAMINIFERAL SEDIMENTS FROM THE PANAMA BASIN

CHIYE YAMASHIRO

School of Oceanography, Oregon State University, Corvallis, Oregon 97331

---

## ABSTRACT

Valid interpretation of sediment assemblages of planktonic foraminifera requires some knowledge of the filters through which the components have passed. Dissolution is the most important process modifying carbonate sediments and it would be useful to separate solution effects from the effects of the other major filter, lateral transport. Indices based on rankings or

foraminiferal species according to the ease of solution and settling velocity of their tests give no clear separation of transport and dissolution. Factor analysis and regression analysis show that whole foraminifera provide information about preservation and that different sizes of fragments, and therefore grain-size analysis, is a more useful indicator of sediment transport.

---

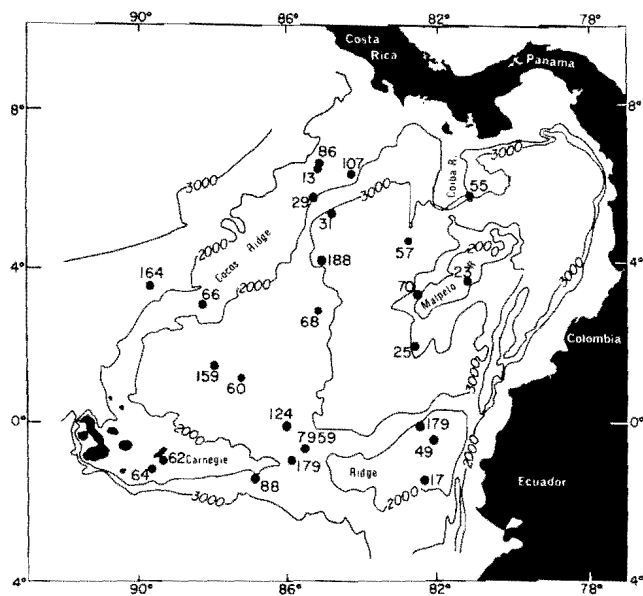
## INTRODUCTION

Where there are carbonate sediments on the ocean floor planktonic foraminifera can be useful sources of information about paleotemperatures, water masses, and surface and bottom circulation. In determining paleo-oceanic conditions from sediment assemblages one must consider the depositional history of the sedimentary components. Solution has long been recognized as a strong modifier of carbonate sediments (Murray and Renard, 1891), the obvious solution effects being a reduction in the final carbonate content and a lowering of total sediment accumulation rate. The solution effect on foraminifera is a weakening of the test as calcite is dissolved away. Berger (1967), Ruddiman and Heezen (1967), and Pytkowicz and Fowler (1968) explored solution effects on different species of planktonic foraminifera. Berger, in his extensive work on the sedimentation of planktonic foraminifera (especially 1968, 1970, 1971) has ranked the foraminifera on the basis of their resistance to solution.

That reworking by bottom currents is widespread

and important in determining the distribution and characteristics of sediment is now recognized. The effects of erosion, winnowing, lateral transport, and redeposition of sediment grains have been pictorially documented by Heezen and Hollister (1971) and discussed by Correns (1939), van Andel and Komar (1969), Johnson (1972), Kennett and others (1972), Watkins and Kennett (1972), Moore and others (1973), van Andel (1973), and Lonsdale and Malfait (in press). Berger and Piper (1972) determined that there is differential settling of foraminiferal species, implying that once deposited, some species can be more easily redeposited by bottom currents than others. Thus currents acting on foraminiferal sediment assemblages may winnow out lighter tests and create fragments from solution-weakened tests, and also enhance dissolution by replacing calcium carbonate saturated water next to tests with "fresh" undersaturated water.

This study attempts to differentiate these effects through analysis of selected components of a foraminiferal assemblage.



TEXT FIGURE 1

Bathymetry of the Panama Basin (contours in meters). Sample locations shown by dots, numbers are accession numbers in the Oregon State University marine sediment laboratory.

## OCEANOGRAPHY AND SEDIMENTATION OF THE AREA

The Panama Basin lies in the east equatorial Pacific in the arm of Central America and South America between lat 8°N. and 4°S. Its oceanic boundaries are the Cocos Ridge on the northwest and the Carnegie Ridge on the south. The oceanography of the area has been described by several authors including Wooster and Cromwell (1959), Wyrтки (1967), Forsbergh (1969), and Stevenson (1970). The waters are characterized by high productivity, much of it due to upwelling. Productivity is highest near the coastal margins and over the Carnegie Ridge (Moore and others, 1973). The basin has a south-north temperature gradient of 22–28°C. The salinity is a low 33.0 to 33.5 ‰, due to dilution by precipitation and runoff.

The sediments are dominated by biogenous components, except near the coast where terrigenous input is large. The distribution and character of the sediments are discussed by Kowsmann (1973), Moore and others (1973), van Andel (1973), and Heath and others (1974). These workers have concluded that dissolution and transport are important in determining the sediment characteristics in the basin.

TABLE 1

Ranking of common species with respect to settling velocities (A-fast ones first), and ease of solution (B-resistant ones first). (Data from Berger, 1968, and Berger and Piper, 1972, except \*-ranking according to morphological considerations.)

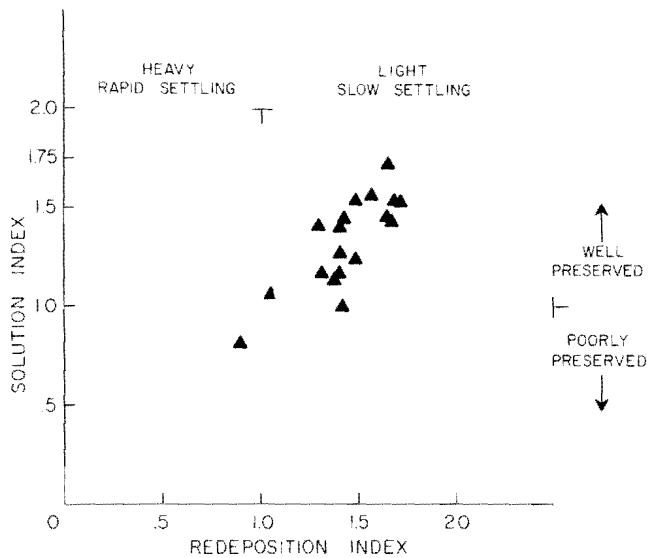
A	B
1. Globorotalia tumida	T. humilis
2. Pulleniatina obliquiloculata	G. tumida
3. Sphaeroidinella dehiscens	S. dehiscens
4. Globoquadrina conglomerata	P. obliquiloculata
5. Globorotalia inflata	G. pachyderma
6. Globorotalia crassaformis	G. dutertrei
7. Globigerina pachyderma	G. menardii
8. Globigerina falconensis	G. crassaformis
9. Globoquadrina dutertrei	G. inflata
10. Globigerinoides conglobatus	G. truncatulinoides
11. Globorotalia menardii	G. hirsuta
12. Globorotalia truncatulinoides	G. conglomerata
13. Globorotalia hirsuta	G. digitata
14. Globigerinoides tenellus	G. hexagona
15. Globigerinoides sacculifer	O. universa
16. Globigerinoides ruber	C. nitida
17. Globigerinella siphonifera	G. falconensis
18. Globigerina calida	G. iota
19. Globigerina bulloides	G. glutinata
20. Globigerina rubescens	G. calida
21. Globoquadrina hexagona	G. bulloides
22. Turborotalita humilis*	G. conglobatus
23. Globigerinita iota	G. sacculifer
24. Globigerinita glutinata	G. siphonifera
25. Orbulina universa	G. tenellus
26. Globigerina digitata	G. rubescens
27. Candeina nitida	G. ruber
28. Hastigerina pelagica	H. pelagica

## METHODS

### SAMPLES AND GRAIN COUNTS

The samples used in this study are the > 62 μ fraction of the tops of 25 cores from the collections of Lamont-Doherty Geological Observatory, Scripps Institution of Oceanography, and Oregon State University. Their locations and identifying numbers are shown in text figure 1. Appendix 1 contains a more complete sample description.

Each sample was separated into a > 177 μ fraction and a 62–177 μ fraction. Each size fraction was further divided with a microsplitter into subsamples of 300–1,200 grains. Species were identified following Parker (1962). In addition to whole foraminifera, globorotaliid and globigerinid fragments were counted. The counts of items used in this study are given in appendix 2.



TEXT FIGURE 2 A

Indices calculated for some Panama Basin samples after the method of Berger (1968).

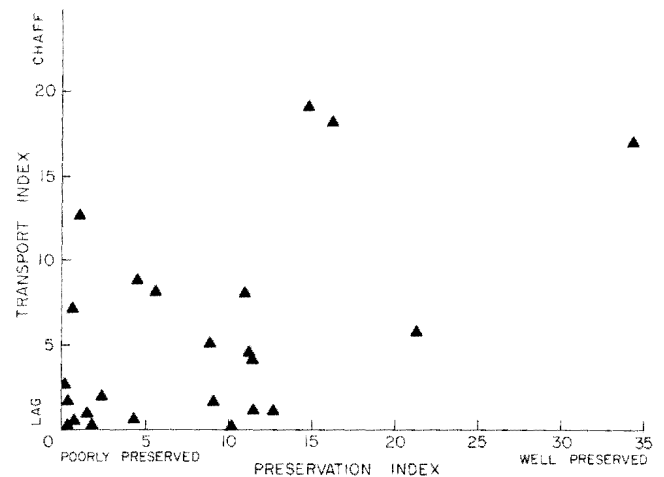
### INDEXING

In a previous study, Berger and Piper (1972) attempted to differentiate dissolution and transport by computing "solution" and "redeposition" indices based on ranking foraminiferal species according to the ease of solution and settling velocity of their tests (table 1). The indices are calculated in this manner: the products of species rank number multiplied by the percentage of the species are summed for a sample and divided by the median rank value (Berger, 1968). Unfortunately, there is a good correlation between the indices (text fig. 2A) because the fastest settling tests are commonly the most resistant to solution and the slowly settling tests the least resistant. Thus, sediment containing heavy resistant foraminifera may result from dissolution of less resistant tests and/or bottom currents winnowing out these lighter tests (Berger and Piper, 1972).

TABLE 2

Ranking of species with respect to ease of transport and ease of solution (A-light, non-resistant, B-heavy, non-resistant).

A	B
1. <i>G. iota</i> + <i>G. glutinata</i>	1. <i>G. conglobatus</i>
2. <i>O. universa</i>	2. <i>G. sacculifer</i> + <i>G. siphonifera</i>
3. <i>G. hexagona</i>	3. <i>G. tenellus</i>
4. <i>T. humilis</i>	4. <i>G. ruber</i>



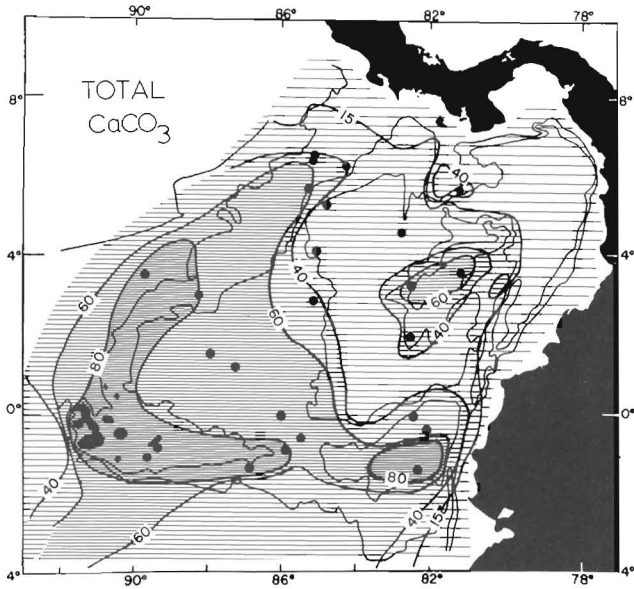
TEXT FIGURE 2 B

Indices calculated for Panama Basin samples according to this paper.

In an attempt to reduce this correlation, "heavy, non-resistant" and "light, resistant" species were selected from table 1 on the basis of greatest difference between solution and settling rankings and ecological considerations. For example, *Globigerinoides ruber* has a rank difference of minus 10: settling rank = 16, solution ranking = 26, and is fairly common in the Panama Basin. *Globigerina falconensis* has a rank difference of minus 8: settling = 8, solution = 16, but because of its rarity in the Panama Basin, was not included. *Globoquadrina hexagona* has a rank difference of plus 8: settling = 21, solution = 13. In this manner 10 species (table 2) were selected. Each species on the "preservation" list is heavier and less solution resistant than each species on the "transport" list. Under current action species on the "transport" list are more likely to be transported whole and survive, whereas species on the "preservation" list are more likely to dissolve and fragmentize in place. Indices based on these rankings (text fig. 2B) were calculated in the same manner as Berger's solution and redeposition indices.

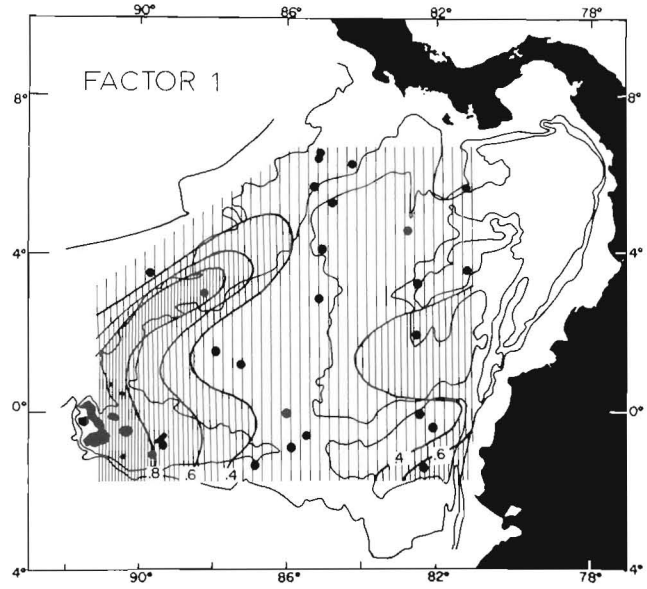
### FACTOR ANALYSIS

Multivariate factor analysis has been shown to be a useful method of organizing species counts into a small number of assemblages or factors (Imbrie and Kipp, 1971). The distribution of these factors can be related to hydrological parameters and bottom processes (for examples, Sachs, 1973). In this study the Q-mode factor analysis program CABFAC (Klovan and Imbrie,



TEXT FIGURE 3

Weight percent calcium carbonate in surface sediment (after Moore and others, 1973).



TEXT FIGURE 4

Distribution of factor 1 dominance, preservation. Higher values indicate greater relative dominance of factor.

1971) was used to resolve the data set of 25 counts (from 25 core tops) and 26 variables. The variables are the percentages of the species in table 2, *Globobulimina conglomerata*, juvenile planktonic foraminifera, globorotaliid fragments, globigerinid fragments and benthic foraminifera, and fragments for each size fraction.

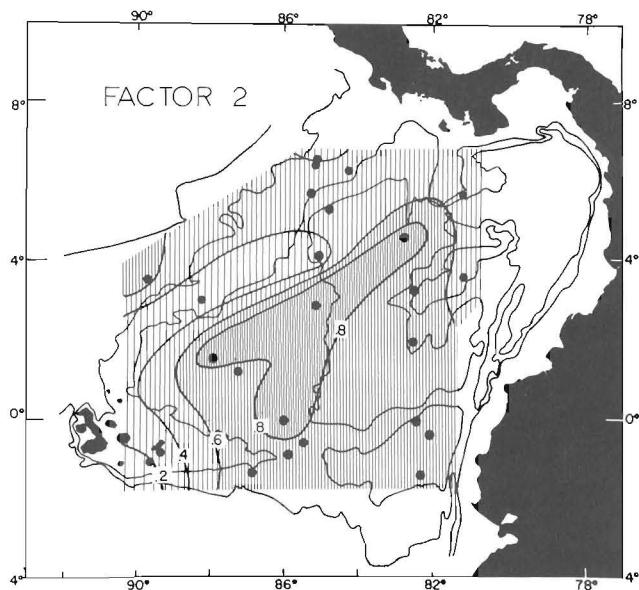
## RESULTS AND DISCUSSION

A low transport index should indicate a winnowed sample, a low preservation index a poorly preserved sample. A high transport index should indicate a sample containing redeposited material, a high preservation index, a well preserved sample. A map of the preservation indices yielded a pattern similar to the distribution of total carbonate (text fig. 3) with the lowest values east of long 83°W. and on the northwestern Cocos Ridge. The deep floor of the basin has higher preservation index values than these areas (indicating somewhat better preservation) which may mean that the index is affected by differences in productivity, which changes significantly across the basin. Certainly the index is affected by foraminiferal input; this should be minimal for the preservation index which is based on species which can tolerate the wide temperature range of the basin. Unfortunately, the planktonic for-

miniferal assemblage data of Bradshaw (1959) is not detailed enough to confirm or deny homogenous input.

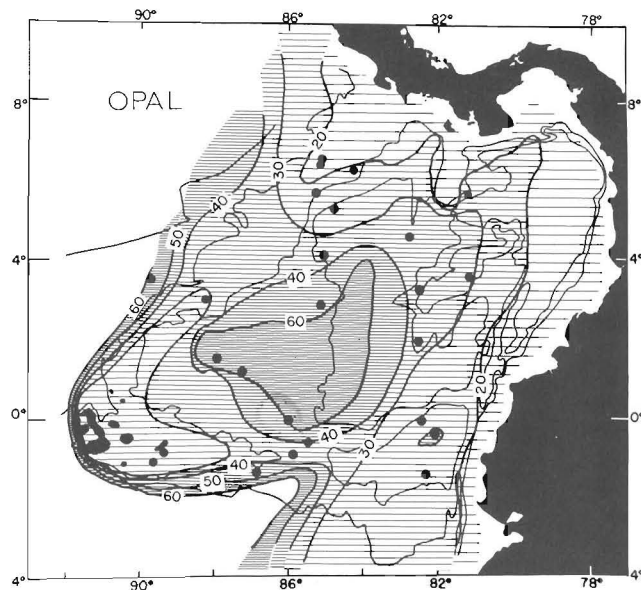
The distribution of the transport indices showed the highest values on the ridge crests. If a high transport index indicates a sample enriched in resistant, easily transported species, one would expect higher values in deeper parts of the basin where fine-grained redeposited material accumulates. Instead, a high value seems to indicate an undisturbed sample. The lower transport indices occurred on both basin floor and ridge crests. That low values are generated by winnowed samples is supported by sample 7959 from a barchan dune. The dune field and sample are described in detail by Lonsdale and Malfait (in press). Current action strong enough to create the dune field where this sample was taken is strong enough to winnow out fine material (ibid.). Thus indexing does not provide a method of determining whether a sample contains redeposited material but does provide information about sample preservation and winnowing.

The factor analysis separated the variables into 3 assemblages or factors which accounts for 97 percent of the variation between samples. The first assemblage is dominated by juvenile planktonic foraminifera with minor contributions from whole adults. Because juveniles are among the most delicate, least solution-resistant foraminifera (Hofker, 1967, Berger, 1971), this factor



TEXT FIGURE 5

Distribution of factor 2 dominance, redeposition. Higher values indicate greater relative dominance of factor.



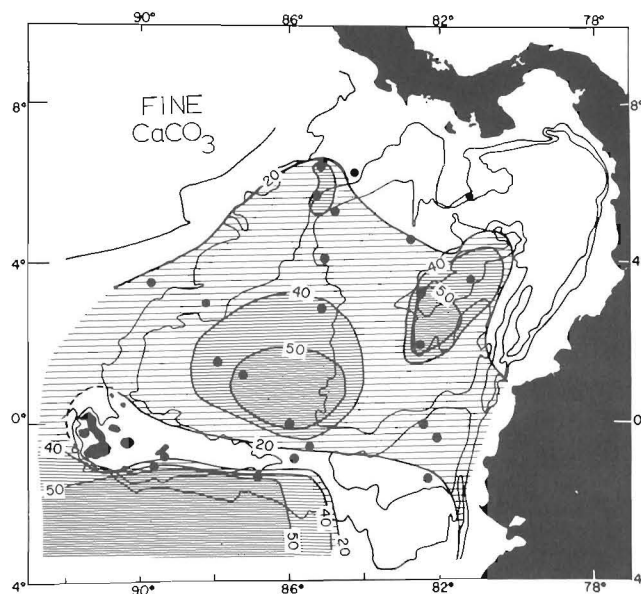
TEXT FIGURE 6

Weight percent opal (carbonate-free) in surface sediment (after Moore and others, 1973).

has been called the "preservation" factor. Its distribution is shown in text figure 4. A low factor 1 dominance indicates a poorly preserved sample. The pattern of preservation presented by factor 1 is similar to the distribution of total carbonate (text fig. 3). Regression analysis showed a good positive correlation between factor 1 and weight percent carbonate.

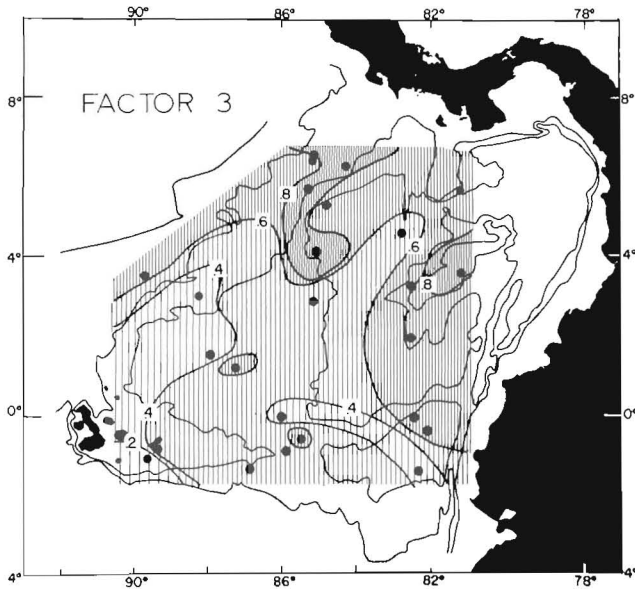
Factor 2 is dominated by smaller ( $62\text{--}177\ \mu$ ) globigerinid fragments. Text figure 5 shows its distribution which increases downslope and is dominant in the deepest part of the basin. The caplike globigerinid fragments should have settling velocities lower than spheres of equivalent volume (Lerman and others, 1974) and therefore require lower critical velocities for transport once settled. The distribution of factor 2 is similar to the distribution of weight percent opal (carbonate-free) (text fig. 6). This distribution is most likely the result of winnowing (Moore and others, 1973) since biogenic opal is by weight more than 90 percent diatoms or fine grained ( $< 62\ \mu$ ). The dominance of fragments may be explained by increased solution. The deeper parts of the basin contain more carbonate than they should if recent calculations on the rate of solution increase with depth are correct (Heath and Culberson, 1970; Morse and Berner, 1972). According to Moore and others (1973) a large part of this "extra" carbonate is fine grained ( $< 62\ \mu$ ) and very likely to have been winnowed from the ridges.

The distribution of factor 2 is also similar to the distribution of fine carbonate (text fig. 7). For these reasons factor 2 has been designated the "chaff" or redeposition factor.



TEXT FIGURE 7

Weight percent (of total sediment) fine-grained ( $< 62\ \mu$ ) calcium carbonate in surface sediment (after Moore and others, 1973).



TEXT FIGURE 8

Distribution of Factor 3 dominance. "In transit." Higher values indicate greater relative dominance of factor.

Factor 3 (text fig. 8) was the most difficult assemblage to analyze. It is dominated by larger ( $> 177 \mu$ ) globigerinid fragments, with somewhat lesser influence from globorotaliid fragments of both  $> 177 \mu$  and  $62-177 \mu$  fractions. The silt mode dispersal patterns determined by van Andel (1973) indicate sediment movement through the areas where factor 3 is dominant. The amphibole distribution determined by Heath and others (1974) which is most likely controlled by bottom currents shows high values and gradients near long  $85^\circ\text{W}$ . where factor 3 is dominant. The dot of factor 3 dominance at lat  $1^\circ\text{S}$ . is produced by the dune sample described previously. Here the pavement is nearly scoured clean of sediments and there are ripples in the facies of the dunes (Lonsdale and Malfait, in press). Because of the associations with current action and moving sediment, factor 3 was called the "in transit" factor.

Factor analysis suggests that grain-size analysis might be a better way of determining redeposition of a sample. There appears to be enough variation in settling velocities of different sizes of the same species (Berger and Piper, 1972) to make an assemblage a function of size only: different species with the same equivalent volume may be transported together and become part of the same sample. Curray (1960) first proposed grain-size analysis of "mixed sediment" to trace com-

ponents. An "original" sediment assemblage would have grain-size modes corresponding to the modes of its components. As the sediment is subjected to current action finer modes are winnowed out.

If the rate controlling step in the dissolution of calcium carbonate is related to surface kinetics and not diffusion, (R. A. Berner, oral commun., Jan. 19-21, 1974; Weyl, 1967) then solution effects in pelagic sediment assemblages should be a function of depth (pressure) and individual species, rather than increased diffusion due to bottom currents. Thus bottom currents and transport should aid in fragmentation much more than dissolution, and a sample whose grain-size distribution is dominated by finer modes is more likely to contain redeposited material.

## CONCLUSIONS

In the interpretation of sediment assemblages of foraminifera sample indexing after the method of Berger (1968) has been shown to be a good indicator of sample preservation. The analysis of whole foraminifera does not provide a method of distinguishing samples which contain redeposited material from those that do not, except by default: a sample with a high transport index is probably an undisturbed sample. However, indices are dependent on assumptions about the species input which require verification by plankton sampling. It would be interesting to compare indices of the plankton assemblages for an area with those of the sediments. Factor analysis shows that different sizes of fragments and therefore grain-size modes are a better indicator of sediment transport than indexing based on species settling velocities. Using both faunal and grain-size analysis one should be able to determine more accurately the depositional history of a sample.

## ACKNOWLEDGMENTS

I thank T. C. Moore, Jr., P. D. Komar, and J. Thiede for advice and assistance. The manuscript was reviewed by J. Thiede. This study was supported by the Office of Naval Research through contract N00014-67-A-0369-0007 under project NR083-102.

## REFERENCES

- BERGER, W. H., 1967, Foraminiferal ooze: Solution at depths: *Science*, v. 156, p. 383-385.  
 ———, 1968, Planktonic foraminifera: Selective solution and paleoclimatic interpretation: *Deep-Sea Research*, v. 15, no. 1, p. 31-43.

- , 1970, Planktonic foraminifera: Selective solution and the lysocline: *Marine Geology*, v. 8, no. 2, p. 111–138.
- , 1971, Sedimentation of planktonic foraminifera, *Marine Geology*, v. 11, p. 325–358.
- BERGER, W. H., and PIPER, D. J. W., 1972, Planktonic foraminifera: Differential settling, dissolution, and redeposition: *Limnology and Oceanography*, v. 17, p. 275–287.
- BRADSHAW, J. S., 1959, Ecology of living planktonic foraminifera in the north and equatorial Pacific Ocean: *Cushman Found. Foram. Research Contr.*, v. 10, p. 25–64.
- CORRENS, C. W., 1939, Pelagic sediments of the North Atlantic Ocean, in Trask, P. D., ed., *Recent marine sediments*; New York, Dover Publications, p. 373–395.
- CURRAY, J. R., 1960, Tracing sediment masses by grain-size modes: *Internat. Geol. Cong., Norden, 21st sess., rept.*, pt. 23, p. 119–130.
- FORSBERGH, E. D., 1969, On the climatology, oceanography and fisheries of the Panama Bight: *Inter-Am. Tropical Tuna Comm. Bull.*, v. 14, p. 49–385.
- HEATH, G. R., and CULBERSON, C., 1970, Calcite: Degree of saturation, rate of dissolution, and the compensation depth in the deep oceans: *Geol. Soc. America Bull.*, v. 81, p. 3151–3160, 4 figs.
- HEATH, G. R., MOORE, T. C., JR., and ROBERTS, G. L., 1974, Mineralogy of the surface sediments from the Panama Basin, eastern equatorial Pacific: *Jour. Geology*, v. 82, p. 145–160.
- HEEZEN, B. C., and HOLLISTER, C. D., 1971, *The face of the deep*: New York, Oxford Univ. Press, 659 p.
- HOFKER, J., JR., 1967, On the internal structure of recent Pacific planktonic foraminifera: 1st Plankt. Conf., Leiden, Proc., p. 273–278.
- IMBRIE, J., and KIPP, N. G., 1971, A new micropaleontological method for quantitative paleoclimatology: Application to a late Pleistocene Caribbean core, in Turekian, K. K., ed., *The late Cenozoic glacial ages*: New Haven, Yale Univ. Press, p. 71–182.
- JOHNSON, D. A., 1972, Ocean floor erosion in the equatorial Pacific: *Geol. Soc. America Bull.*, v. 83, p. 3121–3144.
- KENNETT, J. P., BURNS, R. E., ANDREWS, J. E., CHURKIN, M., JR., DAVIES, T. A., DUMITRICA, P., EDWARDS, A. K., GALEHOUSE, J. S., PACKHAM, G. H., and VAN DER LINGEN, G. J., 1972, Australian-Antarctic continental drift, paleocirculation changes and Oligocene deep-sea erosion: *Nature*, v. 239, p. 51–55.
- KLOVAN, J. E., and IMBRIE, J., 1971, An algorithm and FORTRAN-IV program for large-scale Q-mode factor analysis and calculation of factor scores: *Math. Geol.*, v. 3, p. 61–77.
- KOWSMANN, R. O., 1973, Coarse components in surface sediments of the Panama Basin: *Jour. Geology*, v. 81, p. 473–494.
- LERMAN, A., LAL, D., and DACEY, M. F., 1974, Stokes' settling and chemical reactivity of suspended particles in natural water, in Gibbs, R. J., ed., *Suspended solids in water*: New York, Plenum Press.
- LONSDALE, P. F., and MALFAIT, B., in press, Abyssal dunes of foraminiferal sand on the Carnegie Ridge: *Geol. Soc. America Bull.*
- MOORE, T. C., JR., HEATH, G. R., and KOWSMANN, R. O., 1973, Biogenic sediments of the Panama Basin: *Jour. Geology*, v. 81, p. 458–472.
- MORSE, J. W., and BERNER, R. A., 1972, Dissolution kinetics of calcium carbonate in sea water, II A kinetic origin for the lysocline: *Am. Jour. Sci.*, v. 272, p. 840–851.
- MURRAY, J., and RENARD, A. F., 1891, Report on deep-sea deposits based on the specimens collected during the voyage of H.M.S. Challenger in the years 1872–1876: *Rept. Voyage Challenger*, London, Longmans, 525 pp. (Reprinted by Johnson Reprint Corp., New York, 1965).
- PARKER, F. L., 1962, Planktonic foraminiferal species in Pacific sediments: *Micropaleontology*, v. 8, p. 219–254.
- PYTKOWICZ, R. M., and FOWLER, G. A., 1967, Solubility of foraminifera in seawater at high pressures: *Geochem. Jour.*, v. 1, p. 169–182.
- RUDDIMAN, W. F., and HEEZEN, B. C., 1967, Differential solution of planktonic foraminifera: *Deep-Sea Research*, v. 14, p. 801–808.
- SACHS, H. M., 1973, North Pacific radiolarian assemblages and their relationship to oceanographic parameters: *Jour. Quaternary Research*, v. 3, p. 73–88.
- STEVENSON, M., 1970, Circulation in the Panama Bight: *Jour. Geophys. Research*, v. 75, no. 3, p. 659–671.
- VAN ANDEL, T. J. H., 1973, Texture and dispersal of sediments in the Panama Basin: *Jour. Geology*, v. 81, p. 434–457.
- VAN ANDEL, T. J. H., and KOMAR, P. D., 1969, Ponded sediments of the mid-Atlantic Ridge between 22° and 23° North Latitude: *Geol. Soc. America Bull.*, v. 80, p. 1163–1190.
- WATKINS, N. D., and KENNETT, J. P., 1972, Regional sedimentary unconformities and upper Cenozoic changes in bottom water velocities between Australasia and Antarctica, in Hayes, D. E., ed., *Antarctic Oceanology II: Antarctic Research Ser.*, v. 19, p. 273–293.
- WEYL, P. K., 1967, The solution behavior of carbonate minerals in seawater: *Miami Univ. Studies Tropical Oceanography*, v. 5, p. 178–228.
- WOOSTER, W. S., and CROMWELL, T., 1959, An oceanographic description of the eastern tropical Pacific: *Scripps Inst. Oceanography Bull.*, v. 7, p. 169–282.
- WYRTKI, K., 1967, Circulation and water masses in the eastern Pacific Ocean: *Internat. Jour. Oceanology and Limnology*, v. 1, no. 2, p. 117–147.

APPENDIX 1  
SURFACE SAMPLES

Core	Water Depth (corr. meters)	Sampler	Sample Top (cm)	Sample Bottom (cm)	Lat. (deg. min.)	Long. (deg. min.)	Accession no. PO: OSU PS: SIO PL: LDGO
V15-29	1889	PC	11	14	06.21	085.17	PL00013
V15-31	1417	PC	20	23	-01.30	082.19	PL00017
V17-42	1814	PC	13	16	03.32	081.11	PL00023
V17-43	3147	PC	14	17	01.52	082.37	PL00025
V18-350	1838	PC	8	10	05.42	085.16	PL00029
V18-351	3007	PC	5	8	05.18	084.45	PL00031
V19-27	1373	PC	10	13	-00.28	082.04	PL00049
V21-25	1359	PC	15	18	05.43	081.03	PL00055
V21-26	3081	PC	19	22	04.36	082.44	PL00057
V21-28	2714	PC	11	14	01.05	087.17	PL00060
V21-29	712	PC	12	14	-00.57	089.21	PL00062
V21-30	617	PC	10	13	-01.13	089.41	PL00064
V21-211	1443	PC	7	10	03.00	088.23	PL00066
V21-212	3338	PC	9	12	02.50	085.08	PL00068
V21-213	1966	PC	11	14	03.11	082.25	PL00070
V24-36	1878	PC	0	3	06.30	085.13	PL00086
RC8-102	2180	PC	7	10	-01.25	086.51	PL00088
RC10-250	1734	PC	0	3	06.17	084.19	PL00107
RIS-32P	2770	PC	11	13	-00.09	085.59	PS00124
Y69-73P	2707	PC	26	32	01.27	087.56	PO00159
Y69-75M2	2198	MC	16	19	03.29	089.42	PO00164
Y69-102P	2220	PC	10	17	-01.04	085.51	PO00176
Y69-103P	1808	PC	10	16	-00.05	082.26	PO00179
Y69-108P	3390	PC	10	16	04.09	085.02	PO00188
SOTW-5-2G	2700	GC	0	2	-00.42	085.26	PS07959

APPENDIX 2

Counts of items used in this study. 300 or more grains counted except for badly dissolved samples. Two lines per sample: first line > 177  $\mu$  fraction, second line 62-177  $\mu$  fraction.

Accession Number	G. conglonatus	G. ruber	G. tenellus	G. conglomerata	G. saculifer G. siphonifera	T. humilis	O. universa	G. iota G. glutinata	G. hexagona	Benthic foraminifera and fragments	globigerinid fragments	Juvenile planktonics	globorotaliid fragments	Total Grains Counted
13	2	24	1		8		1	30	3	9	273	4	113	579
13								11		2	220	20	45	325
17	2	84			52		131	6		2	251	392	7	1241
17		2						11		4	489	195	4	728
23					1			1	2	4	551	4	61	665
23										9	390	5	35	439
25		40			31					43	402	38	18	836
25											290	55		350
29		1		1	1					3	239	5	111	394
29			1					2		6	338	6	126	506
31		37			34	1	3	5	5	37	306	33	59	788
31			1			2		9	3	16	248	26	155	475
49		4		3	2			1		11	301	5	54	496
49										4	350	2	17	374
55		7		2			1	5	3	10	375	53	15	501
55						1			1	17	480	5	24	529
57	2	57			28		2	1		121	260	73	33	977
57											287	2		290
60	2	29	1		17		1	8	2	2	280	27	18	589
60		3				1		9		6	407	54	51	543
62		52	3	9	12		2	26	34	25	147	105	17	679
62		7	2	3	1	10		40	57	44	213	159	12	718
64	2	66	8		51		1	15	3	17	146	258	14	753
64		1	1			8		8		8	137	240		522
66	4	237	7	3	148		4	142	5	10	314	258	77	1525
66		6	2		1	32		39	3	15	423	545	44	1322
68	2	18			23		1	3		26	124	15	21	428
68											340	1		350
70	2	18			25		4			31	558	21	64	1162
70											330	10		350
86	1				1					8	255	3	53	324
86										7	300	3	175	499
88	1	17		55	15		2	9	32	20	307	77	43	908
88				3	1	6		20	47	10	603	34	18	795
107		29	1	3	12			4	4	25	379	8	65	696
107		0	2		1			2	1	2	222	22	68	356
124		13	1	4	5			4	1	10	100	19	14	375
124				5		2		27	30	17	470	71	24	650
159	4	8	1	9	9			18	1	9	288	5	65	567
159								6	2	1	435	32	82	597
164	6	20		7	12			3	1	4	173	2	38	363
164		2								7	426	21	33	519
176		8	3		3		5	6	1	1	101	20	13	386
176		1	2					16	6	6	319	36	14	525
179		7			12		6			36	667	37	72	1345
179								1		9	478	14	51	566
188		14	1	7	5		1	4	3	23	147	6	28	325
188		1		1	2	2		15	14	11	555	30	294	942
7959		1			2			3		2	220	0	39	403
7959								5		1	330	14	32	418